Development of Rapid Chromatographic Technologies for Complex Biofermentation Sample Analyses

By

Hassan Alwael, BSc.

A thesis submitted to Dublin City University for the degree of

Doctor of Philosophy

Under the supervision of

Prof. Brett Paull

School of Chemistry

University of Tasmania

and

Dr. Damian Connolly

School of Chemical Sciences

Dublin City University

September 2012

Declaration

I hereby certify that this material, which I now submit for assessment on the programme of study leading to the award of *Doctor of Philosophy* is entirely my own work, that I have exercised reasonable care to ensure that the work is original, and does not to the best of my knowledge breach any law of copyright, and has not been taken from the work of others save and to the extent that such work has been cited and acknowledged within the text of my work.

Signed: _____

ID No.: _____

Date: _____

Table of Contents

Abstract

The recent growth in the biopharmaceutical industry is remarkable due to the introduction of many new therapeutic proteins for the treatment of different diseases. The production processes of the biotherapeutics are complicated and have to be maintained under strict and regulated conditions. Therefore, the development of rapid, sensitive and cost-effective analytical assays is highly demanded for monitoring the biofermentation processes and the key parameters that could affect the final product quality and production consistency.

The overall aim of this research is to develop sensitive and selective analytical methods for the determination of raw material components in highly complex samples supplied from the biopharma industry based on solid phase extraction (SPE) and rapid resolution liquid chromatography (RRLC). This development includes the use of narrow-bore columns packed with sub-2 μm silica particles or made of monolithic materials. The developed methods were applied for the qualitative and quantitative analysis of common monosaccharides, including sialic acid, and cysteine/cystine ratio in a range of biopharmaceutical production samples such as raw material yeast extract powders, fermentation feedstocks, chemically defined media and in-process fermentation broth samples in which they were taken from different lots in order to estimate lot-to-lot variability. For evaluation purposes, standard analytical performance criteria were examined for all the developed methods. In addition, a novel solid phase microextraction in a pipette tip for selective enrichment of galactosylated proteins is presented. The extraction device is fabricated by *in-situ* photopolymerisation of ethylene dimethacrylate porous polymer monolith within the confines of 20 μL polypropylene pipette tip. Then the surface of the monolith was significantly enhanced by immobilising gold nano-particles (AuNPs) which was functionalised with *Erythrina cristagalli* lectin (ECL) afterwards. The ECL-modified tip was successfully applied for the enrichment of galactosylated

proteins versus non-galactosylated proteins from different sample matrices including *Escherichia coli* cell lysate. Reversed-phase capillary LC was used to validate the efficiency and selectivity of the developed extraction device which resulted in an increase in extraction recovery of ~95 % due to the AuNPs enhanced surface area.

List of Publications

1- Development of a rapid and sensitive method for determination of cysteine/cystine ratio in chemically defined media

Hassan Alwael, Damian Connolly, Leon Barron and Brett Paull, *Journal of Chromatography A*, 2010, **1217**, 3863 - 3870.

2- Liquid chromatographic profiling of monosaccharide concentrations in complex cell-culture media and fermentation broths

Hassan Alwael, Damian Connolly and Brett Paull, *Analytical Methods*, 2011, **3**, 62 - 69.

N.B.: Obtained front cover of Analytical Methods (see the next page please).

3- Pipette-tip selective extraction of glycoproteins with lectin modified gold nano-particles on a polymer monolithic phase

Hassan Alwael, Damian Connolly, Paul Clarke, Roisin Thompson, Brendan Twamley, Brendan O'Connor and Brett Paull, *Analyst*, 2011, **136**, 2619 - 2628.

4- Rapid and sensitive chromatographic determination of free sialic acid in bio-pharma fermentation media samples

Hassan Alwael, Damian Connolly and Brett Paull, *Analytical Methods*, in preparation.

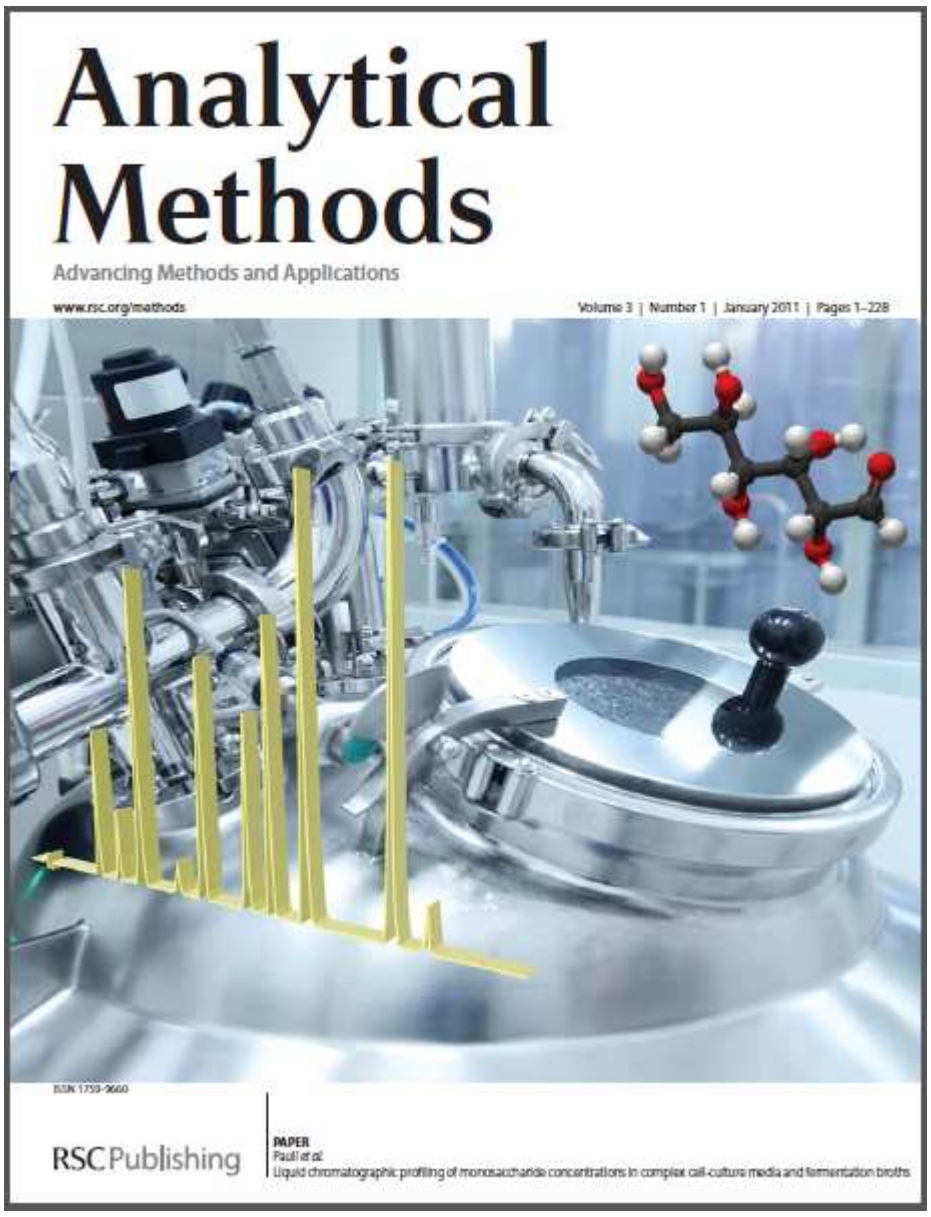
Analytical
Methods
Advancing Methods and Applications
www.rsc.org/methods
Volume 3 | Number 1 | January 2011 | Pages 1–228
ISSN 1759-9660
RSC Publishing
PAPER
Paull et al.
Liquid chromatographic profiling of monosaccharide concentrations in complex cell-culture media and fermentation broths

List of Presentations

A) Oral presentations

1- Lectin affinity extraction of glycoproteins with terminal galactose residues on a gold nano-particle modified polymer monolith in pipette-tip format

Hassan Alwael, Damian Connolly, Paul Clarke, Roisin Thompson, Brendan O'Connor, Brendan Twamley, Brett Paull. The 6th Conference on Analytical Sciences in Ireland, 21-22 February 2011, The Helix Theatre, Dublin City University, Dublin, Ireland.

B) Poster presentations

1- Analysis of monosaccharides in yeastolates and pre-inoculation fermentation media samples.

Damian Connolly, Hassan Alwael and Brett Paull, 12th Symposium on The Interface of Regulatory and Analytical Science for Biotechnology Health Products, Washington DC, USA, January, 2008.

2- Advanced separations and microfluidic platforms.

Mercedes Vazquez, Fernando Benito-Lopez, Dermot Diamond, Hassan Alwael, Damian Connolly, Brett Paull, GlycoScience Ireland Launch, 8th April, Trinity College, Dublin, Ireland.

3- Selective extraction, separation and analysis of monosaccharides in yeastolates and pre-Inoculation fermentation media samples using rapid liquid chromatography with fluorescence detection.

Hassan Alwael, Damian Connolly and Brett Paull, 5th Biennial Conference on Analytical Sciences in Ireland, 7th May 2008, Waterford, Ireland.

4- Rapid and sensitive chromatographic assays for monosaccharides and free sialic acids in bio-fermentation media samples.

Hassan Alwael, Damian Connolly and Brett Paull, Analytical Research Forum, 21-23 July 2008, University of Hull, UK.

5- Application of rapid resolution liquid chromatography in the analysis of monosaccharides and sialic acid in bio-fermentation media samples using fluorescence detection.

Hassan Alwael, Damian Connolly, Kirk Leister, Stephen Gacheru and Brett Paull, International Conference on Trends in Bioanalytical Sciences and Biosensors, 26-27 January 2009, Dublin, Ireland.

6- A study of the redox activity of cysteine/cystine in bio-pharma fermentation feed-stocks by HPLC.

Hassan Alwael, Damian Connolly, Kirk Leister, Stephen Gacheru and Brett Paull, International Conference on Trends in Bioanalytical Sciences and Biosensors, 26-27 January 2009, Dublin, Ireland.

7- Development of a rapid resolution liquid chromatography assay for cysteine/cystine determination in bio-pharma fermentation feed-stocks.

Hassan Alwael, Damian Connolly and Brett Paull, Analytical Research Forum, 13-15 July 2009, Pfizer Global R+D Labs, Kent and University of Kent, Canterbury, UK.

8- Analysis of cysteine/cystine in bio-pharma fermentation feed-stocks using rapid resolution liquid chromatography.

Hassan Alwael, Damian Connolly and Brett Paull. 21st International Ion Chromatography Symposium 21-24 September 2009 Dublin, Ireland.

9- Fabrication of a gold modified polymer monolith in a pipette tip for lectin affinity extraction of selected glycoproteins

Hassan Alwael, Damian Connolly, Paul Clarke, Roisin Thompson, Brendan O'Connor, Brendan Twamley and Brett Paull. 35th International Symposium on High Performance Liquid Phase Separations and Related Techniques, 19-24 June 2010, The Hynes Convention Center & Sheraton Boston Hotel, Boston, MA, USA.

10- Fabrication of a gold modified polymer monolith in a pipette tip for lectin affinity extraction of selected glycoproteins

Hassan Alwael, Damian Connolly, Paul Clarke, Roisin Thompson, Brendan O'Connor, Brendan Twamley and Brett Paull. Analytical Research Forum, 26-28 July 2010, Loughborough University, UK.

11- Fabrication of a gold modified polymer monolith in a pipette tip for lectin affinity extraction of selected glycoproteins

Hassan Alwael, Damian Connolly, Paul Clarke, Roisin Thompson, Brendan O'Connor, Brendan Twamley and Brett Paull. 3rd Annual Meeting of GlycoScience Ireland, 31st August – 1st September 2010, University College Dublin, Dublin, Ireland.

12- Micro-solid phase extraction and selective enrichment of glycoproteins using lectin modified gold nano-particles on a monolithic support

Hassan Alwael, Damian Connolly, Paul Clarke, Roisin Thompson, Brendan O'Connor, Brendan Twamley and Brett Paull. 28th International Symposium on Chromatography, 12-16 September 2010, Valencia Conference Centre, Valencia, Spain.

List of Abbreviations

AA	2-aminobenzoic acid
ABD-F	4-aminosulfonyl-7-fluoro-2,1,3-benzoxadiazole
ABEE	p-aminobenzoic ethyl ester
ACN	Acetonitrile
ADVN	2,2'-azobis(2,4-dimethyl)valeronitrile
AIBN	azobisisobutyronitrile
AMPS	2-acrylamido-2-methyl-1-propanesulfonic acid
AuNPs	Gold nano-particles
BET	Brunauer-Emmett-Teller
BP	Benzophenone
BSA	Bovine serum albumin
BuMA	Butyl methacrylate
CD	Chemically defined
CE	Capillary electrophoresis
CEC	Capillary electrochromatography
CE-LIF	Capillary electrophoresis coupled with laser-induced fluorescence
CHO	Chinese hamster ovary
CMPI	2-chloro-1-methylpyridinium iodide
CMQT	2-chloro-1-methylquinolinium tetrafluoroborate
Cys	Cysteine
Cyss	Cystine
CZE	Capillary zone electrophoresis
DMB	1,2-diamino-4,5-methylenedioxybenzene
DMSO	Dimethyl sulfoxide
DNS-Cl	Dansyl chloride
DPA	2,2-dimethoxy-2-phenylacetophenone

DTNB	5,5´-dithiobis(2-nitrobenzoic acid)
DTSP	3,3′-dithiodipropionic acid di(N-hydroxysuccinimide ester)
DTT	Dithiothreitol
DVB	Divinylbenzene
ECL	*Erythrina cristagalli* lectin
EDMA	Ethylene dimethacrylate
EEM	Excitation-emission matrix fluorescence
EGFR	Epidermal growth factor receptor
ELSD	Evaporative light scattering detection
FDA	Food and Drug Administration
FE-SEM	Field emission scanning electron microscopy
FIA	Flow injection analysis
FLD	Fluorescence detection
Fuc	Fucose
Gal	Galactose
GalN	Galactosamine
GC	Gas chromatography
GC-FID	Gas chromatography with flame ionisation detection
Glc	Glucose
GlcN	Glucosamine
GMA	Glycidyl methacrylate
HPAEC-PAD	High performance anion exchange chromatography with pulsed amperometric detection
HPLC	High performance liquid chromatography
IMAC	Immobilised metal affinity chromatography
LC-ESI-MS	Liquid chromatography electrospray ionisation mass spectrometry
LC-MS/MS	Liquid chromatography tandem mass spectrometry
LLE	Liquid–liquid extraction
LMA	Lauryl methacrylate

MALDI-TOF-MS	Matrix-assisted laser desorption/ionisation time-of-flight mass spectrometry
Man	Mannose
ManN	Mannosamine
MeOH	Methanol
MEPS	Microextraction in a packed syringe
MIP	Molecularly imprinted polymer
MS	Mass spectrometry
NANA	N-acetylneuraminic acid
NDA	New Drug Applications
NGNA	N-glycolylneuraminic acid
NIR	Near-infrared spectroscopy
NSTP	N-succinimidyl-3-thiopropionate
ODS	Octadecylated
OPA	*o*-phthalaldehyde
OPD	*o*-phenylenediamine
PAT	Process Analytical Technology
PEEK	Polyetheretherketone
PEG	Polyethyleneglycols
PEO	Polyethylene oxide
PMP	1-phenyl-3-methyl-5-pyrazolone
QbD	Quality by Design
Rib	Ribose
RP-HPLC	Reversed-phase high performance liquid chromatography
RRLC	Rapid Resolution Liquid Chromatography
SAM	Self-assembled monolayers
SBD-F	7-fluorobenzo-2-oxo-1,3-diazole- 4-sulfonate
SBSE	Stir-bar-sorptive extraction
S.D.	Standard deviation

SEM	Scanning electron microscopy
SPE	Solid phase extraction
SPE-PT	Solid phase extraction in a pipette-tip
SPME	Solid phase microextraction
ST	Styrene
TBA	Thiobarbituric acid
TCA	Trichloroacetic acid
TCEP	Tris(2-carboxyetyl)phosphine
TEMED	*N*,*N*,*N*',*N*'-tetramethylethylenediamine
TEOS	Tetraethoxysilane
TFA	Trifluoroacetic acid
TMOS	Tetramethoxysilane
TMSPM	3-(trimethoxysilyl)propyl methacrylate
TNBT	Tri-nbutylphosphine
TPP	Triphenylphosphine
UPLC	Ultra performance liquid chromatography
UVD	Ultraviolet detection
VAL	2-vinyl-4,4-dimethylazlactone
Xyl	Xylose

Acknowledgments

Praise and thanksgiving to Allah

I express my sincere thanks to my family, especially my parents Omar and Aisha, brothers and sisters for their patience, support and encouragement throughout the period of this work.

I am extremely grateful to my supervisors Prof. Brett Paull and Dr. Damian Connolly for the opportunity given to work in the lab, guidance and encouragement over the duration of this project.

My thanks also go to all the technical staff in the School of Chemical Sciences and National Centre for Sensor Research, colleagues in the lab, friends I made in DCU and Ireland; special big thanks to Hamid Younis, and friends in Saudi.

The financial support from King AbdulAziz University, Saudi Arabia, for this work is really appreciated.

I also acknowledge Bristol-Myers Squibb Company for the provision of samples under the Centre for Bioanalytical Sciences (CBAS) programme.

Chapter 1

An introduction to column stationary phase developments in liquid chromatography

1.1. An introduction to liquid chromatography

Chromatography is a powerful analytical method that is widely used for the separation, identification and determination of the chemical components in complex mixtures [1]. It was first demonstrated by the Russian botanist Mikhail Tswett in 1906 when he separated different plant pigments by passing an extract of the leaves through a glass column packed with calcium carbonate [2]. The term *chromatography* came from the Greek words, *chroma* meaning "colour" and *graphein* meaning "to write" [3]. Tswett's invention went virtually unnoticed for several decades [2]; however, the application of chromatography has grown incredibly since then because of the great need for analytical methods for characterising complex mixtures [3].

Chromatography may be defined as the separation of a mixture of components based on the distribution coefficients for each component between two phases; a stationary phase and a mobile phase as shown in Figure 1.1 [1]. In liquid chromatography, the mobile phase is liquid consisting of a solvent or mixture of solvents and the stationary phase is a solid support. Chromatographic separations can be classified based on the interaction mechanism of the solute with the stationary phase according to the following: (i) Adsorption chromatography; this is the traditional separation mode in which the stationary phase is solid and the mobile phase is liquid. The mixture components adsorb on the surface of the solid phase. The more strongly a solute is adsorbed, the slower it travels through the column [2]. (ii) Partition chromatography; the stationary phase is liquid bonded to a solid support and the mobile phase is a liquid. The separation of the mixture components is based on their equilibration between the liquid on the stationary phase surface and the mobile phase. In the liquid-liquid partition chromatography, if a polar stationary phase with a non-polar mobile phase is used, polar compounds are retained and separated. This is called "normal-phase chromatography". If a non-polar stationary phase with a polar mobile

phase is used, non-polar compounds are retained and separated. This is called "reversed-phase chromatography" [2]. (iii) In ion exchange chromatography, the stationary phase consists of either cationic exchange or anionic exchange groups attached to polymeric or silica materials and the mobile phase consists of an electrolyte. The separation of the mixture components is based on the exchange of ionic analytes with the counter-ions on the stationary phase [4]. (iv) In size exclusion chromatography, the separation of a mixture of components is based on the size of the analyte molecules. Large molecules are excluded from the pores of the stationary phase particles and eluted first, whereas small molecules are retained in the pores for a while before elution [4].

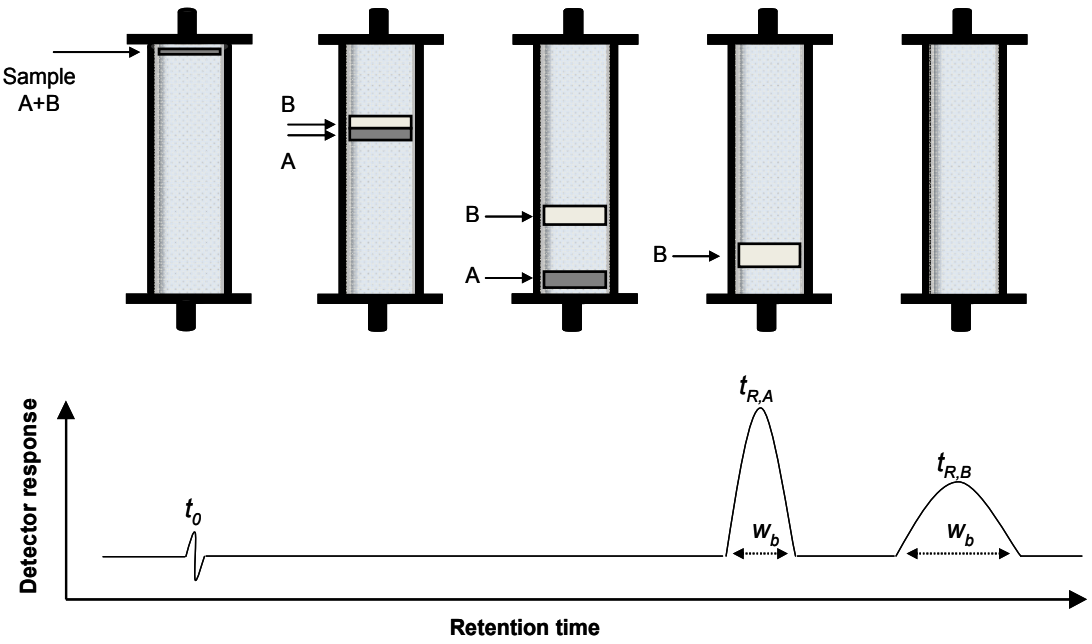

Figure 1.1: Schematic of the chromatographic process showing the separation of sample components during their passage through the column. Adapted from [3].

Until the late 1960s, the passage of the mobile phase through the solid phase in the column was driven by its own weight preventing any attempts for efficient and fast separations. In the late 1950s, the substantial

developments in gas chromatography (GC), which had led to a system with a pump to deliver and control the flow rate of the mobile phase and a detector for on-line monitoring of analytes, were extended to liquid chromatography leading to High Performance Liquid Chromatography (HPLC) [5, 6].

Thus, HPLC is the term used to describe liquid chromatography in which the separation of sample components is accomplished by pumping the liquid mobile phase through a column that contains the stationary phase. The HPLC instrument, as illustrated in Figure 1.2, consists of a pump to deliver the mobile phase through the system, an injector to introduce the sample, a column to separate the sample components, a detector to monitor the separated components and a data collection device for interpretation and storage of results [4, 7].

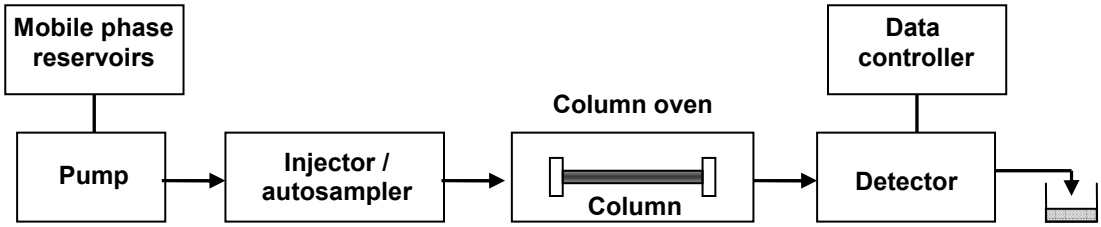

Figure 1.2: Schematic of the major modules of the HPLC instrumentation.

In the last 30 years, HPLC has become one of the most popular analytical instruments for the quantitative analysis of a wide range of pharmaceutical compounds [8, 9]. One of the main objectives of analytical laboratories is to develop rapid and efficient methods for qualitative and quantitative analysis due to a continuously growth in the number of samples [10]. In addition, high-throughput separations are highly demanded in common applications within the pharmaceutical industry such as purity assays, pharmacokinetic studies, and quality control [11] since faster separations are required to enhance productivity and reduce costs [12].

1.2. Column stationary phase developments

1.2.1. Particle-based stationary phases

The column is the heart of the chromatographic system as it contains the most important part, the stationary phase, in which the separation of sample components is achieved. The column chromatographic performance depends on the selectivity and efficiency of the stationary phase where the improvement efforts have been made to achieve faster and more efficient separations since the introduction of HPLC. Typically, the column is constructed from stainless steel for rigidity at high pressures [1, 7] or it can be replaced by titanium or polyetheretherketone (PEEK) for more corrosion resistance [4]. The quality of the packed column and its backpressure, and therefore the separation efficiency are determined by the particle size and its distribution and the quality of the packing of the particles within the column [4, 13]. Most analytical HPLC columns range from 2 to 5 mm in internal diameter and from 30 to 300 mm in length [7]. The most common stationary phases in HPLC columns are those in which the functional group is bonded to silica, which has excellent physical characteristics and chromatographic performance [4, 7].

In theory, it has been known since the early development of chromatography that packing the column with small size particles leads to reduced mass transfer effects and thus high efficiency with reduced analysis time [14, 15]. Great reduction in the size of the particles has been achieved in the last sixty years. For example, the size of the first particles used in the 1950s was approximately 100 µm which has been reduced since then up to the development of sub-2 µm [16]. These small particles were introduced by Horváth and co-worker in 1988 [17] but they were not commercially available until 2004, due to the lack of adequate instrumentations which contain pumps compatible with columns packed with such small particles [10, 18]. Accordingly, column efficiency has been improved significantly. The plate

numbers per column have been increased from 200 to over 30,000 for the columns packed with 100 µm and sub-2 µm respectively [10, 16].

The efficiency of a column is a number that describes peak broadening as a function of retention. Two major theories have been developed to describe the column efficiency. Plate theory was proposed by Martin and Synge, and the rate theory was developed by van Deemter *et al.* [7]. The chromatographic column, as proposed in the plate theory, is considered to consist of a number of thin sections or "plates", each of which allows a solute to equilibrate between the stationary phase and mobile phase [7]. The number of theoretical plates or plate number (N) is a measure of the efficiency of the column. N is defined as the square of the ratio of the retention time divided by the standard deviation of the peak (σ). Since the W_b is equal to 4σ for a Gaussian peak,

$$N = \left(\frac{t_R}{\sigma}\right)^2 = \left(\frac{4\,t_R}{w_b}\right)^2 = 16\left(\frac{t_R}{w_b}\right)^2 \qquad \text{(Eq. 1.1)}$$

Since it is more difficult to measure σ or W_b, a relationship using width at half height ($W_{1/2}$) is often used to calculate N, since $W_{1/2}$ is equal to 2.355σ for a Gaussian peak [4], therefore:

$$N = \left(\frac{t_R}{\sigma}\right)^2 = \left(\frac{2.355\ t_R}{w_{1/2}}\right)^2 = 5.546\left(\frac{t_R}{w_{1/2}}\right)^2 \qquad \text{(Eq. 1.2)}$$

The greater the number of theoretical plates (N), the more efficient the column is considered to be [7].

The movement of a solute along the column is viewed as a stepwise transfer from one theoretical plate to the next. The thinner the theoretical plates, the greater the number that can be envisaged within a given length of column. These terms are related as follows:

$$H = L / N \quad \text{(Eq. 1.3)}$$

Where *L* is the length of the column (mm). Thus, the smaller the height equivalent to a theoretical plate (HETP, or H), the greater is the efficiency of the column. In general, the H value is smaller for small size stationary phase particles, low mobile phase flow rates, less viscous mobile phases [7].

The van Deemter equation was developed in 1950s to explain band broadening in chromatography by correlating HETP or H with linear flow velocity (μ) and describes the contributions to HETP of a column: [4]. It considers the diffusional factors that contribute to band broadening in the column [7]. The contributions of these three parameters to the column efficiency are graphically shown in Figure 1.3. The van Deemter equation may be written as the following:

$$H = A + B/\mu + C\mu \quad \text{(Eq. 1.4)}$$

Where H represents the efficiency of the column and μ is the average linear velocity of the mobile phase. The A term is "eddy diffusion or multi-path effect". When the sample is introduced to the head of the column, the analyte molecules reach the end of the column at different times due to the different paths that they travelled through the stationary phase particles (Figure 1.4). The A term is proportional to particle size d_p and is smaller in well-packed columns [4]. The B term represents "longitudinal diffusion" of the solute band in the mobile phase (Figure 1.4) and is proportional to diffusion coefficient (D_m) [4]. The contribution of longitudinal diffusion to plate height becomes significant only at low mobile phase velocities [7]. The C term is "resistance to mass transfer" which arises from the time lags caused by the slower diffusion of the solute band in and out of the stationary phase (Figure 1.4). It is proportional to (d_p^2/D_m) and contribution from the C term is important at high flow rates [4]. The minimum point on the van Deemter

curve in Figure 1.3 indicates the minimum plate height, H_{min}, and the optimum flow velocity at maximum column efficiency [4].

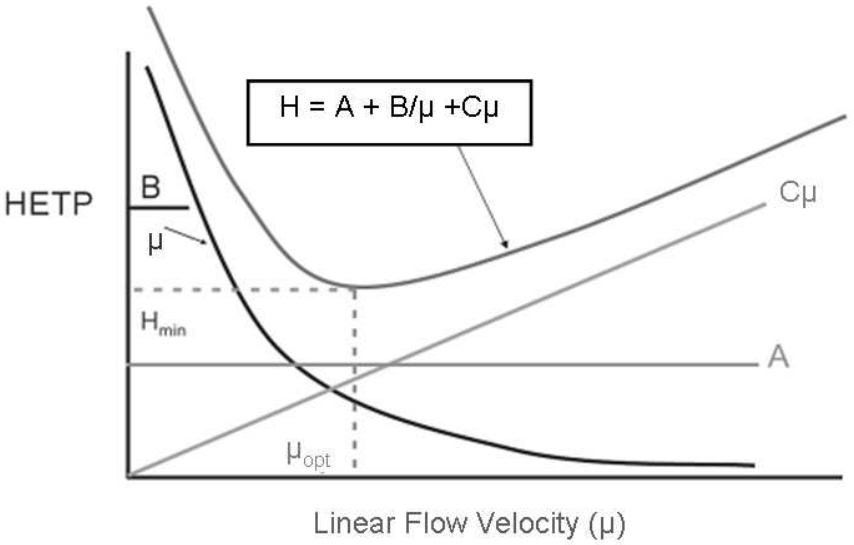

Figure 1.3: Hypothetical van Deemter curve showing the relationship between efficiency and average linear velocity. Adapted from [4].

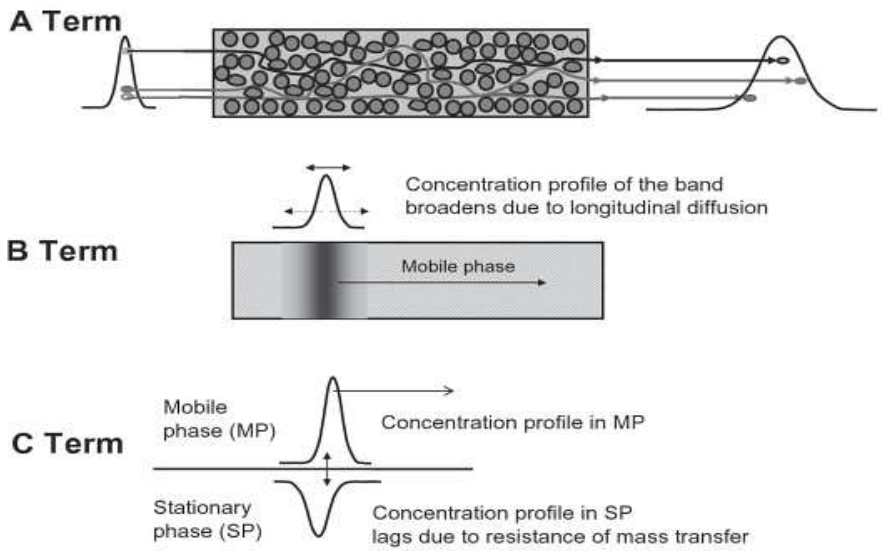

Figure 1.4: Diagrams illustrating the mechanism of various van Deemter terms contributions. Reproduced from [4].

Based on the van Deemter equation, the use of small particles leads to improvements in the column efficiency with reduced analysis time. The main advantage of reducing the size of the particles is the low mass transfer resistance associated with these particles in which high resolution with short analysis time can be achieved at higher and over a wider range linear velocities [10, 18]. The van Deemter plot in Figure 1.5 shows the height equivalent to the theoretical plate (H) versus the linear velocity for different particle sizes. It shows that higher column efficiencies were obtained when the size of the particles decreased. Therefore, columns packed with sub-2-µm particles may obtain better resolution and reduced analysis time whereas the columns packed with larger particles produced a much steeper curves at high linear velocities as the C term in Eq. (1) is proportional to d_p^2 [18].

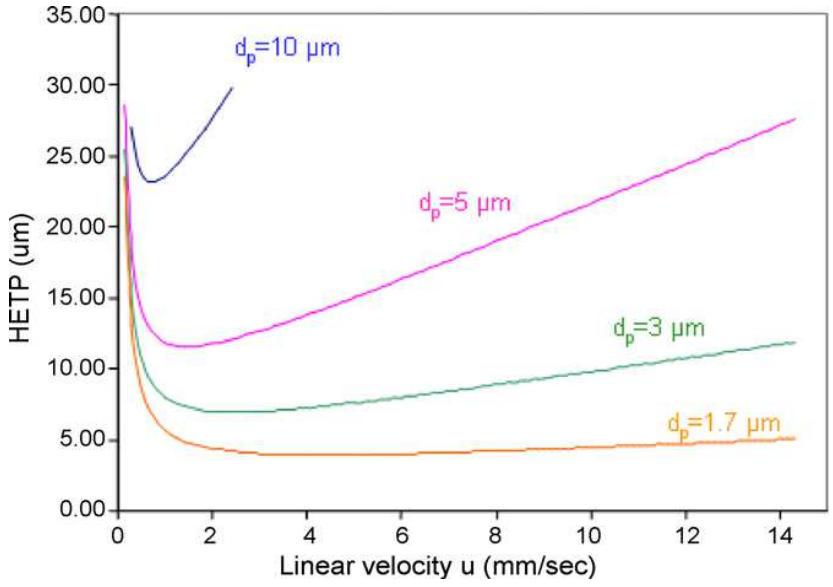

Figure 1.5: Theoretical van Deemter curves plotted for 10, 5, 3 and 1.7 µm particles. Reproduced from [18].

Even though using columns packed with small particles leads to better resolution and rapid analysis time, the high back pressures generated from such columns prevent the use of conventional HPLC instruments. The increase in the pressure is proportional to the cube of the particle diameter

used. For example, a column packed with 1.7 µm particles generates a pressure 27 times higher than that packed with 5 µm particles under the same conditions [10]. Therefore, HPLC instrumentations capable of pumping the mobile phase at high backpressures are required for operating such columns.

1.2.2. Introduction to monolithic stationary phases

Porous monolithic materials are a relatively new class of column stationary phase materials that have proven to be a very good alternative to particle-based columns. The development of monolithic materials for the purpose of chromatographic separation has increased significantly in the last two decades. Monolithic materials are constructed of a porous single piece that contains pores in which the liquid phase flows through and can be compared to a single large “particle” that does not contain interparticular voids typical of packed beds [19-22].

The word “monolith” comes from the Greek and means literally “single stone”. It first appeared as a description of a single piece of functionalised cellulose sponge used for protein separation in 1993 [23] whereas this expression was used afterwards to describe rigid macroporous polymers prepared by bulk polymerisation in a closed mould [24]. Since this stage, this term became standard as it is an easy-to-use word compared to the early names such as “continuous polymer bed” [25], “continuous polymer rod” [26], “porous silica rod” [27] and “continuous column support” [28], which were previously used to describe different porous polymers.

The concept of using monolithic materials as stationary phases in chromatography was first proposed by Mould and Synge in the early 1950s [29, 30]. Later, Kubín *et al.* from the Institute of Macromolecular Chemistry in Prague tested a methacrylate-based polymeric matrix for the purpose of chromatographic separations in size-exclusion mode. However, the low degrees of crosslinking they used led to very low permeability [31]. Even

though the considerable potential advantages of monolithic materials had been proposed a relatively long time ago [32], they were not demonstrated until the introduction of the monolithic stationary phases in the late 1980s and the early 1990s as suitable materials for chromatographic separations, which marked a significant improvement in the column technology [33].

In 1992, a report was published by Svec and Fréchet [26, 34], which described for the first time a much simpler procedure for the *in-situ* fabrication of rigid macroporous polymers. It was prepared by filling a column housing with a mixture consisting of monomers, a free-radical initiator and porogenic solvents and heated in order to form a rigid porous polymer. At the same time, Soga and Nakanishi [35-37] developed a method to synthesise inorganic continuous beds made of porous silica. These materials were then utilised by Tanaka as monolithic columns in HPLC in which he functionalised the surface with octadecyldimethyl-(*N,N*-diethylamino)silane and applied them to the separation of polypeptides [38] and alkylbenzenes [27]. Since the publication of these reports and the promising results obtained, more attention has been drawn towards these materials. Today rapid advances in the development of monolithic materials continue to appear and they now hold an impressively strong position in separation science and other areas of chemistry, achieved due to the tunable properties that lead to broad applications [39-42].

Depending on the nature of the material, monoliths can be divided into two groups: (i) organic polymer-based monoliths, such as acrylamide-based, acrylate- or methacrylate-based, and styrene-based polymers, and (ii) inorganic polymer-based monoliths such as silica, which are prepared by sol-gel technology [13, 43].

The idea of using the monolithic materials as an alternative to packed beds arose from the need to overcome some of the drawbacks associated with particle-based beds, based upon their physical and chemical structures and a number of features and benefits that they possess; mainly, the

achievement of rapid separation with low backpressures and low mass transfer resistance [44, 45].

In general, the fabrication of the monolithic materials is relatively simple; the polymerisation process of a mixture consisting of monomers and porogenic solvents is initiated either thermally or by photo-induction [46]. Monoliths are formed *in-situ* and can be constructed to any shape or confined mould without the requirement for frits to retain the phase. Therefore, some of the problems associated with the manufacture of particle-based stationary phases are avoided, in particular that associated with the use of retaining frits, particularly in capillary column formats [46].

As a result of this high porosity, columns made of monolithic materials can be operated at high flow rates (up to 10 $mL.min^{-1}$ in conventional column formats) using conventional HPLC instruments without generating excessively high backpressures. Figure 1.6 shows a comparison of column backpressures at different flow rates obtained for a monolithic column and particle-based columns packed with 3.5 and 5 µm particles. Obviously, the backpressure obtained by the monolithic column is much lower than that for packed columns [13, 18]. Gaining this advantage, the separation of five β-blocking drugs has been carried out at different flow rates using a silica-based monolithic column (Chromolith Performance RP-18e, 100 mm × 4.6 mm). A baseline separation of the five drugs was achieved within one minute at a flow rate of 9 $mL.min^{-1}$ compared to 12 minutes when the flow rate was 1 $mL.min^{-1}$ without losing the efficiency [13, 18].

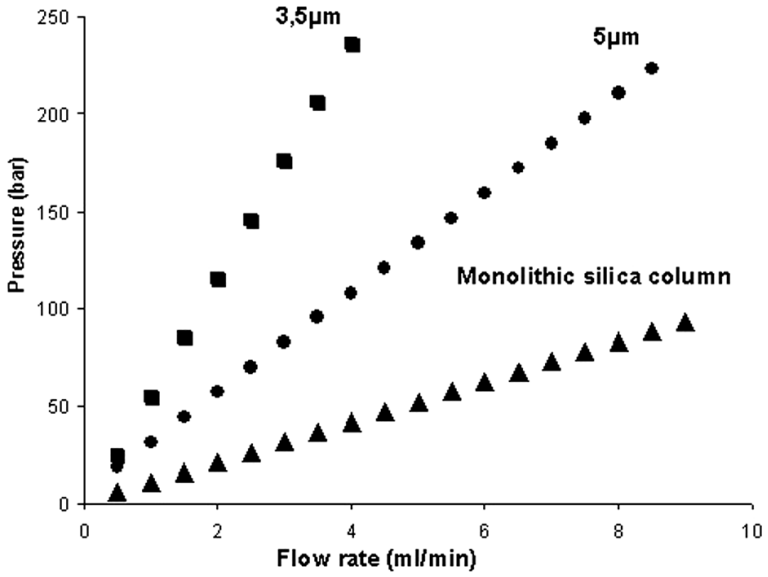

Figure 1.6: Comparison of back pressure in the monolithic and particle-based columns packed with 3.5 and 5 µm particles at different flow rates. Reproduced from [13].

Moreover, monolithic columns require a relatively short-time for column equilibration when a mobile phase gradient is used as well as the easy application of flow-rate gradients and the coupling of several columns together (L >1 m) in order to increase separation efficiency (N >100,000 theoretical plates). This property is important for some applications such as proteomics and metabolomics in which high peak capacity and separation efficiency is required [10, 49].

Furthermore, the structure of the monolithic materials differs from particle-based supports. Monolithic materials consist of continuous rods of interconnected channels totally filling the column. Therefore, all of the mobile phase must flow through the pores of the monoliths rather than around and between the particles in the packed columns due to the lack of interparticular voids in the column [50]. When the van Deemter plots of plate height versus mobile phase linear velocity for particle-based and monolithic columns are compared, one major difference is occurred, the contribution of C term. The contribution of the C term in the monolithic columns is much lower than that in particle-based columns even at high linear velocities. This is owing to

accelerated mass transfer as a result of convection [50]. Consequently, fast separations with high efficiency can be obtained with such materials [46]. Figure 1.7 shows the van Deemter curves for uracil on a particle-based packed with 5 µm particles and a monolithic column indicating that the monolithic column can afford operation at high flow rates without losing efficiency [51].

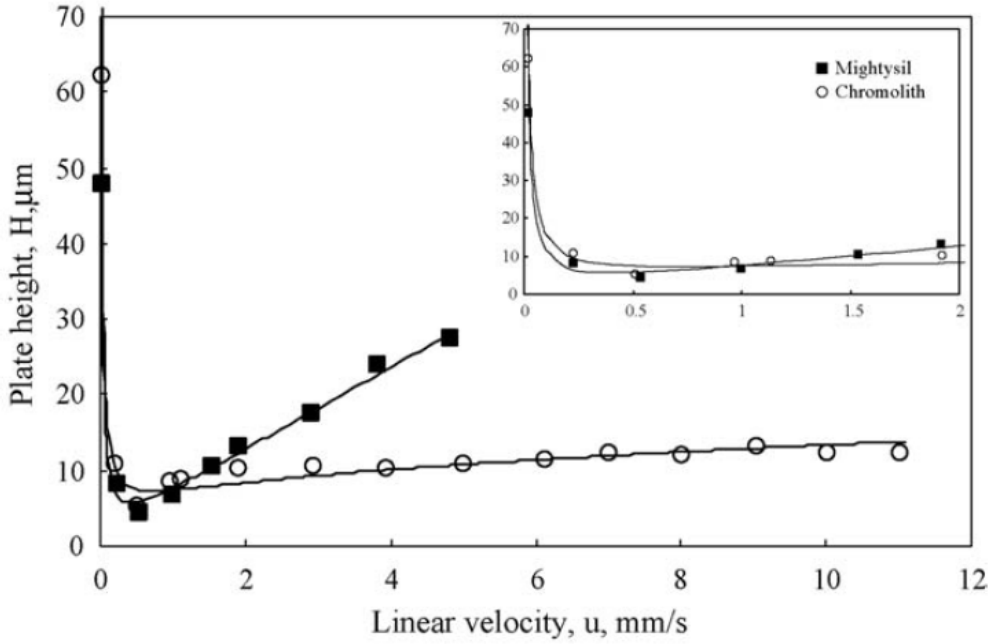

Figure 1.7: Van Deemter plots for uracil obtained for the monolithic (○) and conventional column packed with 5 µm particles (■). Reproduced from [51].

However, monolithic columns have several disadvantages that need to be mentioned which may reduce their applicability. In general, the commercially available monolithic columns do not have a wide range of surface chemistries. In addition, even though it is an advantage to run the monolithic columns (especially with large internal diameters) at high flow rates with low backpressures, this could be a disadvantage at the same time as it consumes large volumes of mobile phase and may not be fully compatible with mass spectrometry [18].

Moreover, silica-based monoliths, in particular, have restricted pH stability. They are only stable at the pH range from 2 to 8 because of the solubility of silica in alkaline solution [52]. Also, the significant shrinkage of the silica-based monoliths that occurs after the preparation of these materials restricts their *in-situ* preparation in typical analytical sizes. For example, if a 4.6 mm rod is desired, a 6 mm rod is prepared first, removed from the mould and then encased within a PEEK tube [13].

In contrast to silica-based monoliths, organic polymer monoliths suffer from significantly lower peak efficiencies in most cases, particularly for small molecules, probably due to the micropores in their structure which negatively affect the efficiency and peak symmetry [53].

1.2.3. Silica-based monolithic stationary phases

1.2.3.1. Introduction

The sol-gel technology, used for the preparation of porous silica-based monoliths, was first invented in the late 1800s [54, 55]. Later, in the early 1990s, a new sol-gel process was developed by Nakanishi and Soga for the production of such materials [35-37]. Based on that, in 1996, Tanaka *et al.* reported the first paper describing the preparation and the application of these materials in HPLC [27], in which they prepared the column based on the hydrolysis and polycondensation of tetramethoxysilane (TMOS) in the presence of water-soluble organic polymers, polyethylene oxide (PEO). The resulting silica monolith is shown in Figure 1.8. Then, the surface chemistry of the column was subsequently modified with C_{18} functionality and then the resulted column was compared with particle-based C_{18} columns packed with 5 μm silica particles. For the separation of alkylbenzenes, the silica-based monolithic column showed a slight tailing with 8000 theoretical plates produced compared to >10,000 produced by the particle-based column.

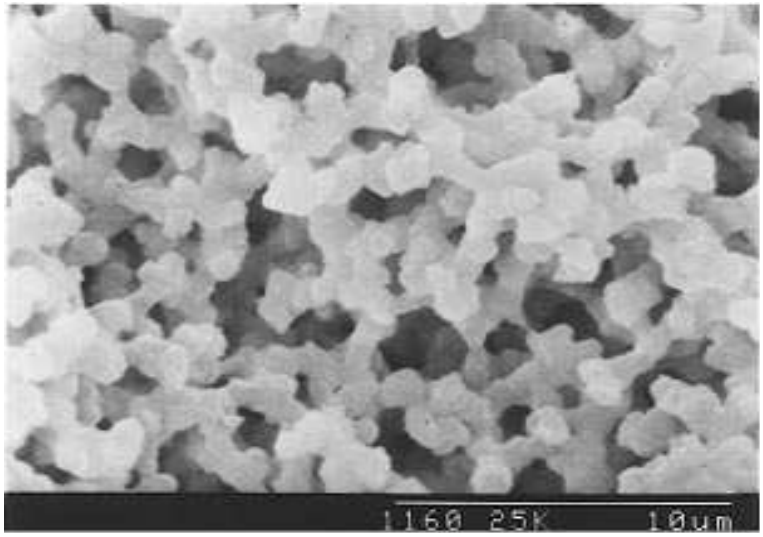

Figure 1.8: SEM image of a porous silica-based monolith. Reproduced from [27].

Simultaneously, an alternative way for the preparation of silica-based monoliths was reported by Fields based on xerogel [28]. The silica xerogel was prepared from a potassium silicate solution. After washing and purging, the surface of the resulting column was derivatised in a subsequent step using a solution of dimethyloctadecylchlorosilane. The column was analysed by scanning electron microscopy (SEM) and the image obtained showed the inhomogeneous continuous structure of the xerogel, which was chemically bonded to the fused silica wall via the surface silanols, as shown in Figure 1.9. For evaluation purposes, the column efficiency was studied using a test mixture consisting of ethyl benzoate and naphthalene with on-line UV detection. The results obtained showed the very low efficiency that the column possesses (5000 plates/m). The efficiency of the column could have been improved by fabricating more homogeneous structures with narrower pore size distributions, since the irregular structure of the stationary phase lead to a subsequent wide distribution of flow paths.

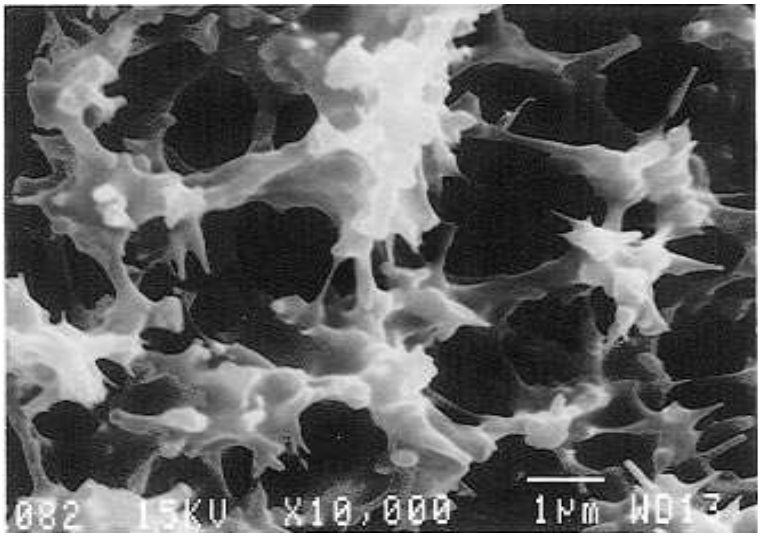

Figure 1.9: SEM image of silica xerogel column end. Reproduced from [28].

In 1998, Asiaie *et al.* [56] published a report describing a different method for preparing silica-based monoliths. The method was based on packing fused silica capillary with octadecylated (ODS) 6 μm particles as the first step. Then, the packed column was thermally treated to form a monolithic structure. In a final step, the column was reoctadecylated *in-situ* with dimethyloctadecylchlorosilane. The resulted monolithic structure is shown Figure 1.10. The column efficiency was evaluated utilising micro-HPLC and capillary electrochromatography (CEC) for the separation of small aromatic compounds. The efficiency of the sintered monolithic column was similar to the column freshly packed with the same particles.

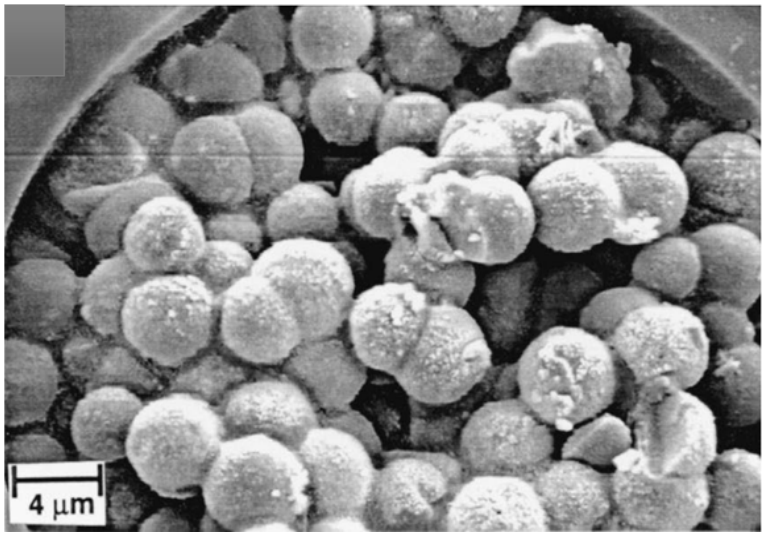

Figure 1.10: SEM image of packed fused silica capillary sintered at 360 ^{o}C with $NaHCO_3$ flux. Reproduced from [56].

The preparation of silica-based monoliths within the fused silica capillaries is relatively straightforward and does not suffer from the shrinkage that occurs after their preparation in conventional analytical sizes, due to attachment between the capillary wall and the monolithic bed. However, capillary columns cannot be operated using the conventional HPLC instrumentations, they require special instrumentation. Silica-based monoliths have become commercially available from Merck KGaA Company (Darmstadt, Germany) in 2000. Based on the work of Nakanishi and co-workers, the company has developed a proprietary technology for the preparation and cladding of 4.6 mm i.d. silica rods with a resistant PEEK polymer.

1.2.3.2. Properties of silica-based monoliths

The essential feature of the silica-based monolithic materials is their unique pore structure. Silica-based monoliths possess a bimodal pore structure which means that the monolithic bed has two kinds of pores; macropores (or through-pores) and mesopores [13]. The macropores size ranges from 1 to 8 µm and allows mobile phase flow through the monolithic

bed, whereas the mesopores on the surface of the macropores range from 10 to 400 nm [57-59]. However, silica-based monoliths with 2 µm macropores and 13 nm mesopores in size are the most widely used [13]. Figure 1.11 shows typical SEM images of the silica-based monolithic structure illustrating the porous structure and the macropores and mesopores. The size of the macropores and mesopores can be controlled independently by controlling the composition of the starting mixture or the concentration of the silanes, such as TMOS, during the preparation process [60]. The porosity of silica-based monoliths is much higher than that of particle-based columns [61]. The total porosity of the silica-based monoliths is about 85 %. This is about 15 - 20 % higher than that for particle-based columns packed with 5 µm particles [13] whereas the external porosity is 65 - 70 % for silica-based monoliths compared to 40 % for particle-based columns [62]. Conventional silica-based monolithic columns that are commercially available have an external porosity of 60 % and 85 % total porosity [27, 63].

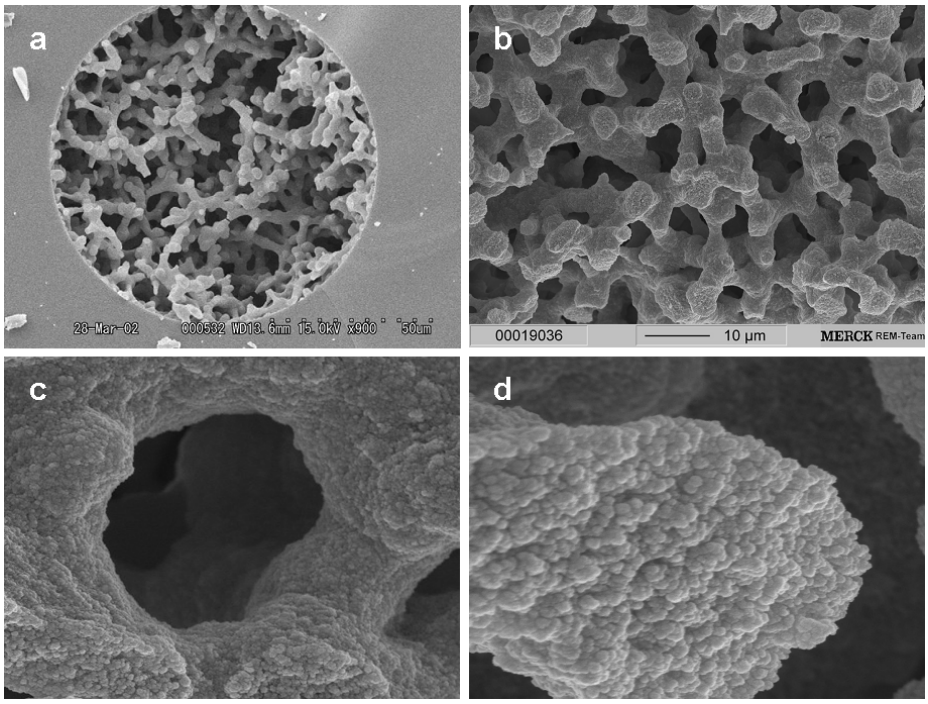

Figure 1.11: SEM images showing the typical porous structure of silica-based monolithic columns. Reproduced from [13].

As a result, the presence of the macropores and mesopores leads to a high permeability with high surface area providing good chromatographic efficiencies comparable to particle-based columns at low backpressures. The permeability of the silica-based monolithic columns has been found to be as much as 30 times higher than a particle-based column packed with 5 µm particles [64] and equivalent to a particle-based column backed with 11 µm particles [65]. Moreover, the column efficiency produced by the commercial silica-based monolith is similar to that produced by a column packed with 3.5 µm particles with a backpressure half of that caused by a column packed with 5 µm particles [13]. These features of the silica-based monoliths allow the coupling of several columns which in turn lead to an efficient separation of complex samples. For example, Cabrera *et al.* have coupled fourteen silica-based monolithic columns to give a total length of 1.4 m. The resulted series has been used for the separation of six alkylbenzenes. The separation was carried out a flow rate of 1 $mL.min^{-1}$ giving a backpressure of 11.7 MPa and plate number of 108,000 [66].

1.2.3.3. Preparation of silica-based monoliths

Silica-based monoliths are produced via sol-gel technology with phase separation. The preparation process mainly involves three reactions: (i) catalysed hydrolysis of an alkoxysilane, (ii) condensation of hydrated silica to form siloxane bonding, and (iii) polycondensation of the linkage of an additional silanol group to form cyclic oligomers as shown in Figure 1.12. [54, 55]. The structure properties of the silica-based monoliths depend on different factors that can be tuned to produce a monolith with desired properties. These factors involve the nature and concentrations of the starting reagents, the nature of the catalyst, pH, temperature, reaction time and the rate of hydrolysis and condensation [54, 55]. The reaction mixture contains silica precursors as starting reagents distributed in a solvent in the presence of water-soluble polymers such as polyethyleneglycols (PEG). The silica precursors are normally alkoxides and the most widely used are

alkoxysilanes such as tetraethoxysilane (TEOS) or TMOS [20, 54, 55, 67]. The average macropores size and skeleton can be controlled by the PEG/silica ratio as this ratio determines the phase separation tendency [60]. The morphology of the monolith is influenced by the additive molecular weight; the larger the additive, the larger the throughpores and mesopores [68]. After the synthesis of the monolith, its surface can be tailored in the ageing step which deals with the enlargement of the mesopores utilising a process called Ostwald Ripening [67].

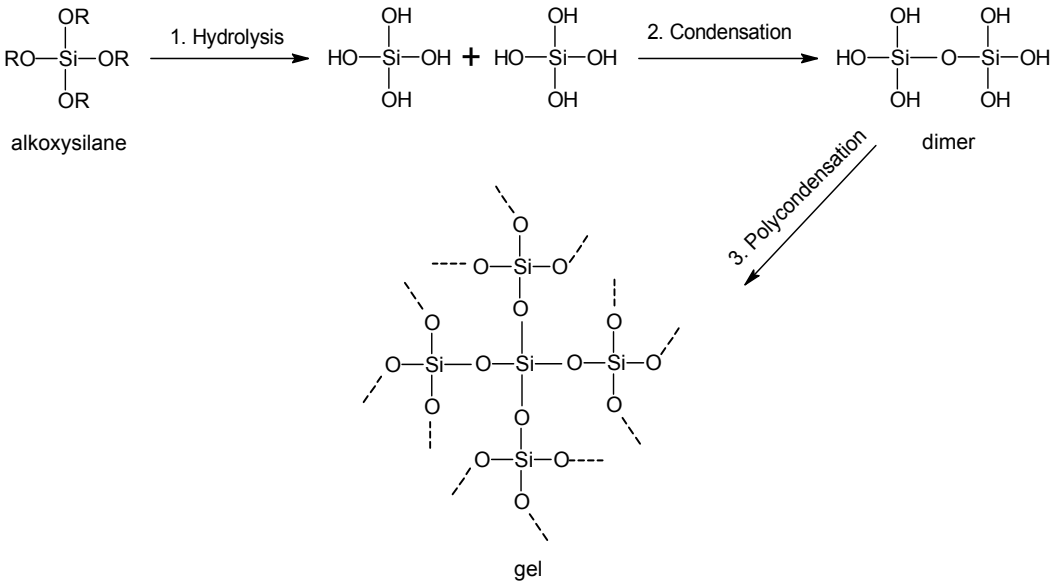

Figure 1.12: Schematic reaction showing typical sol-gel reaction. Adapted from [54].

1.2.4. Organic polymer-based monolithic stationary phases

1.2.4.1. Introduction

In the late 1960s, Kubín *et al.* produced a highly swollen continuous polymeric matrix for chromatographic separations in size-exclusion mode using a redox free-radical initiating system [31]. The fabrication process involves placing 100 mL of the polymerisation mixture that consisted of 22 % aqueous solution of 2-hydroxyethylmethacrylate which contained 0.2 %

ethylene dimethacrylate in a 25 mm i.d. glass tube for 24 h at room temperature [69]. The resulting column was used for the separation of water-soluble polymers. Unfortunately, the permeability of the column was very poor and efficiency was too low for really useful practical separations [21, 41]. In the early 1970s, more permeable open-pore polyurethane foams were developed. They were prepared *in-situ* in large chromatographic columns allowing the separation of small analytes [70-73]. However, none of these early efforts were progressed at the time and the interest in monolithic phases faded for almost two decades [21, 41].

In 1989, Hjertén *et al.* [25, 74] published a report for the first time describing a preparation of highly swollen crosslinked continuous beds by polymerising a dilute solution of *N*,*N*'-methylenebisacrylamide and acrylic acid in the presence of ammonium sulfate. The next step was compression of the resulting polymer to about 17 % of its original length within the confines of a chromatographic column. The compressed bed completely filled the cross section of the column and allowed high flow rates due to its very good permeability. The resulting column was successfully applied to the fast ion-exchange separation of a mixture of proteins (Figure 1.13).

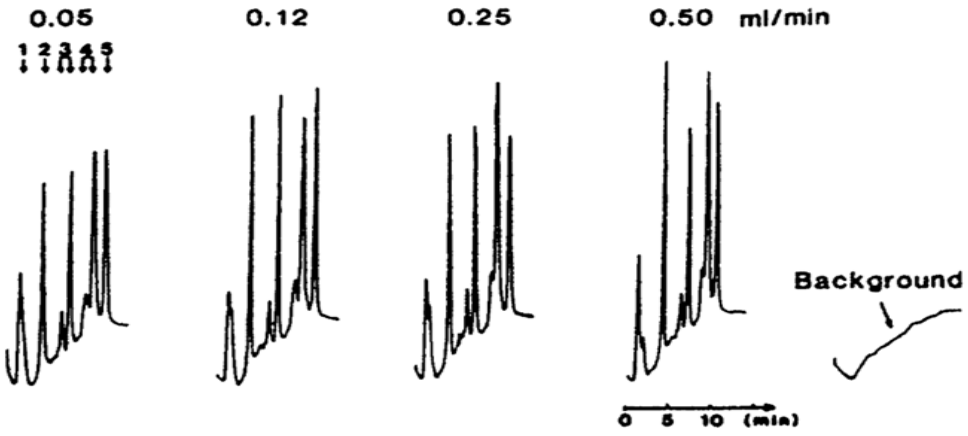

Figure 1.13: HPLC chromatograms of model proteins in cation-exchange mode using compressed continuous gel at different indicated flow rates. Conditions: gel plug 3 × 0.6 cm, linear gradient from 0.01 mol.L^{-1} sodium phosphate buffer pH 6.4 to 0.25 mol.L^{-1} sodium chloride in the buffer, gradient volume 5 mL. Peaks: alcohol dehydrogenase (**1**), horse skeletal myoglobin (**2**), whale myoglobin (**3**), ribonuclease (**4**), and cytochrome c (**5**). Reproduced from [25].

This work was followed by another approach published by Svec and Fréchet in 1992 describing the manufacture of macroporous methacrylate-based monolithic columns for the first time. In their work, the monolith was polymerised *in-situ* in a 30 mm × 8 mm i.d. stainless steel column. The column was filled with the polymerisation mixture consisting of glycidyl methacrylate (GMA) and ethylene glycol dimethacrylate, as monomer and crosslinker, respectively, cyclohexanol and dodecanol as porogens and azobisisobutyronitrile (AIBN) as initiator. The polymerisation was carried out thermally at 70 ^{o}C for 6 hours. The epoxide groups of the GMA were functionalised and the resulting column was applied to the separation of a mixture of proteins in an ion-exchange mode [26]. Even though the chromatogram showed a relatively long run time (~ 35 minutes) as shown in Figure 1.14, it indicated the applicability of such materials as stationary phases for high-performance chromatographic separations and opened the window to the subsequent development of the monolithic materials.

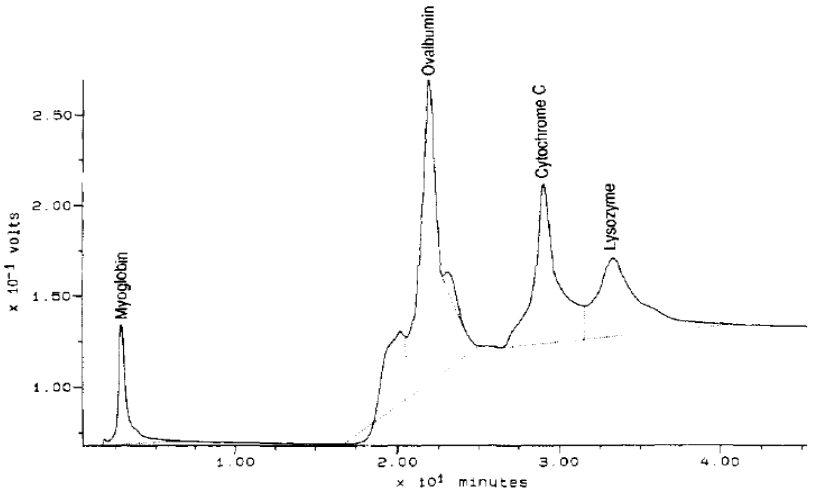

Figure 1.14: Ion-exchange chromatograph of model protein mixture in the porous polymer rod column. Conditions: column 30 × 8 mm i.d., poly(glycidyl methacrylate-co -ethylene dimethacrylate) modified with (diethylamino)hydroxypropyl groups. Mobile phase: 10 min 0.01 mol.L^{-1} Tris-HCI buffer solution at pH 7.6, followed by 10 min gradient of the same buffer from 0 to 7 mol.L^{-1} NaCI, flow rate 0.5 mL.min^{-1}, UV detection: 218 nm, injection 2 pL of a solution containing total 16 mg.mL^{-1} proteins. Reproduced from [26].

1.2.4.2. Preparation of polymer-based monoliths

In comparison to silica-based monoliths, the fabrication of organic polymer-based monoliths by a "moulding" process is simple and relatively-straightforward [75, 76]. The fabrication is achieved by employing a one-step polymerisation approach in which the following components are required: functional monomers (with one or more double bonds) and crosslinkers (with two or more double bonds) to form the monolith skeleton and determine the polarity of the final monolith, porogenic solvents to determine the pores size and distribution, and an initiator to initiate the polymerisation. These components are mixed together in an appropriate ratio, sonicated and deoxygenated with nitrogen [21, 43, 77, 78]. The structural properties of the monoliths can be influenced by different factors such as the polymerisation conditions, e.g. the polymerisation temperature, the content of the crosslinkers, the thermodynamic quality of the porogenic solvents [24, 79, 80].

The fabrication of the organic polymer-based monolithic columns follows the simple scheme illustrated in Figure 1.15. The mould is sealed at one end, filled with the oxygen-free polymerisation mixture and sealed at the other end afterwards. The polymerisation is then initiated. When the polymerisation is finished, the seals are removed and replaced with fittings and then the column is attached to a pump for washing the monolithic column with copious amounts of organic solvent to remove the porogenic solvents and any other unreacted components from the pores of the monolithic column [50, 69]. The mould used for the preparation of the organic polymer-based monolith is typically a tube. A wide range of tube sizes and materials have been used as moulds, such as stainless steel, PEEK, and glass tubes [81-84]. Apart from tubes, polymer-based monoliths could be also prepared in different mould shapes, such as microfluidic chips, syringes, pipette-tips, etc. The preparation of cylindrical monoliths with a homogeneous porous structure and diameter up to about 10 - 25 mm is readily achieved in a single-step polymerisation, whereas larger sizes are

more difficult to prepare [76]. The mould may require a proper pretreatment for its inner-wall for subsequent attachment between the mould and the monolithic bed. This step is crucial to stabilise the monolithic bed inside the mould and to prevent the mobile phase from bypassing the bed and to force it to flow through the monolithic bed. For example, a fused silica capillary surface is first treated with 3-(trimethoxysilyl)propyl methacrylate (TMSPM) before the polymerisation takes place. The reaction between the methoxy groups in TMSPM and silanol groups on the fused silica capillary results in the successful attachment of the ethylene moieties to the capillary inner-wall which participate in the attachment between the monolithic bed and the inner-wall of the capillary afterwards [20, 43].

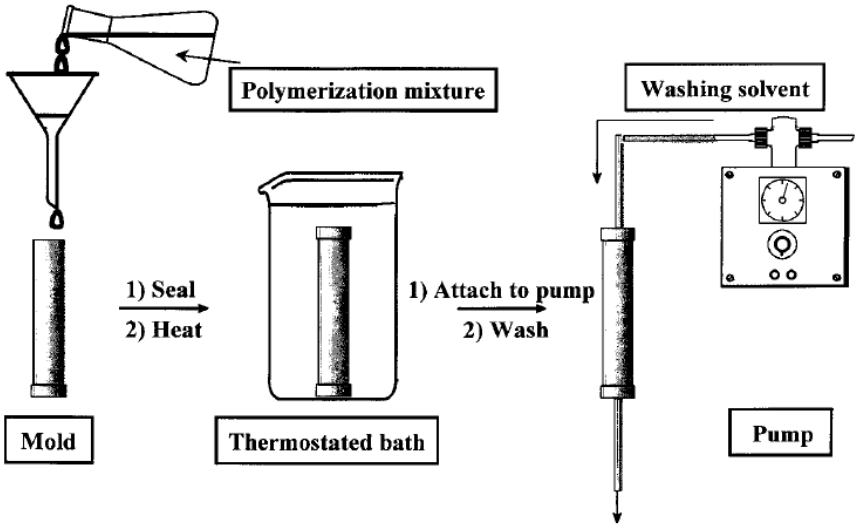

Figure 1.15: Schematic of preparation of macroporous polymer monoliths using "moulding" process. Reproduced from [69].

The mechanism of the monolith formation is as follows. First, the polymerisation is initiated by the decomposition of the initiator forming a free radical. During the polymerisation, the solubility of the polymer chains in the reaction mixture decreases as they grow. Then the polymer chains precipitate to form nuclei. The monomers are thermodynamically better

solvents for the nuclei than the porogens which result in the nuclei being swollen with the monomers. As the polymerisation continues to proceed, the nuclei size increases leading to form microglobules which then cross-link among each other to form the final morphological structure of the monolith, whereas the macropores are filled with the porogens which determine the volume of the macropores [22].

The formation of polymer-based monoliths utilising free-radical polymerisation can be initiated by a number of means such as heating, UV radiation, gamma rays and chemical agents. Thermal-initiation is the most common way for starting the polymerisation. The temperature has to be controlled carefully to obtain monoliths with reproducible and uniform porous structure due to the significant influence of temperature on the growth rate of nuclei. The initiator decomposition and the rate of propagation are faster at high temperatures leading to increase the number of growing nuclei and thus small pore size is obtained. In addition, faster polymerisation may lead to less uniform porous structure. Therefore, lower temperatures are preferred. However, this can be limited by the decomposition temperature of some initiators [22, 85]. The structural properties of the polymer-based monoliths can also be affected by changing the initiators. For example, the decomposition temperatures of di-nitrile or azo initiators such as AIBN are between 60 and 80 ^{o}C. Monoliths with larger pores were obtained when the polymerisation was initiated by di-benzoyl peroxide which decomposes at temperatures of 60 – 140 ^{o}C due to the slower decomposition rate of the initiator [86]. The replacement of AIBN by 2,2'-azobis(2,4-dimethyl)valeronitrile (ADVN) results in a decrease in population of smaller pores which led to a decrease in the total surface area. [87]. Polymerisation can also be initiated utilising UV radiation, which is recommended for the preparation of homogeneous monoliths [88, 89]. UV-initiated polymerisation is usually carried out at room temperature and thus, in contrast to thermal-initiation, volatile solvents with low boiling points can be used as porogens [22]. Moreover, the monolith can be synthesised in a very short time; usually

within few minutes. UV-initiated polymerisation is mostly affected, and thus the structural properties of the monoliths, by the light intensity as well as the nature and the concentration of the initiator [22]. However, UV-initiated polymerisation is limited to UV-transparent monomers and porogenic solvents; and moulds such as fused silica capillaries and UV-transparent microfluidic chips [88-91]. In addition to the above initiation means, gamma radiation is another option for initiating the polymerisation but it is less common than them as it requires strict safety measures [22, 78]. Gamma-initiation has the advantage of direct generation of free radicals from the monomers, without the addition of initiators, which results in a cross-linked product [22, 92-94]. The structural properties of the monoliths are controlled by varying the dose rate. Increasing the dose rate leads to increase the rate of free radical formation and thus accelerates the polymerisation and the crosslinking, which results in monoliths with larger pores [22]. The optimum doses are ranged from 20 to 40 kGy, whereas the optimum dose rates are between 10 and 16 kGy/h [92]. Polymerisation initiation using chemical agents at room temperature is the oldest way [78]. A number of chemical agents have been used for monoliths preparation. For example, ammonium peroxodisulfate with *N*,*N*,*N*',*N*'-tetramethylethylenediamine catalyst has been used for the preparation of poly(butyl methacrylate) [95].

1.2.4.3. Control of surface chemistry

Several methods have been reported for the preparation of organic polymer-based monoliths with a wide variety of surface chemistries in which the application of such materials as chromatographic stationary phases depend on. For example, in reversed-phase mode chromatography, monoliths with hydrophobic moieties are used, while for the separation in ion-exchange mode, ionisable groups must be present on the surface of the monoliths, etc. The desired surface chemistry can be obtained by including the functional monomers in the polymerisation mixture, chemically modifying or photografting the surface of the preformed monoliths.

A) Preparation from functional monomers.

A large variety of surface chemistries can be directly obtained for polymer-based monoliths, due to the large selection of available monomers that can be used for the preparation of such materials. The preparation of a monolith with a desired surface chemistry by inclusion of functional monomers that have the desired chemistry in the polymerisation mixture (i.e. direct copolymerisation) is the most convenient and simple way [21, 22]. Almost any monomer, including water-soluble hydrophilic monomers, can be used in the polymerisation mixture to form a monolith [39]. However, the polymerisation conditions optimised for preparation of a monolith cannot be transferred directly to another one without additional re-optimisation. Thus, the use of new monomer mixtures requires re-optimising the polymerisation conditions to obtain satisfactory permeability of the new resulting monolith [96]. A wide range of monomers and crosslinkers has been used for the preparation of polymer-based monoliths and examples are shown in Figure 1.16. The list of monomers includes a variety of surface functionalities varying from very hydrophilic acrylamide (**8**) and 2-acrylamido-2-methyl-1-propanesulfonic acid (**6**) (AMPS), through reactive monomers such as GMA (**5**), chloromethylstyrene (**2**), 2-vinyl-4,4-dimethylazlactone (**7**) (VAL) and protected functionalities 4-acetoxystyrene (**3**), to rather hydrophobic styrene (**1**) (ST) and butyl methacrylate (**4**) (BuMA), and even zwitterionic (**9**) (N,N-dimethyl-N-methacryloyloxyethyl-N-(3-sulfopropyl)ammonium betaine). The examples of crosslinkers showed in Figure 1.16 include divinylbenzene (DVB) (**10**), *N,N'*-methylenebisacrylamide (**11**), ethylene dimethacrylate (EDMA) (**12**), and trimethylolpropane trimethacrylate (**13**) [50].

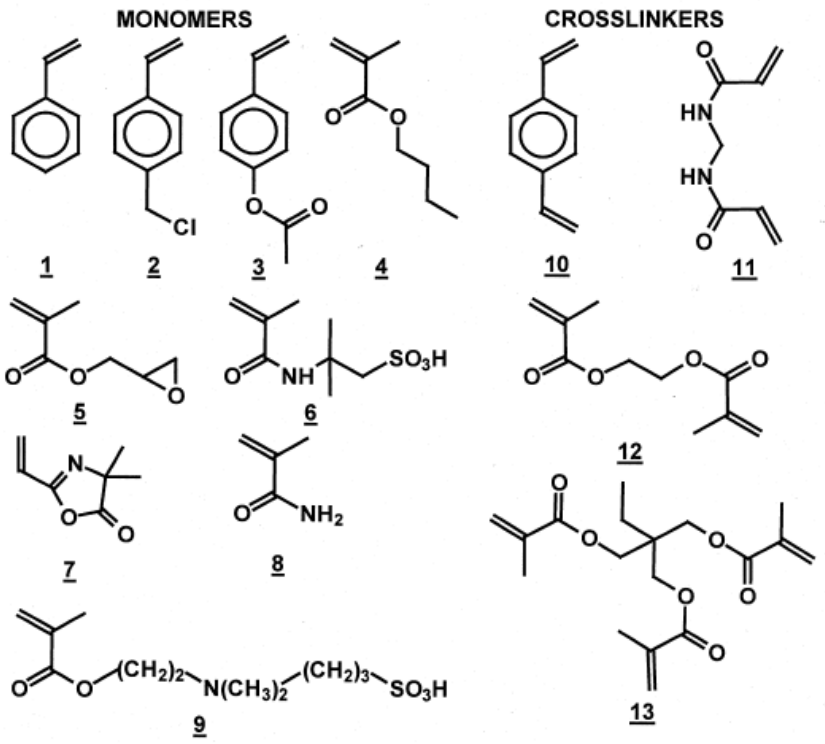

Figure 1.16: Examples of monomers used for the preparation of rigid porous polymer monolithic columns. Reproduced from [50].

Polymethacrylate-based monoliths are materials exhibiting medium polarity, as they contain carboxyl groups, and a hydrophobic framework as shown in Figure 1.17 [43]. The production of such materials can be readily achieved by polymerising a mixture consisting of methacrylate esters as a monomer and EDMA as a crosslinking agent. The monomers used for the production of methacrylate-based monoliths include BuMA, 2-hydroxyethyl methacrylate, GMA and other methacrylate esters [55]. Among them, GMA is often used as a monomer in the polymerisation mixture since it contains reactive epoxide groups which lead to readily subsequent surface modification for numerous applications, such as the extraction of neutral compounds [97] and peptides [98, 99]. The solvents used as porogens include toluene, cyclohexanol, dodecanol, propanol, methanol or acetonitrile. The polymerisation is usually initiated by AIBN, which is activated by heat or UV light. [55, 80, 100, 101].

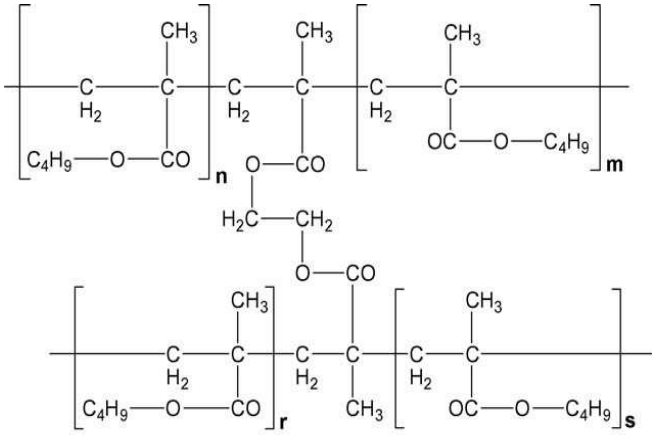

Figure 1.17: Chemical structure of a medium polar poly(butyl methacrylate) monolith. Reproduced from [78].

Polystyrene-based monoliths, as shown in Figure 1.18, are strongly hydrophobic materials. They are prepared by polymerising a mixture consisting of ST or its derivatives, such as 4-(chloromethyl)styrene as monomers and DVB as a crosslinking agent. The polymerisation is carried out in the presence of a diluent which acts as the pore forming agent. It can be a solvent, a nonsolvent or a linear polymer. In the case of a solvating diluent, macroporous monoliths are only produced when the concentration of DVB is high and the monomer concentration is diluted. Whereas in the case of nonsolvating diluent, the macroporous monoliths are formed at lower concentrations of DVB and with less diluted monomers [55]. Since the polystyrene-based monoliths are hydrophobic, they can be used directly in reversed-phase chromatography. However, by using 4-(chloromethyl)styrene as a monomer, reactive groups are obtained for further derivatisation. For example, the poly(chloromethyl)styrene monolith surface has been modified utilising the two-step strategy. It was first reacted with ethylenediamine and then reacted with γ-gluconolactone and chloroacetic acid to produce highly hydrophilic and weak cation-exchange surfaces respectively [102, 103].

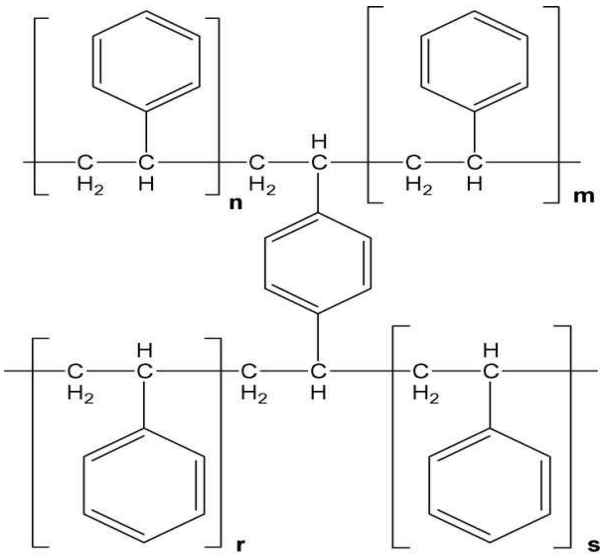

Figure 1.18: Chemical structure of a strongly hydrophobic polystyrene monolith. Reproduced from [78].

Polyacrylamide-based monoliths are highly polar materials with a hydrophilic framework as shown in Figure 1.19. They are prepared by polymerising a mixture including acrylamide or its derivatives as a monomer and *N*,*N*'-methylenebisacrylamide as a crosslinker [25, 104, 105]. The monomers involved in the polymerisation mixture are often acrylamide, piperazine diacrylamide, methacrylamide in the presence of dimethyl sulfoxide (DMSO) and dodecanol as the porogens. In addition, either AMPS or vinylsulfonic acid could be added to the polymerisation mixture for the production of a charged surface, while other monomers such as stearoyl methacrylate or BuMA are used to provide a surface suited to hydrophobic interaction chromatography [55]. The polymerisation reaction is initiated by a catalyst-initiator system of *N*,*N*,*N*',*N*'-tetramethylethylenediamine (TEMED) for the breakdown of ammonium sulfate to form persulfate radicals. The polymerisation is usually carried out overnight at room temperature since it is not thermally-initiated [55]. Polyacrylamide-based monoliths have been used for the extraction of phenols and other acidic species [106-108] as well as in the preparation of molecularly imprinted polymer (MIP) extraction devices [109, 110].

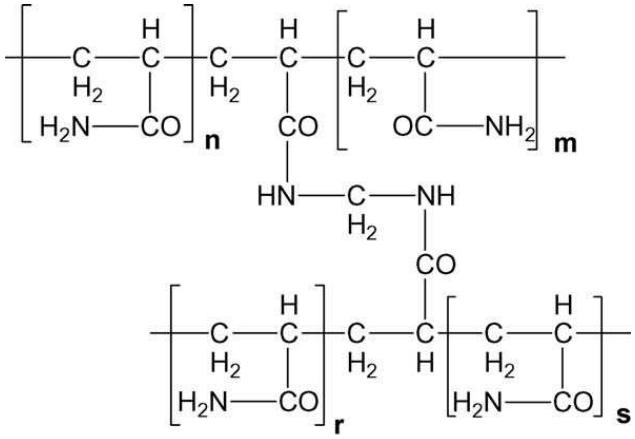

Figure 1.19: Chemical structure of a highly polar polyacrylamide monolith. Reproduced from [78].

B) Chemical modification of the monolith surface.

Chemical modification is another approach that allows the introduction of various functionalities while preserving the original porous structure of the monolithic materials. It increases the number of available chemistries providing stationary phases for various separation modes. The surface modification is readily performed using monoliths prepared from monomers containing reactive groups [21, 39, 50]. For example, GMA is a very popular functional monomer used for monolith preparation. Because of the presence of epoxide groups, it can be readily derivatised for extensive applications [43]. Typically, the pores of the monolith containing reactive groups are filled with the reagent and allowed to react under certain conditions. Then, once the reaction is completed, the monolith is rinsed with a solvent to remove all unreacted components [39]. Examples of chemical surface modifications are shown in Figure 1.20 in which the GMA monolith is treated with diethylamine to obtain a monolith for anion exchange separations [26], while the poly(chloromethylstyrene-*co*-DVB) polarity is converted from hydrophobic to hydrophilic by its treatment with ethylenediamine and then with γ-gluconolactone. [102].

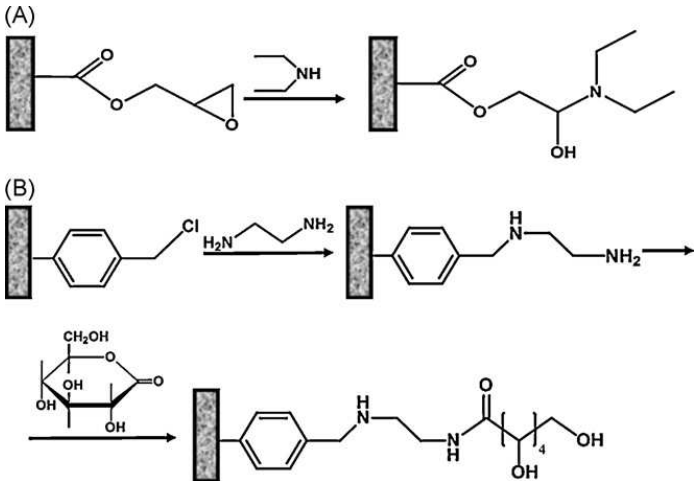

Figure 1.20: Examples of modification of typical porous polymer monoliths containing GMA (A) and chloromethylstyrene (B) units. Reproduced from [39].

C) Grafting the monolith surface.

Grafting can also be utilised to modify the monolith surface chemistry leading to new functional groups without changing the original pore size of monolith morphology. However, in contrast to chemical modification, grafting may produce multiple functionalities by attaching chains of functional polymer to each surface site of the pores rather than introducing only a single functionality at each individual surface site, obtained by chemical modification as illustrated in Figure 1.21. Thus, the sorption capacity of the monolith is significantly increased [22, 39, 50, 111].

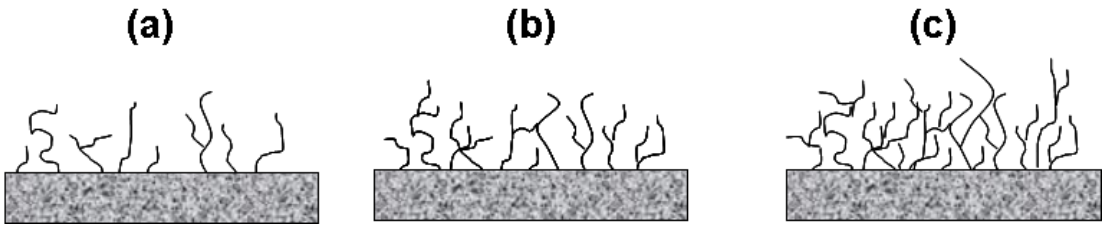

Figure 1.21: Schematic representation of the growing polymer chains during photografting with increasing irradiation time from (a) to (c). Adapted from [90].

Photografting is a photoinitiated method utilised for polymer surface modification using UV irradiation, hydrogen abstracting photoinitiators and reactive vinyl monomers [112]. The desired functionality is introduced in the monolith pore surface by the photoinitiated grafting of suitable polymer chains as shown in Figure 1.22, which can be obtained within a very short period of time [90, 113, 114]. Upon photoexcitation, the photoactive component (e.g. benzophenone (BP)) abstracts hydrogen atoms from the polymer surface and forms free radicals. The resulting surface radicals then initiate surface graft polymerisation [115]. The resulting polymer chains grafted to the surface also contain abstractable hydrogen atoms which also can be a base for new chains to grow, ultimately leading to a branched polymer architecture [39].

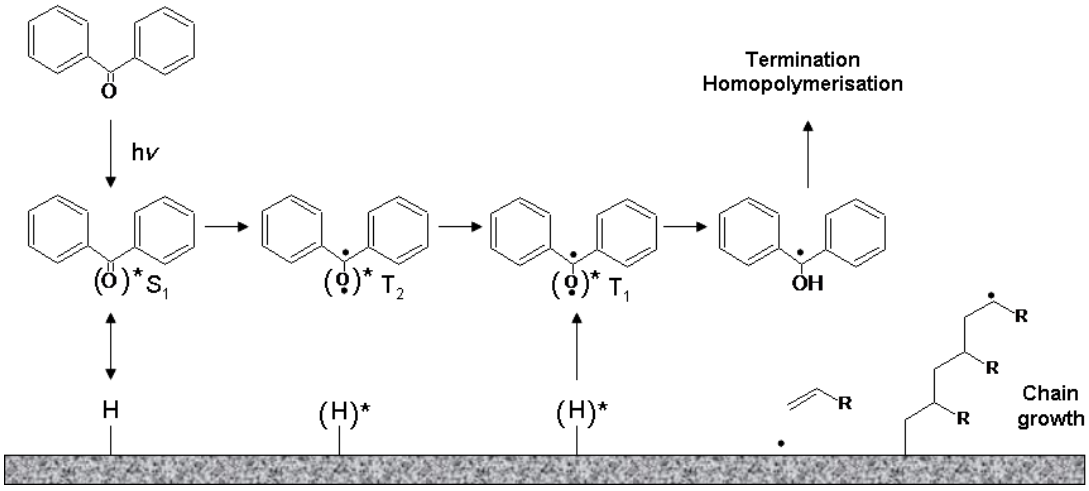

Figure 1.22: Schematic picture of surface grafting onto a substrate with BP and a vinyl monomer, irradiated with UV light. Adapted from [114].

In addition, one of the advantages of UV-initiated grafting is that the location of grafts can be precisely controlled using photomasks which allows the discrete modification of zones within the monolithic rod. This is in contrast with using the chemical modification method in which the entire surface of the monolith is exposed to modification [115]. Rohr *et al.* grafted

distinct areas of the surface of a butyl methacrylate/ethylene glycol dimethacrylate-based monolith with chains of VAL through a mask. VAL amine-reactive groups were labeled with a fluorescent dye, Rhodamine 6G, by reaction with its secondary amine groups. The resulted labeled monolith was visualised by an optical fluorescence microscope and the images in Figure 1.23 show the fluorescent areas (bright spots) [90].

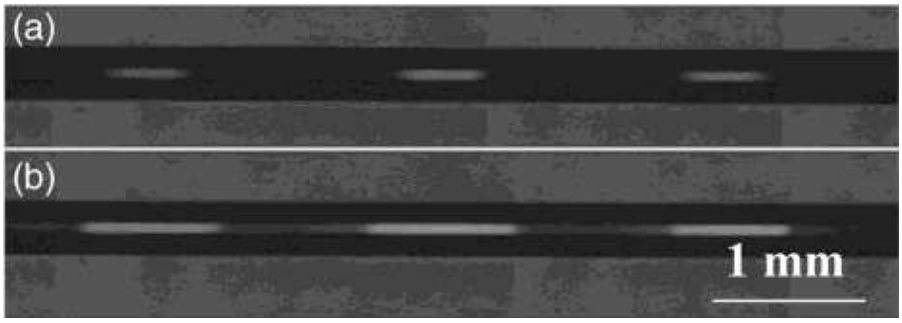

Figure 1.23: Fluorescence microscope image of porous poly-(BuMA-*co*-EDMA) monolith in a 50 µm capillary photografted through a mask with polyVAL chains for 1 (a) and 3 minutes (b) and subsequently reacted with Rhodamine 6G. Reproduced from [90].

1.3. Monolithic solid phase extraction in a pipette-tip format (SPE-PT)

In most cases, biological samples are not compatible with direct analysis utilising HPLC, capillary electrophoresis (CE), mass spectrometry (MS), etc., as such samples are very complex and may contain proteins, salts, acids, bases and other organic compounds with similar properties to the target analytes [116, 117]. Therefore, a pretreatment step is crucial prior to analysis in order to reduce the complexity of such samples. The demand for this is even more when the concentration of the target analyte in the sample is low and close to the detection limit of the analytical instrumentation, or when the detection sensitivity is influenced by the matrix of the sample, as typical in MS [118]. A selective sample preparation step is the front-end and often the key for successful subsequent analysis steps. Thus, the most effort

and a significant amount of time are given to this step. It typically takes about 80 % of the total analysis time [18, 116]. Depending on the desired task, sample preparation, in general, includes (i) concentration of the target analyte to adequate levels for measurement, (ii) removal of interfering-compounds of the sample matrix from the target analyte as the presence of such compounds could complicate or inhibit analysis, and (iii) exchanging the solvent or buffer that the target analyte is dissolved in to be compatible with the analytical method [119]. The sample preparation technique can be considered successful if the following features are obtained: (i) low sample loss (i.e. high recovery), (ii) complete removal of coexisting components, (iii) convenient and fast sample treatment, and (iv) low-cost analysis [116, 117].

Ultra-centrifugation, liquid–liquid extraction (LLE) and solid phase extraction (SPE) are the most common techniques that have been employed for sample preparation [18, 119]. Ultra-centrifugation is used to remove proteins from the biological samples. In contrast, LLE and SPE are useful techniques regularly employed for efficient sample clean-up based on partition or adsorption of the target analytes. These techniques are efficient and reliable for extracting the majority of pharmaceutical compounds from sample matrices and can produce clean extracts for subsequent analysis [116, 117]. Traditional LLE, however, suffers from a number of limitations. Specifically, difficulties in choosing a non-miscible solvent for polar and ionic compound extraction from water. The need for large volumes of organic solvents also results in a dilute extract [116].

SPE, among others, is a simple, effective and versatile sample preparation technique that plays a crucial role in the analysis of biological matrices [120-122]. This is due to high analyte recovery, short extraction time, ease of operation, high enrichment factor and low consumption of organic solvents, together with ease of automation [123, 124]. It is a powerful tool applicable for purification, desalting, preconcentration and selective capturing prior to introducing the sample to advanced analytical techniques. [43, 119, 125].

SPE first appeared in the late 1970s to avoid the use of environmentally unfriendly chlorinated solvents in LLE techniques. It has gained increased importance as a sample preparation technique utilised for reducing sample complexity, and has gradually replaced the position of LLE as the preferred sample preparation technique for biological samples [126-128]. SPE is defined as "a method of sample preparation that concentrates and purifies analytes from solution by sorption onto a disposable solid-phase cartridge, followed by elution of the analyte with solvent appropriate for instrumental analysis" [121]. Therefore, the extraction of the target analytes is based on partitioning between two phases: a liquid phase (the sample) and a solid phase (the extraction bed). The sample solution is passed through the solid phase and the analyte of interest is retained and then eluted with another solvent. The analyte of interest must have greater affinity for the solid phase than for the sample matrix to be retained, which may involve polar, non-polar or ionic interactions with a wide range of solid phase chemistries that can be used for the extraction of various compounds from aqueous or organic matrices [18, 116]. The key factor in optimising an extraction method for the target analyte is choosing the solid phase in which the extraction is going to take place on. The choice depends on the analyte and its properties and the sample matrix [18, 116].

The most popular format of SPE is a 1 – 6 mL open syringe-barrel or cartridge type containing a sorbent between frits. It is typically filled with 40 – 60 µm packing materials [119, 128, 129]. The first SPE devices were made of stainless steel packed with porous poly(ST-*co*-DVB) beads and used as pre-columns. These expensive columns were then replaced with disposable column-like containers manufactured from polyethylene or polypropylene [127].

However, one of the recent trends in sample preparation method development is the use of miniaturised extraction devices. Miniaturisation is driven by the limited availability of valuable samples, the requirement of fast and simple handling of small volumes (1 – 100 µL), and the need to

minimise sample dilution in the elution step. Therefore, studies have recently focused on the development of methods that reduce the sample volumes required for analysis, the analysis time, the organic solvent consumption or even elimination of chlorinated solvents [18, 117, 119]. Solid phase microextraction (SPME) is a successful miniaturised extraction technique that requires low sample and solvent volume, is simple and easily automated [43]. It was invented by Pawliszyn in the early 1990s as a one-step, simple, time-efficient and solvent-free sample preparation technique. The extraction is based on the partitioning of the target analyte between the sample matrix and a solid phase coating on a fused silica fibre and attached to a modified microsyringe [130-132]. This invention was a significant step towards the development of miniaturised sample preparation techniques and since then various miniaturised techniques such as chip-based microextraction [133], stir-bar-sorptive extraction (SBSE) [134], microextraction in a packed syringe (MEPS) [135], microextraction based on a monolithic spin column [136] have been described.

Solid phase extraction in a pipette-tip (SPE-PT), in particular, is another approach towards miniaturisation which was introduced in the late 1990s [129]. It is a simple and rapid method that has recently gained increased attention as a sample preparation tool within the field of bioanalytical chemistry and utilised for purification, desalting, preconcentration and selective capturing prior to introducing the sample to the advanced analytical techniques [137-139]. SPE-PT is an off-line sample pretreatment tool that can be utilised for processing one or several samples simultaneously either manually using multi-channel hand-held pipettors or automatically using commercially available robotic liquid handling systems [117]. Moreover, the operation process of this microextraction device is based on bi-directional flow in which the handling of the samples includes repeated smooth aspiration/desorption cycles [43, 140]. The extraction procedure is simple and easy as there is no special equipment required. As illustrated in Figure 1.24, the extraction sorbent is conditioned first and then

the sample solution is withdrawn through the sorbent and the analyte is adsorbed. Following that, the sorbent is washed and the analyte is eluted with a suitable organic solvent [141, 142]. The technique has several advantages, including the ease of use, faster extraction time, small sample and solvent consumption, low operating costs and inexpensive and disposable usage compared to conventional SPE [43, 128, 129, 143].

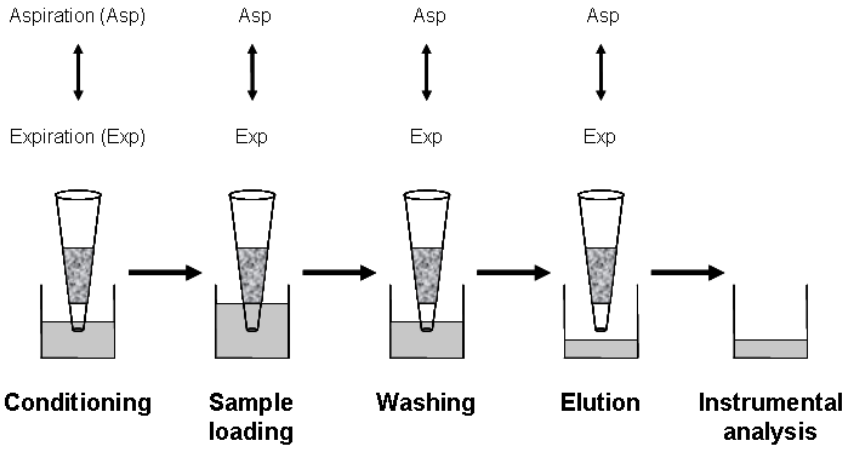

Figure 1.24: Extraction procedures for SPE-PT. Adapted from [142].

An SPE-PT device contains a chromatographic sorbent (solid phase), in which the extraction takes place, positioned at the bottom-end of a pipette-tip. The chromatographic materials used for the preparation of these devices are required to be (i) amenable to fluidic flow, which means low backpressure is produced, (ii) physically stable at the bottom-end of the pipette-tip, so no dead volume at the end of the tip or void between the solid phase and the wall of the tip is produced, (iii) able to eliminate any possible interference or carry-over that could arise as these devices are single-use, and (iv) available in different surface functionalities such as reversed-phase, ion exchange, immobilised metal affinity chromatography (IMAC), etc., in order to be applicable to as wide range of sample matrices as possible [117, 128].

Among other sorbents, silica particles or silica-based and organic polymer-based monoliths are the most common chromatographic materials used for the fabrication of the SPE-PT devices. Regarding the fabrication of SPE-PT packed with silica beads, the key concerns associated with such devices are how the beads are going to be retained in the packing mold, how easy and reproducible is the packing procedure, and the robustness of the packed column, etc. [118, 144]. Packed SPE-PT devices have been reported before for the enrichment, purification, desalting and fractionation of different biological samples using either home-made or commercially available tips. Several reports have been published on packing a bottom-end squeezed GELoader tip (Eppendorf, Hamburg, Germany) with a slurry of chromatographic media (Figure 1.25) [139, 145-150]. The bottom-end of the tip was carefully squeezed using a pair of flat pliers to reduce the inner diameter of the lower end of the tip. This modification is necessary to prevent leakage of the chromatographic media, but still allows the passage of solvent. Then the modified tips were filled with a suspension of different chromatographic media for various purposes. For example, the tip was packed with reversed-phase media to form a purification column for clean-up and preconcentration of peptide mixtures [139, 145, 146], with and immobilised Fe(III) affinity media, TiO_2 beads for purification, enriching and characterisation of phosphorylated peptides [147, 148], immobilised-trypsin for protein digestion [149]. In addition, Jiang and Lucy reported a method for the preparation of an off-line ion-exchange SPE-PT. They have packed a 200 µL pipette-tip with 50 mg of Bio-Rad AG1-X8 anion exchanger beads which were stabilised with glass wool. The resulted tip was used for the enrichment of herbicide glyphosate from river water samples prior to CE analysis [150].

'ZipTip' from Millipore (Billerica, MA, USA) was the first commercially available tip, developed in the late 1990s. It is a fritless SPE-PT consisting of beads incorporated into a matrix of supportive material [145]. It has been widely used for desalting, preconcentration and purification of different

sample matrices [137, 138, 151, 152]. For example, Bagshaw *et al.* have reported a method for desalting and sample clean-up using 'ZipTip' C_{18} tips prior to analysis with matrix-assisted laser desorption/ionisation time-of-flight mass spectrometry (MALDI-TOF-MS). The results obtained showed a great improvement in the signal-to-noise ratio of in-gel peptide digests leading to more reliable peptide mass fingerprinting [152]. Even though 'ZipTip' tips are very popular, their capacity is too small for quantitative studies [153] and their binding properties have been found to be unsatisfactory [154].

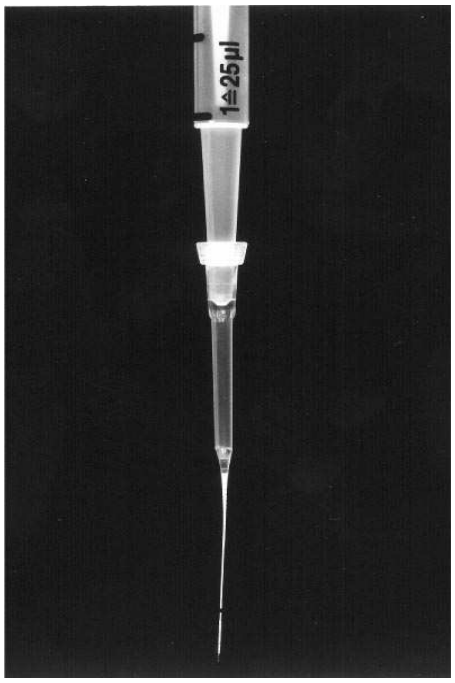

Figure 1.25: Image showing an example of a packed SPE-PT. Reproduced from [146].

However, there are some difficulties and limitations associated with the preparation of packed tips. The main issues are the need for frits for retaining the beads and the ease of packing these beads reproducibly within the confines of the polypropylene tip. Furthermore, the narrow pH stability range and low surface area because of large particles used in order not to produce high backpressures are some other limitations that restrict the use of packed SPE-PT [117, 142, 144, 155].

On the other hand, monolithic materials have shown great potential for the preparation of such extraction devices and can be an alternative to overcome many packed sorption material drawbacks. Both silica-based and organic polymer-based monoliths are becoming more common due to the advantages they posses compared to packed beads [155]. In general, these include the ease and low-cost of preparation, in particular, for microscale utilisation as there is no need for frits. Also, they take the shape of the mould in which they are prepared in. In addition, polymer monoliths are chemically stable over a wide pH range and can be synthesised with a wide variety of surface functionalities. They are also physically stable, as they are attached to the inner-wall of the tip providing no voids or dead volume. Moreover, the structure of the monoliths is highly permeable and thus operation at low backpressures and higher linear velocities is possible [117, 155, 156]. Furthermore, monoliths for bioanalytical applications, in particular for large molecules such as proteins and peptides, are gaining popularity due to the favourable mass transfer characteristics they possess [127, 157].

Silica-based monoliths are manufactured by sol–gel technology when the continuous sol–gel network is created by the gelation of sol solution. These materials have been previously used as sorbents in SPE-PT. Miyazaki *et al.* prepared a monolithic silica bed fixed in a 200 µL pipette-tip in which the silica surface was modified with a C_{18} phase or coated with a titania phase. The C_{18}-bonded tip was used for sample concentration, desalting and removal of detergents, whereas the titania-coated tip was applied for purification and concentration of phosphorylated peptides from β-casein tryptic digestion [158]. The commercially available silica-based tips 'MonoTip' from GL Sciences Inc. (Tokyo, Japan) have also been extensively used for the pretreatment of various biological samples for drugs analysis. For example, Kumazawa *et al.* [159, 160] and Hasegawa *et al.* [161, 162] used 'MonoTip' C_{18} for the extraction of antihistamines from human plasma [159, 161] as well as methamphetamine and amphetamine from human urine [160] and human whole blood [162]. In addition, Ota *et al.* reported a

successful method for the preparation of the trypsin-immobilised silica-based tip which was achieved via an aminopropyl group. The effectiveness of the tip was shown through its ability to rapidly digest reduced and alkylated proteins prior to chromatographic analysis [163].

Although monoliths, in general, have the advantages mentioned above, the preparation of silica monoliths, however, is time-consuming in comparison with organic polymer monoliths. It manufactured by sol-gel technology with phase separation and takes over 64 hours, whereas the polymer monolith takes less than 2 hours. In addition, the shrinkage of silica monoliths which occurs during the preparation cannot be completely avoided and it needs special apparatus to be overcome which may not be available in every lab [43]. In contrast, polymer-based monoliths can be readily prepared *in-situ* in polypropylene pipette-tips as shrinkage is not serious in the preparation of such materials [43]. The inner-wall of the tip is pretreated in order to get subsequent bonding to the monolithic bed. This treatment is required to stabilise the bed and to prevent sample loss due to the void between the bed and the inner-wall of the tip [164]. Organic polymer monoliths are produced by a one-step polymerisation of a mixture consisting of organic monomers, crosslinkers, porogenic solvents and initiators. The mixture is typically sonicated, purged under nitrogen, filled into the tip itself and in most cases polymerised using UV irradiation. In addition, a wide range of the monolith surface functionalities can be obtained either by copolymerisation of a suitable functional monomer or by post-modification utilising simple modification or photografting. Although polymer-based monolithic SPE-PT has drawn attention recently as an off-line sample preparation tool for bioanalysis, they have not yet been extensively applied for large biomolecules analysis.

Hsu *et al.* [118] described a preparation of an 'EasyTip', which is an EDMA-based polymer monolith fabricated in a 20 µL polypropylene pipette-tip by photopolymerisation. Instead of bonding the monolithic bed to the wall of the pipette-tip, they used a 1 mm ring that was cut from the sharp end of

the tip to stabilise the bed. Due to high backpressure originated from the small porosity of the monolithic bed which prevents using the manual micropipettors, the authors created a main flow-through channel by inserting a piece of fused capillary-silica during the polymerisation which was removed afterwards. The surface of the monolith was functionalised with C_{18} beads and IMAC beads by blending the beads with the polymerisation mixture and then the suspended slurry was photopolymerised *in-situ*. The effectiveness of the C_{18} beads functionalised tip was evaluated by applying it to desalt and preconcentrate the tryptic-digested hemoglobin and in-gel digest of epidermal growth factor receptor (EGFR) protein from A431 cell lysate. Whereas the IMAC beads functionalised monolith was applied to extract the signal of tryptic phosphopeptides of β-casein prior to MALDI-MS. Later, they prepared the SPE-PT device by an oil-in-water emulsion technique in order to increase the pore size and permeability of the monolithic bed and therefore overcome the high backpressure preventing the use of the manual micropipettors and facilitate the sample handling with low backpressures. By using this technique, they increased the pore size of the bed over five times compared to conventional photopolymerisation [165].

Hsieh *et al.* [166] developed a SPE-PT device following the same preparation strategy described by Hsu *et al.* [118] in which they functionalised the surface of the polymer monolith with titanium dioxide (TiO_2) nanoparticles for entrapping phosphorylated peptides. The TiO_2-embedded tip coupled with MALDI-MS was successfully applied to selectively identify phosphorylated peptides from tryptic-digested α-casein and β-casein spiked into bovine serum albumin (BSA) nonphosphorylated peptides. The same target analytes, phosphorylated peptides, were analysed by Rainer and co-workers [167] utilising a SPE-PT with a DVB backbone. The selectivity of the device towards the target analytes was achieved by incorporating TiO_2 and zirconium dioxide (ZrO_2) nanoparticles in the polymer monolith skeleton. The selectivity was demonstrated by enriching a digest of the *in vitro* phosphorylation of extracellular signal

regulated kinase prior to identification by MALDI-MS-MS. In addition, the sample handling was automated using a 12-channel robotic system allowing a highly reproducible process and analysis of many samples simultaneously.

Recently, Hahn *et al.* [168] immobilised trypsin on GMA-*co*-DVB monolith for in-tip digestion of proteins. In their method, the protein solution was aspirated into the trypsin-immobilised tip and then the tip was placed in a microwave oven for highly efficient and time saving digestion. Then the protein digests were eluted from the tip and injected in the MALDI-TOF-MS and liquid chromatography electrospray ionization mass spectrometry (LC-ESI-MS) for analysis. The method was fully automated using a robotic system for fast and reproducible sample handling. Myoglobin, bovine serum albumin and α-casein were used as test proteins for evaluation purposes whereas the method was applied for the analysis of in-tip trypsin-digested serum sample and the results were good in comparison with in-solution digestion.

Altun *et al.* [164, 169-171] carried out a series of experiments developing a high-throughput methacrylate polymer-based SPE-PT for drug analysis using 96-well pipette-tips (Figure 1.26) allowing the handling of the samples in 2 minutes by a Personal Pipettor robot (PP-550N-MS, Apricot Designs, Monrovia, CA, USA). The inner-wall of the tip was modified using BP as photoinitiator to generate radicals at the surface for subsequent covalent attachment between the monolithic bed and the tip inner-wall [164]. The sampling procedures include passing the sample through the tip to target analyte, washing the bed with water to remove the interferences, and then eluting the analyte with organic solvent. The tips were successfully applied to extract different drugs from human plasma samples.

Figure 1.26: UV-polymerised 96-tips packed with monolithic methacrylate polymer. Reproduced from [143].

1.4. References

[1] D. A. Skoog, D. M. West, F. J. Holler, Fundamentals of Analytical Chemistry, seventh ed., Sunders College Publishing, USA, 1996.

[2] G. D. Christian, Analytical chemistry, sixth ed., Wiley and Sons, USA, 2004.

[3] D. A. Skoog, F. J. Holler, T. A. Nieman, Principles of Instrumental Analysis, fifth ed., Brooks/Cole, USA, 1998.

[4] M. W. Dong, Modern HPLC for Practicing Scientists, Wiley and Sons, USA, 2006.

[5] C. Horváth, B.A. Preiss, S.R. Lipsky, *Anal. Chem.* 1967, **39**, 1422 - 1428.

[6] J.H. Knox, *Anal. Chem.* 1966, **38**, 253-261.

[7] A. Weston, P, R, Brown, HPLC and CE Principles and Practice, Academic Press, USA, 1997.

[8] W. Wieder, C.P. Bisjak, C.W. Huck, R. Bakry, G.K. Bonn, *J. Sep. Sci.* 2006, **29**, 2478 - 2484.

[9] P. Pruim,M. Ohman, Y. Huo, P.J. Schoenmakers, W. T. Kok, *J. Chromatogr. A* 2008, **1208**, 109 - 115.

[10] D. T. Nguyen, D. Guillarme, S. Rudaz, J. L. Veuthey, *J. Sep. Sci.* 2006, **29**, 1836 - 1848.

[11] M. A. Al-Sayah, P. Rizos, V. Antonucci, N. Wu, *J. Sep. Sci.* 2008, **31**, 2167 - 2172.

[12] S. A. C. Wren, P. Tchelitcheff, *J. Chromatogr. A* 2006, **1119**, 140 - 146.

[13] K. Cabrera, *J. Sep. Sci.* 2004, **27**, 843 - 852.

[14] J. Knox, *J. Chromatogr. Sci.* 1977, **15**, 352 - 364.

[15] J. E. MacNair, K.D. Patel, J. W. Jorgenson, *Anal. Chem.* 1999, **71**, 700 – 708.

[16] R.E. Majors, *LC-GC N Am*, 2005, **23**, 1248 – 1255.

[17] K. Kalghati, C. Horváth, *J. Chromatogr.* 1988, **443**, 343 - 354.

[18] L. Nováková, H. Vlčková, *Anal. Chim. Acta* 2009, **656**, 8 - 35.

[19] F. Svec, *J. Sep. Sci.* 2004, **27**, 1419 - 1430.

[20] G. Guiochon, *J. Chromatogr. A* 2007, **1168**, 101 - 168.

[21] J. Urban, P. Jandera, *J. Sep. Sci.* 2008, **31**, 2521 - 2540.

[22] E. G. Vlakh, T. B. Tennikova, *J. Sep. Sci.* 2007, **30**, 2801 - 2813.

[23] R. Noel, A. Sanderson, L. Spark, in *Cellulosics: Materials for Selective Separations and other Technologies* (Eds.: J.F. Kennedy, G.O. Phillips, P.A. Williams). Horwood, New York 1993, pp. 17 - 24.

[24] C. Viklund, F. Svec, J. M. J. Fréchet, K. Irgum, *Chem. Mater.* 1996, **8**, 744 - 750.

[25] S. Hjertén, J. L. Liao, R. Zhang, *J. Chromatogr.* 1989, **473**, 273 - 275.

[26] F. Svec, J.M.J. Fréchet, *Anal. Chem.* 1992, **64**, 820 - 822.

[27] H. Minakuchi, K. Nakanishi, N. Soga, N. Ishizuka, N. Tanaka, *Anal. Chem.* 1996, **68**, 3498 - 3501.

[28] S.M. Fields, *Anal. Chem.* 1996, **68**, 2709 - 2712.

[29] D. L. Mould, R. L. M. Synge, *Analyst* 1952, **77**, 964 - 970.

[30] D. L. Mould, R. L. M. Synge, *Biochem. J.* 1954, **58**, 571 - 585.

[31] M. Kubín, P. Špacek, R. Chromecek, *Coll. Czechosl. Chem. Commun.* 1967, **32**, 3881 - 3887.

[32] J.H. Knox, Personal communication, 1972.

[33] M. Al-Bokari, D. Cherrak, G. Guiochon, *J. Chromatogr. A* 2002, **975**, 275 - 284.

[34] F. Svec, J. M. J. Fréchet, *Science* 1996, **273**, 205 - 211.

[35] K. Nakanishi, N. Soga, *J. Am. Ceram. Soc.* 1991, **74**, 2518 - 2530.

[36] K. Nakanishi, N. Soga, *J. Non Cryst. Solids* 1992, **139**, 1 - 13.

[37] K. Nakanishi, N. Soga, *J. Non Cryst. Solids* 1992, **139**, 14 - 24.

[38] N. Tanaka, N. Ishizuka, K. Hosoya, K. Kimata, H. Minakuchi, K. Nakanishi, N. Soga, , *Kuromatogurafi* 1993, **14**, 50 - 51.

[39] F. Svec, J. Chromatogr. A 2010, **1217**, 902 - 924.

[40] M. R. Buchmeiser, *Polymer* 2007, **48**, 2187 - 2198.

[41] F. Svec, C. G. Huber, *Anal. Chem*. 2006, **78**, 2100 - 2107.

[42] M. Fernández, HMG-S Miguel, J. M. Estela, V. Cerdá *Trends Anal. Chem.* 2009, **28**, 336 - 346.

[43] L. Xu, Z. G. Shi, Y. Q. Feng, *Anal. Bioanal. Chem.* 2010, **399**, 3345 - 3357.

[44] M. W. H. Roberts, C. M. Ongkudon, G. M. Forde, M. K. Danquah, *J. Sep. Sci.* 2009, **32**, 2485 - 2494.

[45] A. M. Siuoffi, *J. Chromatogr. A* 2003, **1000**, 801 - 818.

[46] N. W. Smith, Z. Jiang, *J. Chromatogr. A* 2008, **1184**, 416 - 440.

[47] A. Jungbauer, R. Hahn, *J. Chromatogr. A* 2008, **1184**, 62 - 79.

[48] K. Miyabe, G. Guiochon, *J. Sep. Sci.* 2004, **27**, 853 - 873.

[49] L. Nováková, L. Matysová, D. Solichová, M. A. Koupparis, P. Solich, *J. Chromatogr. B* 2004, **813**, 191-197.

[50] F. Svec*, J. Sep. Sci.* 2004, **27**, 747 - 766.

[51] H. Kobayashi, D. Tokuda, J. Ichimaru, T. Ikegami, K. Miyabe, N. Tanaka, *J. of Chromatogr. A* 2006, **1109**, 2 - 9.

[52] D. T. T. Nguyen, D. Guillarme, S. Rudaz, J. L. Veuthey, *J. Sep. Sci.* 2006, **29**, 1836 - 1848.

[53] D. Lubda, K. Cabrera, K. Nakanishi, W. Lindner, *Anal. Bioanal. Chem.* 2003, **377**, 892 - 901.

[54] M. Kato, K. Sakai-Kato, T. Toyo'oka, *J. Sep. Sci.* 2005, **28**, 1893 - 1908.

[55] C. Legido-Quigley, N. D. Marlin, V. Melin, A. Manz, N. W. Smith, *Electrophoresis* 2003, ***24,*** 917 - 944.

[56] R. Asiaie, X. Huang, D. Farnan, C. Horváth, J. Chromatogr. A 1998, **806**, 251 - 263.

[57] K. Nakanishi, J. Porous Mater. 4 (1997) 67 - 112.

[58] T. Hara, H. Kobayashi, T. Ikegami, K. Nakanishi, N. Tanaka, *Anal. Chem.* 2006, **78**, 7632 - 7642.

[59] N. Ishizuka, H. Minakuchi, K. Nakanishi, K. Hirao, N. Tanaka, *Colloids Surf. A* 2001, **187–188**, 273 - 279.

[60] O. Núñez, K. Nakanishi, N. Tanaka, *J. Chromatogr. A* 2008, **1191**, 231 - 252.

[61] N. Tanaka, H. Kobayashi, N. Ishizuka, H. Minakuchi, K. Nakanishi, K. Hosoya, T. Ikegami, *J. Chromatogr. A* 2002, **965**, 35 - 49.

[62] N. Ishizuka, H. Minakuchi, K. Nakanishi, N. Soga, K. Hosoya, N. Tanaka, *Anal. Chem.* 2000, **72**, 1275 - 1280.

[63] N. Tanaka, H. Kobayashi, K. Nakanishi, H. Minakuchi, N. Ishizuka, *Anal. Chem.* 2001, **73**, 420A - 429A.

[64] N. Ishizuka, H. Kobayashi, H. Minakuchi, K. Nakanishi, K. Hirao, K. Hosoya, T. Ikegami, N. Tanaka, *J. Chromatogr. A* 2002, **960**, 85 - 96.

[65] F. C. Leinweber, U. Tallarek, *J. Chromatogr. A* 2003, **1006**, 207 - 228.

[66] T. Ikegami, E. Dicks, H. Kobayashi, H. Morisaka, D. Tokuda, K. Cabrera, K. Hosoya, N. Tanaka, *J. Sep. Sci.* 2004, **27**, 1292 - 1302.

[67] L. Rieux, H. Niederländer, E. Verpoorte, R. Bischoff, *J. Sep. Sci.* 2005, **28**, 1628 - 1641.

[68] M. C. Breadmore, S. Shrinivasan, K. A. Wolfe, M. E. Power, J. P. Ferrance, B. Hosticka, P. M. Norris, J. P. Landers, *Electrophoresis* 2002, **23**, 3487 - 3495.

[69] F. Svec, T. B. Tennikova, Z. Deyl, (Eds.), Monolithic Materials: Preparation, Properties, and Applications, Elsevier, Amsterdam 2003.

[70] W.D. Ross, R.T. Jefferson, *J. Chromatogr. Sci.* 1970, **8**, 386 - 389.

[71] F.D. Hileman, R.E. Sievers, G.G. Hess, W.D. Ross, *Anal. Chem.* 1973, **45**, 1126 - 1130.

[72] L.C. Hansen, R.E. Sievers, *J. Chromatogr.* 1974, **99**, 123 - 133.

[73] T.R. Lynn, D.R. Rushneck, A.R. Cooper, *J. Chromatogr. Sci.* 1974, **12**, 76 - 79.

[74] S. Hjertén, Y.M. Li, J.L. Liao, J. Mohammad, K. Nakazato, G. Pettersson, *Nature* 1992, **356**, 810 - 811.

[75] K. K. Unger, R. Skudas, M. M. Schulte, *J. Chromatogr. A* 2008, **1184**, 393 - 415.

[76] F. Svec, J.M.J. Fréchet, *Ind. Eng. Chem. Res.* 1999, **38**, 34 - 48.

[77] S. Eeltink, J. M. Herrero-Martinez, G. P. Rozing, P. J. Schoenmakers, W. Th. Kok, *Anal. Chem.* 2005, **77**, 7342 - 7347.

[78] K. Štulík, V. Pacáková, J. Suchánková, P. Coufal, *J. Chromatogr. B* 2006, **841**, 79 - 87.

[79] E. C. Peters, M. Petro, F. Svec, J. M. J. Fréchet, *Anal. Chem.* 1997, **69**, 3646 - 3649.

[80] E. C. Peters, M. Petro, F. Svec, J. M. J. Fréchet, *Anal. Chem.* 1998, **70**, 2288 - 2295.

[81] Q. C. Wang, F. Svec, J. M. J. Fréchet, *Anal. Chem*. 1993, **65**, 2243 - 2248.

[82] F. Svec, J. M. J. Fréchet, *Biotechnol. Bioeng*. 1995, **48**, 476 - 480.

[83] F. Svec, J. M. J. Fréchet, *J. Chromatogr. A* 1995, **702**, 89 - 95.

[84] E. C. Peters, F. Svec, J. M. J. Fréchet, *Chem. Mater.* 1997, **9**, 1898 - 1902.

[85] F. Svec, J. M. J. Fréchet, *Macromol. Symp.* 1996, **110**, 203 - 216.

[86] F. Svec, J. M. J. Fréchet, *Macromolecules* 1995, **28**, 7580 - 7582.

[87] H. Aoki, T. Kubo, T. Omegami, N. Tanaka, K. Hosoya, D. Tokuda, N. Ishizuka, *J. Chromatogr. A* 2006, **1119**, 66 - 79.

[88] C.Viklund, E. Ponte, B. Glad, K. Urgum, P. Horsted, F. Svec, *Chem. Mater.* 1997, **9**, 463 - 471.

[89] C. Yu, F. Svec, J.M.J. Fréchet, *Electrophoresis* 2000, **21**, 120 - 127.

[90] T. Rohr, E. F. Hilder, J. J. Donovan, F. Svec, J. M. J. Fréchet, *Macromolecules* 2003, **36**, 1677 - 1684.

[91] A. Tan, S. Benetton, J. D. Henion, *Anal. Chem.* 2003, **75**, 5504 - 5511.

[92] A. Sáfrány, B. Beiler, K. Laszlo, F. Svec, *Polymer* 2005, **46**, 2862 - 2871.

[93] M. Grasselli, E. Smolko, P. Hargittai, A. Sáfrány, *Nucl. Instr. Meth. Phys. Res. B* 2001, **185**, 254 - 261.

[94] B. Beiler, A. Vincze, F. Svec, A. Sáfrány, *Polymer* 2007, **48**, 3033 - 3040.

[95] P. Holdšvendová, P. Coufal, J. Suchánková, E. Tesařová, Z. Bosáková, *J. Sep. Sci.* 2003, **26**, 1623 - 1628.

[96] Q. Wang, F. Svec, J. M. J. Fréchet, *J. Chromatogr. A* 1994, **669**, 230 - 235.

[97] Y. Wen, Y. Wang, Y. Q. Feng, *J. Sep. Sci.* 2007, **30**, 2874 - 2880.

[98] L. Zhang, L. Zhang, W. Zhang, Y. Zhang, *Electrophoresis* 2005, **26**, 2172 - 2178.

[99] N. M. Vizioli, M. L. Rusell, M. L. Carbajal, C. N. Carducci, M. Grasselli, *Electrophoresis* 2005, **26**, 2942 - 2948.

[100] L. Zhang, G. Ping, L. Zhang, W. Zhang, Y. Zhang, J. Sep. Sci. 2003, **26**, 331 - 336.

[101] E.C. Peters, M. Petro, F. Svec, J.M.J. Fréchet, *Anal. Chem.* 1998, **70**, 2296 - 2302.

[102] Q. C. Wang, F. Svec, J. M. J. Fréchet, *Anal. Chem.* 1995, **67**, 670 - 674.

[103] Q. Luo, Y. Wei, T. Liu, G. Lei, X. Geng, *Chin. Chem. Lett.* 1999, **10**, 215 - 218.

[104] C. Fujimoto, J. Kino, H. Sawada, *J. Chromatogr. A* 1995, **716**, 107 - 113.

[105] D. Hoegger, R. Freitag, *J. Chromatogr. A* 2001, **914**, 211 - 222.

[106] Y. Fan, M. Zhang, Y. Q. Feng, *J. Chromatogr. A* 2005, **1099**, 84 - 91.

[107] Y. Fan, M. Zhang, S. L. Da, Y. Q. Feng, *Analyst* 2005, **130**, 1065 - 1069.

[108] H. J. Zhang, J. S. Li, H. Wang, Y. Q. Feng, *Anal. Bioanal. Chem.* 2006, **386**, 2035 - 2042.

[109] S. W. Zhang, C. J. Zou, N. Luo, Q. F. Weng, L. S. Cai C. Y. Wu, J. Xing, *Chin. Chem. Lett.* 2010, **21**, 85 - 88.

[110] S. W. Zhang, J. Xing, L. S. Cai, C. Y. Wu, *Anal. Bioanal. Chem.* 2009, **395**, 479 - 487.

[111] S. Eeltink, E. F. Hilder, L. Geiser, F. Svec, J. M. J. Fréchet, G. Rozing, P. J. Schoenmakers, W. Th. Kok, *J. Sep. Sci.* 2007, **30**, 407 - 413.

[112] B. Rånby, Z.M. Gao, A. Hult, P.Y. Zhang, Polym. Prepr. 1986, **27**, 38 - 39.

[113] B. Rånby, W. T. Yang, O. Tretinnikov, *Nucl. Instr. Meth. Phys. Res. B* 1999, **151**, 301 - 305.

[114] E. F. Hilder, F. Svec, J. M. J. Fréchet, *Electrophoresis* 2002, **23**, 3934 - 3953.

[115] T. B. Stachowiak, F. Svec, J. M. J. Fréchet, *Chem. Mater.* 2006, **18**, 5950 - 5957.

[116] H. Kataoka, *Trends Anal. Chem.* 2003, **22**, 232 - 244.

[117] H. Kataoka, *Anal. Bioanal. Chem.* 2010, **396**, 339 - 364.

[118] J. L. Hsu, M. K. Chou, S. S. Liang, S. Y. Huang, C. J. Wu, F. K. Shi, S. H. Chen, *Electrophoresis*, 2004, **25**, 3840 - 3847.

[119] M. Gilar, E. S. P. Bouvier, B. J. Compton, J. Chromatogr. A 2001, **909**, 111 - 135.

[120] J. S. Fritz, *Analytical Solid-Phase Extraction*, Wiley-VCH, New York, USA, 1999.

[121] E. M. Thurman, M.S. Mills, *Solid Phase Extraction – Principles and Practice*, Wiley, New York, USA, 1998.

[122] C. F. Poole, *Trends Anal. Chem.* 2003, **22**, 362 - 373.

[123] D. Martinez, M. J. Cugat, F. Borrull, M. Calull, *J. Chromatogr. A* 2000, **902**, 65 - 89.

[124] G. L. Duan, L. X. Zheng, J. Chen, W. B. Cheng, D. Li, *Biomed. Chromatogr.* 2002, **16**, 282 - 286.

[125] J. L. Luque-Garcia, T. A. Neubert, *J. Chromatogr. A* 2007, **1153**, 259 - 276.

[126] E.M. Thurman, K. Snavely, *Trends Anal. Chem.* 2001, **19**, 18 - 26.

[127] F. Svec, J. Chromatogr. B 2006, 841, 52 - 64.

[128] L. G. Blomberg, *Anal. Bioanal. Chem.* 2009, **393**, 797 - 807.

[129] A. Żwir-Ferenc, M. Biziuk, *Polish J. of Environ. Stud.* 2006, **15**, 677 - 690.

[130] C. L. Arthur, J. Pawliszyn, *Anal. Chem*. 1990, **62**, 2145 - 2148.

[131] J. Pawliszyn, *Solid phase microextraction: theory and practice.* Wiley-VCH, New York, 1997.

[132] D. W. Lou, X. Lee, J. Pawliszyn, *J. Chromatogr. A.* 2008, **1201**, 228 - 234.

[133] E. A. Moschou, A. D. Nicholson, G. Jia, J.V. Zoval, M. J. Madou, L. G. Bachas, S. Daunert, *Anal. Bioanal. Chem.* 2006, **385**, 596 - 605.

[134] X. Huang, D. Yuan, B. Huang, *Talanta* 2008, **75**, 172 - 177.

[135] M. Abdel-Rehim, *J. Chromatogr. A* 2010, **1217**, 2569 - 2580.

[136] A. Namera, A. Nakamoto, M. Nishida, T. Saito, I. Kishiyama, S. Miyazaki, M. Yahata, M. Yashiki, M. Nagao, *J. Chromatogr. A* 2008, **1208**, 71 - 75.

[137] N. S. Tannu, J. Wu, V. K. Rao, H. S. Gadgil, M. J. Pabst, I. C. Gerling, R. Raghow, *Anal. Biochem.* 2004, **327**, 222 - 232.

[138] M. G. Pluskal, A. Bogdanova, M. Lopez, S. Gutierrez, A. M. Pitt, *Proteomics* 2002, **2**, 145 - 150.

[139] J. Gobom, E. Nordhoff, E. Mirgorodskaya, R. Ekmanb, P. Roepstorff, *J. Mass Spectrom.* 1999, **34**, 105 - 116.

[140] M. W. J. van Hout, R. A. de Zeeuw, G. J. de Jong, *J. Chromatogr. A* 1999, **858**, 117 - 122.

[141] A. Namera, A. Nakamoto, T. Saito, S. Miyazaki, *J. Sep. Sci.* 2011, **34**, 901 - 924.

[142] T. Kumazawa, C. Hasegawa, X. P. Lee, K. Sato, *Forensic Toxicol.* 2010, **28**, 61 - 68.

[143] Z. Altun, C. Skoglund, M. Abdel-Rehim, *J. Chromatogr. A* 2010, **1217**, 2581 - 2588.

[144] R. Bakry, D. Gjerde, G. K. Bonn, *J. Proteome Res.* 2006, **5**, 1321 - 1331.

[145] M. R. Larsen, S. J. Cordwell, P. Roepstorff, *Proteomics* 2002, **2**, 1277 - 1287.

[146] M. Kussmann, E. Nordho, H. Rahbek-Nielsen, S. Haebel, M. Rossel-Larsen, L. Jakobsen, J. Gobom, E. Mirgorodskaya, A. Kroll-Kristensen, L. Palmp and P. Roepstor, *J. Mass Spectrom.* 1997, **32**, 593 - 601.

[147] A. Stensballe, S. Andersen, O. N. Jensen, *Proteomics* 2001, **1**, 207 - 222.

[148] M. R. Larsen, T. E. Thingholm, O. N. Jensen, P. Roepstorff, T. J. D. Jørgensen, *Mol. Cell. Proteomics* 2005, **4**, 873 - 886.

[149] J. Gobom, E. Nordhoff, R. Ekman, P. Roepstorff, *Int. J. Mass Spectrom. Ion Processes* 1997, **169-170**, 153 - 163.

[150] J. Jiang, C. A. Lucy, *Talanta* 2007, **72**, 113 - 118.

[151] M. Palmblad, J. S. Vogel, *J. Chromatogr., B: Anal. Technol. Biomed. Life Sci.* 2005, **814**, 309 - 313.

[152] R. D. Bagshaw, J. W. Callahan, D. J. Mahuran, Anal. Biochem. 2000, **284**, 432 - 435.

[153] C. Hasegawa, T. Kumazawa, X. P. Lee, A. Marumo, N. Shinmen, H. Seno, K. Sato, *Anal. Bioanal. Chem.* 2007, **389**, 563 - 570.

[154] F. K. Liu, Y. T. Hsu, C. H. Wu, *J. Chromatogr. A* 2005, **1083**, 205 - 214.

[155] K. C. Saunders, A. Ghanem, W. B. Hon, E. F. Hilder, P. R. Haddad, *Anal. Chim. Acta.* 2009, **652**, 22 - 31.

[156] D. Moravcová, V. Kahle, H. Řehulková, J. Chmelík, P. Řehulka, *J. Chromatogr. A* 2009, **1216**, 3629 - 3636.

[157] R. N. Xu, L. Fan, M. J. Rieser, T. A. El-Shourbagy, *J. Pharm. Biomed. Anal.* 2007, **44**, 342 - 355.

[158] S. Miyazaki, K. Morisato, N. Ishizuka, H. Minakuchi, Y. Shintani, M. Furuno, K. Nakanishi, *J. Chromatogr., A* 2004, **1043**, 19 - 25.

[159] T. Kumazawa, C. Hasegawa, X. P. Lee, A. Marumo, N. Shimmen, A. Ishii, H. Seno, K. Sato, *Talanta* 2006, **70**, 474 - 478.

[160] T. Kumazawa, C. Hasegawa, X. P. Lee, K. Hara, H. Seno, O. Suzuki, K. Sato, *J. Pharm. Biomed. Anal.* 2007, **44**, 602 - 607.

[161] C. Hasegawa, T. Kumazawa, X. P. Lee, M. Fujishiro, A. Kuriki, A. Marumo, H. Seno, K. Sato, *Rapid Commun. Mass Spectrom.* 2006, **20**, 537 - 543.

[162] C. Hasegawa, T. Kumazawa, X. P. Lee, A. Marumo, N. Shinmen, H. Seno, K. Sato, *Anal. Bioanal. Chem.* 2007, **389**, 563 - 570.

[163] S. Ota, S. Miyazaki, H. Matsuoka, K. Morisato, Y. Shintani, K. Nakanishi, *J. Biochem. Biophys. Methods* 2007, **70**, 57 - 62.

[164] Z. Altun, A. Hjelmström, M. Abdel-Rehim, L.G. Blomberg, *J. Sep. Sci.* 2007, **30**, 1964 - 1972.

[165] S.S. Liang, S. H. Chen, *J. Chromatogr. A* 2009, **1216**, 2282 - 2287.

[166] H. C. Hsieh, C. Sheu, F. K. Shi, D. T. Li, *J. Chromatogr. A* 2007, **1165**, 128 - 135.

[167] M. Rainer, H. Sonderegger, R. Bakry, C. W. Huck, S. Morandell, L. A. Huber, D. T. Gjerde, G. K. Bonn, *Proteomics* 2008, **8**, 4593 - 4602.

[168] H. W. Hahn, M. Rainer, T. Ringer, C. W. Huck, G. K. Bonn, *J. Proteome Res.* 2009, **8**, 4225 - 4230.

[169] Z. Altun, A. Hjelmström, L. G. Blomberg, M. Abdel-Rehim, *J. Liq. Chromatogr. Relat. Technol.* 2008, **31**, 743 - 751.

[170] Z. Altun, L. Blomberg, M. Abdel-Rehim, *J. Liq. Chromatogr. Relat. Technol.* 2006, **29**, 1477 - 1489.

[171] M. Abdel-Rehim, C. Persson, Z. Altun, L. Blomberg, *J. Chromatogr. A* 2008, **1196-1197**, 23 - 27.

Chapter 2

Nature of the samples forming the basis of this study

2.1. Introduction

Since the United States Food and Drug Administration (FDA) approval of recombinant insulin more than two decades ago [1], there has been an accelerated drive towards the development and manufacturing of therapeutic proteins. This is due to the high specificity and effectiveness of such drugs for the treatment of various diseases, including several types of cancer, diabetes, anemia and hepatitis [2-5]. Up to 2009, nearly 100 proteins with human therapeutic applications have entered the market [6] and more than 370 are currently under development [7]. The biopharmaceutical industry has grown significantly in the last decade and continues to grow at a rapid rate with a predicted annual growth of 12 % [8]. The global market value has increased in the last decade from $12 billion to $99 billion [9, 10] and is expected to reach $125 billion by the year 2015 [11]. Therefore, due to the increase in demand for therapeutic proteins, there is a growing need to develop technologies to achieve better productivity [12].

Quality by Design (QbD) is a framework that ensures better understanding of biofermentation processes and the various parameters which affect product quality and process consistency [13]. QbD is gaining industry acceptance as an approach towards development and commercialisation of bio-therapeutic products expressed via microbial or mammalian cell lines [14]. Manufacturers who submit New Drug Applications (NDA) for novel bio-therapeutic products have an obligation to clearly demonstrate the application of the QbD approach, which is defined as: ‘a systematic approach to development that begins with predefined objectives and emphasises product and process understanding and process control, based on sound science and quality risk management’ [15-17]. Some of the key activities that are performed during QbD implementation include: (i) identification of the quality target product profile and the critical quality attributes based on impact on product safety and/or efficacy, (ii) design of the process and a robust control strategy to deliver consistently the desired

product quality, (iii) validation and filing of the process to demonstrate the effectiveness of the control strategy, and (iv) ongoing monitoring to ensure robust process performance over the life cycle of the product [18, 19].

Process Analytical Technology (PAT) has been defined by the United States FDA as 'a system for designing, analysing, and controlling manufacturing through timely measurements of critical quality and performance attributes of raw and in-process materials and processes, with the goal of ensuring final product quality' [20]. The main goal of this approach is to design and develop well-characterised processes which will consistently ensure a predefined quality at the end of the manufacturing process.

In contrast to small molecule medicines (i.e. < 1 kDa), which are typically synthesised by chemical means, therapeutic proteins are macromolecules composed of long chains of amino acid subunits and usually produced in living systems through microbial fermentation or by mammalian cell culture. The structure and functionality of the protein is determined by its sequence of amino acids which determines its three dimensional structure [21, 22]. Producing such therapeutics is a complicated, time-consuming and expensive process. Many years can be spent in just identifying the proteins, determining its gene sequence and developing the process to produce the molecule in commercial quality. Once the production process is optimised and scaled up, large batches can be produced [22]. Most of the therapeutic proteins are produced in bacteria (*Escherichia coli*), yeast (*Saccharomyces cerevisiae*) or mammalian cell culture (Chinese hamster ovary cells, CHO) [23-25], beside other production systems under development which include the yeast (*Pichia pastoris*), insect cell culture and transgenic animals and plants [1]. However, cultivated mammalian cells have become the dominant production system due to their capacity for proper protein folding and their ability to perform extensive post-translational modification [26]. Therefore, the quality and effectiveness of a protein can be superior when expressed in mammalian cells compared to

other hosts such as bacteria, plants and yeast. Today, about 60 - 70 % of all recombinant protein pharmaceuticals are produced in mammalian cells [27]. In addition, glycosylation, which refers to the covalent attachment of carbohydrate to the protein surface, is required for most of the therapeutic proteins to ensure proper folding, biological function and activity. At the moment about 60 % of the therapeutic proteins market are glycoproteins [4, 28, 29]. The production of therapeutic proteins that are glycosylated has mostly required mammalian cells that have the ability to mimic human glycosylation, and cannot be produced in standard prokaryotic expression systems because of the lack of proper glycosylation machinery. Prokaryotic hosts, e.g. *E. coli*, do not glycosylate proteins and lower eukaryotic expression systems such as yeast and insect cells are typically unable to provide mammalian glycosylation [21, 29].

A number of mammalian cell lines are used for recombinant protein production including CHO, mouse myeloma (NS0), baby hamster kidney (BHK), human embryo kidney (HEK-293) and human retinal cell lines [27]. Among them, CHO cells, which are derived from a partially inbred female adult Chinese hamster [30], are widely used in combination with the dihydrofolate reductase (DHFR)-selectable and amplifiable marker to produce therapeutic proteins [31], due to the high viability and the high densities achieved by these cells [32]. The number of licensed therapeutic proteins produced in CHO cells between the years 1987 and 2006 was 27, out of 38 drugs produced by mammalian cells [24]. CHO cells have gained their popularity from their ability to modify the protein products with glycosylation patterns similar to those in humans as well as their ability to grow to high densities in bioreactors [32, 33].

2.2. Cell culture media and yeast extract samples

2.2.1. Introduction

In vitro cell cultivation techniques play a key role in the production of therapeutic proteins [34-36]. Thus, mammalian cells (e.g. CHO cells) are cultivated in bioreactors under strictly controlled conditions in an aqueous-based media formulated for this task. Cell culture media used for the cultivation of mammalian cells is more complex and costly than that used for bacteria or yeast [37]. The cell culture media is very important to produce the correct physiological environment and allow effective *in vitro* culturing of mammalian cells as it provides survival and growth requirements [38]. The formulation of suitable culture media is critical and requires accurate selection of different components since the physiological environments of most cells are not fully defined and the exact compositions vary significantly based on the cell line used. In addition, different parameters are required for growth promotion and protein production enhancement, depending on the cell line used [39, 40]. The cell culture media must provide an energy source and all of the cell nutrients required for growth, while maintaining pH and osmolarity. Therefore, the cell culture media tend to be highly complex mixtures, containing a variety of amino acids, inorganic salts, organic acids, buffers, carbohydrates, vitamins, cofactors, and other materials [41].

Research on hosts for producing therapeutic proteins is focusing increasingly on the development of more cost-effective and high performance novel expression systems with improved characteristics to meet the increased demands for therapeutic proteins [21, 29]. Therefore, increasing the yield of the final product and improving the stability of the protein expression are of considerable value to the manufacturer. Such improvements have been mainly obtained, over recent years, from optimising downstream processes and media development [27].

An example of cell culture media development is shown in the following. The final product titers in CHO cells have been increased to reach

the gram per liter range, representing a 100-fold increase. In the late 1980s, a maximum cell density of 1 - 2 million cells.mL^{-1} yielding 50 - 100 mg.L^{-1} with a typical batch culture production run lasted about 7 days. By comparison, the recent fed-batch production run can last up to 21 days with a maximum cell density of 10 - 15 million cells.mL^{-1} yielding 1 - 5 g.L^{-1} [27, 42]. This significant improvement in the yield has been achieved mostly by reformulation of the serum-free medium and development of the cell culture feeding process, and in bioprocess modifications [27, 43]. The components of the cell culture media can be complex or chemically-defined (CD) mixtures.

2.2.2. Media with complex components

There are two types of cell culture media that contain complex components: basal media or feed media. Basal media, in addition to other important growth factors, are added at the initial bioreactor inoculation step to provide specific cell nutrients, whereas feed media are used in fed-batch processes. Media supply is strictly controlled to optimise growth rate, product yield, and quality, while preventing the formation of unwanted metabolites [38]. In addition, the presence of metabolisable materials in the cell culture media is a key to the production. Originally, serum was used to promote growth and enhance protein production. However, the risks of using serum as supplements are high, and include the possible presence of large proteins that may be difficult to remove and the possibility of infectious agents [44, 45]. Moreover, not having serum in the cell culture media offers improved biosafety and makes regulatory approval simpler but that can limit the cell growth and protein production. Instead, a digest of biological materials, such as yeast extracts or plant hydrolysates, have become popular as a substitute for serum in cell culture to increase productivity [39]. Supplementing the culture media with these hydrolysates have been shown to improve protein production by twofold or more [39, 46, 47]. However, the drawback of such

supplements is that these hydrolysates contain unknown materials and undefined levels of nutrients, which can result in lot-to-lot variation in fed-batch performance and protein production consistency [39, 48].

2.2.3. Chemically defined media

CD media is made of chemically defined ingredients added to purified water in which the identity and quantity of every component in the CD media is known. It contains no biogenic ingredients such as proteins, hydrolysates, or constituents of unknown composition. It is composed of only a carbon source, essential and non-essential amino acids, vitamins, and trace elements [39, 49, 50]. CD media are well suited for fundamental studies of metabolism which could greatly help the success of prospective commercial fermentation processes. CD media have become more popular for therapeutic protein production in the industrial scale, although complex media continue to be dominant in this field because of lower cost and higher productivity [51, 52]. There are some advantages related to using CD media instead of complex media. The major one is the absence of animal-derived components which is desirable from a regulatory point of view. Another important advantage and desired characteristic for any industrial fermentation process is greater reproducibility in the production of the target protein. This is due to the reduced performance variability of the cells in such media, since all the components and their amount in the media are known. In addition, CD media offer cleaner downstream processing steps and simplicity in the analysis of the end product. Also, as the CD media is more easily characterised compared to the complex media, it offers the potential for improved process control and monitoring [49, 51].

However, despite the advantages of the CD media, it must be optimised to meet the specific nutritional requirements of each individual expression system. This can be a lengthy process and expensive, limiting their use in the commercial processes, since each system has specific

nutritional requirements and expensive growth factors such as L-amino acids and vitamins. Even following these significant efforts, the optimised CD media may still produce lower yields than complex media [49, 51].

Therefore, semi-defined media can provide a balance for high productivity with reduced downstream processing. Semi-defined media are composed mostly of CD media supplemented with a small amounts (0.05 - 0.5 %) of complex nutrients such as yeast extracts. Such small amount may provide enough nutrients to enhance microorganisms' growth and protein production by over twofold without interfering with recovery or analysis of products [39, 49, 51].

2.2.4. Yeast extracts

Yeast extract is a highly filterable extract of autolysed baker's or brewer's yeast (*S. cerevisiae*) that includes the water-soluble components of the yeast cell. Yeast extract, which has good nutritional characteristics, is a non animal-derived powder consisting of peptides, free amino acids, nitrogen, carbohydrates, nucleotides, vitamins, especially vitamin B complex, trace elements, growth factors and salts, in addition to a significant amount of unknown materials [39, 51-56].

Yeast extract is generally manufactured from the baker's yeast, *S. cerevisiae* via a controlled autolysis process which releases the intracellular components. *S. cerevisiae* is allowed to grow to a high cell density for a designated period of time optimised for the particular yeast strain. Then the batch is exposed to a controlled temperature or osmotic shock that causes the yeast cells to die. However, even though these conditions lead to the death of the cells, the yeast's endogenous enzymes are still active and the autolysis is begun. The cells are allowed to autolyse for a predetermined period of time. Autolysis of yeasts causes the release of amino acids, proteins, nucleic acid and other products. Moreover, yeast's own digestive enzymes (particularly proteases and nucleases) are responsible for the

degradation of yeast proteins and nucleic acids which are broken down into peptides and amino acid derivatives and nucleotides, respectively. Once the autolysis is finished, the insoluble materials are centrifuged and filtered and the filtrate is concentrated and spray dried [49, 57-59].

Yeast extract is a typical raw material used as a supplement in the culture media for the cultivation of cells which are used in the production of therapeutic proteins. It is a low-cost valuable source of various substances and a key medium component providing much of the nutritional requirements, particularly amino acids and vitamins, for growing CHO cells, and has shown a significant positive influence on cell growth and protein production [39, 49, 60-64].

However, since yeast extracts are complex, ill-defined mixtures of natural origin, they exhibit significant lot-to-lot variability or variability between different vendors [65-67]. A variation by almost 50 % in biomass and growth-promoting activity was reported when different lots from the same manufacturing process were used [68]. This variability is due to the complex substrates and less controlled fermentation conditions used for yeast cultivation and to the variations in downstream processes [53]. As a result, the variability of such raw materials may have a significant impact on CHO cell growth and performance which could adversely affect the final product quality and yield [55, 64]. Therefore, such variation in the raw materials requires a development of extensive ‘use testing’ of different lots to ensure the invariability of such materials which, in turn, is reflected on the growth and performance of the cells and consistency of the final product [53, 55, 69].

2.3. Characterisation of cell culture media and yeast extract samples

2.3.1. Introduction

Cell culture productivity plays a major role in reducing the overall manufacturing costs, whereas variability could lead to problems in downstream processes. Therefore, it is desirable to have a better understanding of cellular metabolism to understand the factors that contribute to productivity and variability [70, 71]. Process control is a critical factor in regulating cellular metabolism during cell cultivation to increase cell performance and productivity [72]. The presence of optimal concentrations of nutrients and the reduction of accumulating waste lead to successful cell growth, viability and protein production [73]. However, cell culture media and fermentation broths are complex mixtures of nutrients and other undefined components sourced from supplements, such as yeast, and limited information is available on the complex metabolisms of these cell lines. Thus, a variation in the fermentation performance may occur due to the lot-to-lot variation inherently associated with these ill-defined components [51, 74, 75]. Therefore, these exists a need to develop rapid, efficient and sensitive analytical methods to observe compositional changes and to ensure efficient and reliable process control for improving the yield and consistency of the target product [38, 41].

It is important to determine the concentration of specific components of the cell culture media, such as the main carbon and energy sources, and to monitor other factors, such as pH, when developing and optimising cell culture processes [76]. For example, characterisation of amino acid composition and concentrations in the cell culture and fermentation broth media is important because the presence or absence of specific amino acids could affect the yield and the quality of the desired products. Also, each cell line demands specific media compositions for obtaining maximum

productivity. Furthermore, monitoring of such nutrients during the fermentation is demanded since amino acids in the media might be consumed or released by the cells [75, 76]. Carbohydrates, which serve as carbon sources for many microorganisms, are essential for cell growth and product synthesis. It is desirable to characterise the carbohydrates, in these cell cultures and fermentation broths to avoid any adverse influence on the yield or quality of the target product [77]. Metabolism of glutamine and glucose produces ammonia and lactate, respectively. The concentrations of such metabolites should be monitored since the cell growth and productivity are inhibited at higher concentrations [78].

2.3.2. Characterisation of amino acids and carbohydrates

Amino acids and carbohydrates have been characterised in a number complex media such as mammalian cell culture media and fermentation broths [70, 71, 74-76, 79-83] utilising different analytical techniques such as high performance anion exchange chromatography with pulsed amperometric detection (HPAE-PAD) [70, 75, 76, 80, 81, 83], gas chromatography with flame ionisation detection (GC-FID) [71], ultra performance liquid chromatography (UPLC) [82] and MALDI-TOF-MS [74].

Genzel *et al*. developed a method for direct separation and detection of amino acids based on anion exchange chromatography with integrated pulsed amperometric detection [76]. The optimised method was applied for the analysis of typical mammalian cell culture broth samples taken over the entire process time. In their method, the samples had to be analysed at two dilutions due to the wide range of amino acid concentrations in the samples as a result of the medium composition and cell metabolism. Using the same separation technique, Hanko and Rohrer reported a direct method for quantitative analysis of tryptophan content of bovine serum albumin (BSA). The method was also used to monitor free tryptophan of *E. coli* cell culture and Bacto Yeast Peptone Dextrose (YPD) Broth and during an *E. coli*

fermentation [80]. Hanko *et al.* also published the successful use of anion exchange chromatography to simultaneous determination of carbohydrates and all common amino acids in cell culture and fermentation broth media [75, 83]. In their method, the separation between carbohydrates and amino acids was achieved by varying the initial NaOH eluent concentration and its duration.

Mohabbat and Drew developed a rapid (< 7 minutes) GC-FID for the simultaneous identification and quantification of 33 amino acids and dipeptides in cell culture media. The complex media samples were pretreated using the EZ:faast^{TM} (Phenomenex) amino acid sample testing kit [71].

Using UPLC with fluorescence detection, Fiechter and Mayer have developed a method for the separation of 21 amino acids utilising a sub-2 µm C_{18} column [82]. Amino acids were derivatised with 6-aminoquinolyl-N-hydroxysuccinimidyl carbamate and the derivatives were separated within 12 minutes. The method was applied to characterise changes in the free (FAA) as well as total amino acid (TAA) profiles specific to culture media at three distinctive stages of fermentation: starting medium (before fermentation), inoculated fermentation broth after cell mass production prior to induction and after product expression at the end of fermentation.

Free amino acids in mammalian cell culture media have also been quantified using MALDI-TOF-MS [74]. The technique was capable of quantifying 12 amino acids without derivatisation using α-cyano-4-hydroxycinnamic acid as the internal standard. It was applied for the analysis of bioreactor samples from five time points in the process.

Krömer *et al.* have compared four common detection systems coupled to reversed-phase high performance liquid chromatography (RP-HPLC) for the determination of L-alanyl-L-glutamine, a stable source of L-glutamine, in cell culture media [84]. They used fluorescence detection (FLD) after precolumn derivatisation with *o*-phthaldialdehyde, direct quantification using ultraviolet detection (UVD), evaporative light scattering

detection (ELSD), and liquid chromatography electrospray ionisation tandem mass spectrometry (LC-ESI-MS/MS). The direct quantification of L-alanyl-L-glutamine using UVD or ELSD was prevented by sample matrix effects, whereas FLD allowed the quantification over a wide concentration range and ESI-MS/MS showed the highest sensitivity.

Giuffrida *et al.* studied the effect of genetic modification on the autolysis of yeast [85]. In their study, they determined L- and D-forms of the major amino acids released from yeast. The determination method of the released amino acids includes a pre-column derivatisation with fluorescein isothiocyanate. The derivatives were identified and quantified using chiral micellar electrokinetic chromatography with laser-induced fluorescence detection (chiral-MEKC-LIF). The results obtained from comparing conventional and transgenic yeasts showed that higher amounts of L-amino acids were released to the medium as a result of the genetic modification which had lead to a faster autolysis of the yeast.

Rao and co-workers simultaneously determined six of the critical cellular thiols in the sulfur metabolic pathway using a liquid chromatographic method with mass spectrometric detection [86]. Sample preparation included the extraction of thiols from yeast using water in an ultrasonic bath for 10 minutes with an extraction recovery of more than 97 %. The extracted disulfides were treated with tris(2-carboxyethyl)phosphine (TCEP) to reduce the disulfide bond and then thiols were derivatised with p-(hydroxymercuri)benzoate. The determined thiols were cysteine, homocysteine, glutathione, cysteinyl-glycine, γ-glutamyl-cysteine, and S-adenosyl-homocysteine.

The carbon sources, carbohydrates, and the metabolism products, sugar alcohols and glycols, were analysed simultaneously in growing yeast (*S. cerevisiae*) cultures and their final fermentation broths using HPAE-PAD [77]. The changes of carbohydrate concentrations in the yeast culture media during fermentation were monitored over 1 day. The results obtained showed a drop in glucose concentration over time and an increase in

glycerol. Male *et al.* also developed a method for on-line monitoring of glucose during mammalian cell cultivation. The method was based on a flow injection analysis (FIA) mediated-biosensor system, using immobilised glucose oxidase and the mediator 1,1'-dimethylferricinium (DMFe+)-cyclodextrin [78].

2.3.3. Characterisation of nucleotides and metabolism intermediates

Cordell *et al.* developed a method utilising ion-pair HPLC tandem electrospray ionisation-mass spectrometry for the quantitative profiling of over twenty nucleotides and related phosphorylated species [87]. The method was applied to profile changes in intracellular nucleotides in cultured CHO cells and to study their response to drug treatments. VanDusen and co-workers reported a method for the measurement of free adenine content in yeast extracts or the adenine concentrations found in CD and complex fermentation samples [88]. The method used for the quantitation of adenine was RP-HPLC with fluorescence detection. Adenine was derivatised with chloroacetaldehyde to form the fluorescent adenine adduct 1,N^6-ethenoadenine. The method was utilised to study the adenine nutritional requirements of adenine auxotrophs of recombinant *S. cerevisiae*. The adenine content of individual yeast extracts was determined in relation to the cell mass (dry cell weight, DCW) achieved in culture media formulated with these extracts. As a result, a general increase in DCW was observed with increasing adenine concentration in the yeast extract. Jérôme *et al.* determined the concentration of methylamine, an intermediate in biopharmaceutical industry, in fermentation broths using a developed GC assay [89]. The validated method was used for monitoring methylamine concentration in a fed-batch bioprocess producing a dye-linked formaldehyde dehydrogenase in *Hyphomicrobium zavarzinii* ZV 580 cultures.

2.3.4. Characterisation of vitamins

Cataldi *et al.* and Nardiello *et al.* reported a developed method based on capillary electrophoresis coupled with laser-induced fluorescence (CE-LIF) for the analysis of water-soluble riboflavin, or vitamin B2, in baker's yeast as it is a good source for riboflavin. Since riboflavin has an intrinsic fluorescent nature, it was selectively detected in such complex samples without interference [90]. In the same sample matrix, Gliszczyńska *et al.* quantified and identified riboflavin and its derivatives utilising HPLC with fluorescence detection [91].

2.3.5. Characterisation using spectroscopic methods

The use of spectroscopic methods in biopharmaceutical industry has been increased and their applications could exist at all manufacturing stages such as raw materials characterisation, monitoring of product formation and quality control in packaging [55]. In addition, they are suitable for online, *in-situ* and *in vivo* measurements [38]. Kasprow *et al.* used near-infrared spectroscopy as a rapid screening method for yeast extract qualifying. NIR spectroscopy was performed by scanning yeast extract samples at the wavelengths in the range 1100 - 2500 nm. Mathematical treatment of the raw spectra was performed utilising chemometric methods for correlation between yeast extract variations and fermentation product yields [55]. However, since the samples under investigation in this field are prepared in water, much of the analyte spectral detail is masked in a technique such as near-infrared (NIR) spectroscopy due to the very strong water signals [41]. Ryan *et al.* [38] and Li *et al.* [41, 92, 93] have investigated the use of rapid 'holistic' analytical methods for routine screening of cell culture media and yeast extracts used in industrial biotechnology. Due to the insufficient spectra obtained for characterising complex samples such as culture media by conventional single excitation wavelength spectroscopy, they used

excitation-emission matrix (EEM) fluorescence and Raman spectroscopy. In combination with chemometric methods, rapid and efficient assays were demonstrated for the qualitative and quantitative characterisation and quality assessment of complex and CD cell culture media and yeastolate components used for CHO cells cultivation for the purpose of recombinant proteins production.

2.4. Thesis objectives

Biotherapeutic drugs are very effective for treating different diseases such as cancer, diabetes, etc. This effectiveness has accelerated their development and manufacturing and the growth in the biopharmaceutical industry in the last decade is remarkable due to the introduction of many new therapeutic proteins. The production processes of such drugs are complicated and have to be maintained under strict and regulated conditions to ensure the consistency of the processes and to produce high quality drugs. Therefore, the development of rapid, sensitive and cost-effective analytical assays is highly demanded for monitoring the biofermentation processes and the key parameters that could affect the final product quality and production consistency.

Chromatography is a powerful analytical technique that is widely used for the separation, identification and determination of the chemical components in complex mixtures. In the last 30 years, HPLC has become one of the most popular analytical instruments for the quantitative analysis of a wide range of pharmaceutical compounds. One of the main objectives of analytical laboratories is to develop rapid and efficient methods for qualitative and quantitative analysis. In addition, high-throughput separations are highly demanded in common applications within the pharmaceutical industry such as purity assays, pharmacokinetic studies, and quality control since faster separations are required to enhance productivity and reduce costs.

The aim of this thesis was to develop selective, rapid and efficient analytical methods based on solid phase extraction (SPE) and rapid resolution liquid chromatography (RRLC) for the analysis of real samples sourced from the biopharma industry and to evaluate lot-to-lot variability. The samples include fermentation feedstocks, CD cell culture media, raw materials (i.e. yeastolate) and in-process samples. The samples are complex and comprised a variety of components. The challenge is to develop methods for the determination of the target analytes with minimal interference from sample matrices. The development of the chromatographic methods includes the use of narrow-bore columns packed with sub-2 μm silica particles or the use of columns made of monolithic materials. The aim was also to develop a novel solid phase microextraction in a pipette tip for selective enrichment of galactosylated proteins by immobilising gold nano-particles on the surface of the preformed monolith.

2.5. References

[1] B. A. Rasala, M. Muto, P. A. Lee, M. Jager, R. M. F. Cardoso, C. A. Behnke, P. Kirk, C. A. Hokanson, R. Crea, M. Mendez, S. P. Mayfield, *Plant Biotech. J.* 2010, **8**, 719 - 733.

[2] G. Woodnutt, B. Violand, M. North, *Curr. Opin. Drug Discovery Dev.* 2008, **11**, 754 - 61.

[3] B. Leader, Q. J. Baca, D. E. Golan, Nat. Rev. Drug Discovery 2008, **7**, 21 - 39.

[4] R. J. Solá and K. Griebenow, *Biodrugs* 2010, **24**, 9 - 21.

[5] R. Werner, K. Kopp, M. Schlueter, *Acta Paediatr Suppl.* 2007, **96**, 17 - 22.

[6] D. L. Hacker, M. D. Jesus, F. M. Wurm, *Biotechnol. Adv.* 2009, **27**, 1023 - 1027.

[7] J. Xu, X. Ge, M. Dolan, *Biotechnol. Adv.* 2011, **29**, 278 - 299.

[8] L. Deakin, *Filtration and separation* 2011, **48**, 20 - 22.

[9] G. Walsh, *Nat. Biotechnol*. 2000, **18**, 831 - 833.

[10] G. Walsh, *Nat. Biotechnol.* 2010, **28,** 917 - 924.

[11] Decision Resources, 2009, http://www. decisionresources. Com

[12] M. Zhou, Y. Crawford, D. Ng, J. Tung, A. F. J. Pynn, A. Meier, I. H. Yuk, N. Vijayasankaran, K. Leach, J. Joly, B. Snedecora, A. Shen, *J. Biotechnol.* 2011, **153**, 27 - 34.

[13] A. S. Rathore, *Trends Biotechnol.* 2009, **27**, 546 - 553.

[14] R. Bhambure, K. Kumar, A. S. Rathore, *Trends Biotechnol.* 2011, **29**, 127 - 135.

[15] International Conference of Harmonisation (ICH), Harmonised Tripartite Guideline: Q8(R2) Pharmaceutical Development, 2008, http://www.ich.org/LOB/media/MEDIA4986.pdf, accessed 30th July 2010.

[16] International Conference of Harmonisation (ICH), Harmonised Tripartite Guideline: Q9 Quality Risk Management, 2005, http://www.ich.org/LOB/media/MEDIA1957.pdf, accessed 30th July 2010.

[17] International Conference of Harmonisation (ICH), Harmonised Tripartite Guideline: Q10 Pharmaceutical Quality Systems, 2008, http://www.ich.org/LOB/media/MEDIA3917.pdf, accessed 30th July 2010.

[18] A. S. Rathore, H. Winkle, *Nat. Biotechnol.* 2009, **27**, 26 - 34.

[19] A. S. Rathore, *Trends Biotechnol.* 2009, **27**, 546 - 553.

[20] U.S. Department of Health and Human Services, Food and Drug Administration (2004) Guidance for Industry: PAT - A Framework for Innovative Pharmaceutical Development, Manufacturing, and Quality Assurance (http://www.fda.gov/downloads/Drugs/GuidanceComplianceRegulatoryInformation/Guidances/ucm070305.pdf).

[21] T. Gerngross, *Nat. Biotechnol.* 2004, 22, 1409 - 1414.

[22] A. A. Hajare, A. S. Dange, Y. T. Shetty, *Indian J. Pharm. Educ. Res.* 2008, **42**, 104 - 112.

[23] G. Walsh, *Nat. Biotechnol.* 2003, **21**, 865 - 870.

[24] G. Walsh, *Nat. Biotechnol.* 2006, **24**, 769 - 776.

[25] A. L. Demain, P. Vaishnav, *Biotechnol. Adv*. 2009, **27**, 297 - 306.

[26] A. Traunecker, O. Filipo, K. Karajalainen, *Trends Biotechnol.* 1991, **9**, 109 - 113.

[27] F. M. Wurm, *Nat. Biotechnol.* 2004, **22**, 1393 - 1398.

[28] A. Humphreys, C. Boersig, *Med. Ad. News* 2003, **22**, 42 - 57.

[29] K. D. Pourcq. K. D. Schutter, N. Callewaert, *Appl. Microbiol. Biotechnol.* 2010, **87**, 1617 - 1631.

[30] T. T. Puck, S. J. Cieciura, A. Robinson, *J. Exp. Med.* 1958, **108**, 945 - 959.

[31] L. M. Barnes, C. M. Bentley, A. J. Dickson, *Biotechnol. Bioeng.* 2003, **81**, 631 - 639.

[32] J. J. Cacciatore, L. A. Chasin, E. F. Leonard, *Biotechnol. Adv.* 2010, **28**, 673 - 681.

[33] K. P. Jayapal, K. F. Wlaschin, W. S. Hu, M. G. S. Yap, *Chem. Eng. Prog.* 2007, **103**, 40 - 52.

[34] I. Martin, D. Wendt, M. Heberer, *Trends Biotechnol.* 2004, **22**, 80 - 86.

[35] Y. Martin, P. Vermette, *Biomaterials* 2005, **26**, 7481 - 7503.

[36] J. N. Warnock, M. Al-Rubeai, *Biotechnol. Appl. Biochem.* 2006, **45**, 1 - 12.

[37] T. H. J. Kwaks, A. P. Otte, *Trends Biotechnol.* 2006, **24**, 137 - 142.

[38] P. W. Ryan, B. Li, M. Shanahan, K. J. Leister, A. G. Ryder, *Anal. Chem.* 2010, **82**, 1311 - 1317.

[39] L. W. Dick Jr., J. A. Kakaley, D. Mahon, D. Qiu, K. C. Cheng, *Biotechnol. Prog.* 2009, **25**, 570 - 577.

[40] T. Cartwright, G. P. Shah, CultureMedia. In: J.M. Davis , Editor,Basic Cell Culture (2nd ed.), Oxford University Press Inc. New York, 2002, pp. 69 - 106.

[41] B. Li, P. W. Ryan, B. H. Ray, K. J. Leister, N. M. S. Sirimuthu, A. G. Ryder, *Biotechnol. Bioeng.* 2010, **107**, 290 - 301.

[42] M. Butler, *Appl. Microbiol. Biotechnol.* 2005, **68**, 283 - 291.

[43] M. D. Jesus, F. M. Wurm, *Eur. J. Pharm. Biopharm.* 2011, **78**, 184 - 188.

[44] M. J. Keen, N. T. Rapson. *Cytotechnology* 1995, **17**, 153 - 163.

[45] M. C. Glassy, J. P. Tharakan, P. C. Chau, *Biotech. Bioeng.* 1988, **32**, 1015 - 1028.

[46] J. Mols, C. Peeters-Joris, R. Wattiez, S. N. Agathos, Y. J. Schneider, *In Vitro Cell Dev. Biol. Anim.* 2005, **41**, 83 - 91.

[47] C. C. Bureau, F. R. Verhoeye, J. F. Mols, J. S. Ballez, S. N. Agathos, Y. J. Schneider, *In Vitro Cell Dev. Biol. Anim.* 2003, **39**, 291 - 306.

[48] Y. Luo, G. Chen, *Biotechnol. Bioeng.* 2007, **15**, 1654 - 1659.

[49] BD Bionutrients Technical Manual, Advanced Bioprocessing, Becton Dickinson, Franklin Lakes, NJ, 3rd edn, 2006, http://www.bdbiosciences.com/documents/bionutrients_tech_manual.pdf, accessed 24th October 2011.

[50] J. Kuchibhatla, C. Hunt, S. Holdread, J. W. Brooks, As presented at the IBC Bioprocess International Conference, Boston, MA, 2004.

[51] J. Zhang, R. Greasham, Appl. Microbiol. Biotechnol. 1999, 51, 407 - 421.

[52] J. Stephenne, *Vaccine* 1990, **8**, S69 - S73.

[53] J. Zhang, J. Reddy, B. Buckland, R. Greasham, *Biotechnol. Bioeng*. 2003, **82**, 640 - 652.

[54] R. G. Rhodes, W. Coy, D. R. Nelson, *BMC Microbiology* 2009, **9**, 108 - 123.

[55] R. P. Kasprow, A. J. Lange, D. J. Kirwan, *Biotechnol. Prog.* 1998, **14**, 318 - 325.

[56] C. P. Champagne, H. Gaudreau, J. Conway, *Electron. J. Biotechnol.* 2003, **6**, 185 - 197.

[57] H. J. Peppler, *Economic Microbiol.* 1982, **7**, 293 - 392.

[58] H. Tangüler, H. Erten, *Turk. J. Agric. For.* 2009, **33**, 149 - 154.

[59] R. Sommer, *Food Australia* 1998, **50**, 181 - 183.

[60] J. S. Smith, A. J. Hiller, G. J. Lees, G. R. Jago, *J. Dairy Res.* 1975, **42**, 123 - 138.

[61] E. Selmer-Olsen, T. Sorhaug, *Milchwissenschaft* 1998, **53**, 367 - 370.

[62] X. Y. Fu, D. Z. Wei, W. Y. Tong, *J. Chem. Technol. Biotechnol.* 2006, **81**, 1866 - 1871.

[63] V. P. Hanko, J. S. Rohrer, *Anal. Biochem.* 2000, **283**, 192 - 199.

[64] M. S. Donaldson, L. Shuler, *Biotechnol. Prog.* 1998, **14**, 573 - 579.

[65] T. M. Larson, M. Gawlitzek, H. Evans, U. Albers, J. Cacia, *Biotechnol. Bioeng.* 2002, **77**, 253 - 263.

[66] A. O. Kirdar, K. D. Green, A. S. Rathore, *Biotechnol. Prog.* 2008, **24**, 720 - 726.

[67] R. Fike, B. Dadey, R. Hassett, R. Radominski, D. Jayme, D. Cady, *Cytotechnology* 2001, **36**, 33 - 39.

[68] J. Potvin, E. Fonchy, J. Conway, C. P. Champagne, *J. Microbial. Methods* 1997, **29**, 153 - 160.

[69] C. F. Shen, T. Kiyota, B. Jardin, Y, Konishi, A. Kamen, *Cytotechnology* 2007, **54**, 25 - 34.

[70] T. M. Larson, M. Gawlitzek, H. Evans, U. Albers, J. Cacia, *Biotechnol. Bioeng.* 2002, **77**, 553 - 563.

[71] T. Mohabbat, B. Drew, *J. Chromatogr. B* 2008, **862**, 86 - 92.

[72] H. Kurokawa, Y. S. Park, S. Lijima, T. Kobayashi, *Biotechnol. Bioeng.* 1994, **44**, 95 - 103.

[73] M. R. Riley, H. M. Crider, M. E. Nite, R. A. Garcia, J. Woo, R. M. Wegge, *Biotechnol. Prog.* 2001, **17**, 376 - 378.

[74] J. E. Dally, J. Gorniak, R. Bowie, C. M. Bentzley, *Anal. Chem.* 2003, **75**, 5046 - 5053.

[75] V. P. Hanko, J. S. Rohrer, *Anal. Biochem.* 2004, **324**, 29 - 38.

[76] Y. Genzela, S. König, U. Reichl, *Anal. Biochem.* 2004, **335**, 119 - 125.

[77] V. P. Hanko, J. S. Rohrer, Anal. Biochem. 2000, **283**, 192 - 199.

[78] K. B. Male, P. O. Gartu, A. A. Kamen, J. H. T. Luong, *Biotechnol. Bioeng.* 1997, **55**, 497 - 504.

[79] A. Mulchandani, A. S. Bassi, *Biosens. Bioelectron.* 1996, **11**, 271 - 280.

[80] V. P. Hanko, J. S. Rohrer, *Anal. Biochem.* 2002, **308**, 204 - 209.

[81] P. Jandik, J. Cheng, D. Jensen, S. Manz, N. Avdalovic, *Anal. Biochem.* 2000, **287**, 38 - 44.

[82] G. Fiechter, H. K. Mayer, *J. Chromatogr. B* 2011, **879**, 1353 - 1360.

[83] V. P. Hanko, A. Heckenberg, J. S. Rohrer, *J. Biomol. Tech.* 2004, **15**, 317 - 324.

[84] J. O. Krömer, S. Dietmair, S. S. Jacob, L. K. Nielsen, *Anal. Biochem.* 2011, **416**, 129 - 131.

[85] A. Giuffrida, L. Tabera, R. González, V. Cucinotta, A. Cifuentes, *J. Chromatogr. B* 2008, **875**, 243 - 247.

[86] Y. Rao, B. Xiang, E. Bramanti, A. D'Ulivo, Z. Mester, *J. Agric. Food Chem.* 2010, **58**, 1462 - 1468.

[87] R. L. Cordell, S. J. Hill, C. A. Ortori, D. A. Barrett, *J. Chromatogr. B* 2008, **871**, 115 - 124.

[88] W. J. VanDusen, J. Fu, F. J. Bailey, C. J. Burke, W. K. Herber, H. A. George, *Biotechnol. Prog.* 1997, **13**, 1 - 7.

[89] V. Jérôme, M. Hermann, F. Hilbrig, R. Freitag, J. Chromatogr. B 2008, **861**, 88 - 94.

[90] T. R.I. Cataldi, D. Nardiello, V. Carrara, R. Ciriello, G. E. D. Benedetto, *Food Chem.* 2003, **82**, 309 - 314.

[91] A. Gliszczyńska, A. Koziolowa, *J. Chromatogr. A* 1998, **822**, 59 - 66.

[92] B. Li, P. W. Ryan, M. Shanahan, K. J. Leister, A. G. Ryder, *Appl. Spectrosc.* 2011, **65**, 1249 - 1249.

[93] B. Li, N. M. S. Sirimuthu, B. Ray, A. G. Ryder, *J. Raman Spectrosc.* In press, 2011.

Chapter 3

Application of rapid resolution liquid chromatography with fluorescence detection to the analysis of monosaccharides in bio-fermentation media samples

3.1. Introduction

The development of robust quality control assays for key components in the raw materials and during production process is absolutely critical, since yeastolate raw materials and other cell hydrosylates exhibit significant lot-to-lot variability, or variability between different vendors [1-3].

Several analytical methods of varying degrees of complexity have been developed for the determination of monosaccharides in aqueous samples and sample extracts, including GC [4], HPAEC-PAD [5-10], capillary zone electrophoresis (CZE) [11-15] RP-HPLC [11, 16-23]. Methods developed specifically for the characterisation of biofermentation broth samples for monosaccharide profiles are relatively few, and most are limited to two or three monosaccharides, present at relatively high concentrations [24-27]. In RP-HPLC, monosaccharides cannot be determined using direct UV absorbance or FLD, due to the lack of suitable chromophores and fluorophores. Some methods on complex media samples have been described using HPAEC-PAD [5], although this particular detection approach is prone to interference, especially with samples like yeastolates, which contain excess concentrations of undefined components. Alternative detection options, such as refractive index detection and related methods, suffer from limited concentration sensitivity and lack of specificity [28]. For these reasons, pre-column derivatisation of monosaccharides is crucial for highly sensitive and selective detection [29]. There are a variety of reagents developed for this application, including 2-aminobenzoic acid (AA) [11, 17], benzamidine [18], FMOC-hydrazine (9-fluorenylmethylchloroformate) [19] and aminopyrazine [20] for FLD, and p-aminobenzoic ethyl ester (ABEE) [21, 22] and 1-phenyl-3-methyl-5-pyrazolone (PMP) [23] for UV absorbance detection. Of the above options, labelling monosaccharides with AA has several advantages, not least the high sensitivity compared to the others. Additionally, AA can be used for quantitation of both neutral and amino

monosaccharides without N-acetylation, whereas using other labelling tags requires monosaccharides to be N-acetyled [30].

This Chapter describes a selective and robust RPLC-FLD based method developed specifically for the profiling of up to 10 monosaccharides, with a chromatographic run-time of approx. 20 minutes, for a range of complex biological samples originating from a biopharmaceutical CHO based process. Specifically, the assay was developed to allow selective quantification of glucosamine, mannosamine, galactosamine, galactose, mannose, glucose, ribose, xylose, fucose and sialic acid, without interferences from the extracts of yeastolate feedstock, basal media preparations and fermentation process samples.

3.2. Experimental

3.2.1. Reagents and materials

Galactose (Gal, 99 %), glucose (Glc, 99.5 %), mannose (Man, Sigma-Ultra), glucosamine (GlcN, 99 %), galactosamine (GalN, 98 %), ribose (Rib, 99 %), fucose (Fuc, 98 %), sodium cyanoborohydride (95 %), sodium acetate (99 %), boric acid (99.5 %) and diethyl ether were purchased from Sigma-Aldrich (Tallaght, Dublin, Ireland). Xylose (Xyl, 99 %), mannosamine (ManN, 98 %), and anthranilic acid (AA, 98 %) were purchased from Fluka (Buchs, Switzerland). Methanol (MeOH) and acetonitrile (ACN) were of HPLC grade from Labscan (Tallaght, Dublin, Ireland). Acetic acid (96 %) was from Riedel-de-Haen (Seelze, Germany). All chemicals were used as received, without any further purification.

3.2.2. Instrumentation

The chromatographic separation was performed using an Agilent 1200 Series Rapid Resolution Liquid Chromatography (RRLC) system (Agilent Technologies, CA, USA), which comprised an on-line degasser, a binary pump, an autosampler with temperature control, a column oven and a UV-Vis detector. The AA-monosaccharide derivatives were separated on a 2.1 mm × 50 mm, 1.8 µm ZORBAX Eclipse XDB-C_{18} column (Agilent Technologies, CA, USA) at a flow rate of 0.4 $mL.min^{-1}$ and a column temperature of 20 ^{o}C. Mobile phase A was 50 $mmol.L^{-1}$ sodium acetate buffer (pH 4.3) and mobile phase B was ACN. The gradient program was: 0-12 minutes (2 % B), 12.1-17 minutes (10 % B) and 17.1-25 minutes (2 % B). The injection volume was 700 nL with FLD (Waters 470 fluorescence detector, Waters Corporation, MA, USA) at excitation: 360 nm and emission: 424 nm. Sample preparation prior to derivatisation was achieved with a C_{18} solid phase extraction cartridge (Phenomenex Strata C_{18}-E, 55 µm, 70 Å, 50 mg/mL, Phenomenex, Macclesfield, UK). A GFL water bath model 1013 (GFL, Burgwedel, Germany) was used for derivatisation and the balance used was a Sartorius Model ED124S (Sartorius, Goettingen, Germany). The pH meter used (Orion 2 Star) was purchased from Thermo Electron Corporation (Thermo, PA, USA). The water used for preparations was purified using Millipore Direct Q 5 system (Millipore, France).

3.2.3. Sample preparation

The samples analysed originate from an actual industrial scale biofermentation process facility for a commercial biotherapeutic drug and were supplied by Bristol–Myers Squibb.

Yeastolate samples were supplied as solid materials and stored in the fridge at 4 ^{o}C. Cell culture media were sampled and aliquotted under sterile conditions and shipped from the US to Ireland at low temperature. These

samples were then aliquotted to smaller volumes and stored frozen at -70 ^{o}C. The samples were further transferred from Galway to Dublin at low temperature and stored at -70 ^{o}C. When analysed, the samples were removed from the freezer and defrosted at room temperature (~ an hour). The desired sample volume was aliqotted and then treated as described below, whereas the remaining sample was retuned to the freezer until further use. Samples identities are listed in Table 3.1.

Table 3.1
Identification and description of different sample types

Sample#	Sample ID	Description
Yeastolate samples		
Sample 1	ITP-2006-000113	Bacto TC Yeastolate
Sample 2	ITP-2006-000567	Bacto TC Yeastolate
Sample 3	ITP-2006-000566	Bacto TC Yeastolate
Sample 4	ITP-2006-000528	Bacto TC Yeastolate
Sample 5	ITP-2006-000527	Bacto TC Yeastolate
Sample 6	ITP-2006-000112	Bacto TC Yeastolate
Sample 7	ITP-2006-000114	Bacto TC Yeastolate
Basal media samples (Lot A)		
Sample A1	ITP-2006-000615	Lonza Initial After Load
Sample A2	ITP-2006-000616	Lonza Initial After Load
Sample A3	ITP-2006-000617	Lonza Initial After Load
Sample A4	ITP-2006-000618	Lonza Initial After Load
Sample A5	ITP-2006-000619	Lonza Initial After Load
Sample A6	ITP-2006-000620	Lonza Initial After Load
Sample A7	ITP-2006-000621	Lonza Initial After Load
Basal media samples (Lot B)		
Sample B1	ITP-2006-000025	Bioreactor 4 Initial After Load
Sample B2	ITP-2006-000091	Bioreactor 4 Initial After Load
Sample B3	ITP-2006-000308	Bioreactor 4 Initial After Load
Sample B4	ITP-2006-000401	Bioreactor 4 Initial After Load
Sample B5	ITP-2006-000234	Bioreactor 4 Initial After Load
Sample B6	ITP-2006-000186	Bioreactor 4 Initial After Load
Sample B7	ITP-2006-000447	Bioreactor 4 Initial After Load

Table 3.1 (continued)
Identification and description of different sample types

Sample#	Sample ID	Description
In-process samples (Lot A)		
Sample A1	ITP-2006-000137	Bioreactor 1 Media Start (Day 0)
Sample A2	ITP-2006-000238	Bioreactor 1 Media End
Sample A3	ITP-2006-000239	Bioreactor 1 End Passage 7
Sample A4	ITP-2006-000223	Bioreactor 2 Initial After Load
Sample A5	ITP-2006-000253	Bioreactor 2 Prior to Transfer
Sample A6	ITP-2006-000232	Bioreactor 3 Initial After Load
Sample A7	ITP-2006-000246	Bioreactor 3 Prior to Transfer
Sample A8	ITP-2006-000255	Bioreactor 4 Initial After Load
Sample A9	ITP-2006-000247	Bioreactor 4 After Inoculation
Sample A10	ITP-2006-000268	Bioreactor 4 Day 5 Post Inoculation
Sample A11	ITP-2006-000297	Bioreactor 4 Day 10 Post Inoculation
Sample A12	ITP-2006-000310	Bioreactor 4 Prior to Transfer
In-process samples (Lot B)		
Sample B1	ITP-2005-000002	Bioreactor 1 Media Start (Day 0)
Sample B2	ITP-2005-000003	Bioreactor 1 Media End
Sample B3	ITP-2006-000001	Bioreactor 1 End Passage 7
Sample B4	ITP-2006-000005	Bioreactor 2 Initial After Load
Sample B5	ITP-2006-000004	Bioreactor 2 Prior to Transfer
Sample B6	ITP-2006-000003	Bioreactor 3 Initial After Load
Sample B7	ITP-2006-000018	Bioreactor 3 Prior to Transfer
Sample B8	ITP-2006-000014	Bioreactor 4 Initial After Load
Sample B9	ITP-2006-000017	Bioreactor 4 After Inoculation
Sample B10	ITP-2006-000036	Bioreactor 4 Day 5 Post Inoculation
Sample B11	ITP-2006-000038	Bioreactor 4 Day 10 Post Inoculation
Sample B12	ITP-2006-000043	Bioreactor 4 Prior to Transfer

All samples were dissolved and diluted using GlcN as an internal standard. A number of representative samples had previously been tested and found to contain no detectable levels of GlcN. Therefore, for yeastolate analysis (received as dry powders) 15 mg of yeastolate was dissolved in 1 mL of 150 $mmol.L^{-1}$ GlcN. For the analysis of basal media samples, 50 mL of

the sample was diluted by a factor of 5 using spiking solution (175 mmol.L^{-1} GlcN). For the determination of Glc levels in these samples, 20 mL of the above diluted sample was further diluted by a factor of 80 using the spiking solution. In-process samples were collected at specific time-points during a commercial biofermentation process and were provided after removal of CHO cells by centrifugation. These samples were diluted by a factor of 5 using spiking solution (175 mmol.L^{-1} GlcN). A further dilution of the diluted sample was carried out by a factor of 20, 50 or 60 depending on the relative levels of Gal and Glc which were present at high levels in many of these samples.

3.2.4. Sample cleanup by solid phase extraction (SPE)

A C_{18} SPE cartridge was conditioned with 1 mL of methanol followed by 1 mL of water. A volume of diluted sample (200 µL) was passed through the cartridge and collected in a clean polypropylene centrifuge tube, followed by a further 100 µL water wash; the unretained hydrophilic monosaccharides were subsequently derivatised with AA as described is Section 3.2.5.

3.2.5. Fluorescent labelling of monosaccharides

3.2.5.1. Preparation of derivatisation reagent

A methanol acetate borate solution (MABS) was prepared by dissolving 240 mg sodium acetate and 200 mg boric acid in 10 mL methanol. This solution was stable for one week at 4 ^{o}C. The derivatisation reagent was prepared by dissolving 30 mg of amino benzoic acid (AA) and 20 mg of sodium cyanoborohydride in 1 mL of MABS, which was prepared fresh prior to use [17].

3.2.5.2. Derivatisation of monosaccharides

Pre-column derivatisation was achieved by mixing 100 µL of sample/standard with 100 µL of the AA reagent in a 2 mL screw-top polypropylene plastic tube. The mixture was heated in a water bath at 80 ^{o}C for 80 minutes followed by dilution with 800 µL of mobile phase A. The mixture was centrifuged and the supernatant was transferred for further use. The reaction scheme is shown in Figure 3.1.

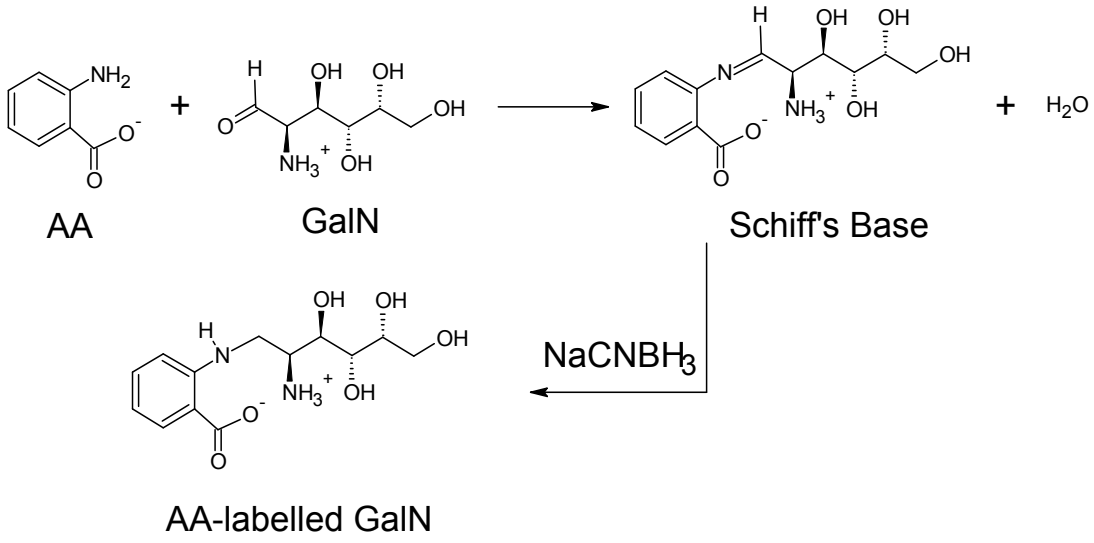

Figure 3.1: Reaction scheme for the labelling of monosccharides with AA [30].

3.2.6. Liquid-liquid extraction of excess derivatisation reagent

An aliquot of the derivatised sample (250 µL) was transferred to a 1.5 mL centrifuge tube and shaken with 1 mL of diethyl ether for 1 minute. The top layer (ether) was removed with a micropipette and another 1 mL of ether was added to the bottom layer and the procedure repeated. A total of three ether extractions were performed after which the bottom layer was transferred to a glass HPLC vial for injection.

3.2.7. SPE recovery of monosaccharide standards and real samples

The recovery of monosaccharides standards from SPE was studied by comparing the peak areas of two different aliquots of the same standard solution. One of the aliquots was passed through the SPE cartridge as in Section 3.2.4., collected and derivatised, whereas the other was derivatised without SPE treatment. For spike recovery study, a yeastolate sample was spiked with known concentrations of monosaccharide standards prior to SPE and derivatisation.

3.3. Results and discussion

3.3.1. Optimisation of chromatographic conditions

The method described here has its origin within the pioneering paper on the separation of AA monosaccharide derivatives by RPLC-FLD initially reported by Anumula [17]. However, the chromatographic method developed by Anumula utilising a 5 µm 0.46 mm × 25 cm C_{18} column was only capable of the separation of six to seven monosaccharides in a run-time of approx. 50 minutes, with a large tailed reagent peak masking the elution window from 20 to 35 minutes, and thus limiting the practical application of the method. In an effort to simultaneously reduce chromatographic run-time, mobile phase consumption and increase peak capacity to allow the separation of a larger suite of monosaccharides (including sialic acid), the method described herein utilised a short (2.1 mm × 50 mm) 1.8 µm, C_{18} column (ZORBAX Eclipse XDB), which under optimised conditions allowed the separation of all 10 target AA-monosaccharide derivatives within 20 minutes. In addition, the method used considerably less solvent while running at lower flow rates (in this instance 0.4 $mL.min^{-1}$).

The effect of the mobile phase pH was investigated in detail over two different pH ranges. 'Range 1' was from pH 3.6 to pH 5.2 at 0.4 unit intervals. The retention time of the last eluting peak decreased by about 50 % when the pH was increased from 3.6 to 5.2, however, the overall resolution of the analyte peaks was almost lost at this pH (5.2), whereas a reasonable separation was obtained at pH 4.4 as shown in Figure 3.2(**a**). Therefore, a further investigation over a narrower range from pH 4.0 to pH 4.5 at 0.1 unit intervals, i.e. 'Range 2', was carried out. There was no significant effect upon retention times across this range, as they only increased by approximately 7 %, when the pH was decreased from 4.5 to 4.0, whereas a greater effect was seen on the resolution between Man, Glc and Rib peaks as shown in Figure 3.2(**b**). For example, at pH 4.0 the resolution of the Man/Glc pair was 1.9 and 0.92 for Glc/Rib, whereas at pH 4.5 Man/Glc resolution was 0.96 and Glc/Rib was 1.55. However, at pH 4.3 these were 1.5 and 1.4, respectively, as shown in Figure 3.3. The resolution between Glc and Rib was the highest at pH 4.8, although at this pH co-elution of Man/Glc and ManN/GalN peak pairs was also observed, with lower resolution between sialic acid and a late eluting system peak. Therefore, it was concluded that the optimum working pH in terms of retention and resolution was pH 4.3. In addition, the effect of sodium acetate buffer concentration on the separation was also investigated in the range between 10 and 50 mmol.L^{-1}. However, there was no significant influence of the concentration either on the separation or on the retention time.

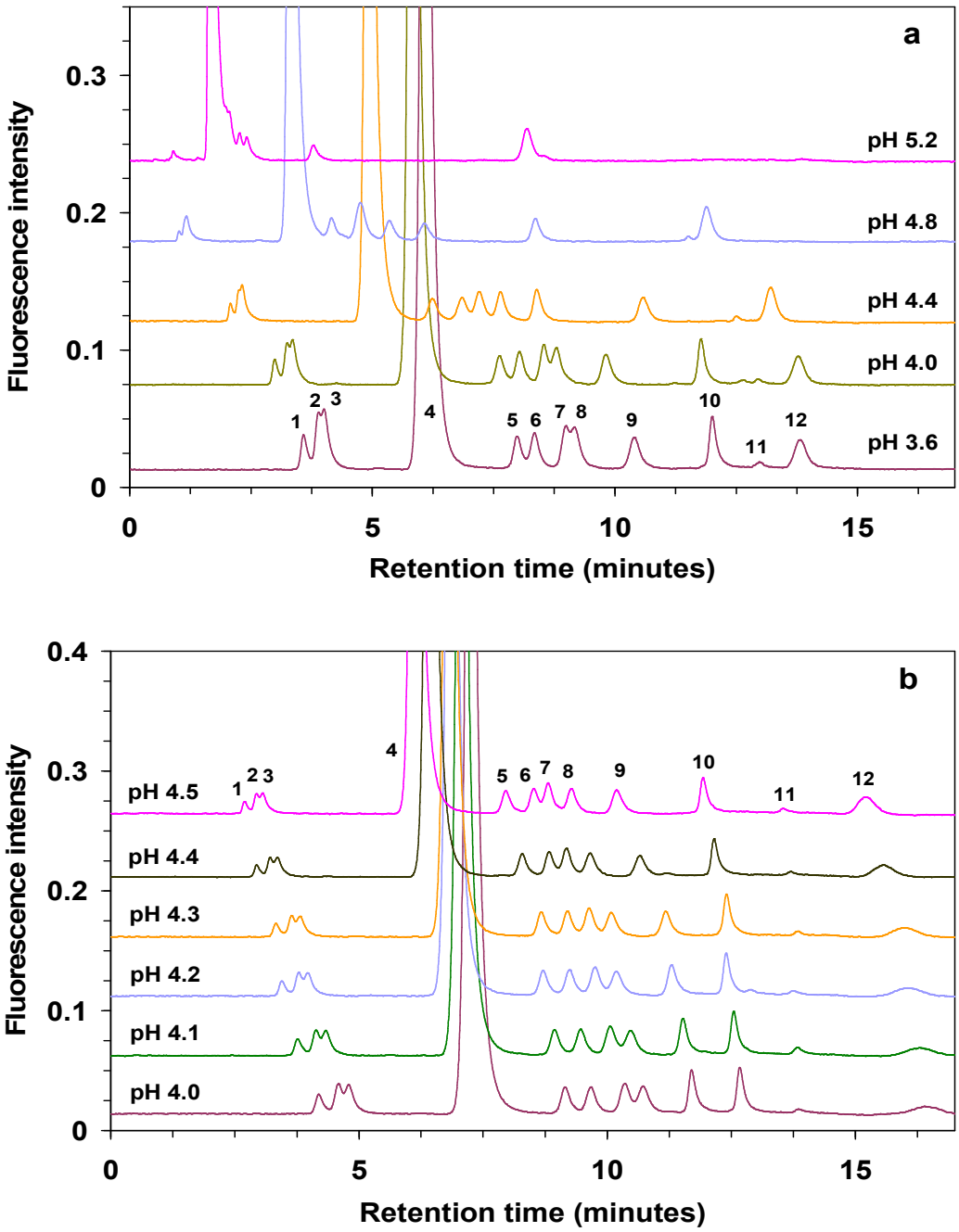

Figure 3.2: The effect of mobile phase pH on the separation of the ten AA-monosaccharide derivatives at pH 'Range 1' (**a**) and pH 'Range 2' (**b**). Column: 2.1 mm × 50 mm, 1.8 µm Zorbax Eclipse XDB-C_{18}. Mobile phase A: 50 mmol.L^{-1} sodium acetate, mobile phase B: 100 % ACN. Gradient program: 0-4 minutes (2 %), 5-8 minutes (4 %), 9-12 minutes (8 %), 12.1-20 (2 %). Flow rate: 0.43 mL.min^{-1}. Column temperature: 20 ^{o}C. Injection volume: 700 nL. Detection: excitation @ 360 nm and emission @ 425 nm. Peaks: (**1**) GlcN, (**2**) ManN, (**3**) GalN, (**4**) excess AA, (**5**) Gal, (**6**) Man, (**7**) Glc, (**8**) Rib, (**9**) Xyl, (**10**) Fuc, (**11**) sialic acid, and (**12**) blank peak.

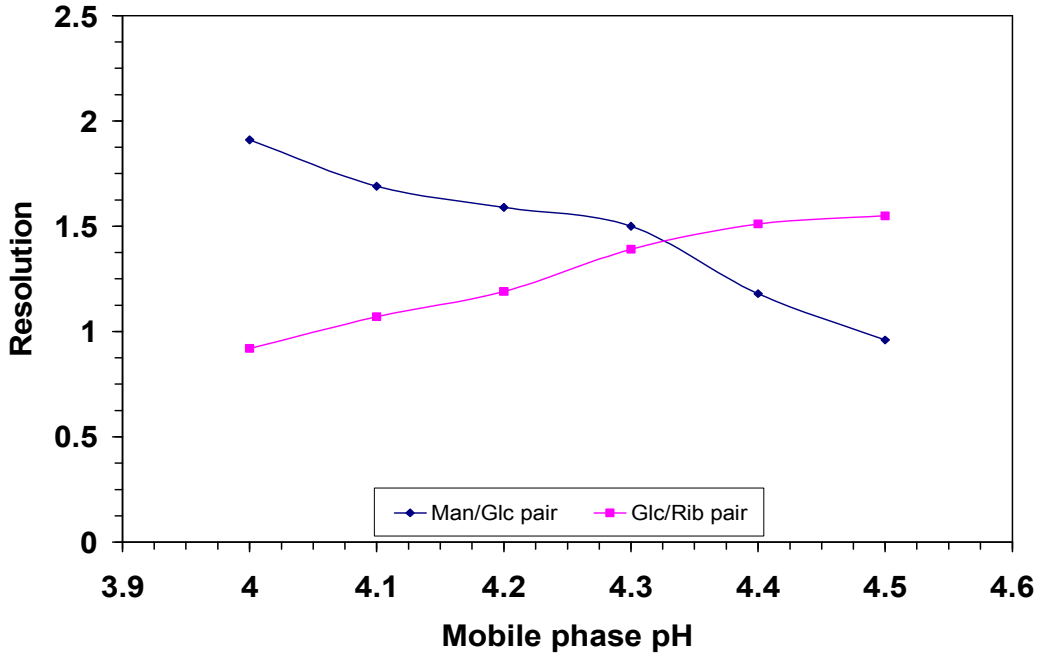

Figure 3.3: The influence of mobile phase pH on the resolution of Man/Glc and Glc/Rib peak pairs.

The effect of column temperature upon the separation of the derivatives was also examined in the range between 15 ^{o}C and 50 ^{o}C at 5 ^{o}C intervals and the results are shown in Figure 3.4. Even though the peaks were sharper and eluted earlier by over 50 % at 50 ^{o}C compared to 15 ^{o}C, the resolution between the peaks decreased significantly and, in particular, co-elution of ManN/GalN and sialic acid/system peak pairs was observed. Improved resolution was obtained when the separation was carried out at lower temperatures. However, column temperatures below 20 ^{o}C lead to broadened peaks and increased retention times and so 20 ^{o}C was selected for all sample analyses.

Figure 3.5 shows the separation of the AA-monosaccharide derivatives under the optimised conditions. As it can be seen, the AA-monosaccharide derivative peaks are well separated from each other and from the blank peaks.

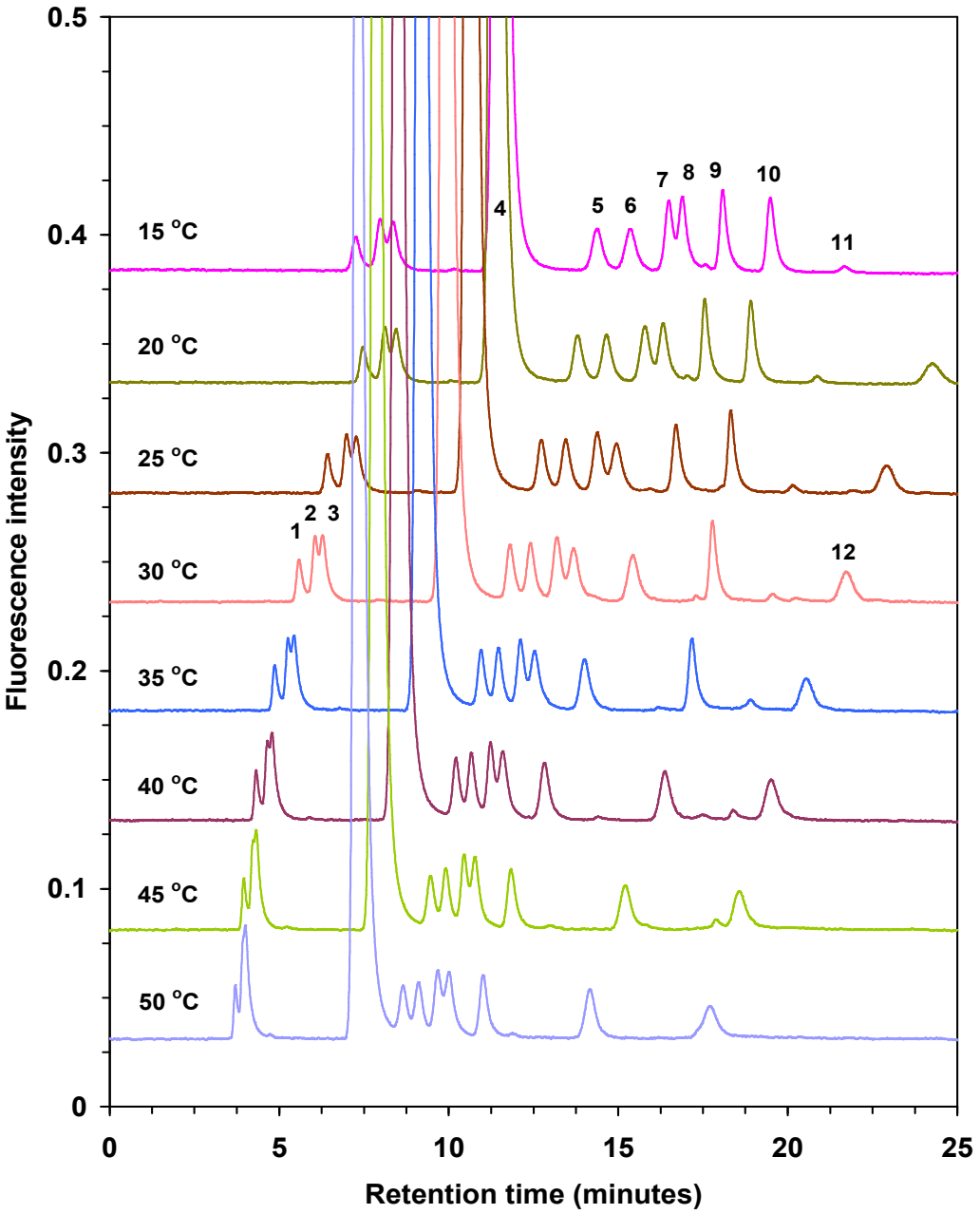

Figure 3.4: The effect of column temperature on the separation of the ten AA-monosaccharide derivatives. Chromatographic conditions are as descriced in Figure 3.2 except the following: Mobile phase A: 50 mmol.L^{-1} sodium acetate pH 4.1. Gradient program: 0-4 minutes (2 %), 6-12 minutes (4 %), 13-20 minutes (8 %), 21-25 (2 %). Flow rate: 0.3 mL.min^{-1}. Peaks: (**1**) GlcN, (**2**) ManN, (**3**) GalN, (**4**) excess AA, (**5**) Gal, (**6**) Man, (**7**) Glc, (**8**) Rib, (**9**) Xyl, (**10**) Fuc, (**11**) sialic acid, and (**12**) blank peak.

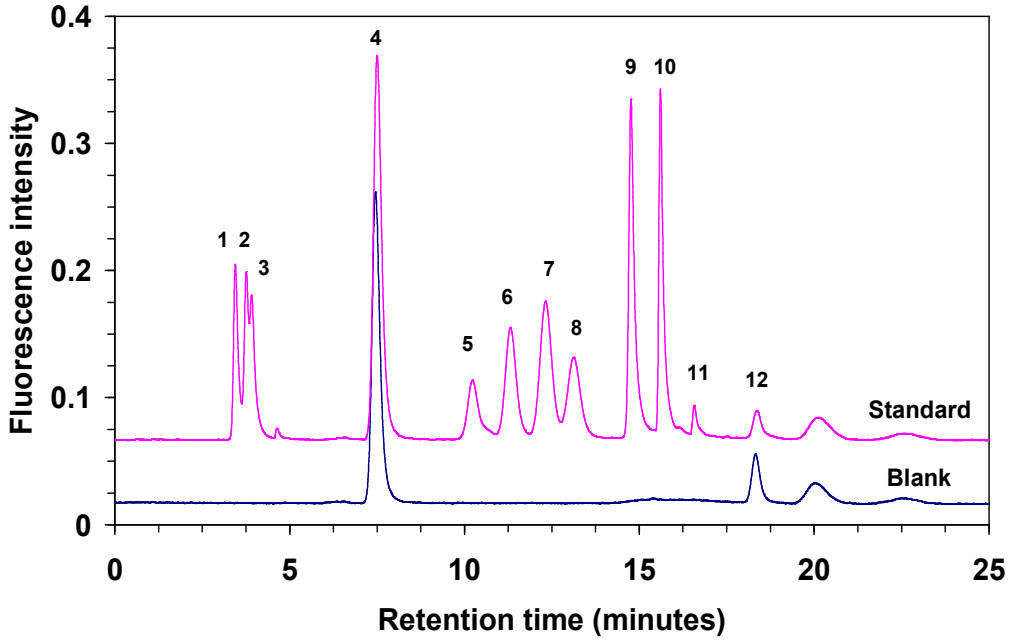

Figure 3.5: Optimum separation of the ten AA-monosaccharide derivatives overlaid with a blank. Column: 2.1 mm × 50 mm, 1.8 µm Zorbax Eclipse XDB-C_{18}. Mobile phase A: 50 mmol.L^{-1} sodium acetate pH 4.3, mobile phase B: 100 % ACN. Gradient program: 0-12 minutes (2 %), 12.1-17 minutes (10 %), 17.1-25 minutes (2 %). Flow rate: 0.4 mL.min^{-1}. Injection volume: 700 nL. Column temperature: 20 ^{o}C. Detection: excitation @ 360 nm and emission @ 425 nm. Peaks: (**1**) GlcN, (**2**) ManN, (**3**) GalN, (**4**) excess AA, (**5**) Gal, (**6**) Man, (**7**) Glc, (**8**) Rib, (**9**) Xyl, (**10**) Fuc, (**11**) sialic acid, and (**12**) blank peak.

3.3.2. Labelling of monosaccharides with AA

Figure 3.1 shows the reaction scheme for tagging the monosaccharides with AA. An investigation of the time required for formation of the AA-monosaccharide derivatives was carried out by performing the derivatisation at 80 ^{o}C for different time periods ranging from 0 to 120 minutes. The optimum time for the derivatisation reaction which gave the highest peak areas for the AA-monosaccharide derivatives was 80 minutes as indicated in Figure 3.6. Peak areas for AA-monosaccharides derivatives were increased by 11.2 % for GlcN, 5.5 % for ManN, 4.2 % for GalN, 1.9 % for Gal, 3.8 % for Man, 4.0 % for Glc, 2.9 % for Rib, 3.1 % for Xyl, 3.3 % for Fuc and 33.3 %

for sialic acid compared to the original assay, [17] in which the derivatisation was carried out for 60 minutes in an oven.

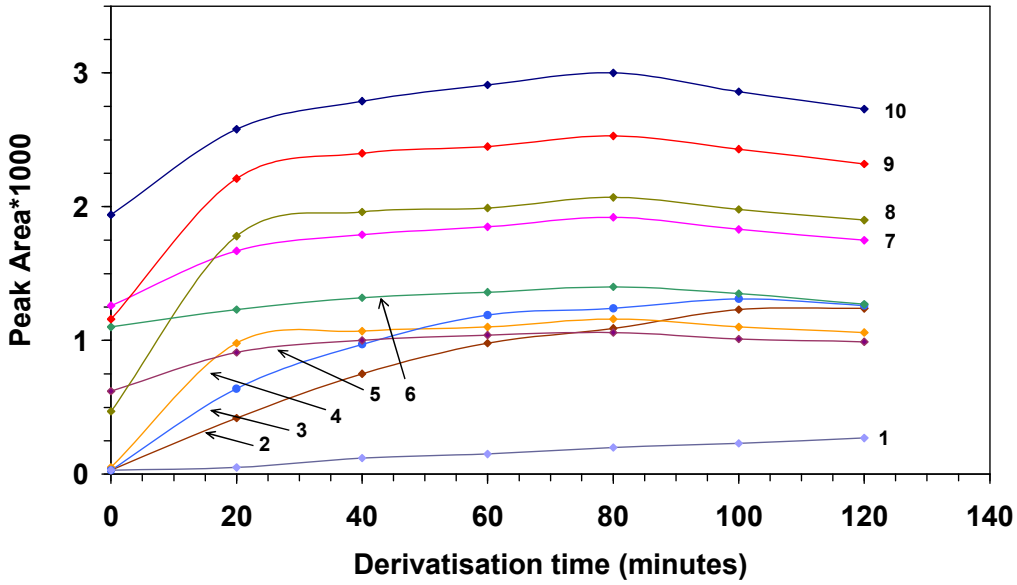

Figure 3.6: The effect of the time of derivatisation on the peak area of standard monosaccharides derivatives. The other derivatisation conditions are as described in Section 3.2.5. Curve assignment: (**1**) sialic acid, (**2**) GlcN, (**3**) GalN, (**4**) ManN, (**5**) Gal, (**6**) Rib, (**7**) Man, (**8**) Glc, (**9**) Fuc, (**10**) Xyl.

3.3.3. Liquid-liquid extraction of the excess derivatisation reagent

The concentration of AA reagent used for the derivatisation of samples as first reported produced an unacceptably large tailed reagent peak within the centre of the chromatogram which interfered with the accurate determination of Gal and probably Man [17]. Within the sample set under investigation in this study, monosaccharide concentrations varied greatly, particularly for basal media samples and in-process samples, which both had been supplemented with additional Glc. Therefore, for practical application a method to reduce the excessive reagent concentration within the prepared sample was necessary. Since the intention of this study was to develop a single derivatisation protocol for all three sample types (i.e. yeastolate, basal media and in-process samples), no attempt was made to reduce the reagent peak size by optimising the concentration of AA (30 $mg.mL^{-1}$) for each

individual sample type. Instead the excess reagent could be readily extracted into diethyl ether without adversely affecting either the separation or the recovery of monosaccharides. Figure 3.7 shows standard chromatograms of AA-monosaccharide derivatives before and after diethyl ether extraction. The peak area for the AA reagent peak(s) (including Peak 12) was selectively reduced by a factor of ten, while the extraction recovery for all monosaccharides was not adversely affected as detailed in Table 3.2.

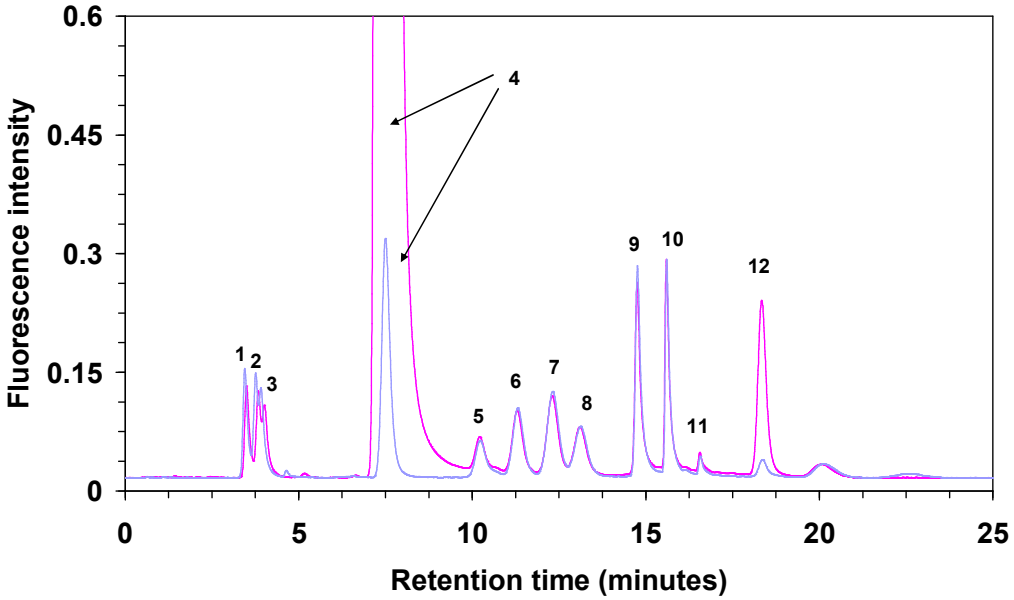

Figure 3.7: Separation of ten AA-monosaccharide derivatives before (pink) and after (dark blue) diethyl ether extraction of excess AA. Chromatographic conditions and peak assignment are as described in Figure 3.5.

3.3.4. Method validation

3.3.4.1. Solid phase extraction (SPE) recovery studies

Given the complex nature of the samples, SPE was used as an initial cleanup step for all samples under study. The samples were subjected to SPE to trap vitamins and peptides but to allow the unretained monosaccharides to run straight through for collection and derivatisation as such components could overload binding sites on the column. The SPE phase selected for study was a C_{18} bonded phase used in non-retentive SPE

mode, since monosaccharides were not expected to be retained due to their hydrophilic nature, relative to peptides and other hydrophobic small molecules. Thus the sample was passed through the SPE bed and unretained monosaccharides immediately collected for analysis. To recover any monosaccharides which were held up within the dead volume of the SPE cartridge, a water rinse was combined with the collected monosaccharide fraction. Rinse volumes ranging from 100 µL to 400 µL were investigated in an effort to maximise recovery while minimising unnecessary dilution effects. While an average recovery value of 62 % was obtained when no water rinse was used, a minimum rinse volume of 100 µL resulted in recovery values > 97 %, as detailed in Table 3.2. The recovery of a known concentration of monosaccharides spiked into a yeastolate sample prior to SPE and derivatisation was also examined and results are also detailed in Table 3.2. The spike recovery was > 90 % for all monosaccharides.

Table 3.2
Recovery (%) studies of monosaccharides from SPE and diethyl ether extractions[a]

Monosaccharide	Solid phase extraction recovery (standards)	Solid phase extraction recovery (spiked sample)	Diethyl ether extraction recovery	Average recovery (combined SPE and solvent extraction, *n* = 6 inj.)
Glucosamine	100	112	114	108
Mannosamine	98	102	111	104
Galactosamine	98	105	118	107
Galactose	102	103	122	109
Mannose	100	91	115	102
Glucose	97	102	117	105
Ribose	98	90	110	99
Xylose	101	91	113	102
Fucose	97	94	104	98
Sialic acid	102	122	109	111

[a] Individual recovery data based upon duplicate injections for all monosaccharides.

3.3.4.2. Linearity

The linear range of the method was examined using standard solutions of the ten monosaccharides. Each monosaccharide was prepared at five different concentrations (n = 5), derivatised and injected in duplicate. The method provided linear standard curves (R^2 > 0.999) for each monosaccharide of interest over a wide concentration range (Table 3.3).

3.3.4.3. Precision

A mixture of ten monosaccharides was derivatised and injected seven times for testing peak area and retention time precision, resulting in % RSD values < 2.2 % and < 0.4 %, respectively as listed in Table 3.3. A yeastolate sample which had previously been found to contain detectable levels of Man, Glc, Xyl and Fuc was selected to study the reproducibility of sample preparation, i.e. SPE and subsequent derivatisation. The sample was divided into five aliquots, which were each individually treated as described in the Experimental section using GlcN as an internal standard. Duplicate injections of each individually processed sample aliquot resulted in peak area % RSD values of 1.9 % (Man), 3.1 % (Xyl), 3.0 % (Fuc) and 2.0 % (Glc).

3.3.4.4. Sensitivity

The limit of detection (LOD) was determined for each monosaccharide by injecting low concentrations of each analyte and extrapolating peak heights to a signal-to-noise (S/N) ratio of 3 (Table 3.3). Based upon a 700 nL injection volume, absolute detection limits were in the 10-350 fmol range for the complete group of monosaccharides investigated.

Table 3.3
Analytical performance criteria

Monosaccharide	Area precision % RSD (*n* = 7)	RT precision % RSD (*n* = 7)	LOD µ µmol.L^{-1} (fmol)[a]	Linear range (µmol.L^{-1})	Linearity (*n* = 5)
Glucosamine	0.7	0.4	0.56 (39)	4.2-83.3	0.999
Mannosamine	0.7	0.4	0.19 (13)	1.4-41.7	0.999
Galactosamine	0.7	0.3	0.37 (26)	1.9-55.6	0.999
Galactose	0.8	0.2	0.37 (26)	1.9-55.6	0.999
Mannose	0.8	0.2	0.37 (26)	2.8-83.3	0.999
Glucose	1.2	0.1	0.37 (26)	2.8-55.6	0.999
Ribose	2.2	0.1	0.37 (26)	1.9-55.6	0.999
Xylose	0.6	0.1	0.14 (10)	1.4-41.7	0.999
Fucose	1.0	0.1	0.14 (10)	1.4-27.8	0.999
Sialic acid	1.3	0.1	0.50 (35)	5-500	0.999

[a] Based on a 700 nL injection.

3.3.5. Monosaccharide profile of yeastolate, basal media and in-process samples

For evaluation purposes, the developed method was applied to the qualitative analysis of monosaccharide profiles in a variety of complex samples supplied from the biopharmaceutical industry. The samples were treated as described in the Experimental section and analysed with the developed method. The presence of monosaccharides in the samples was confirmed by a comparison with a standard chromatogram.

3.3.5.1. Analysis of yeastolate samples

The concentration of yeastolate used in this study was 15 mg.mL^{-1}. The choice of this concentration was based on a preliminary study in which a series of yeastolate sample concentrations ranging from 10 to 100 mg.mL^{-1} was prepared and injected. At the optimum concentration, the target analyte peaks were well separated from each other and from the other peaks.

Figure 3.8 shows the HPLC chromatograms obtained from the analysis of the yeastolate samples, seven samples in total. As it can be seen, all the AA-monosaccharide derivatives were well separated with no observed interference from unknown sample components. All samples were injected in duplicate and Man, Glc, Xyl and Fuc were found in all samples tested. As previously mentioned, GlcN was used as an internal standard in order to minimise possible quantification errors stemming from SPE or derivatisation procedures. Relative peak areas (relative to GlcN) are listed in Table 3.4 and shown graphically in Figure 3.9. From the results obtained the amount of most of the monosaccharides in the yeastolate samples lies within one standard deviation of the mean. The average % RSD for the seven yeastolate samples is 14 % (except for Xyl, % RSD = 37 %). Although the basic monosaccharide chromatographic profile for all batches was very similar (Figure 3.8), the variability in monosaccharide relative peak areas between different lots of yeastolate (particularly for the two high level monosaccharides, Man and Glc) was significant, since it could possibly have an impact on the consistency of product quality. Interestingly, the sample chromatograms showed a number of unidentified peaks eluting between 14 and 17 minutes, which were not present in the standard or blank. Through sample spiking, both Xyl and Fuc could be seen in low levels within the yeastolate, but sialic acid could not be seen under these conditions.

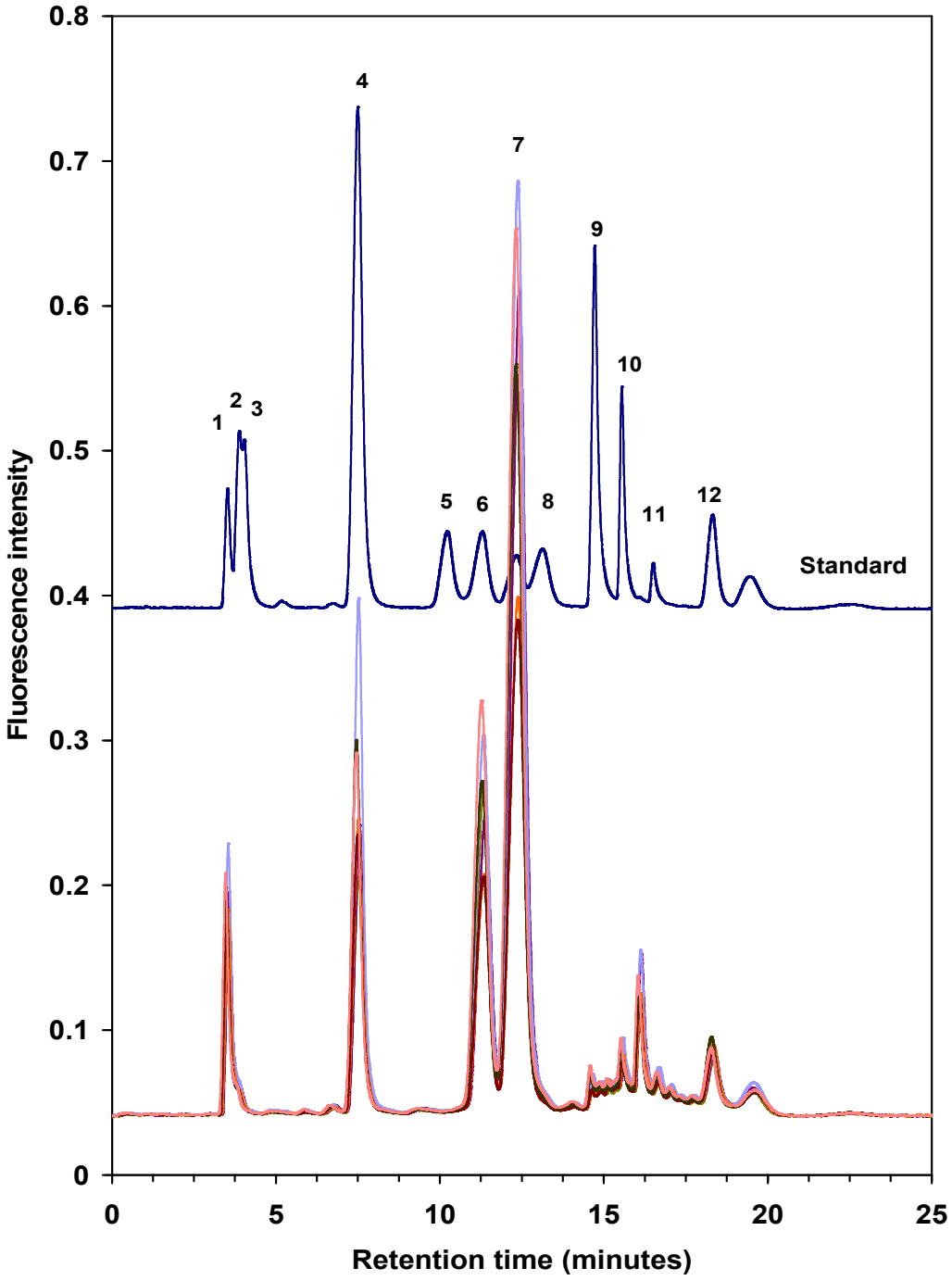

Figure 3.8: HPLC chromatograms of yeastolate samples overlaid with a standard. Chromatographic conditions are as described in Figure 3.5. Peaks: (**1**) GlcN, (**2**) ManN, (**3**) GalN, (**4**) excess AA, (**5**) Gal, (**6**) Man, (**7**) Glc, (**8**) Rib, (**9**) Xyl, (**10**) Fuc, (**11**) sialic acid, and (**12**) blank peak.

Table 3.4
Semi-quantitative evaluation of monosaccharide levels in yeastolate samples. Date of analysis: 11/01/2008.

Sample number	Relative peak area*			
	Man	Glc	Xyl	Fuc
Sample 1	2.98	7.73	0.05	0.11
Sample 2	2.53	8.13	0.04	0.08
Sample 3	2.71	7.71	0.04	0.01
Sample 4	2.22	5.55	0.02	0.10
Sample 5	2.21	5.41	0.020	0.1
Sample 6	2.80	7.34	0.05	0.11
Sample 7	3.32	8.29	0.055	0.12
S.D. (% RSD)	0.40 (15 %)	1.20 (16.7 %)	0.01 (36.8 %)	0.01 (10.2 %)

*Relative peak areas w.r.t GlcN internal standard

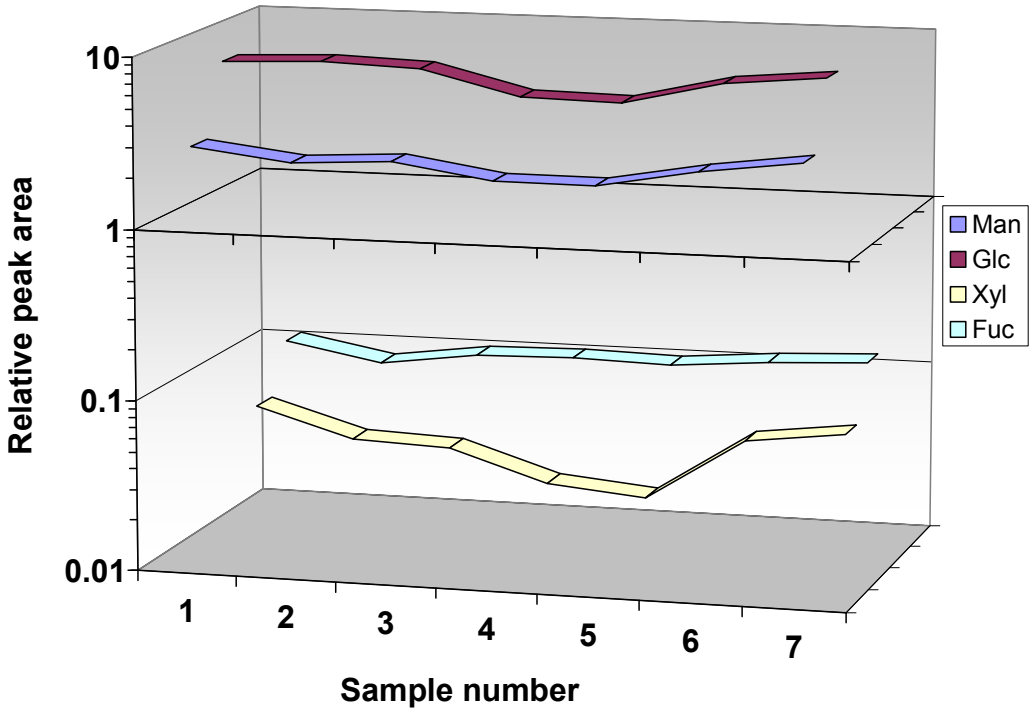

Figure 3.9: Monosaccharide profiles in the yeastolate samples.

3.3.5.2. Analysis of basal media samples

Fourteen samples of basal media were supplied from industry, in this case sourced from two different manufacturing facilities producing the same biotherapeutic (seven samples from each facility, referred to hereafter as ‘‘**Lot A**’’ and ‘‘**Lot B**’’). Since the majority of samples were supplemented with relatively high levels of Glc, two dilution factors were employed for sample analysis (1/5 for all monosaccharides, except Glc for which 1/400 dilution factor was used). Figures 3.10 and 3.11 (**a** and **b**) show an overlay of HPLC chromatograms for basal media (**Lot A** and **Lot B**) samples with small and large dilution factors, respectively. The samples were treated as described earlier and injected in the HPLC system in duplicate. The presence of the target analytes was confirmed by a comparison with a standard chromatogram. Relative peak areas of all monosaccharides existing in the samples were quantified with respect to GlcN internal standard and the results are listed in Table 3.5. Figures 3.12, 3.13 and 3.14 show the intra- and inter-lot profile of each monosaccharide in these samples. All samples were found to contain Man, Glc and sialic acid. As shown in Table 3.5 and Figure 3.11(**b**), Sample **B1** was the only sample containing detectable levels of Gal as well as over twice the amount of Glc relative to all other samples from **Lot B**. Although Glc levels were very high relative to Man for all samples tested, quantification of Man was still possible. Interestingly, mean Glc and Man levels were notably higher in the samples within **Lot B** relative to **Lot A**. The % RSD for Glc was 10 % in **Lot A** compared with 68 % in **Lot B**. Finally, there was a large variation in levels of free sialic acid present in both lots of samples (% RSD: 112 % for **Lot A** and 65 % for **Lot B**).

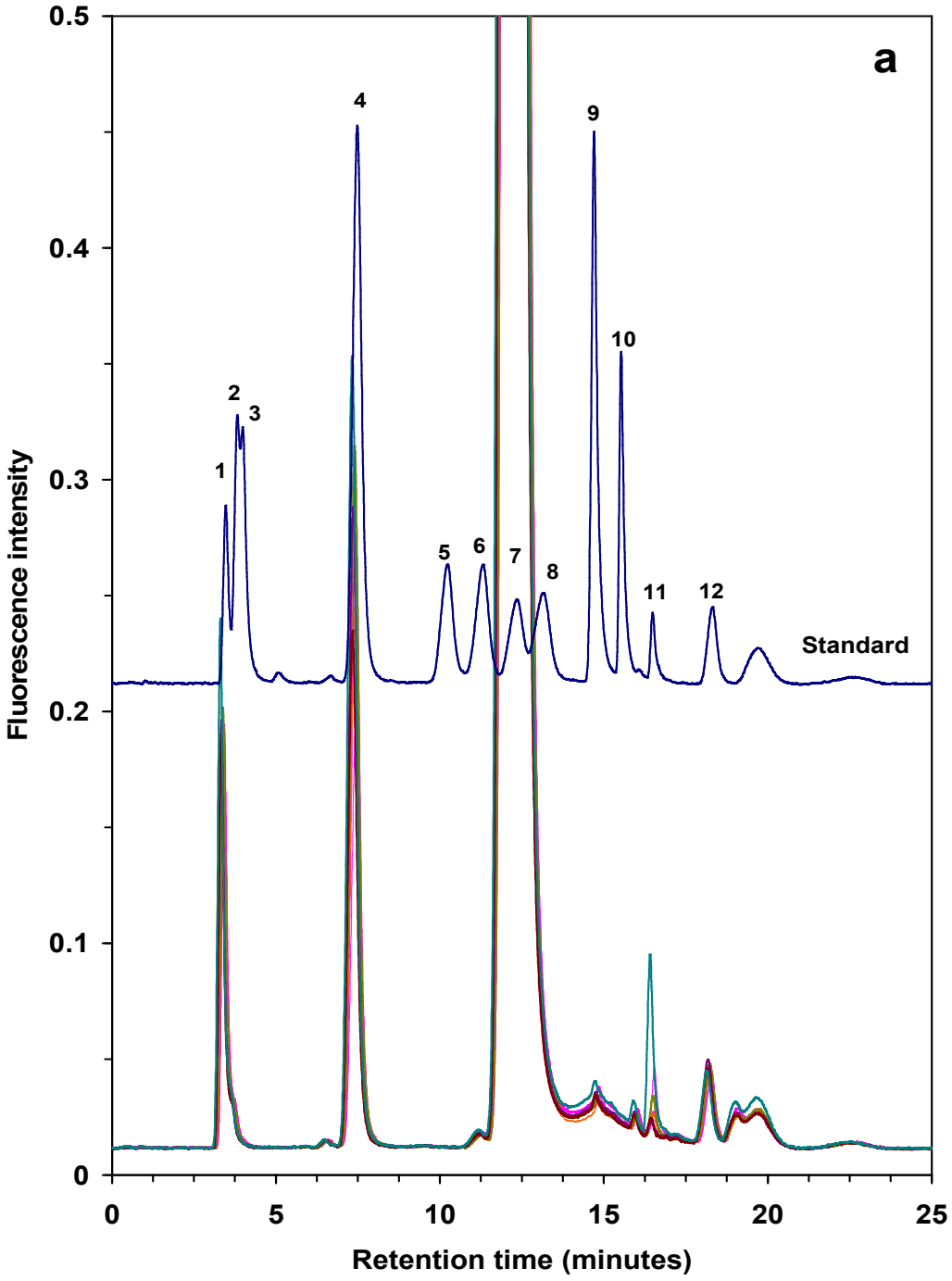

Figure 3.10(a): HPLC chromatograms of **Lot A** of basal media samples (diluted by a factor of 1/5) overlaid with a standard. Chromatographic conditions are as described in Figure 3.5. Peaks: (**1**) GlcN, (**2**) ManN, (**3**) GalN, (**4**) excess AA, (**5**) Gal, (**6**) Man, (**7**) Glc, (**8**) Rib, (**9**) Xyl, (**10**) Fuc, (**11**) sialic acid, and (**12**) blank peak.

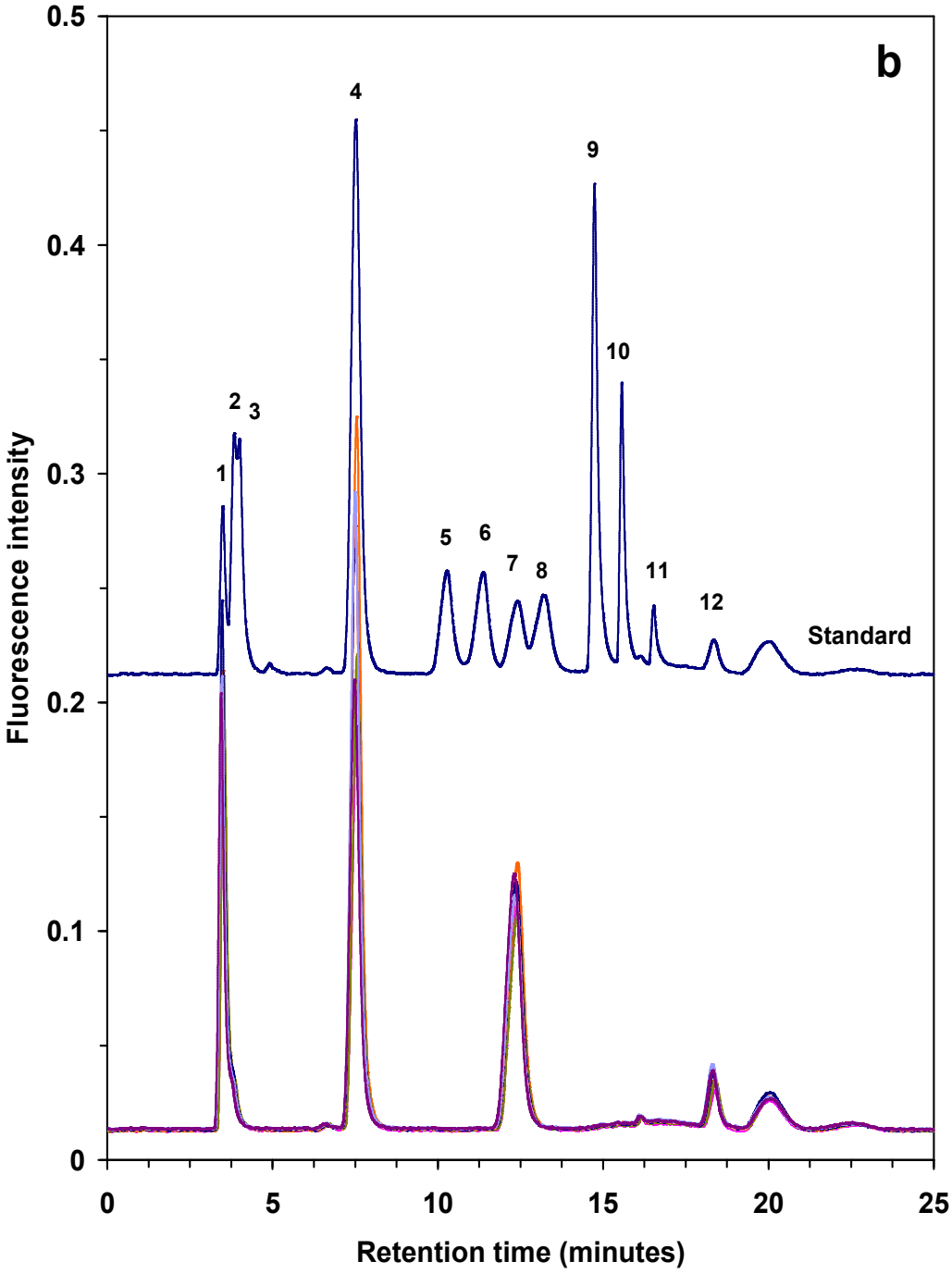

Figure 3.10(b): HPLC chromatograms of **Lot A** of basal media samples (diluted by a factor of 1/400) overlaid with a standard. Chromatographic conditions are as described in Figure 3.5. Peaks: (**1**) GlcN, (**2**) ManN, (**3**) GalN, (**4**) excess AA, (**5**) Gal, (**6**) Man, (**7**) Glc, (**8**) Rib, (**9**) Xyl, (**10**) Fuc, (**11**) sialic acid, and (**12**) blank peak.

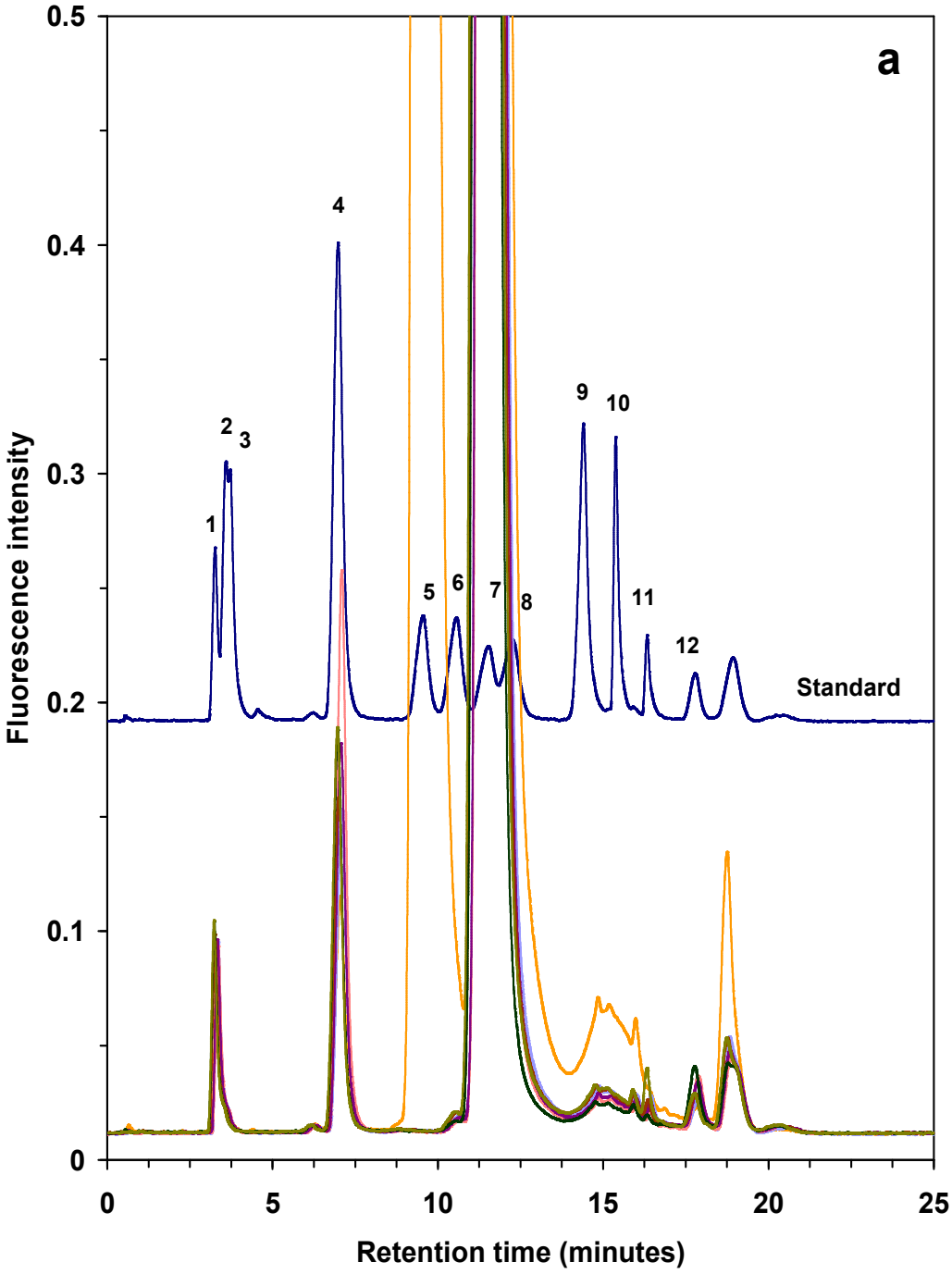

Figure 3.11(a): HPLC chromatograms of **Lot B** of basal media samples (diluted by a factor of 1/5) overlaid with a standard. Chromatographic conditions are as described in Figure 3.5. Peaks: (**1**) GlcN, (**2**) ManN, (**3**) GalN, (**4**) excess AA, (**5**) Gal, (**6**) Man, (**7**) Glc, (**8**) Rib, (**9**) Xyl, (**10**) Fuc, (**11**) sialic acid, and (**12**) blank peak.

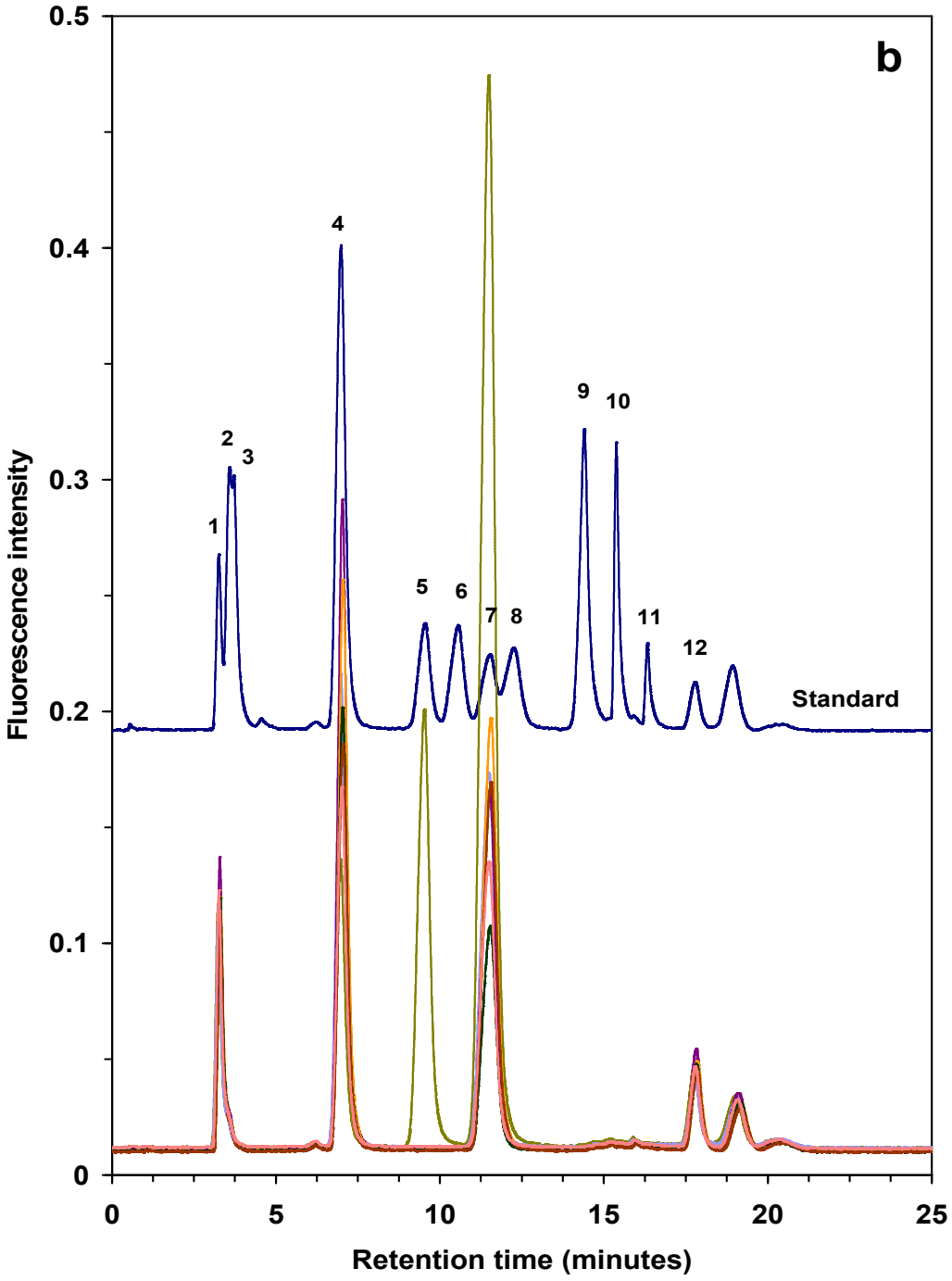

Figure 3.11(b): HPLC chromatograms of **Lot B** of basal media samples (diluted by a factor of 1/400) overlaid with a standard. Chromatographic conditions are as described in Figure 3.5. Peaks: (**1**) GlcN, (**2**) ManN, (**3**) GalN, (**4**) excess AA, (**5**) Gal, (**6**) Man, (**7**) Glc, (**8**) Rib, (**9**) Xyl, (**10**) Fuc, (**11**) sialic acid, and (**12**) blank peak.

Table 3.5
Semi-quantitative evaluation of monosaccharide levels in basal media samples. Date of analysis: 14-16/01/2008.

Sample number	Relative peak area*			
	Gal	Man	Glc	Sialic acid
Basal media samples (Lot A)				
Sample A1	ND**	0.01	1.28	0.13
Sample A2	ND**	0.02	1.33	0.03
Sample A3	ND**	0.01	1.11	0.04
Sample A4	ND**	0.01	1.07	0.07
Sample A5	ND**	0.02	1.21	0.03
Sample A6	ND**	0.01	1.17	0.03
Sample A7	ND**	0.02	1.38	0.30
S.D. **(% RSD)**		0.0015 (10.7 %)	0.116 (9.5 %)	0.10 (112 %)
Basal media samples (Lot B)				
Sample B1	4.8	ND**	10.2	0.18
Sample B2	ND**	0.03	3.69	0.11
Sample B3	ND**	0.04	2.56	0.05
Sample B4	ND**	0.04	2.84	0.08
Sample B5	ND**	0.04	3.97	0.08
Sample B6	ND**	0.03	1.99	0.03
Sample B7	ND**	0.04	3.50	0.20
S.D. **(% RSD)**		0.0046 (12.8 %)	2.77 (67.5 %)	0.07 (64.7 %)

*Relative peak areas w.r.t GlcN internal standard
**None detected

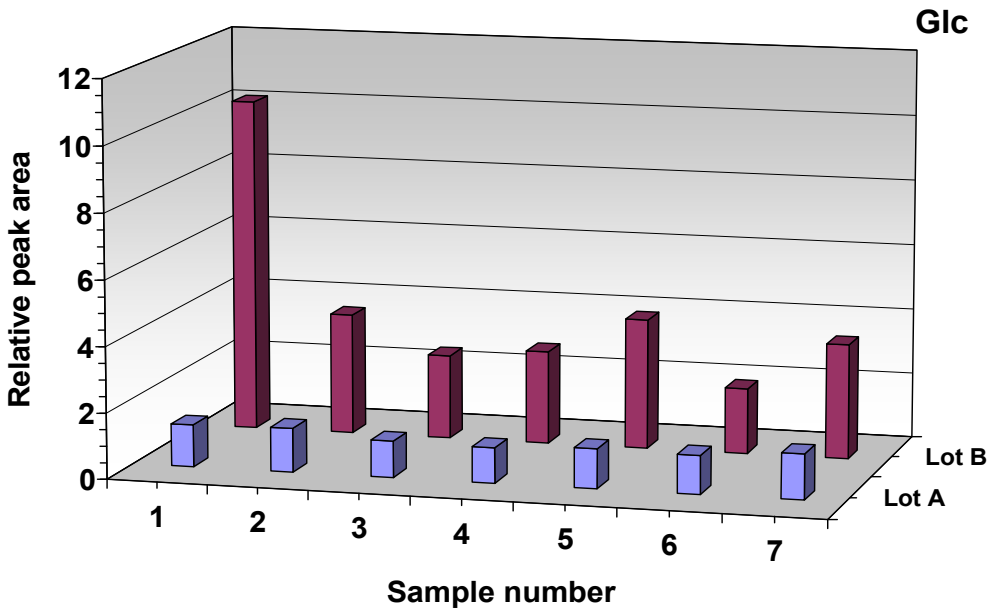

Figure 3.12: Glc profile in the basal media samples.

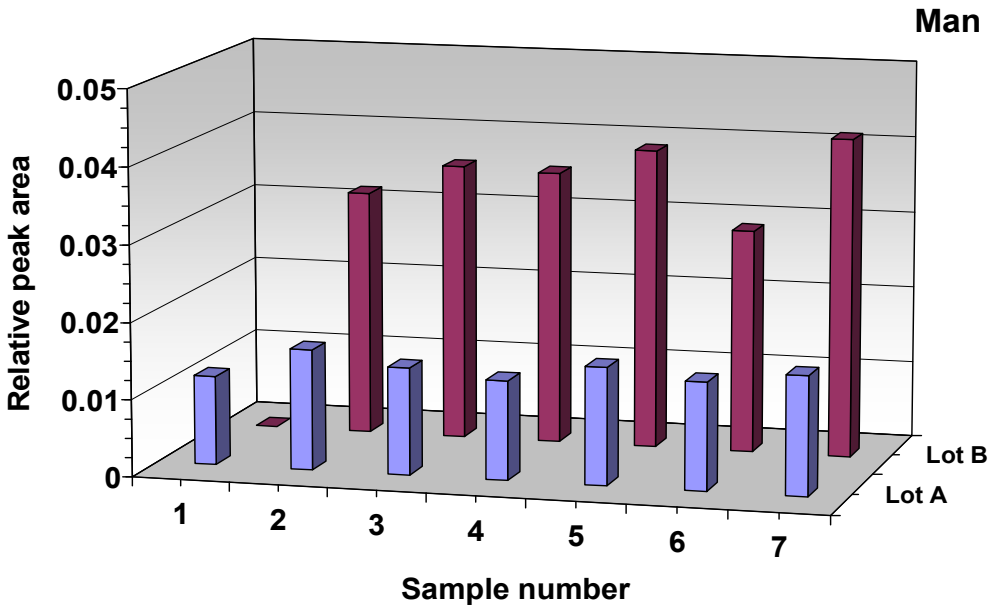

Figure 3.13: Man profile in the basal media samples.

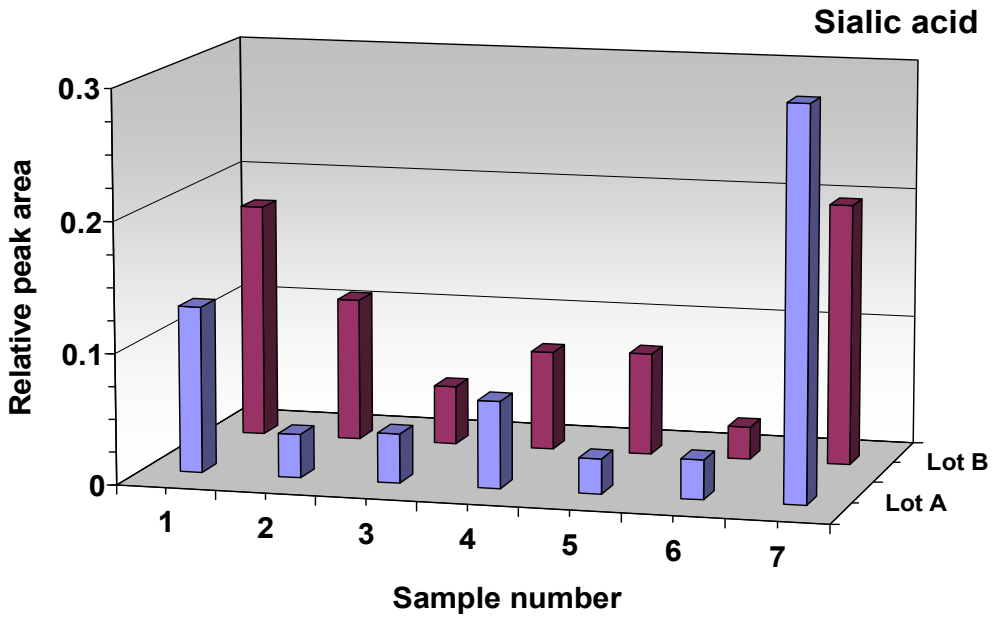

Figure 3.14: Sialic acid profile in the basal media samples.

3.3.5.3. Analysis of in-process samples

Figure 3.15 (**a** and **b**) shows chromatograms of in-process samples (24 samples in total). The samples sourced from two different manufacturing facilities producing the same protein. These in-process samples were collected from fed-batch CHO cell cultures at different time-points as described in Table 3.1. They were obtained prior to and after bioreactor inoculation as described earlier. The samples were treated and derivatised using the optimised procedure and injected in duplicate. The utility of the developed method for the in-process determination of monosaccharide levels in a bioreactor is clearly demonstrated in Figure 3.15. The displayed chromatograms demonstrate the potential of the method for monitoring changing levels of Gal and Glc over time. After the treatment of the samples under the optimised conditions, Glc was found in all samples tested and Gal and Man in some of them. Relative peak areas are listed in Table 3.6. Figures 3.16, 3.17 and 3.18 show the intra- and inter-lot profiles of each monosaccharide existing in the samples. The graphs show a close similarity between lots indicating a clearly well controlled process. In addition, Figure

3.19 illustrates that trace levels of Man can still be determined in in-process samples which contain significantly higher levels of Gal and Glc.

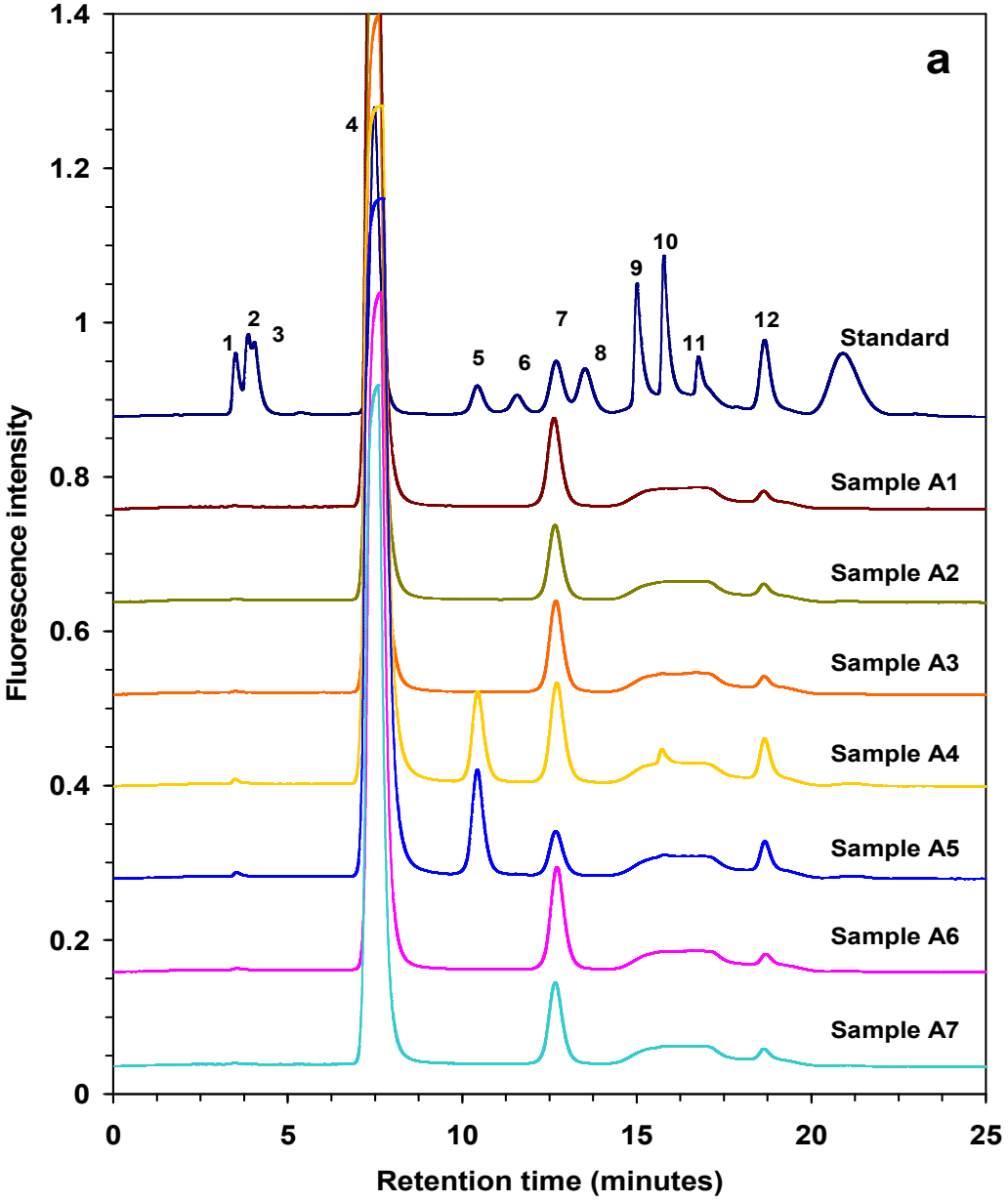

Figure 3.15(a): HPLC chromatograms of **Lot A** of in-process samples (diluted to different extents) overlaid with a standard. Chromatographic conditions are as described in Figure 3.5. Peaks: (**1**) GlcN, (**2**) ManN, (**3**) GalN, (**4**) excess AA, (**5**) Gal, (**6**) Man, (**7**) Glc, (**8**) Rib, (**9**) Xyl, (**10**) Fuc, (**11**) sialic acid, and (**12**) blank peak.

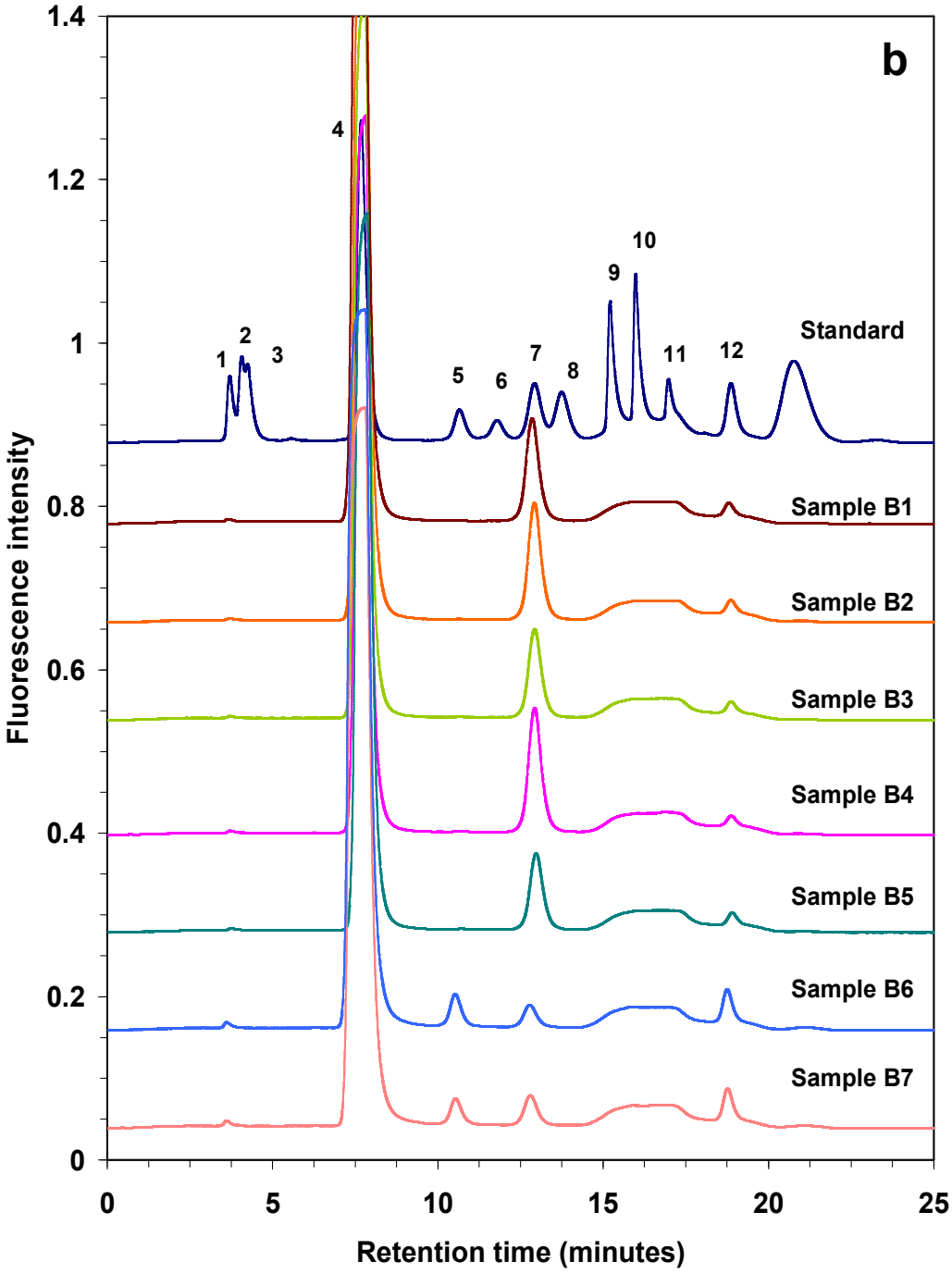

Figure 3.15(b): HPLC chromatograms of **Lot B** of in-process samples (diluted to different extents) overlaid with a standard. Chromatographic conditions are as described in Figure 3.5. Peaks: (**1**) GlcN, (**2**) ManN, (**3**) GalN, (**4**) excess AA, (**5**) Gal, (**6**) Man, (**7**) Glc, (**8**) Rib, (**9**) Xyl, (**10**) Fuc, (**11**) sialic acid, and (**12**) blank peak.

Table 3.6
Semi-quantitative evaluation of monosaccharide levels in in-process samples. Date of analysis: 05-06/03/2008.

Sample number (dilution factor)	**Relative peak area***		
	Gal	**Man**	**Glc**
In-process samples (Lot A)			
Sample A1 (50)	ND**	0.020	153.2
Sample A2 (50)	ND**	0.018	170.5
Sample A3 (50)	ND**	0.031	111.4
Sample A4 (50)	ND**	0.015	137.6
Sample A5 (50)	ND**	0.044	151.5
Sample A6 (50)	ND**	0.015	159.8
Sample A7 (50)	ND**	0.034	144.8
Sample A8 (50)	0.025	0.020	149.8
Sample A9 (50)	0.008	0.024	130.4
Sample A10 (20)	1.96	0.058	131.5
Sample A11 (20)	17.1	0.41	17.6
Sample A12 (20)	16.9	0.43	15.1
In-process samples (Lot B)			
Sample B1 (50)	ND**	0.016	148.3
Sample B2 (50)	ND**	0.014	117.6
Sample B3 (50)	ND**	0.043	89.7
Sample B4 (50)	ND**	0.017	104.6
Sample B5 (50)	ND**	0.044	76.9
Sample B6 (50)	ND**	0.015	132.5
Sample B7 (50)	ND**	0.039	81.8
Sample B8 (50)	ND**	0.014	133.3
Sample B9 (50)	ND**	0.031	103.3
Sample B10 (20)	2.25	0.091	14.1
Sample B11 (20)	6.92	0.081	9.2
Sample B12 (20)	7.78	0.094	5.8

*Relative peak areas w.r.t GlcN internal standard
**None detected

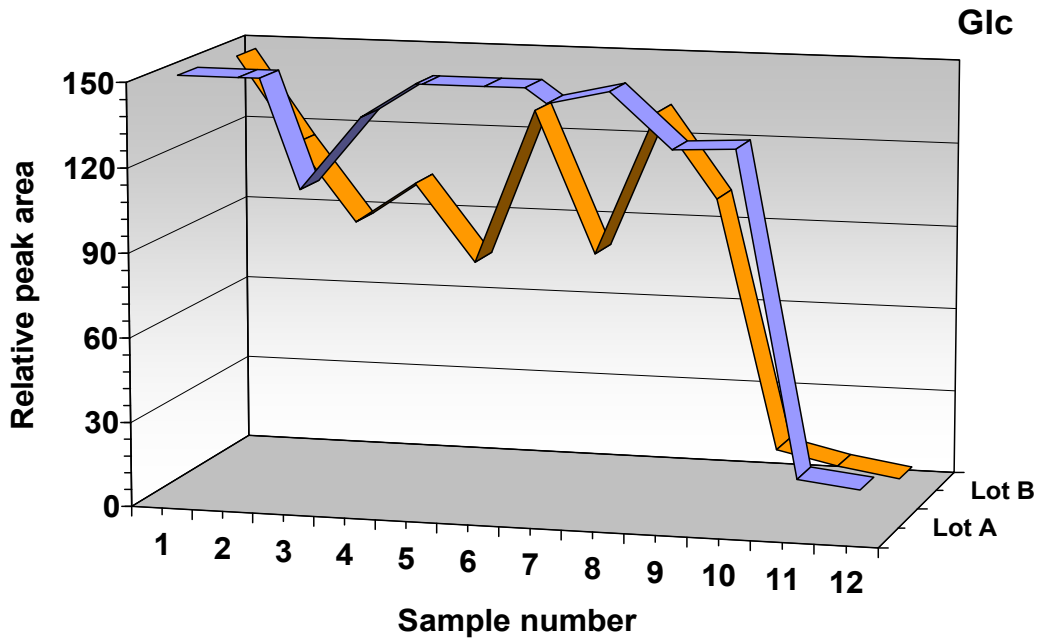

Figure 3.16: Glc profile for two different lots of biofermentetion in-process broth samples.

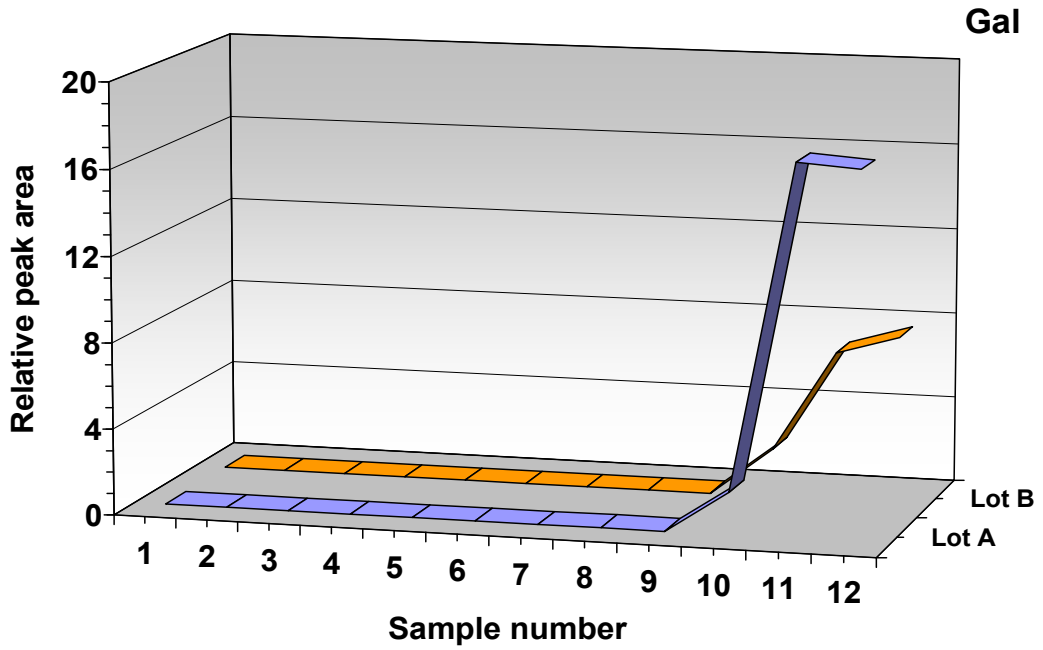

Figure 3.17: Gal profile for two different lots of biofermentetion in-process broth samples.

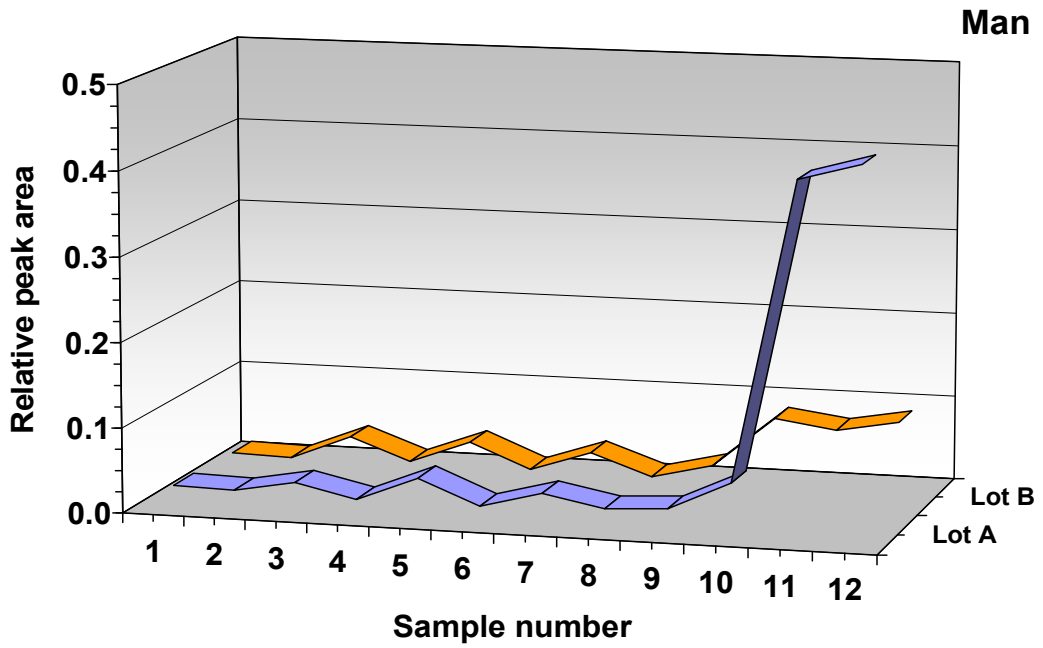

Figure 3.18: Man profile for two different lots of biofermentetion in-process broth samples.

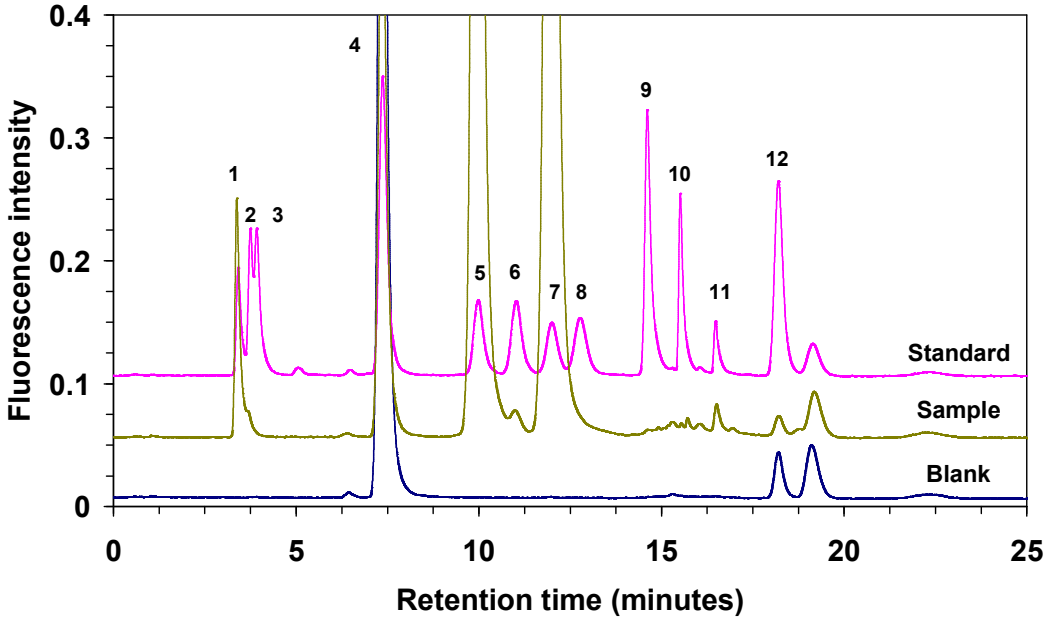

Figure 3.19: HPLC chromatograms obtained for an in-process sample overlaid with a standard and a blank. Chromatographic conditions are as described in Figure 3.5. Peaks: (**1**) GlcN, (**2**) ManN, (**3**) GalN, (**4**) excess AA, (**5**) Gal, (**6**) Man, (**7**) Glc, (**8**) Rib, (**9**) Xyl, (**10**) Fuc, (**11**) sialic acid, and (**12**) blank peak.

3.4. Conclusion

A relatively rapid, robust RPLC-FLD based method was developed for the determination (both qualitative and semi-quantitative) of up to 10 monosaccharides (glucosamine, mannosamine, galactosamine, galactose, mannose, glucose, ribose, xylose, fucose and sialic acid) in a range of complex samples originating from the biofermentation production process within the biopharmaceutical industry. Standard analytical performance criteria were used for evaluation purposes, with the method having been found to be both linear and precise, and with LODs meeting the requirements for routine and potentially process monitoring of these important solutes, for both process optimisation and quality control. This work demonstrates for the first time a single chromatographic method directly applicable to analysis of all three sample matrices and provides the ever increasing biopharmaceutical industry with a new assay to investigate both material quality and complex in-process biochemical processes and interactions, currently not fully understood.

3.5. References

[1] T. M. Larson, M. Gawlitzek, H. Evans, U. Albers, J. Cacia, *Biotechnol. Bioeng.* 2002, **77**, 253 - 563.

[2] A. O. Kirdar, K. D. Green, A. S. Rathore, *Biotechnol. Prog.* 2008, **24**, 720 - 726.

[3] R. Fike, B. Dadey, R. Hassett, R. Radominski, D. Jayme, D. Cady, *Cytotechnology* 2001, **36**, 33 - 39.

[4] C. Rumpel, M. Dignac, *Soil Biol. Biochem.* 2006, **38**, 1478 - 1481.

[5] V. P. Hanko, J. S. Rohrer, *Anal. Biochem.* 2000, **283**, 192 - 199.

[6] R. Andersen, A. Sørensen, *J. Chromatogr. A* 2000, **897**, 195 - 204.

[7] P. Kerhervé, B. Charrière, F. Gadel, *J. Chromatogr. A* 1995, **718**, 283 - 289.

[8] L. Liang, P. Zhang, Y. Cai, S. Mou, *Chin. J. Anal. Chem.* 2006, **34**, 1371 - 1374.

[9] C. Panagiotopoulos, R. Sempéré, R. Lafont, P. Kerhervé, *J. Chromatogr. A* 2001, **920**, 13 - 22.

[10] A. Meyer, H. Fischer, Y. Kuzyakov, K. Fischer, *J. Plant Nutr. Soil Sci.* 2008, **171**, 917 - 926.

[11] K. Račaityté, S. Kiessig, F. K. álmán, *J. Chromatogr. A* 2005, **1079**, 354 - 365.

[12] S. Santos, A. Duarte, V. Esteves, *Talanta* 2007, **72**, 165 - 171.

[13] S. Rovio, J. Yli-Kauhaluoma, H. Siren, *Electrophoresis* 2007, **28**, 3129 - 3135.

[14] S. Rovio, H. Simolin, K. Koljonen, H. Siren, *J. Chromatogr. A* 2008, **1185**, 139 - 144.

[15] A. Jarmeus, A. Emmer, *Chromatographia* 2008, **67**, 151 - 155.

[16] Z. Ying, H. Lin-Juan, W. Zhong-Fu, *Chin. J. Chem.* 2007, **25**, 1522 - 1528.

[17] K. Anumula, *Anal. Biochem.* 1994, **220**, 275 - 283.

[18] H. Kakita, H. Kamishima, K. Komiya, Y. Kato, *J. Chromatogr. A* 2002, **961**, 77 - 82.

[19] Y. Yuh, J. Chen, C. Chiang, *J. Pharm. Biomed. Anal.* 1998, **16**, 1059 - 1066.

[20] W. Wu, K. Hamase, M. Kiguchi, K. Yamamoto, K. Zaitsu, *Anal. Sci.* 2000, **16**, 919 - 922.

[21] D. Gomis, D. Tamayo, J. Alonso, *Anal. Chim. Acta* 2001, **436**, 173 - 180.

[22] H. Kwon, J. Kim, *Anal. Biochem.* 1993, **215**, 243 - 252.

[23] X. Yang, Y. Zhao, Q. Wang, H. Wang, Q. Mei, *Anal. Sci.* 2005, **21**, 1177 - 1180.

[24] W. J. Schmidt, W. Kuhlmann, K. Schugerl, *Biotechnology* 1985, **21**, 78 - 84.

[25] G. A. Marko-Varga, *Anal. Chem.* 1989, **61**, 831 - 838.

[26] G. Marko-Varga, E. Dominguez, B. Hahn-Hagerdal, L. Gorton, H. Irth, G. J. De Long, R. W. Frei, U. A. Th. Brinkman, *J. Chromatogr. A* 1990, **523**, 173 - 188.

[27] H. Liden, T. Buttler, H. Jeppsson, G. Marko-Varga, J. Volc, L. Gorton, *Chromatographia* 1998, **47**, 501 - 508.

[28] Q. Wang, Y. Fang, *J. Chromatogr. B: Anal. Technol. Biomed. Life Sci.* 2004, **812**, 309 - 324.

[29] S. Honda, E. Akao, S. Suzuki, M. Okuda, K. Kakehi, J. Nakamura, *Anal. Biochem.* 1989, **180**, 351 - 357.

[30] K. Anumula, *Anal. Biochem.* 2000, **283**, 17 - 26.

Chapter 4

Rapid and sensitive chromatographic determination of total sialic acid in bio-pharma fermentation media samples

4.1. Introduction

Sialic acids are a family of nine-carbon carboxylated monosaccharides and are generally found in the terminal position of the carbohydrate chains of glycoconjugates (glycoproteins, glycolipids and lipopolysaccharides); they are rarely found in free form (3%) [1, 2]. Sialic acids have many biological roles and the importance of sialic acids to a glycoprotein's half-life emphasises the need to determine sialic acid content of a glycoprotein when examining its function and activity as therapeutic [3]. There are more than 40 compounds have been associated to sialic acid family [4]. However, the main representative and the most abundant forms of sialic acid are the acylated compound, which are known as N-acetylneuraminic acid (NANA), and N-glycolylneuraminic acid (NGNA), where a glycolyl group is bound to the amino group at C5 (Figure 4.1) [5].

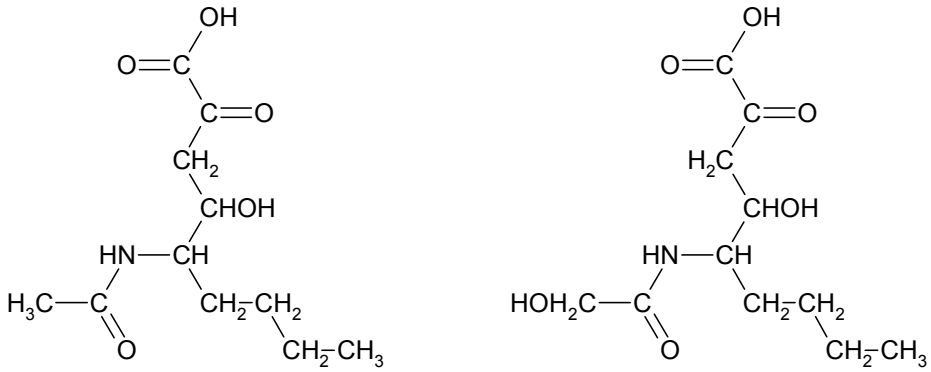

N-acetylneuraminic acid

N-glycolylneuraminic acid

Figure 4.1: Chemical structures of N-acetylneuraminic acid and N-glycolylneuraminic acid.

Sialic acid levels in biological samples have been determined using various methods. Traditional determination has been performed by a number of colorimetric methods. The most commonly used are the resorcinol-based method [6] and the thiobarbituric acid (TBA) method [7]. However, the TBA

method is preferable due to its specificity and sensitivity [8]. This method determines free sialic acids only; bound sialic acids have to be released first utilising acid hydrolysis [9, 10] or enzymatic hydrolysis [11]. The TBA does not distinguish the two types of sialic acid because both of them give β-formylpyruvic acid upon oxidation with periodic acid [12]. Therefore, it determines the total sialic acid. The TBA method was first introduced by Waravdekar and Saslaw [13] for the determination of 2-deoxyribose which produces malonaldehyde upon periodate oxidation, which then reacts with TBA to form a red complex with an absorption maximum at 532 nm. The method was later modified for the assay of sialic acids as described by Warren [7] and Aminoff [14]. The product of sialic acid oxidation is β-formylpyruvic acid which forms a red complex after derivatisation with TBA that has an absorbance maximum at 549 nm.

Sialic acids have also been determined using several other instrumental techniques such as GC [15], HPAEC-PAD [3, 16, 17], CE [18-20] and HPLC using different detection techniques [12, 21-30] and liquid chromatography tandem mass spectrometry (LC-MS/MS). Rohrer *et al.* [3] described a HPAEC-PAD method for the analysis of sialic acid content in glycoproteins. However, this technique in general suffers from other sample components interfering in complex matrices such as biological samples [31, 32]. The TBA method has been adapted to HPLC for sialic acid determination in biological samples for enhanced sensitivity and reduced interference because sialic acids are usually present at trace levels in such complex matrices. The derivatised sialic acid was separated from other interfering substances on a C_{18} reversed phase column [12, 21, 22]. Anumula [27] reported a HPLC method for the determination of sialic acids in which sialic acids were derivatised with *o*-phenylenediamine (OPD) and monitored using fluorescence detection. The method was used for the analysis of sialic acid in glycoproteins. Martín *et al.* [28] also described a HPLC method for sialic acid determination in which they used another derivatisation agent, i.e. 1,2-diamino-4,5-methylenedioxybenzene (DMB),

and the method was applied to determine sialic acid content in infant formulas.

This Chapter describes a rapid, sensitive and reproducible method specifically for the quantitative determination of total sialic acid in a range of complex biological samples employing TBA as pre-column tagging agent after the oxidation of sialic acid with periodic acid. The derivatised sialic acid was separated from 2-deoxy-D-ribose and the other components in less than 90 seconds utilising a short C_{18} monolithic column. The method was successfully applied to quantify sialic acid in a range of complex samples, e.g. yeastolate powders, basal media and in-process samples supplied by Bristol-Myers Squibb.

4.2. Experimental

4.2.1. Reagents and materials

N-acetylneuraminic acid (NANA, 98 %), 2-thiobarbituric acid (TBA, 98 %), periodic acid (98 %), sodium hydroxide (NaOH, 98 %), sodium phosphate monobasic monohydrate (98-102 %), sodium phosphate dibasic (99 %), 2-deoxy-D-ribose (97 %), sodium thiosulfate (98 %) and trifluoroacetic acid (TFA, 98 %) were purchased from Sigma-Aldrich (Tallaght, Dublin, Ireland). Methanol (MeOH) was of HPLC grade and purchased from Labscan (Dublin, Ireland). All chemicals were used as received, without any further purification.

4.2.2. Instrumentation

All instrumentation used was as described in Section 3.2.2 with the exception of the following. The derivatives were separated on a 4.6 mm × 100 mm Chromolith Flash RP-18e monolith column (**Column A**) and a 4.6

mm × 25 mm Chromolith Flash RP-18e monolith column (**Column B**) at flow rates of 2.5 $mL.min^{-1}$ and 4.5 $mL.min^{-1}$, respectively, and a column temperature of 45 ^{o}C for both columns. The separation was performed using TFA (pH 2.3, 0.05 %) as mobile phase A and MeOH as mobile phase B. The separation mode for **Column A** was isocratic at 20 % mobile phase B, whereas for **Column B** was used with a gradient of: 0-30 seconds (11 % B), 30-39 seconds (11-35 % B) and 39.6-90 seconds (11 % B). The injection volume was 100 µL and the derivatives were monitored at 549 nm.

4.2.3. Sample preparation

All samples described in Section 3.2.3 were analysed for sialic acid utilising the method described in this chapter. Here, the samples were dissolved and diluted using sodium phosphate buffer (pH 6.5, 10 $mmol.L^{-1}$). For yeastolate powder samples, 15 mg of the sample was dissolved in 1 mL of phosphate buffer whereas for the analysis of the liquid samples (basal media and in-process samples), 150 µL of the sample was diluted by a factor of 2 using phosphate buffer.

4.2.4. Sample cleanup by solid phase extraction (SPE)

All samples obtained from Section 4.2.3 were subjected to clean up using a C_{18} SPE cartridge. The cartridge was first conditioned with 1 mL of MeOH followed by 1 mL of water. Then 250 µL of the sample was passed through the cartridge and collected in a clean polypropylene centrifuge tube, followed by a further 80 µL phosphate buffer (pH 6.5, 10 $mmol.L^{-1}$) which was collected and combined with the 250 µL.

4.2.5. Labelling of sialic acid with TBA

4.2.5.1. Oxidation of sialic acid

300 µL of standard/sample collected in Section 4.2.4 was placed in a 2 mL screw-top polypropylene sample tube. Sialic acid was oxidised by the addition of 25 µL of 50 mmol.L^{-1} periodic acid and 40 µL of 0.22 mol.L^{-1} HCl. The tube was shaken and placed in a water bath at 37 ^{o}C for 40 minutes. Then the oxidation was terminated by the addition of 60 µL of 2 % sodium thiosulfate and shaking the sample tube until the yellow-brown colour appeared upon the addition of thiosulfate had vanished. The oxidation is shown in Figure 4.2.

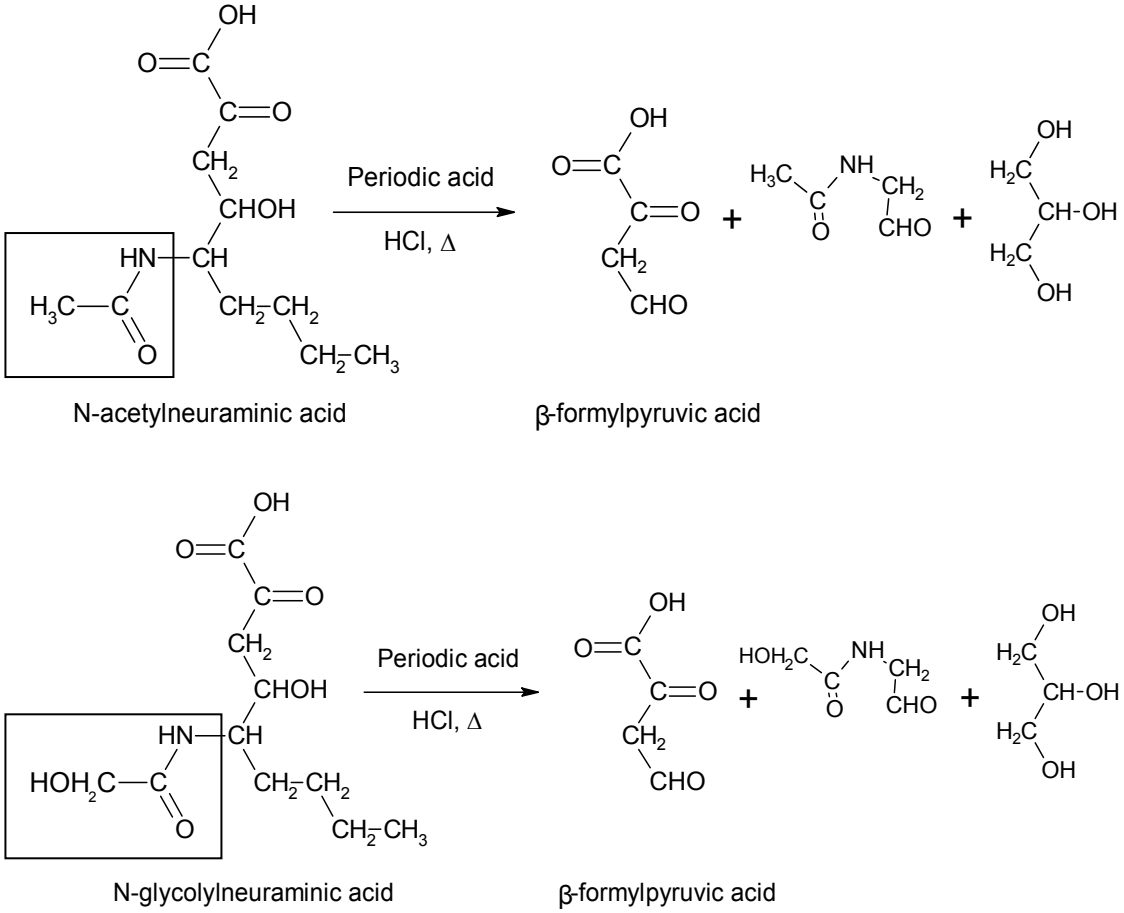

Figure 4.2: Reaction scheme shows the oxidation of N-acetylneuraminic acid and N-glycolylneuraminic acid with periodic acid.

4.2.5.2. Derivatisation of sialic acid

To the oxidised standard/sample obtained from Section 4.2.5.1, 250 µL of 0.1 mol.L^{-1} TBA prepared in 70 mmol.L^{-1} NaOH was added. The sample tube was shaken and heated in a water bath at 100 ^{o}C for 8 minutes. After that the tube was removed and placed in an ice bath for 5 minutes. The derivatised sample was then centrifuged and the supernatant was transferred to an HPLC vial for injection.

4.3. Results and discussion

4.3.1. Optimisation of chromatographic conditions

Throughout this study, NANA was used as a representative of sialic acid. The separation of the sialic acid peak from 2-deoxy-D-ribose peak, which is a possible source of interference as described in Section 4.3.4.2, was performed on an Agilent 1200 series RRLC chromatograph using a monolithic column. One of the advantages of monolithic materials that they can be operated at high flow rates with low backpressures due to the porous structure of the monolith which leads to rapid sample analysis as achieved in this study.

Initially, the separation was developed using **Column A**. The effective parameters on the separation such as the pH of the mobile phase, the % of the organic solvent and the column temperature were investigated.

The effect of the mobile phase pH was studied in the range 2.3 to 4.3. Even though the range was narrow, the influence of the pH on the retention factor of sialic acid was significant. The retention factor of sialic acid increased from 0.85 for pH 4.3, to over 4.3 for pH 2.3 at a column temperature of 25 ^{o}C and 5 % MeOH in the mobile phase. Decreasing the pH to 2.3 and thus increasing the retention factor allowed the use of

elevated column temperatures and higher organic solvent which lead to sharper peaks and lower running times as described below.

The effect of the organic solvent in the mobile phase was examined. The peaks were eluted earlier using ACN instead of MeOH. However, the resolution of sialic acid both from the void peak and 2-deoxy-D-ribose was low, thus using less organic solvent in the mobile phase, low column temperatures and low mobile phase pH are required to improve the resolution. Instead, using MeOH as organic modifier allowed running the samples at high column temperatures and high organic solvent ratio which sharpened the peaks as indicated in Figure 4.3.

Figure 4.4 shows the effect of the column temperature upon the separation. In general, decreasing the column temperature lead to an increase in the retention times and broadening of the peaks. Therefore, the column temperature of 45 ^{o}C was selected as an optimum temperature.

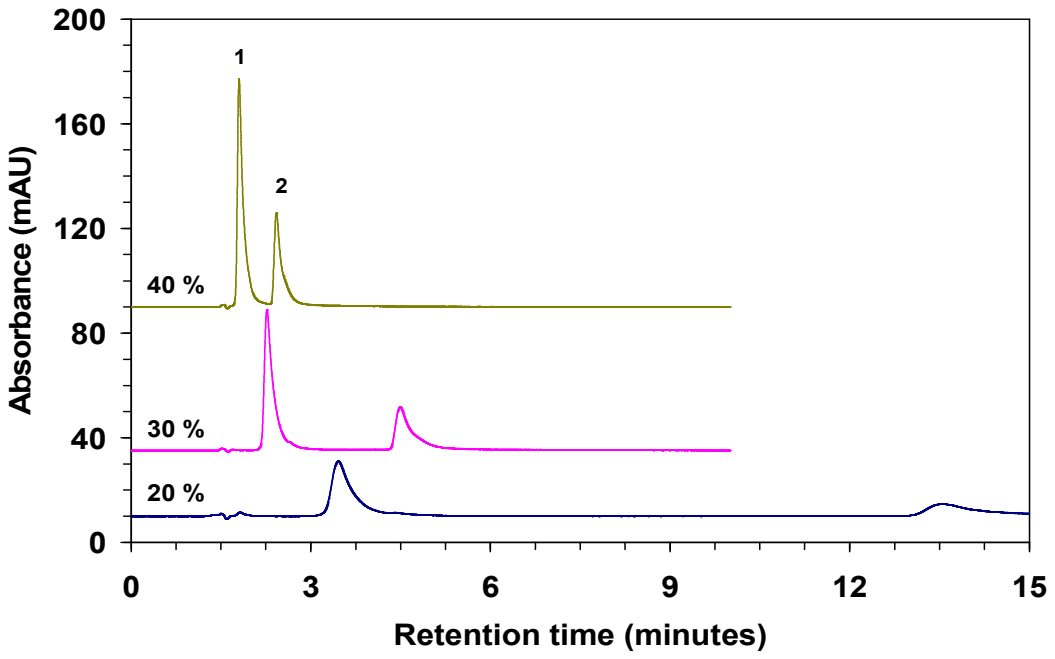

Figure 4.3: The effect of MeOH percentage on the separation between sialic acid (**1**) and 2-deoxy-D-ribose (**2**). Column: **Column A**. Mobile phase: 0.05 % TFA, pH 2.3/MeOH. Elution mode: isocratic. Flow rate: 1 mL.min^{-1}. Injection volume: 10 µL. Column temperature: 25 ^{o}C. Detection @ 549 nm.

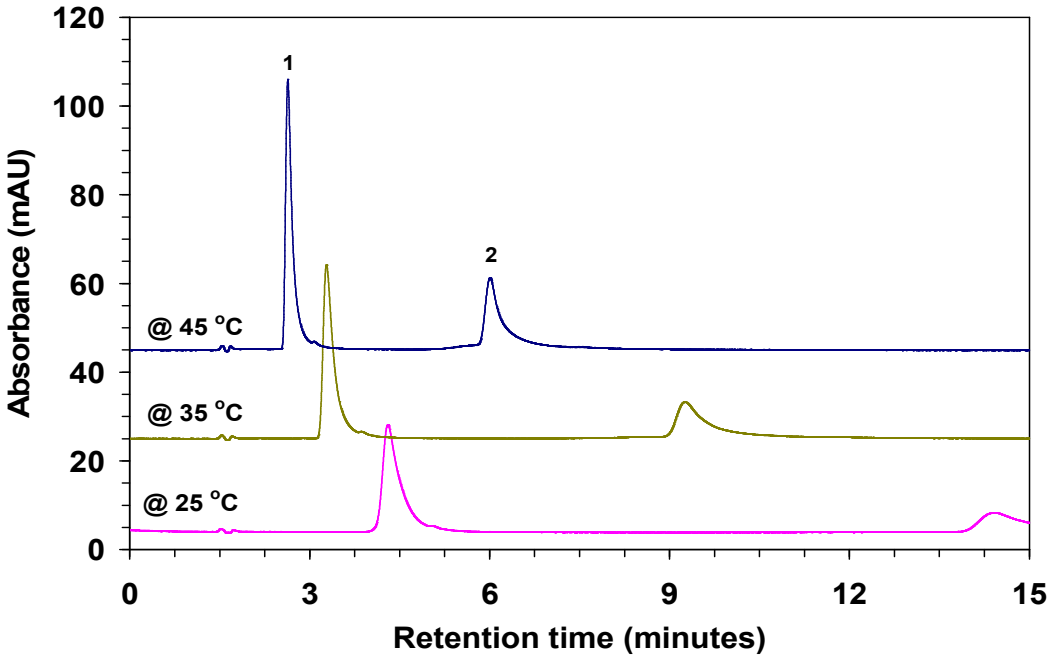

Figure 4.4: The effect of column temperature on the separation between sialic acid (**1**) and 2-deoxy-D-ribose (**2**). Chromatographic conditions are as described in Figure 4.3 except that the % of MeOH was 20 %.

Using 20% MeOH in TFA pH 2.3 as the mobile phase in an isocratic mode at a column temperature of 45 ^{o}C resulted in a good separation of sialic acid from 2-deoxy-D-ribose in less than 4 minutes as illustrated in Figure 4.5. Under the optimised conditions, the column was operated at a backpressure of 121 bars.

In order to achieve a faster run time, the separation was transferred to a shorter column (**Column B**) using the same conditions described above except that the separation mode was gradient instead of isocratic. Using high MeOH percentages resulted in a good peak shapes but the resolution of sialic acid from the void peak was low (retention factor < 1). Therefore, gradient elution was used for a combination of good resolution and peak shape which resulted in the separation showed in Figure 4.6. Under the optimised conditions, the separation obtained was over 70 % faster than the previous TBA-HPLC methods [12, 21, 22].

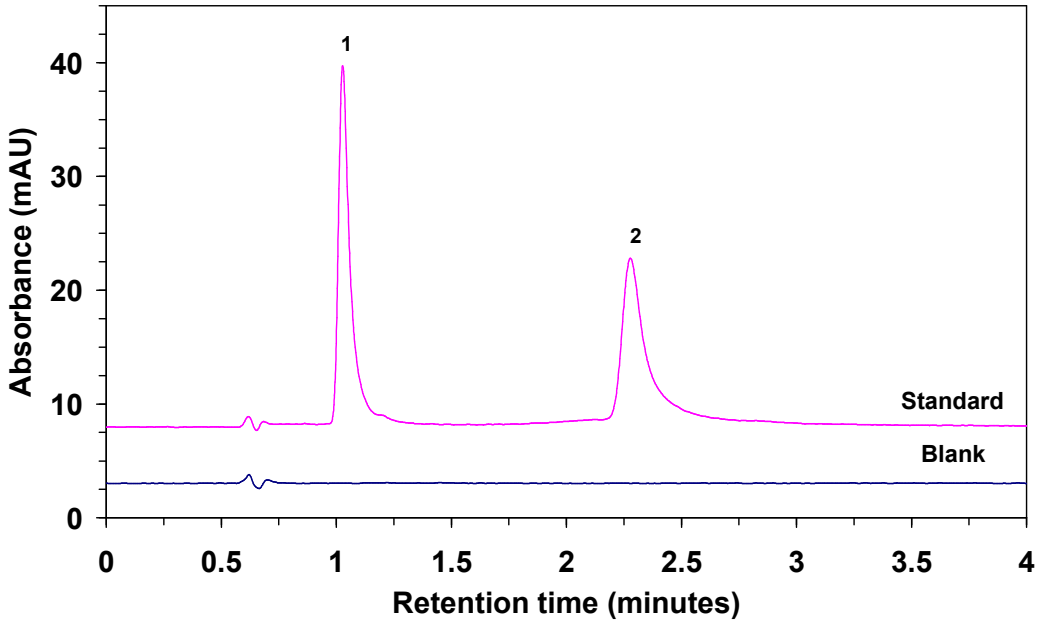

Figure 4.5: HPLC chromatograms show a separation of standard of 0.25 mmol.L^{-1} sialic acid (**1**) and 0.25 mmol.L^{-1} 2-deoxy-D-ribose (**2**) overlaid with a blank. Column: **Column A**. Mobile phase: 0.05 % TFA, pH 2.3/MeOH (80:20). Flow rate: 2.5 mL.min^{-1}. Injection volume: 10 µL. Column temperature: 45 ^{o}C. Detection @ 549 nm.

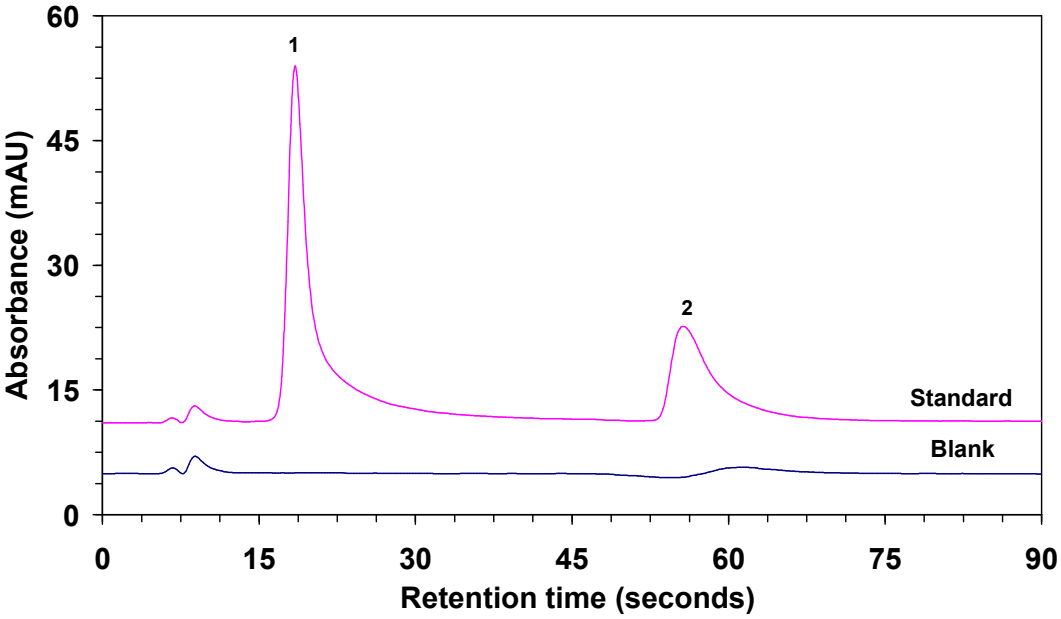

Figure 4.6: HPLC separation of 0.01 mmol.L^{-1} sialic acid (**1**) and 0.01 mmol.L^{-1} 2-deoxy-D-ribose (**2**) overlaid with a blank media which contains all reagents except the analytes. Column: **Column B**. Gradient program: 11 % for 0.5 minute, 0.5-0.65 minutes (11-35 %) and 0.66-1.5 minutes (11 %). Flow rate: 4.5 mL.min^{-1}. Injection volume: 100 µL. Column temperature: 45 ^{o}C. Detection @ 549 nm.

4.3.2. Labelling of sialic acid with TBA

4.3.2.1. Periodate-oxidation of sialic acid

The oxidation of sialic acid with periodate leads to form β-formylpyruvic acid which then reacts with TBA to form a red complex. Oxidation of 1 mole of sialic acid using periodic acid yields 1 mole of β-formylpyruvic acid as illustrated in Figure 4.2.

The effect of the periodic acid concentration and volume on the oxidation of sialic acid was studied. Figure 4.7 shows that the presence of excess oxidising agent lead to a decrease in peak area. This could be because (1) the presence of excess oxidising agent oxidised the aldehyde formed from sialic acid to carboxylic acid, (2) the presence of excess oxidising agent lead to an increase in acidity of the solution causing degradation of sialic acid which is acid-labile [14].

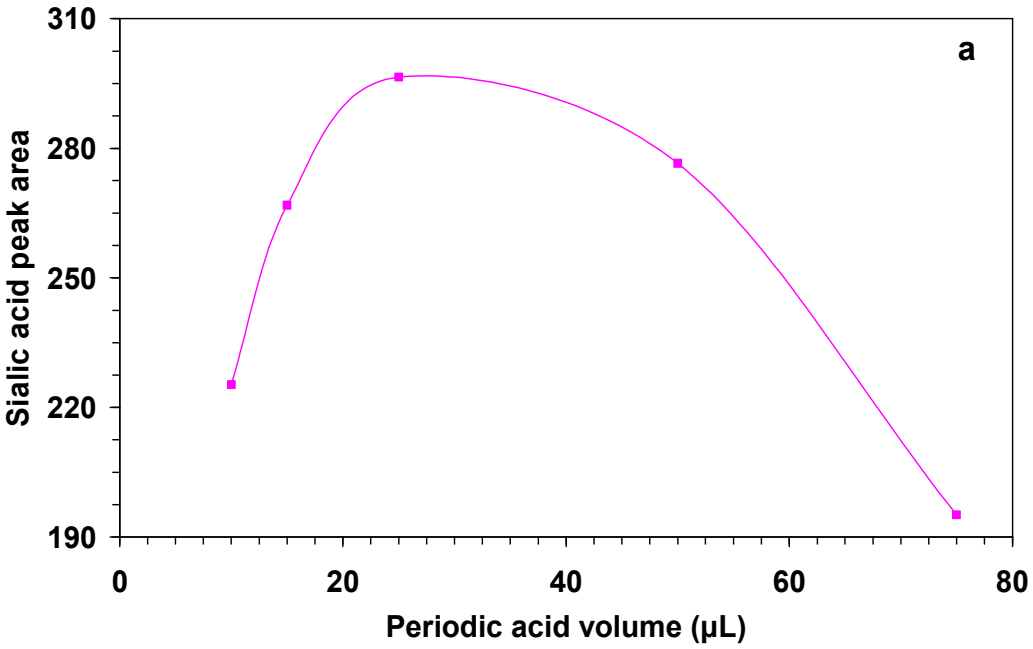

Figure 4.7(a): The effect of periodic acid volume on the oxidation of sialic acid. The concentratopn of periodic acid was 0.05 mol.L^{-1}.

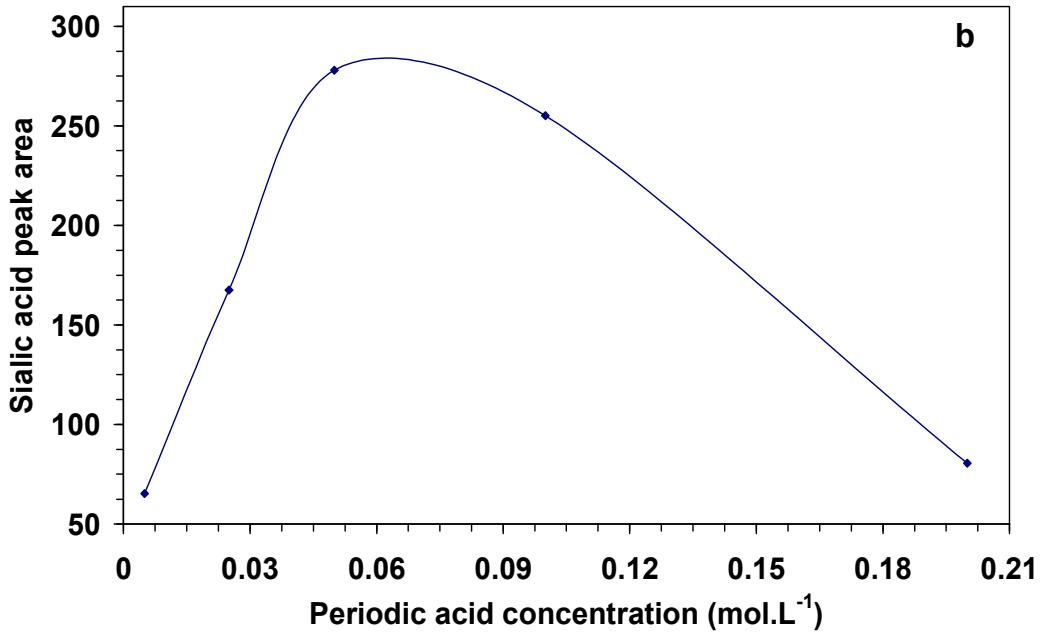

Figure 4.7(**b**)**:** The effect of periodic acid concentration on the oxidation of sialic acid. The added volume of periodic acid was 25 µL.

Figure 4.8 shows the effect of acidifying the environment of oxidation. This was investigated by adding different amounts of HCl with the periodic acid. As a result of this study, the peak area of sialic acid was increased by a maximum of 36 % compared to the peak area of the derivative obtained from the oxidation of sialic acid in which there was no addition of HCl. However, increasing the amount of the acid over the optimum concentration caused degradation of sialic acid [14].

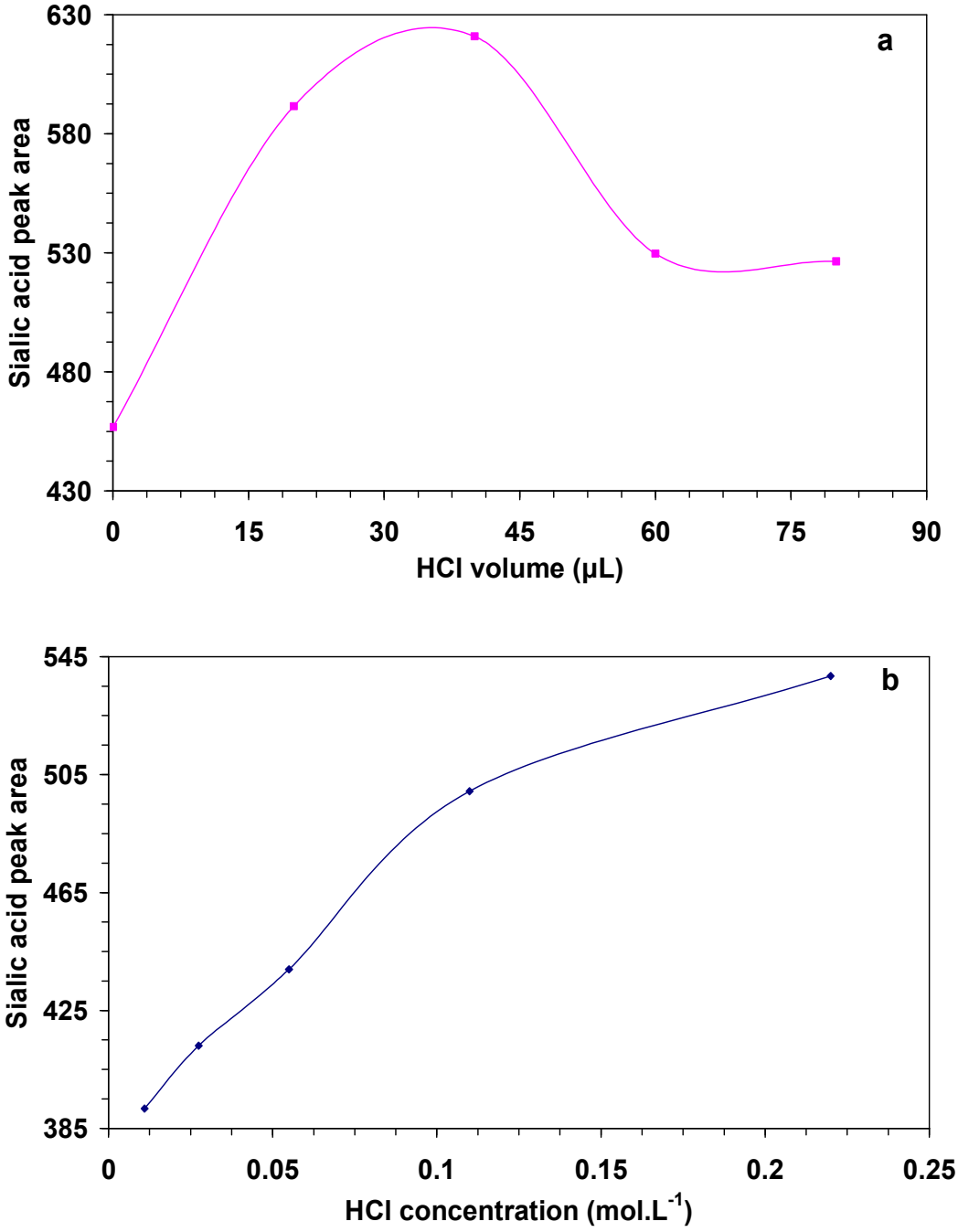

Figure 4.8: (**a**) The effect of HCl volume on the oxidation of sialic acid with periodic acid. The HCl concentration was 0.22 mol.L^{-1}. (**b**) The effect of HCl concentration on the oxidation of sialic acid with periodic acid. The added volume of HCl was 40 µL.

The period and temperature of oxidation of sialic acid in the water bath was investigated. The results are obtained in Figure 4.9. Generally,

increasing the temperature accelerated the oxidation. However, the maximum peak area of sialic acid was obtained after the oxidation of sialic acid at 37 ^{o}C for 40 minutes. This temperature is in agreement with Aminoff [14] whereas Warren [7] found that at 37 ^{o}C less colour was formed compared to room temperature. The sialic acid peak area was increased by about 13 % when the time of oxidation increased to 40 minutes against 30 minutes in the original assay [14].

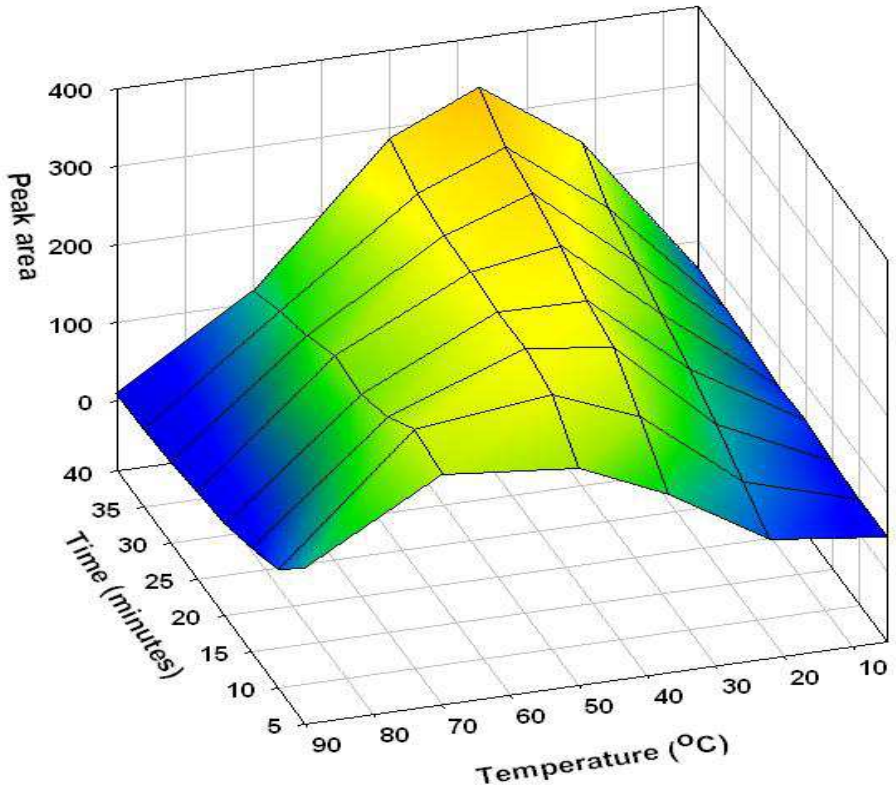

Figure 4.9: Effect of reaction time and temperature on sialic acid derivatisation.

The oxidation reaction was terminated by destroying the excess of the oxidation agent with sodium thiosulfate. The amount of thiosulfate required for this task was investigated and the results are plotted in Figure 4.10. Increasing the concentration of thiosulfate resulted in increasing the pH of the medium of the reaction, therefore preventing the condensation of β-formylpyruvic acid with TBA.

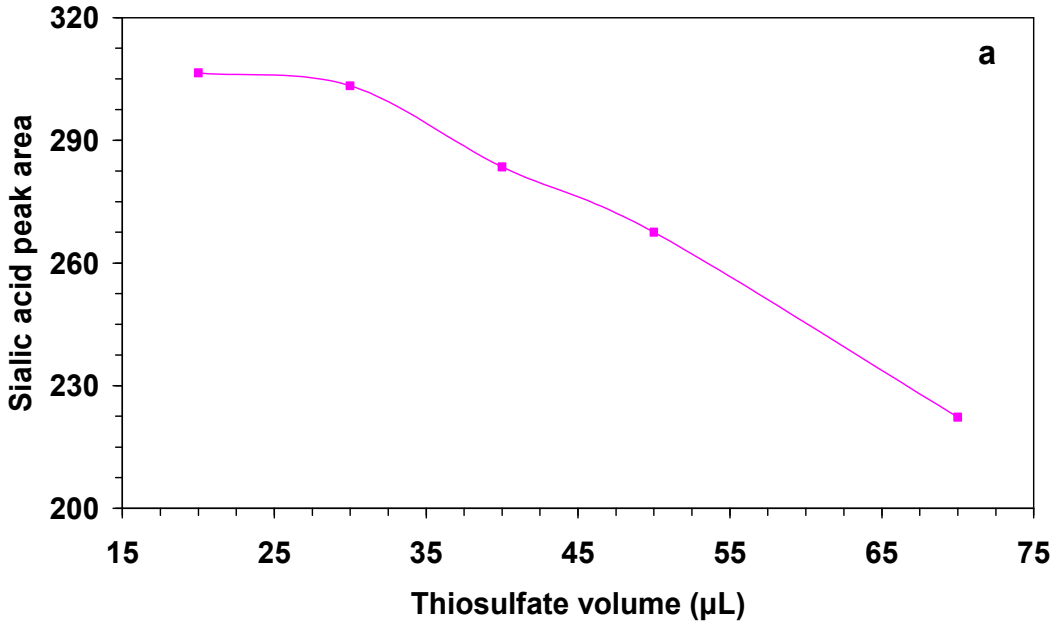

Figure 4.10(**a**)**:** The effect of thiosulfate volume on the red complex formation. The thiosulfate concentration was 5 %.

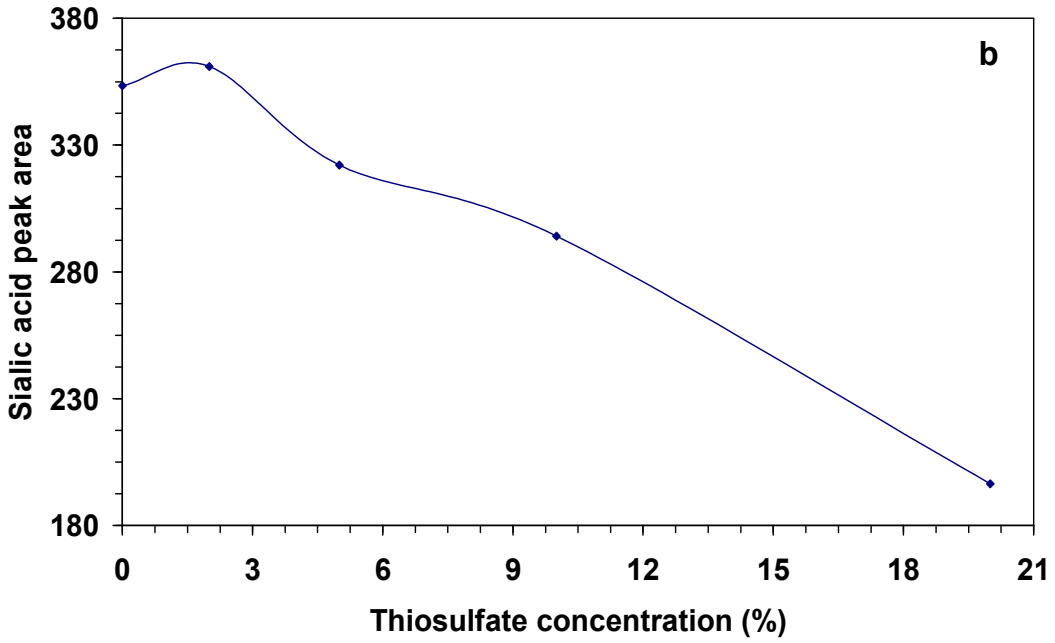

Figure 4.10(**b**)**:** The effect of thiosulfate concentration on the red complex formation. The added volume of thiosulfate was 20 µL.

4.3.2.2. Derivatisation of sialic acid

The red complex is formed from the condensation reaction between TBA and β-formylpyruvic acid, which was produced from the oxidation of sialic acid (Figure 4.11). This condensation was carried out in acidic medium, in which the formed chromophore is stable [7, 8]. The possibility of increasing the pH of the solution comes from either adding excess thiosulfate as mentioned above or from adding excess TBA, as TBA is only soluble in alkaline solution. The addition of excess TBA lead to increase the pH of the reaction medium and thus decrease the formation of the red complex as shown in Figure 4.12.

The derivatisation was performed in a water bath at 100 ^{o}C. The time of the derivatisation was studied to reach completion. As it can be seen from Figure 4.13 the maximum absorbance was increased by about 23 % in 8 minutes compared to 15 minutes in the original assay by Warren [7]. This is almost in agreement with Aminoff [14] as he carried out the derivatisation for 7.5 minutes.

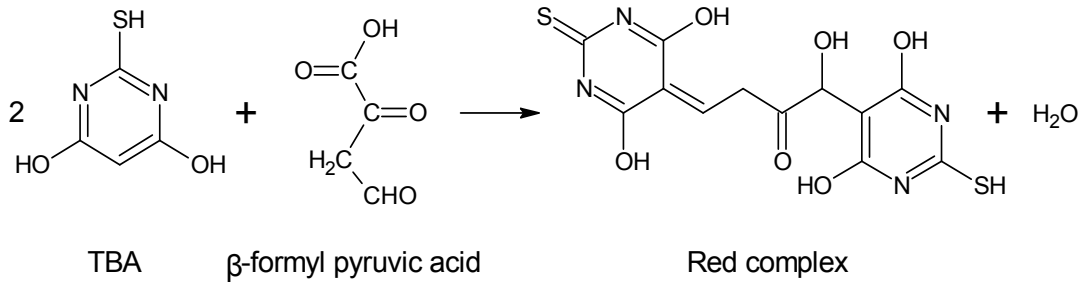

Figure 4.11: Reaction scheme show the formation of the red complex resulted from the condensation of β-formylpyruvic acid and TBA.

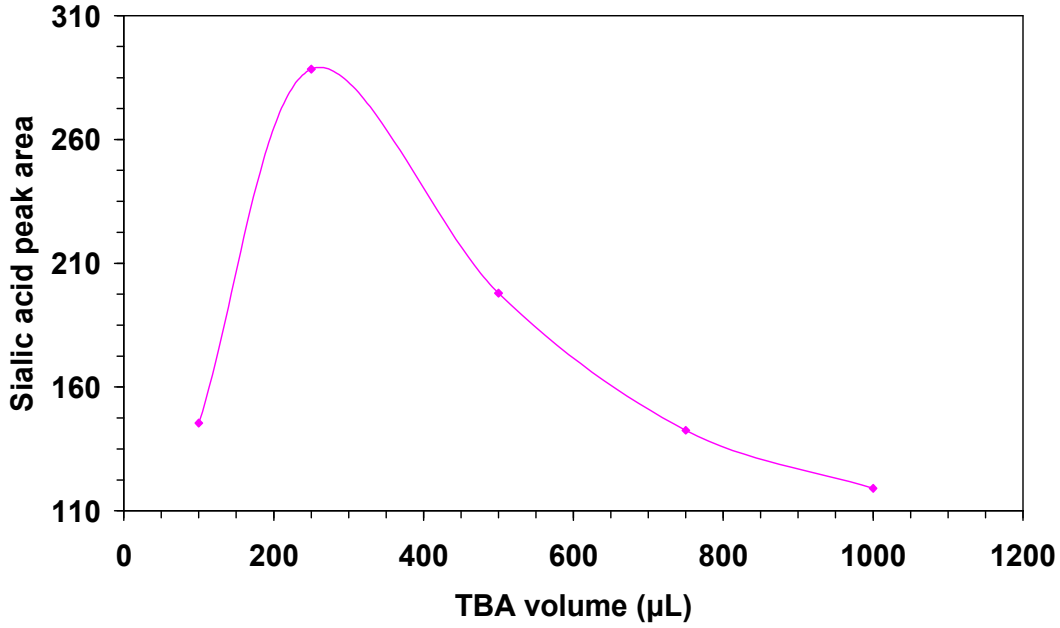

Figure 4.12: The effect of adding excess TBA on the peak area of the red complex formed from the condensation of β-formylpyruvic acid and TBA. The concentration of TBA was 0.1 mol.L^{-1}.

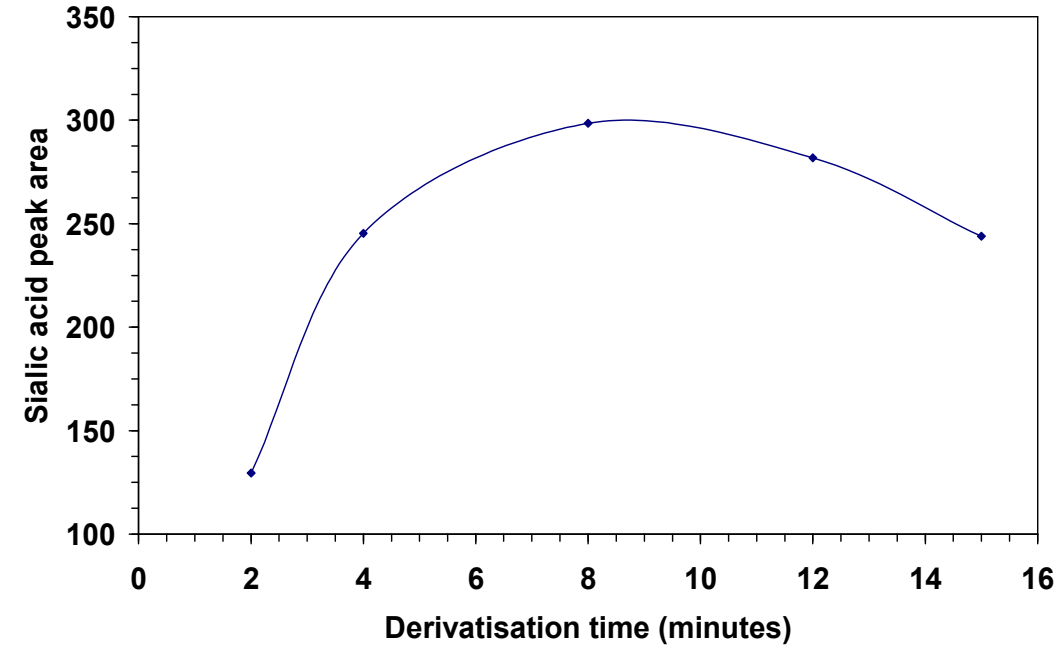

Figure 4.13: Effect of derivatisation time on the amount of the red complex formed between β-formylpyruvic acid and TBA at 100 ^{o}C. The derivatisation conditions are as described in Section 4.2.5.

4.3.3. Effect of organic solvents on the colour intensity

Extracting the red complex in *n*-butanol or cyclohexanone or adding water miscible solvents, such as MeOH, ethanol (EtOH) and DMSO, to the red complex solution after derivatisation are known to enhance the intensity of the colour and thus the absorbance of red complex in the UV-Vis detector [7, 8, 12, 14]. Here, the samples were mixed with different organic solvents after derivatisation; i.e. MeOH, EtOH and DMSO. The final concentration of the organic solvent in the sample was 20 %. The colour of the samples was significantly intensified. However, the use of such organic solvents in this study, particularly in the case of MeOH, had an adverse influence on the retained sialic acid as shown in Figure 4.14. The obtained results were expected because the concentration of the organic solvent added to the sample was stronger than the percentage of the organic modifier in the mobile phase. Therefore, sialic acid will not be retained in the column. The results obtained here is in a disagreement with the results obtained by Powell and Hart [12]. Powell and Hart showed in their work that the absorbance of the red complex varied by the addition of different amounts of MeOH to the sample. They diluted the derivatised sample in a buffer containing different amounts of MeOH. For example, the absorbance of the red complex was increased by about 15 % when the amount of MeOH increased from 5 % to 45 %.

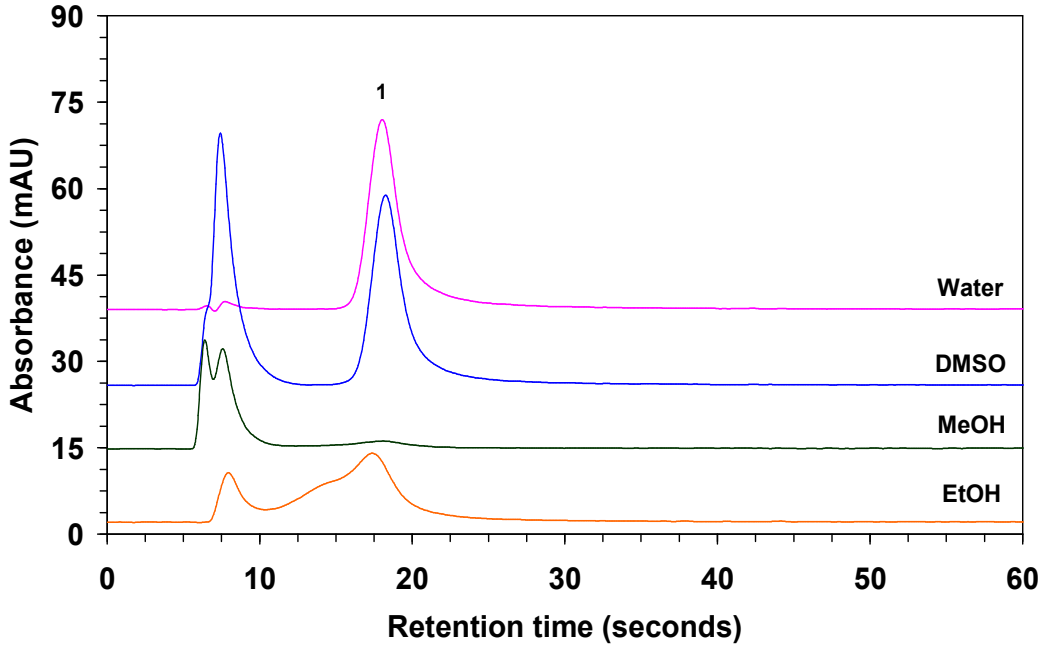

Figure 4.14: Effect of organic solvents on signal intensity. Chromatographic conditions are as described in Figure 4.6 except the separation mode, it was isocratic at 11 % MeOH. Peaks: (**1**) sialic acid standard.

4.3.4. Method validation

4.3.4.1. SPE recovery study of sialic acid standard

The recovery of sialic acid standard from SPE (Table 4.1) was studied by comparing the peak area of sialic acid produced from two different aliquots of the same standard solution. One of the aliquots was passed through the SPE cartridge as described in Section 4.2.4, collected, oxidised with periodic acid and derivatised with TBA as described in Section 4.2.5, whereas the other aliquot was oxidised and derivatised as described in Section 4.2.5 without SPE treatment. In order to minimise the dilution of the sample or the standard, the volume of the phosphate buffer required for rinsing the SPE cartridge after passing the sialic acid solution was also investigated. The cartridge was rinsed with 250, 125 and 50 µL phosphate buffer and the same volume was added to the non-extracted standards and compared. In all cases the recovery was good (111.8, 99.3 and 99.4 %

respectively). However, the minimum volume chosen for rinsing the cartridge was 80 µL.

Table 4.1
Analytical performance data

	Sialic acid
Area precision % RSD (*n* = 6)	1.31 %
RT precision % RSD (*n* = 6)	0.57 %
Oxidation/derivatisation precision % RSD (*n* = 6)	1.71 %
LOD	842 fmol
Linear range (µmol.L^{-1})	0.25-25
Linearity	0.9994
SPE recovery	99.4 %

4.3.4.2. Selectivity of the method

Possible interference could arise from monosaccharides or amino acids present in the samples tested in this study. Therefore, in order to prove the selectivity of the method, the following nine common monosaccharides and twenty amino acids were treated through the whole optimised procedure: 0.1 mmol.L^{-1} of galactose, mannose, glucose, ribose, galactosamine, mannosamine, glucosamine, xylose, fucose, L-phenylalanine, L-leucine, D-threonine, L-proline, L-arginine, L-thyrosine, D-methionine, L-histidine, L-methionine, L-aspartic acid, L-isoleucine, L-valine, L-serine, trans-4-hydroxy-l-proline, L-lysine, L-thyreonine, L-alanine, L-glutamine, L-glutamic acid, L-asparagine, L-typtophan, D-typtophan and D-valine. As a consequence, all of the nine monosaccharides and the twenty amino acids gave no colour confirming the selectivity of TBA. This results in agreement with what has been described previously by Warren [7] and Aminoff [14] in which they investigated some of the compounds listed above. Figure 4.15 shows an illustrative example of one of the twenty amino acids (D-methionine) and one of the nine monosaccharides (Gal) after oxidation

with periodic acid and derivatisation with TBA in which there is no detectable peaks observed.

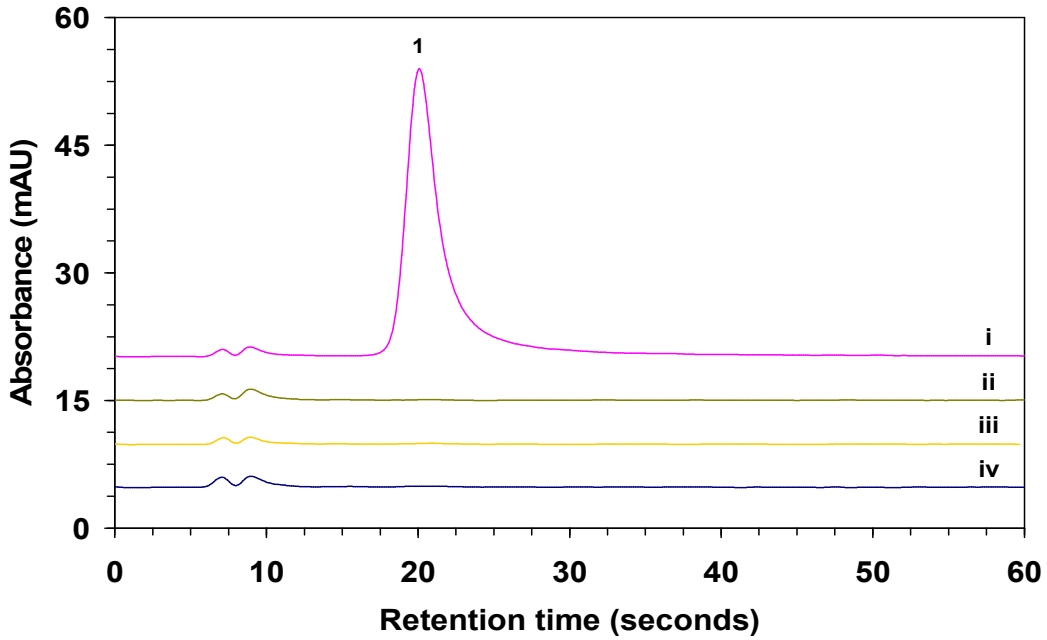

Figure 4.15: HPLC chromatograms of derivatised samples of galactose (**ii**) and D-methionine (**iii**) overlaid with sialic acid standard (**i**) and a blank (**iv**). Chromatographic conditions are as described in Figure 4.6 except the separation mode, it was isocratic at 11 % MeOH. Peaks: (**1**) sialic acid.

2-deoxy-D-ribose is another source of interference [7, 8, 14] as it gives malonaldehyde as a product of periodate oxidation. Malonaldehyde reacts with TBA to form an intense red complex that has a slightly lower λ_{max} (532 nm). This interference has been separated from sialic acid using HPLC as described previously [12, 22] and within the present method as well (Figure 4.6)

4.3.4.3. Linearity

A linear curve for sialic acid was established based on duplicate injections of each standard solution in the concentration range of 0.25 - 25

μmol.L^{-1} (Figure 4.16) revealing a good correlation between the peak areas and concentrations, with the correlation coefficient being > 0.999 (Table 4.1).

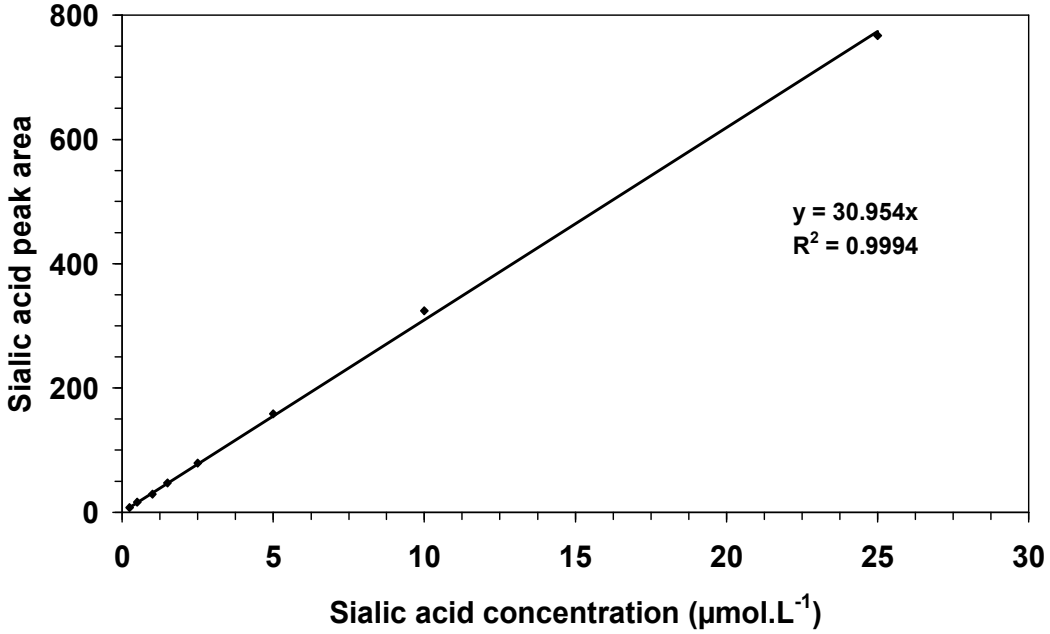

Figure 4.16: Linearity response of derivatised sialic acid standards.

4.3.4.4. Reproducibility

Reproducibility of the assay was investigated in two different ways: reproducibility of the oxidation/derivatisation steps and reproducibility of the chromatographic method. The precision of the oxidation/derivatisation steps was studied by derivatising six different standard solutions and the supernatants were injected in duplicate. The precision of the instrument was confirmed by injecting a single sialic acid six times consecutively and the % RSD was calculated using the peak areas and the retention times. From the results obtained in Table 4.1 it can be confirmed that the assay is highly reproducible.

4.3.4.5. Sensitivity

The sensitivity of the method was obtained by minimising the effect of the sample dilution and by increasing the injection volume. The volume of the sample that can be injected in the column was investigated. A linear plot was obtained from plotting the injection volume in the range against the peak area with the correlation coefficient being 0.9999 and good column efficiency over the range studied (Figures 4.17 and 4.18). Under the optimised conditions, the sensitivity was determined by preparing a series of sialic acid standard solutions ranging from 500 nmol.L^{-1} down to 1 nmol.L^{-1}. The series was oxidised and derivatised as described in the Experimental Section, followed by a duplicate injection in the HPLC system. The LOD of the assay was based on a signal-to-noise ratio of 3 and found to be 842 fmol (Table 4.1). This method is more sensitive than previously published TBA-HPLC based methods. The sensitivities reported by Powell *et al.* and Romero *et al.* were 2000 fmol and 6500 fmol, respectively [12, 21].

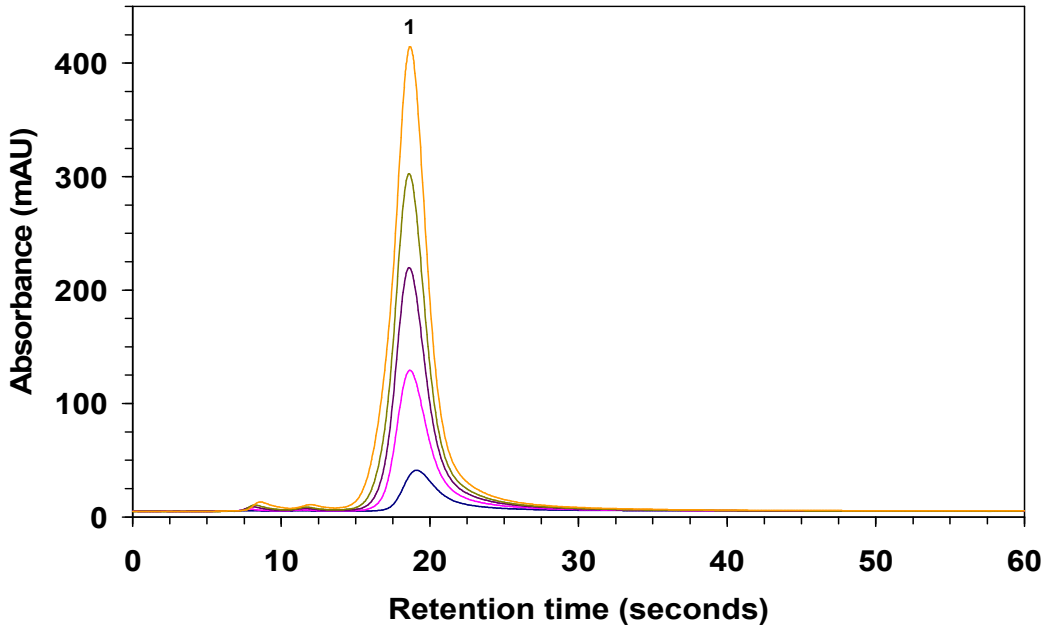

Figure 4.17: HPLC chromatograms of sialic acid injected in the column at different volumes. The volumes were: 10, 30, 50, 70 and 100 µL. The concentration of sialic acid was 1 µmol.L^{-1}. Chromatographic conditions are as described in Figure 4.6 except the separation mode, it was isocratic at 11 % MeOH. Peaks: (**1**) sialic acid.

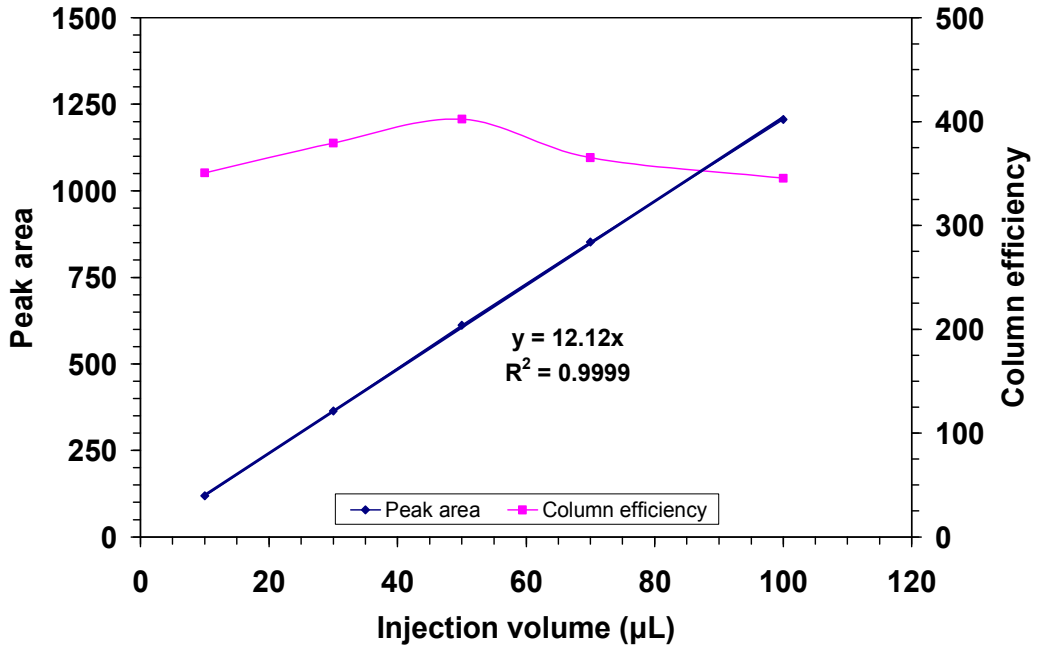

Figure 4.18: Linearity response of sample injection volume of sialic acid.

4.3.5. Quantitative analysis of yeastolate, basal media and in-process samples

In order to evaluate the applicability of the developed method, a number of yeastolate samples (powder samples) as well as basal media and in-process samples (liquid samples) sourced from the biopharmaceutical industry were analysed. The condensation reaction between β-formylpyruvic acid and TBA is highly pH dependant. For this reason, all of the samples were dissolved and diluted using phosphate buffer (pH 6.5, 10 mmol.L^{-1}). The presence of sialic acid in the samples was verified by a comparison with a standard chromatogram. The samples were prepared and derivatised with TBA as described in Sections 4.2.3, 4.2.4 and 4.2.5. Due to the high specificity of the TBA method, there was no interference from unknown peaks in all samples tested.

4.3.5.1. Analysis of yeastolate samples

The concentration of the sample used for analysis was 15 $mg.mL^{-1}$. This concentration was selected based on the results obtained in Figure 4.19. Logically, the higher the concentration of the sample used, the greater the peak area obtained. However, contrary to expectation, the peak areas were inversely proportional to the concentration. This could be due to the fact that the pH of the yeastolate sample itself is around seven whereas the overall pH of the medium after the addition of the reagents must be acidic in which the red complex is formed. However, increasing the concentration of the yeastolate sample lead to an increase the overall pH of the medium (even though the samples were prepared in a buffer), and thus decrease the possibility of the red complex formation. In addition, the peak area of sialic acid resulting from the analysis of yeastolate samples at the concentration of 15 $mg.mL^{-1}$ was high enough to be quantified. Therefore, it was not necessary to prepare the samples in higher concentrations. Moreover, a decrease in the retention time of sialic acid was obtained by increasing the concentration of the sample. This might be due to column overloading with the complex sample matrix.

Figure 4.20 shows the chromatograms obtained from the yeastolate samples. In total, seven yeastolate samples were analysed and sialic acid was found in all samples tested and the presence was confirmed by a comparison with a standard chromatogram. All samples were injected in duplicate and sialic acid was quantified against a linear curve of sialic acid standard and the results are listed in Table 4.2. The results showed that the variability between samples is low with a % RSD of 6.8 %. The average concentration of sialic acid found in the samples was 4.2 $ng.mg^{-1}$ (S.D. = 0.3 $ng.mg^{-1}$) and ranged between 4.76 and 3.98 $ng.mg^{-1}$. Figure 4.21 shows the sialic acid profile in these samples. As it can be seen, sialic acid in all the samples is deviated within one standard deviation from the average (except Sample 7) indicating that the sialic acid sourced from the yeastolate samples is invariable. Interestingly, sialic acid was not detected in the yeastolate

samples using the AA method (as described in Chapter 3) which confirms the value of developing this method.

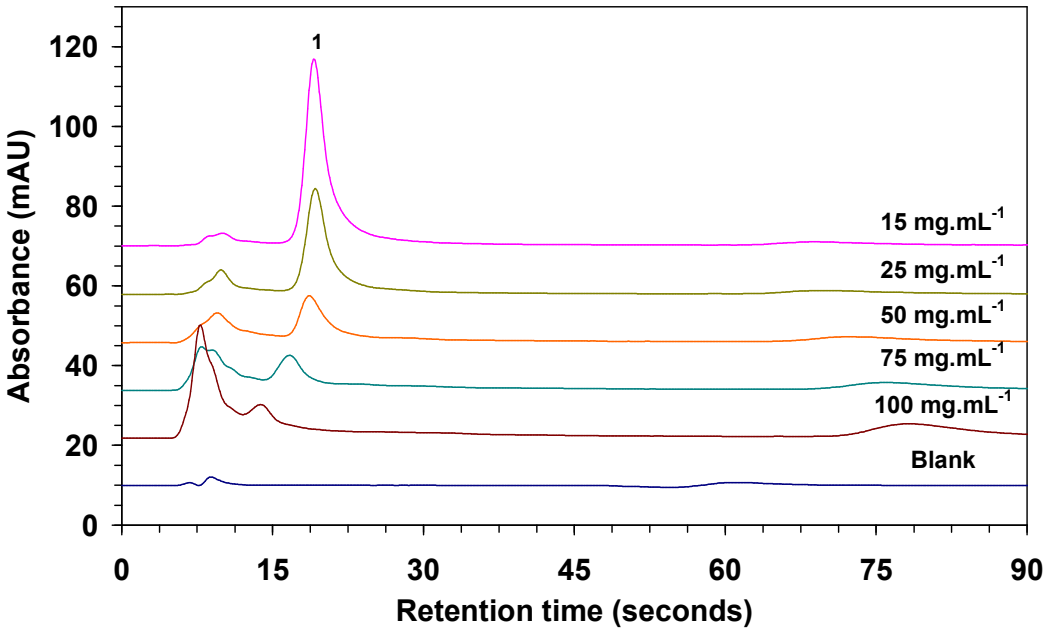

Figure 4.19: HPLC chromatograms of a yeastolate sample prepared at the different concentrations. Chromatographic conditions are as described in Figure 4.6 except the separation mode, it was isocratic at 11 % MeOH. Peaks: (**1**) sialic acid.

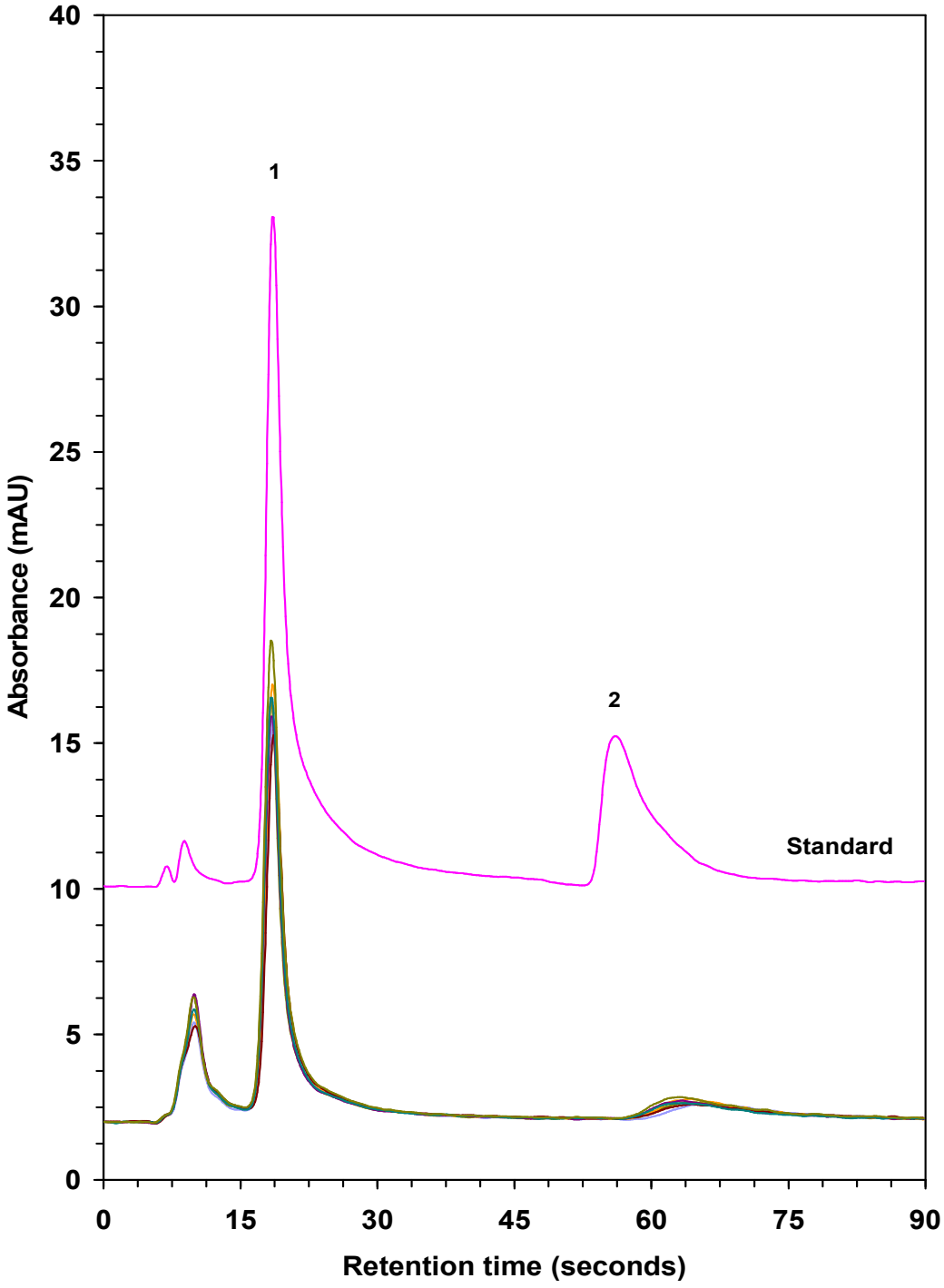

Figure 4.20: HPLC chromatograms obtained from the analysis of the yeastolate samples overlaid with a sialic acid standard. Chromatographic conditions are as described in Figure 4.6. Peaks: (**1**) sialic acid, (**2**) 2-deoxy-D-ribose.

Table 4.2
Quantitative data of sialic acid in the yeastolate samples. Date of analysis: 01/07/2008.

Sample number	Sialic acid found ($ng.mg^{-1}$)
Yeastolate samples	
Sample 1	4.04
Sample 2	4.02
Sample 3	4.39
Sample 4	4.01
Sample 5	3.98
Sample 6	4.24
Sample 7	4.76
S.D. **(% RSD)**	0.3 (6.8 %)

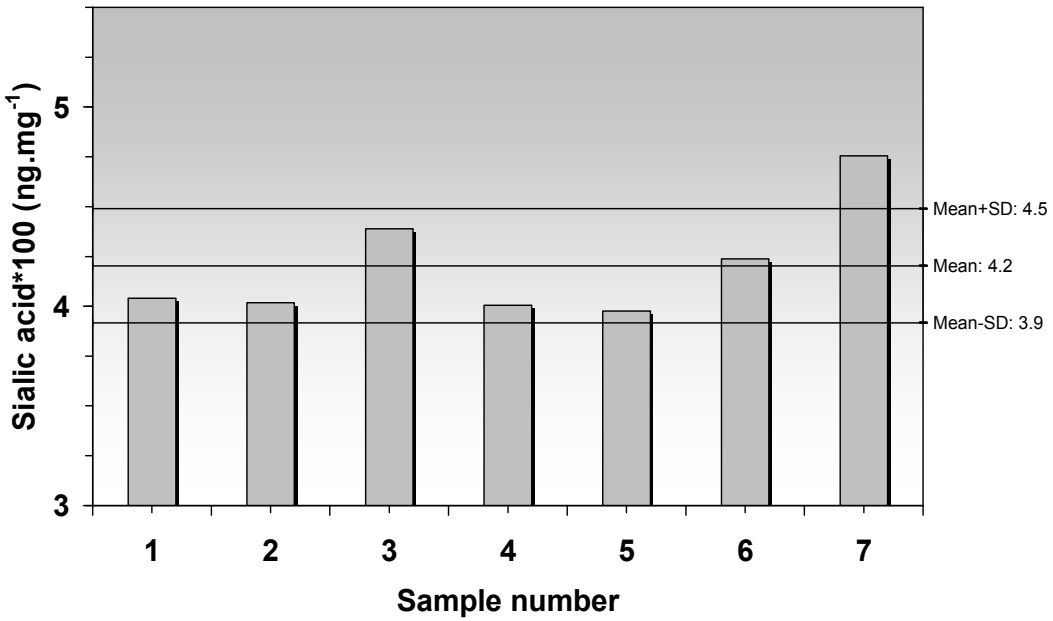

Figure 4.21: Sialic acid profile for the yeastolate samples.

4.3.5.2. Analysis of basal media samples

Figures 4.22 and 4.23 show an overlay of HPLC chromatograms obtained from the analysis of basal media samples. The samples, fourteen in total, were sourced from two different manufacturing facilities producing the same biotherapeutic as described earlier (Section 3.2.3). The samples were pretreated as described in the Experimental section and injected in the HPLC system in duplicate. Sialic acid was found in all samples tested. It was confirmed by a comparison with a standard chromatogram of sialic acid and quantified against a linear curve of sialic acid standard. The results are listed in Table 4.3 and the profile of sialic acid is as shown in Figure 4.24. From the results obtained, the variation in sialic acid level in **Lot B** (% RSD = 110.1 %) is much higher than **Lot A** (% RSD = 8.2 %). This is because sialic acid presented in one of the samples in **Lot B** (Sample **B1**) is about five times higher than the second highest sample in the same lot. The same results from the same sample were obtained in Chapter 3 regarding Glc, in which its level was higher in this particular sample compared to the others in the same lot. However, this was not the case for sialic acid in Chapter 3. Apart from Sample **B1**, the % RSD of **Lot B** is about 11 %, which is almost the same as **Lot A**. The average concentration of sialic acid found in the **Lot A** was 19.4 $pg.\mu L^{-1}$ (S.D. = 1.6 $pg.\mu L^{-1}$) and ranged between 21.8 and 17.5 $pg.\mu L^{-1}$ whereas the average in **Lot B** was 21.9 $pg.\mu L^{-1}$ (S.D. = 2.5 $pg.\mu L^{-1}$) and the range is between 24.0 and 17.8 $pg.\mu L^{-1}$. Sample **B1**, in particular, contains 131.0 $pg.\mu L^{-1}$ of sialic acid.

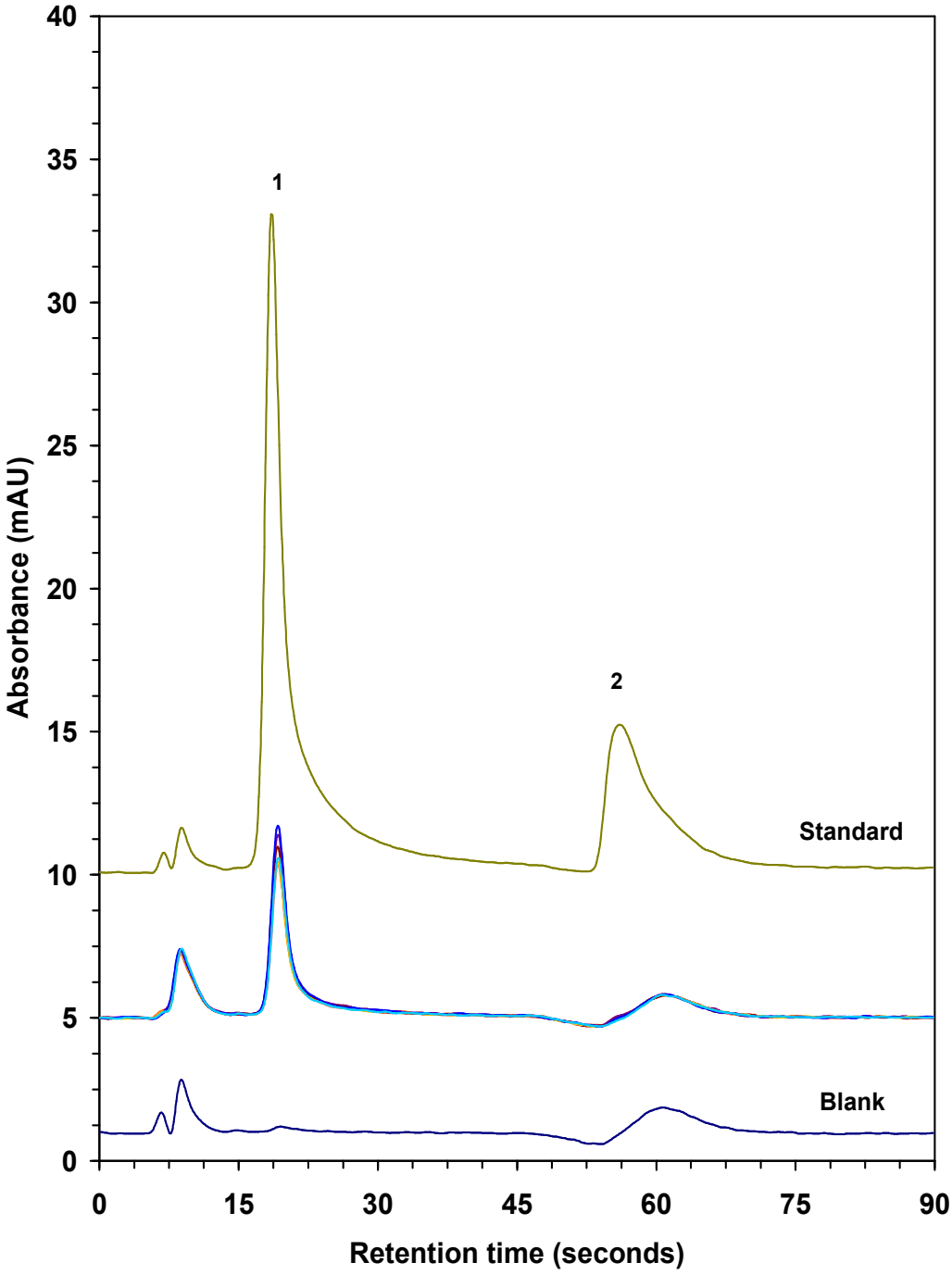

Figure 4.22: HPLC chromatograms obtained from the analysis of the basal media samples (**Lot A**) overlaid with a sialic acid standard and blank. Chromatographic conditions are as described in Figure 4.6. Peaks: (**1**) sialic acid, (**2**) 2-deoxy-D-ribose.

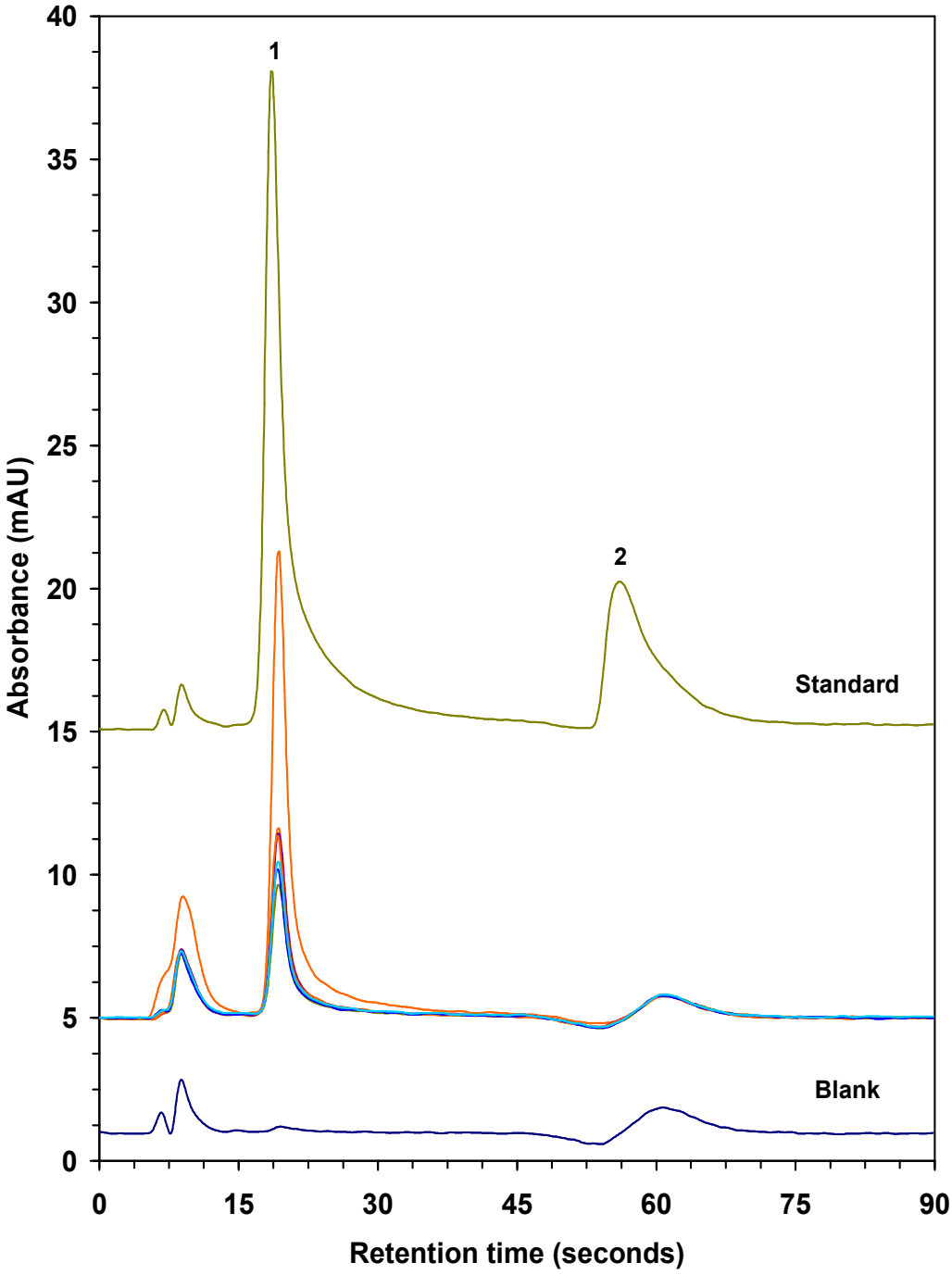

Figure 4.23: HPLC chromatograms obtained from the analysis of the basal media samples (**Lot B**) overlaid with a sialic acid standard and blank. Chromatographic conditions are as described in Figure 4.6. Peaks: (**1**) sialic acid, (**2**) 2-deoxy-D-ribose.

Table 4.3
Quantitative data of sialic acid in the two lots of basal media samples. Date of analysis: 04/07/2008.

Sample number	Sialic acid found ($pg.\mu L^{-1}$)
Basal media samples (Lot A)	
Sample A1	18.4
Sample A2	18.8
Sample A3	21.8
Sample A4	17.5
Sample A5	18.4
Sample A6	21.2
Sample A7	20.1
S.D. **(% RSD)**	1.6 (8.2 %)
Basal media samples (Lot B)	
Sample B1	131.0
Sample B2	22.9
Sample B3	24.0
Sample B4	17.8
Sample B5	24.5
Sample B6	20.8
Sample B7	21.4
S.D. **(% RSD)**	41.3 (110.1 %)

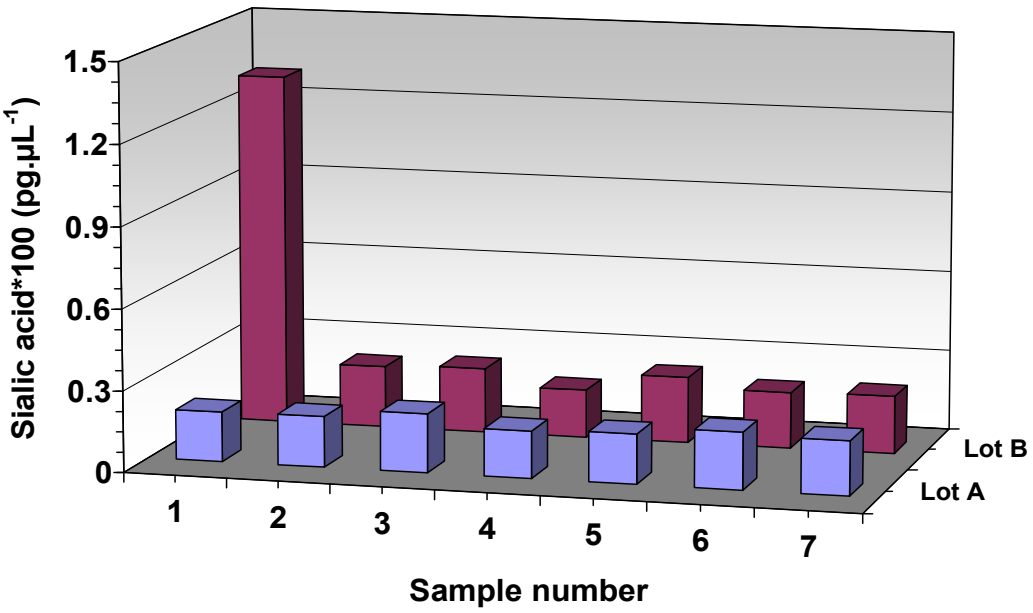

Figure 4.24: Sialic acid profile for the two lots of basal media samples.

4.3.5.3. Analysis of in-process samples

Finally, 12 in-process samples were analysed and the chromatograms are shown in Figure 4.25. The samples were treated and derivatised using the optimised procedure and injected in duplicate. Sialic acid was found in all samples tested and the results are listed in Table 4.4. Sialic acid in these samples ranges from 30.0 to 93.3 $pg.\mu L^{-1}$. These in-process samples were collected from fed-batch CHO cell cultures at different time-points as described in Table 3.1. They were obtained prior to and after bioreactor inoculation. The level of free sialic acid throughout the production of the biotherapeutic can be monitored in the bioreactor vessel. Figure 4.26 shows the profile of sialic acid for the 12 samples that have been taken from different time-points during the production process of a biotherapeutic.

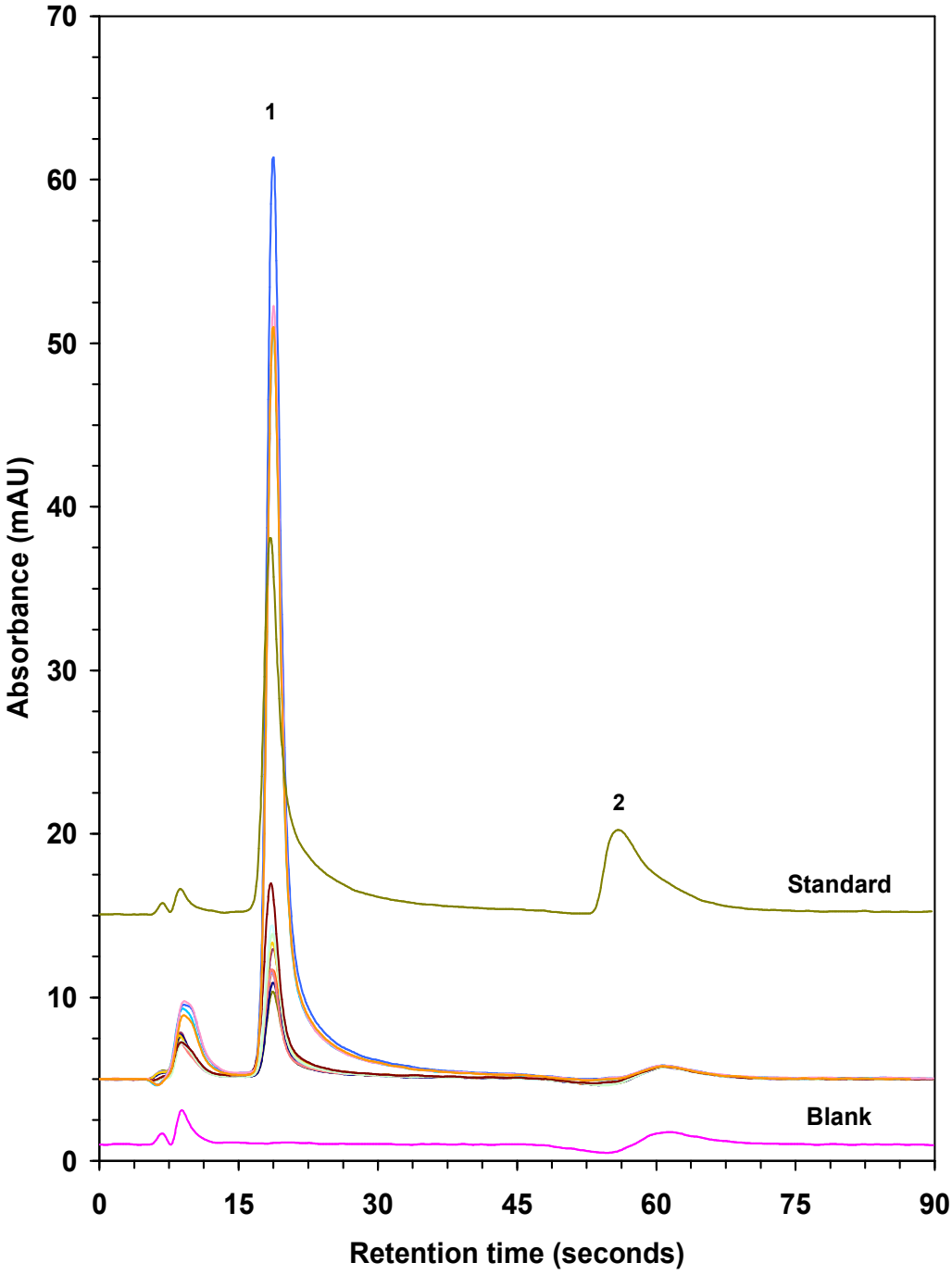

Figure 4.25: Selected HPLC chromatograms obtained from the analysis of the in-process samples overlaid with a sialic acid standard. Chromatographic conditions are as described in Figure 4.6. Peaks: (**1**) sialic acid, (**2**) 2-deoxy-D-ribose.

Table 4.4
Quantitative data of sialic acid in the in-process samples. Date of analysis: 05/07/2008.

Sample number	Sialic acid found ($pg.\mu L^{-1}$)
In-process media samples (Lot A)	
Sample A1	40.7
Sample A2	30.0
Sample A3	42.8
Sample A4	34.2
Sample A5	45.0
Sample A6	45.8
Sample A7	38.1
Sample A8	53.9
Sample A9	47.9
Sample A10	80.9
Sample A11	93.3
Sample A12	54.8

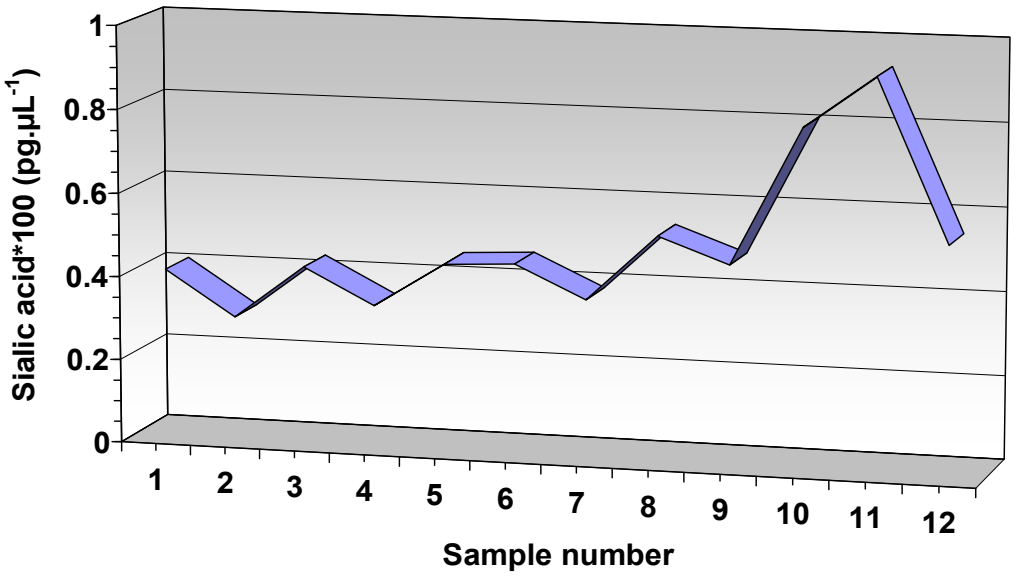

Figure 4.26: Sialic acid profile for the in-process samples.

4.4. Conclusion

In conclusion, a rapid, sensitive and accurate RRLC-UV-Vis method for quantitative determination of sialic acid was developed. The method consists of pre-column oxidation of sialic acid with periodic acid followed by derivatisation with TBA to form a red complex. The sialic acid was separated from other components on a short monolithic column within 90 seconds. The method was used for sialic acid determination in a range of complex samples sourced from the biopharmaceutical industry. The method was found to be linear over the range, reproducible and sensitive. The method is reliable to use in the quantification analysis of total sialic acid in a variety of sample types within the production process and quality assurance of the pharmaceutical industry.

4.5. References

[1] J.W. Dennis, M. Granovsky, C.E. Warren, *Biochim. Biophys. Acta, Gen. Subj.* 1999, **1473**, 21 - 34.

[2] R. Lacomba, J. Salcedo, A. Alegría, M. J. Lagarda, R. Barberá, E. Matencio, *J. Pharm. Biomed. Anal.* 2010, **51**, 346 - 357.

[3] J. S. Rohrer, J. Thayer, M. Weitzhandler, N. Avdalovic, *Glycobiology*, 1998, **8**, 35 - 43.

[4] A. Varky, R. Cummings, J. Esko, H. Freeze, G. Hart, J. Marth (Eds.), Essentials of glycobiology, CSHL Press, New York, 1999, pp. 25 - 40.

[5] J. Salcedo, R. Lacomba, A. Alegría, R. Barbera, E. Matencio, M. J. Lagarda, *Food Chem.* 2011, **127**, 1905 - 1910.

[6] L. Svennerholm, *Biochim. Biophys. Acta* 1957, **24**, 604 - 611.

[7] L. Warren, *J. Biol. Chem.* 1959, **234**, 1971 - 1975.

[8] G. B. Paerels, J. Schut, *Biochem. J.* 1965, **96**, 787 - 792.

[9] M. Van der Ham, B. H. C. M. T. Prinsen, J. G. M. Huijmans, N. G. G. M. Abeling, B. Dorland, R. Berger, T. J. deKoning, M. G. M. D. S. V. Velden, *J. Chromatogr. B* 2007, **848**, 251 - 257.

[10] M. H. E. Spyridiaki, P. A. Siskos, *J. Chromatogr. A* 1999, **831**, 179 - 189.

[11] K. Sugahara, K. Sugimoto, O. Nomura, T. Usui, *Clin. Chim. Acta* 1980, **108**, 493 - 498.

[12] L. D. Powell, G. W. Hart, *Anal. Biochem.* 1989, **157**, 179 - 185.

[13] V. S. Waravdekar, L. D. Saslaw, *Biochim. Biophys. Acta* 1957, **24**, 439.

[14] D. Aminoff, *Biochem. J.* 1961, **81**, 384 - 392.

[15] J. P. Zanetta, A, Pons, M. Iwersen, C. Mariller, Y, Leroy, P. Timmerman, R. Schauer, *Glycobiology* 2001, **11**, 663 - 676.

[16] T. Kun-Tian, L. Li-Na, C. Ya-Qi, M. Shi-Fen, *Chin. J. Anal. Chem*. 2008, **36**, 1535 - 1538.

[17] J. S. Rohrer, *Anal. Biochem.* 2000, **283**, 3 - 9.

[18] F. Che, X. Shao, K. Wang, Q. Xia, *Electrophoresis* 1999, **20**, 2930 - 2937.

[19] A. Taga, M. Sugimura, S. Suzuki, S. Honda, *J. Chromatogr. A* 2002, **954**, 259 - 266.

[20] X. Dong, X. Xu, F. Han, X. Ping, X. Yuang, B. Lin, *Electrophoresis* 2001, **22**, 2231 - 2235.

[21] E. L. Romero, M. F. Pardo, S. Porro, S. Alonso, *J. Biochem. Biophys. Methods* 1997, **35**, 129 - 134.

[22] A. Freyberger, *Exp. Toxic. Pathol.* 1996, **48**, 526 - 528.

[23] S. Hara, Y. Takemori, M. Yamaguchi, M. Nakamura, Y.Ohkura, *Anal. Biochem.* 1987, **164**, 138 - 145.

[24] P. G. Stanton, Z. Shen, E. A. Kecorius, P. G. Burgon, *J. Biochem. Biophys. Methods* 1995, **30**, 37 - 48.

[25] T. Hikita, K. Tadano-Aritomi, N. Iida-Tanaka, H. Toyoda, A. Suzuki, T. Toida, T. Imanari, T. Abe, Y. Yanagawa, I. Ishizuka, *Anal. Biochem.* 2000, **281**, 193 - 201.

[26] G. N. Tzanakakis, A. Syrokou, I. Kanakis, N. K. Karamanos, *Biomed. Chromatogr.* 2006, **20**, 434 - 439.

[27] K. R. Anumula, *Anal. Biochem.* 1995, **230**, 24 - 30.

[28] J. Martín, E. Vázquez, R. Rueda, *Anal. Bioanal. Chem.* 2007, **387**, 2943 - 2949.

[29] S. Hara, M. Yamaguchi, Y. Takemori, K. Furuhata, H. Ogura, M. Nakamura, *Anal. Biochem.* 1989, **179**, 162 - 166.

[30] M. Ito, K. Ikeda, Y. Suzuki, K. Tanaka, M. Saito, *Anal. Biochem.* 2002, **300**, 260 - 266.

[31] N. Tomiya, T. Suzuki, J. Awaya, K. Mizuno, A. Matsubara, K. Nakano, M. Kurono, *Anal. Biochem.* 1992, **206**, 98 - 104.

[32] Y. Yuh, J. Chen and C. Chiang, *J. Pharm. Biomed. Anal.* 1998, **16**, 1059 - 1066.

Chapter 5

Quantitative analysis of cysteine/cystine in chemically defined media utilising a developed rapid and sensitive chromatographic assay

5.1. Introduction

Since these CD media often contain mixtures of vitamins and amino acids, the temporal stability of these components is crucial for the production of a therapeutic protein with high yield. Cysteine (Cys) is an important amino acid for protein folding and function due to disulphide linkages and is a very important component of CD media. However, Cys can be readily oxidised to cystine (Cyss) in such complex environments, and this ratio has significance as a redox indicating quality assay for CD media which contain Cys.

A number of analytical methods such as GC-MS [1,2], CZE [3-6], LC-MS [7-10] and HPLC with pre- or post-column thiol derivatisation followed by UV detection [11-22] or fluorometric detection [23-28], have been reported for the separation and determination of Cys in different sample matrices such as urine [12, 15, 18, 21, 23], human plasma [4, 8, 11, 16, 17, 20, 22, 23, 27], human blood [10, 24, 25] and yeast [7]. However, very few chromatographic methods are available to quantitate Cys and Cyss in complex media, and none that exist can be termed simple or rapid [29].

Cys cannot be detected by UV absorption or fluorescence due to the lack of a suitable UV chromophore, therefore, derivatisation is important for sensitive and selective detection. Derivatisation also stabilises thiols by blocking the labile sulfhydryl group and thus improves chromatographic performance [30]. The derivatisation reagents should react rapidly and specifically with the thiol group to form stable thiol derivatives with sufficient absorption or fluorescent yield for trace concentration detection. Furthermore, the derivatisation reaction should be carried out at the lowest possible temperatures and weakly acidic pH to prevent oxidation of the analytes leading to inaccurate results [30, 31]. Several reagents have been used for this purpose, such as 2-chloro-1-methylpyridinium iodide (CMPI) [22, 32, 33], 2-chloro-1-methylquinolinium tetrafluoroborate (CMQT) [5, 11–13, 15-19, 21], 7-fluorobenzo-2-oxo-1,3-diazole- 4-sulfonate (SBD-F) [26, 34], monobromobimane [3, 23-25], 4-aminosulfonyl-7-fluoro-2,1,3-

benzoxadiazole (ABD-F) [4], dansyl chloride (DNS-Cl) [14], *o*-phthalaldehyde (OPA) [27, 28] and 5,5´-dithiobis(2-nitrobenzoic acid) (DTNB, Ellman's reagent) [9, 35]. Among these, CMQT is preferable as a tagging reagent due to the very mild reaction conditions (i.e. immediate reactivity at room temperature in neutral medium) and due to its high specificity for thiol-containing compounds.

However, Cyss cannot be derivatised with CMQT directly, since it has no free thiol group. Therefore, the reduction of its disulfide bond must be first carried out, prior to derivatisation and subsequent separation as CMQT-Cys. Reduction of the disulfide bond can be carried out using several reducing agents including tri-nbutylphosphine (TNBT) [4, 21, 32, 34], tris(2-carboxyetyl)phosphine (TCEP) [5, 7, 13, 16-18, 20, 34, 36], sodium borohydride ($NaBH_4$) [11, 12, 19], triphenylphosphine (TPP) [3, 24, 25] and dithiothreitol (DTT) [37]. However, of the above, TCEP is clearly the most suitable to-date, as it is water soluble, odourless, selective towards disulfide bonds, stable in both acidic and basic solutions and, perhaps most important, the reduction is quantitative and takes no more than 5 minutes at room temperature [34, 38, 39, 40].

In this Chapter, the development of rapid, selective and quantitative monolithic RPLC and RPLC-MS assays for Cys/Cyss in complex CD media is reported. The complexity of the media samples was such that a thiol selective pre-separation derivatisation step was essential, with a rapid sample reduction step allowing accurate determination of the Cys and Cyss ratio in a total analysis time of less than 30 minutes for the monolithic RPLC–UV method. The method is based on reducing Cyss (oxidised form) to Cys (reduced form) with TCEP and then tagging the total Cys with CMQT, followed by ion-pairing reversed-phase LC separation on a narrow-bore C_{18} monolithic column and UV detection.

5.2. Experimental

5.2.1. Reagents and materials

Cysteine (Cys, 97 %), cystine (Cyss, 99.5 %), trichloroacetic acid (TCA, 99.5 %), lithium hydroxide (LiOH, 99 %), potassium phosphate monobasic (99 %), potassium phosphate dibasic (99 %), sodium hydroxide (NaOH, 98 %), hydrochloric acid (HCl, 37 %), ammonium acetate (99 %), 2-chloroquinoline (99 %), trimethyloxonium tetrafluoroborate (95 %), diethyl ether (99.9 %) and nitromethane (99.0 %) were purchased from Sigma-Aldrich (Dublin, Ireland). TCEP (98 %) was purchased from Alfa Aesar (Heysham, UK). ACN and MeOH were of HPLC grade and purchased from Labscan (Tallaght, Dublin, Ireland). Ammonia solution (35 %) was purchased from BDH Laboratory Supplies (Poole, England). Acetic acid (96 %) was obtained from Riedel-deHaen (Seelze, Germany). All chemicals were used as received, without any further purification. CMQT was prepared in the laboratory as described in Section 5.2.4.

5.2.2. Instrumentation

All instrumentation used was as described in Section 3.2.2 with the exception of the following. The sample was mixed using a VX100 vortex mixer purchased from Labnet. The derivatisation and reduction were carried out in a capped 2-mL polypropylene sample tube (Sarstedt, Germany).

For LC-ESI-MS analysis, a Bruker Daltonics Esquire~LC (Bremen, Germany) ion trap instrument with electrospray interface was employed using Bruker Daltonics NT 4.0 software. For direct infusion-MS, a Cole Parmer 74900 series threaded screw syringe type pump was filled with sample and infused at 250 $\mu L.h^{-1}$. Conditions were optimised by direct sample infusion of a solution of CMQT (1 $\mu g.L^{-1}$) in 80:20 H_2O/MeOH and the optimised parameters are listed in Table 5.1.

Table 5.1
Optimisation of ESI-MS parameters for CMQT

Parameter	Optimised value
Capillary (V)	4000
End plate offset (V)	-500
Capillary exit offset (V)	95.0
Trap drive	55.0
Octopole RF (Vpp)	150
Lens 1	-5.0
Lens 2	-60
N_2 drying gas flow ($L.min^{-1}$)	8
Dry gas temperature (^oC)	300
Nebulizer pressure (psi)	55
Scan range (*m/z*)	50 - 2200
Averages (spectra)	5
Ion polarity	positive

5.2.3. Chromatographic conditions

5.2.3.1. Isocratic method

The column used was a 2.0 mm × 50 mm Phenomenex Onyx monolithic C_{18} column. The mobile phase used was (86:14) 50 $mmol.L^{-1}$ TCA/ACN (pH 2.5) delivered isocratically at 1.5 $mL.min^{-1}$. Column temperature was set at 45 ^oC, the injection volume was 40 µL and detection was by UV absorbance at 355 nm.

5.2.3.2. Gradient method

Using the same column as described above, a LC gradient method was developed. Mobile phase A was 10 $mmol.L^{-1}$ ammonium acetate buffer (pH 5) with ACN as mobile phase B, and a gradient program of 0-1 minutes (2 % B), 1.1-5 minutes (10 % B), 5.1-7 minutes (2 % B) delivered at 1.5

$mL.min^{-1}$. Injection volume was 100 µL with a column temperature of 25 ^{o}C and detection at 355 nm. This method was further adapted for ESI-MS detection by reducing the flow rate to 0.3 $\mu L.min^{-1}$ and modifying the gradient program as the following: 0-5 minutes (2 % B), 5.5-25 minutes (10 % B), 25.1-35 minutes (2 % B). The optimised ESI-MS conditions are listed in Table 5.1.

5.2.4. Synthesis of CMQT

CMQT was prepared as described by Bald and Glowacki [15]. Briefly, into a standard glass test tube a small stirring bar was placed followed by 1.0 g of 2-chloroquinoline and 1.0 g of trimethyloxonium tetrafluoroborate. The mixture was stirred over a magnetic stirring plate after adding 1.2 mL of nitromethane. After the evolution of dimethyl ether had ceased, 4 mL of diethyl ether was added slowly in a 1-mL aliquots to precipitate CMQT. The white precipitate was filtered off under vacuum. The precipitate was washed with a further 4 mL of diethyl ether in two 2-mL aliquots and left under vacuum for 60 minutes. CMQT was further recrystallised as described in Appendix I.

5.2.5. Derivatisation procedure for Cys/Cyss analysis in standard solutions

In all cases, Cys and Cyss standards were prepared in 1 $mol.L^{-1}$ HCl in order to match the pH of the industry samples provided, which was 1 $mol.L^{-1}$. For sample analysis, samples were divided into two aliquots. The first was analysed for Cys after pre-column derivatisation with purified CMQT. The second was analysed for Cyss (detected and quantified as Cys by peak area subtraction) after an initial reduction step with TCEP followed by pre-column CMQT derivatisation. Initial studies were performed with a derivatisation pH

of 7.6. Quantitative sample analysis was performed at pH 6.2 in order to minimise matrix effects.

5.2.5.1. Cys determination

A solution containing 75 µL of Cys standard was neutralised with 75 µL of 1 mol.L^{-1} ammonium hydroxide followed by the addition of 50 µL of 50 mmol.L^{-1} HCl and 75 µL of 1 mol.L^{-1} ammonium acetate pH 6.2. The addition of 10 µL CMQT (50 mmol.L^{-1}) was followed by a 2 minutes incubation after which the mixture was acidified with 30 µL of 0.5 mmol.L^{-1} HCl and injected into the chromatograph.

5.2.5.2. Cyss determination

A solution containing 75 µL of Cyss standard was neutralised with 75 µL of 1 mol.L^{-1} ammonium hydroxide followed by the addition of 50 µL of 50 mmol.L^{-1} HCl and 10 µL of 50 mmol.L^{-1} TCEP prepared in 1 mol.L^{-1} ammonium acetate (pH 6.2). Following a 3 minutes incubation, 65 µL of 1 mol.L^{-1} ammonium acetate (pH 6.2) was added along with 10 µL of 50 mol.L^{-1} CMQT and incubated for a further 2 minutes. The solution was then acidified with 30 µL of 0.5 mol.L^{-1} HCl prior to injection.

5.2.6. CD cell culture media samples treatment

A total of 31 CD CHO acid I samples originate from an actual industrial scale biofermentation process facility for a commercial biotherapeutic drug were supplied by Bristol–Myers Squibb as liquids and they contain mainly amino acids. CD media were sampled and aliquotted under sterile conditions and shipped from the US to Ireland at low temperature. The samples were further transferred from Galway to Dublin at low temperature and stored at -70 ^{o}C. When analysed, the samples were removed from the freezer and defrosted at room temperature (~ an hour). The desired sample volume was

aliqotted and then treated as described in Section 5.2.6.1, whereas the remaining sample was retuned to the freezer until further use. The samples identities are listed in Table 5.5.

5.2.6.1. Sample derivatisation

CD CHO acid I media samples were first neutralised with 1 mol.L^{-1} ammonium hydroxide on a 1:1 volume to volume basis. Then the neutralised sample was divided into two aliquots as described in Figure 5.1. For Cys determination, 150 µL of the neutralised sample was treated as described above, with an additional 1/5 dilution with 10 mmol.L^{-1} ammonium acetate (pH 5) prior to injection. For Cyss determination 10 µL of the neutralised sample was diluted to 150 µL with water and treated as described above, again with an additional 1/5 dilution with 10 mmol.L^{-1} ammonium acetate (pH 5) prior to injection.

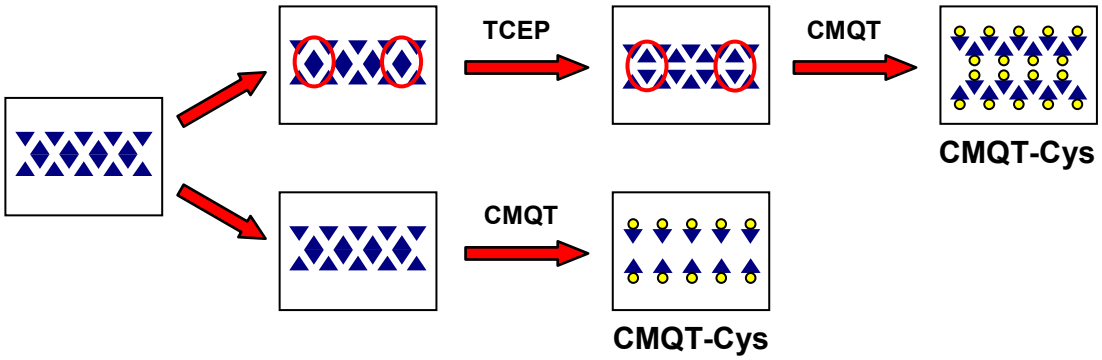

Figure 5.1: Schematic diagram showing the analysis of Cys (▲) and Cyss (◆) in CD media samples.

5.3. Results and discussion

5.3.1. Labelling of Cys/Cyss with CMQT

Due to the lack of suitable chromophores and fluorophores, Cys was labelled with CMQT as a UV-tagging reagent. The reaction between Cys and CMQT is rapid, specific for thiol-containing compounds and occurs under mild conditions across a pH range of 7-9 [15]. In addition, the λ_{max} of CMQT and CMQT-Cys derivative are not the same which leads to less interference in the case of using excess reagent. The chemical reaction is shown in Figure 5.2 in which it involves a nucleophilic displacement of chlorine atom by sulphur atom in the Cys molecule [15]. To ensure the completion of Cys labelling with CMQT, the amount of CMQT and the time period required for labelling of Cys were investigated. As shown in Figure 5.3 the, effect of CMQT concentration on the derivatisation of Cys was studied in the range from 10 mmol.L^{-1} to 150 mmol.L^{-1}. The derivatisation reaction was completed within 1 minute using 50 mmol.L^{-1} of CMQT. However, reaction time was chosen to be 2 minutes to ensure the complete conversion.

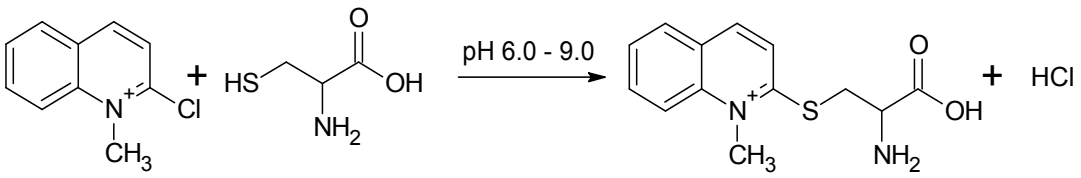

Figure 5.2: Reaction scheme of labelling Cys with CMQT.

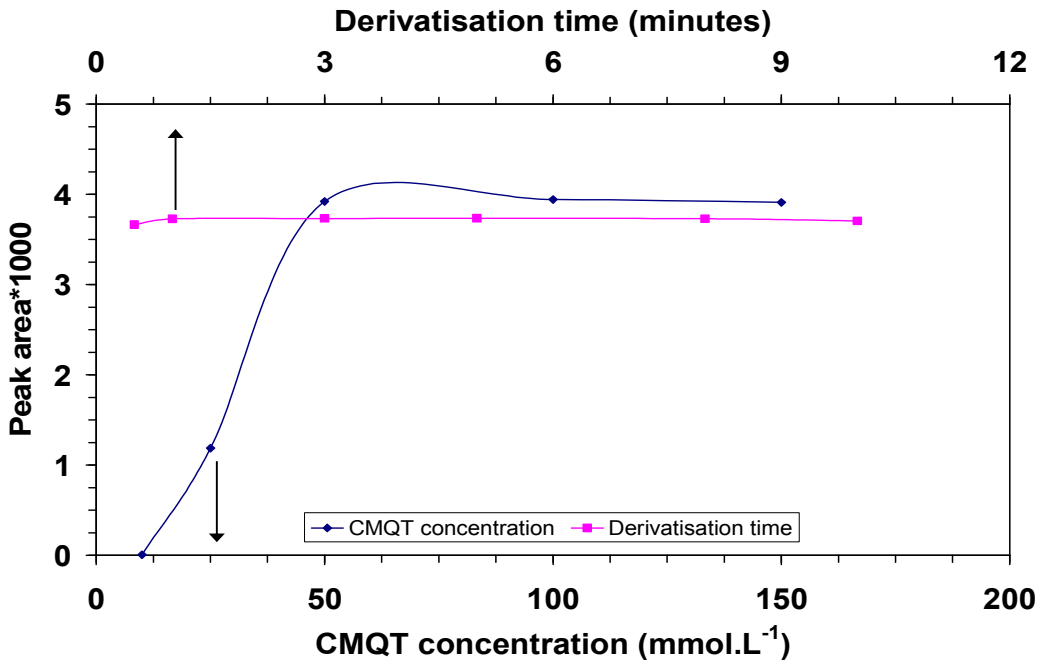

Figure 5.3: Optimisation of CMQT concentration and derivatisation time required for Cys labelling with CMQT.

Cyss has a disulfide bond and does not have free thiol group and thus it cannot be tagged with CMQT. Therefore, the reduction of the disulfide bond is demanded. For this task, TCEP was used as reducing agent due to the advantages that it has compared to other reducing agents (e.g. sodium borohydride, dithiothreitol) since it is water soluble, odour-free, does not produce gases during its use (which can lead to poor reproducibility), and can be used across a wide pH range (pH 1.5 - 11.1). Reduction of the disulfide bond is shown in Figure 5.4. It is worth noting that reducing one mole of Cyss gives two moles of Cys. Therefore, the peak area obtained from Cyss is double the peak area obtained from the same concentration of Cys.

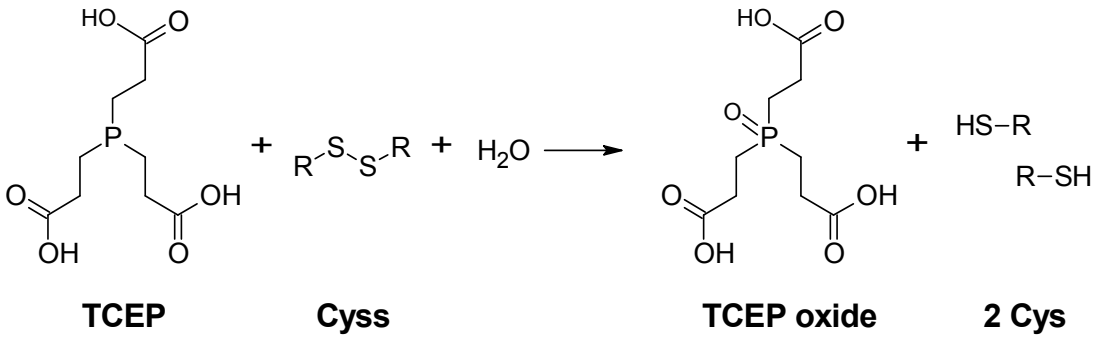

Figure 5.4: Reaction scheme of reducing the disulphide bonds using TCEP.

The influence of TCEP concentration and the time period required for Cyss reduction were investigated and the results are shown in Figure 5.5. The effect of TCEP concentration was studied in the range from 50 to 250 mmol.L^{-1}. As it can be seen, increasing TCEP concentration leads to decrease the peak area of the CMQT-Cys. This is in agreement with the results reported by Kozich *et al.* [34]. This decrease in the peak area could be due to the fact that the TCEP is an acidic solution with a pH of about 2.5 whereas the derivatisation reaction between CMQT and Cys is carried out at pH 7.0 - 9.0. Therefore, increasing the TCEP concentration leads to decrease the final pH of the medium, thus decrease the possibility of CMQT-Cys derivative formation. Moreover, the time period of reduction was also studied. The time period investigated ranged from 0.5 to 10 minutes, however the peak area of CMQT-Cys was not significant. The peak area increased by about 10 % when the time increased from 0.5 to 10 minutes.

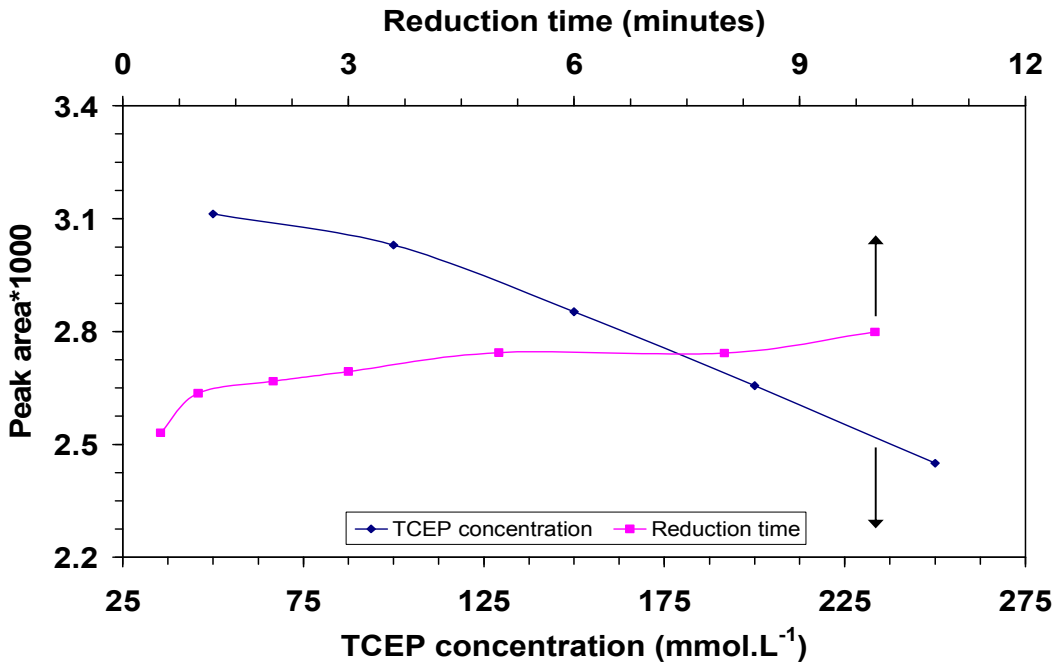

Figure 5.5: Optimisation of TCEP concentration and reduction time required for Cyss reduction.

5.3.2. Chromatographic determination of Cys

5.3.2.1. Isocratic monolithic RPLC

The separation of the CMQT-Cys peak from unreacted CMQT reagent and reaction by-product peaks was achieved using the separation conditions described by Bald and Glowacki [15] with slight modifications. However, here the separation was developed utilising a micro-bore monolithic C_{18} column instead of a conventional particulate column. The column temperature was also increased from 25 ^{o}C to 45 ^{o}C, resulting in a reduction in retention of the CMQT-Cys peak by 50 % and improved peak shape. The optimised separation is shown in Figure 5.6. Peak efficiency for the CMQT-Cys derivative peak was calculated using the equation $n = 5.55 (t_R/W_{½})^2$ as 20,250 N/m, with all reagent and standard peaks eluting in under 2 minutes.

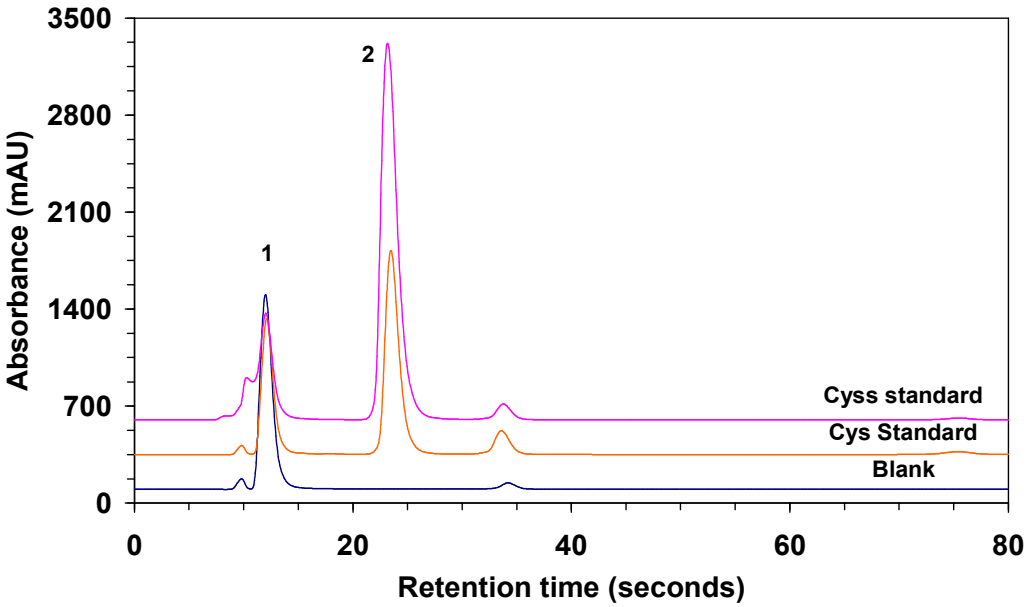

Figure 5.6: HPLC chromatograms of Cys and Cyss standards overlaid with a blank. Column: 50 mm × 2 mm Phenomenex Onyx C_{18} monolith. Mobile phase: 50 mmol.L^{-1} TCA pH 2.5/ACN (86:14). Flow rate: 1.5 mL.min^{-1}. Injection volume: 40 µL. Column temperature: 45 ^{o}C. Detection UV at 355 nm. Peaks: (**1**) excess CMQT, (**2**) CMQT-Cys.

The isocratic method was applied to the analysis of industry supplied CD media fermentation feed-stocks samples. The presence of Cys in the sample was confirmed by spiking the sample with a Cys standard as illustrated in Figure 5.7. The retention time variation between standard solution and diluted complex media sample was approximately 4 % (t_R greater for the media sample) indicating the column capacity for the sample was sufficient and that the complex sample matrix resulted in some small 'salting out' effect for the analyte complex. As can be seen from the sample chromatogram shown, the presence of multiple unidentified peaks existed in the derivatised sample, greatly exceeding the number of known thiol-containing species within the CD media sample. However, all peaks were sufficiently resolved from the target CMQT-Cys peak and all were eluted before 3 minutes and so the method could still be justified as relatively rapid.

To determine whether the sample contained unknown components which absorbed at 355 nm along with CMQT derivatives, the sample was injected directly without derivatisation. This underivatised sample did not produce any peaks that absorbed at 355 nm. Furthermore, the extra peaks were not seen in derivatised Cys standards, bar the reagent impurity peak eluting at 34 seconds (Figure 5.6), and thus were not by-products of the CMQT-Cys reaction. Therefore, the additional peaks observed were deemed to result from the derivatisation of the sample with CMQT, either being derivatised unknown sample components or other specific sample reagent reaction artefacts.

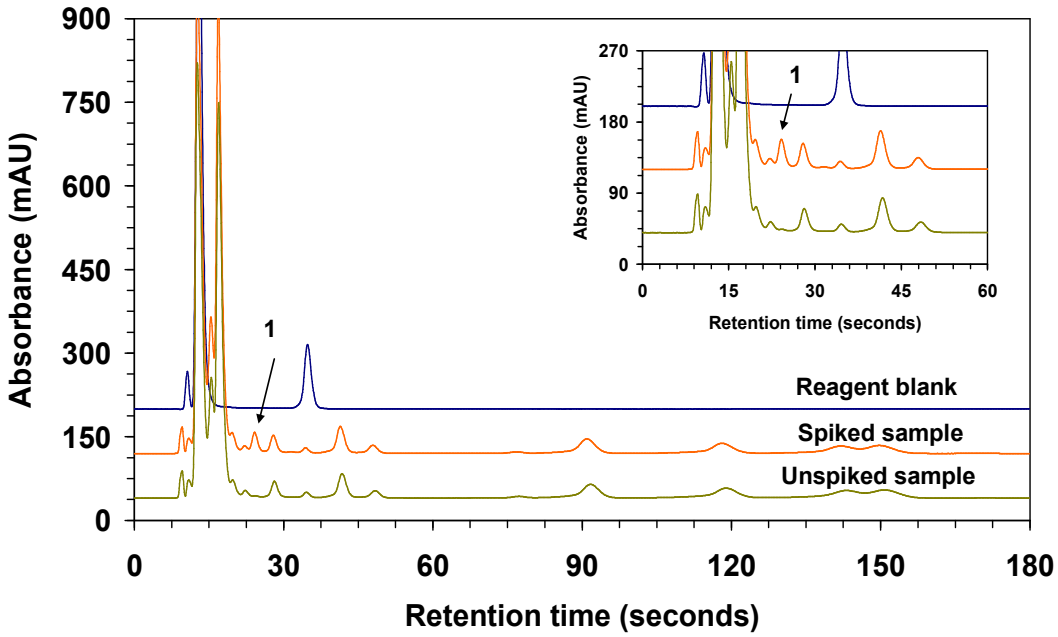

Figure 5.7: HPLC chromatograms of unspiked CD CHO acid I media sample and Cys-spiked CD media sample overlaid with a reagent blank. Chromatographic conditions are as described in Figure 5.6. Peaks: (**1**) CMQT-Cys.

5.3.2.2. Gradient monolithic RPLC

Figure 5.8 shows the optimised separation of CMQT-Cys derivative from the reagent peak using the gradient mode. The gradient mode was developed in order to further improve resolution of the Cys peak from the

matrix peaks. Ammonium acetate was used as mobile phase buffer instead of TCA in order to facilitate simultaneous ESI-MS detection. The same micro-bore monolithic column was utilised as described above, with the mobile phase delivered at 1.5 mL.min^{-1} for simple RPLC, and 0.3 mL.min^{-1} for RPLC-ESI-MS.

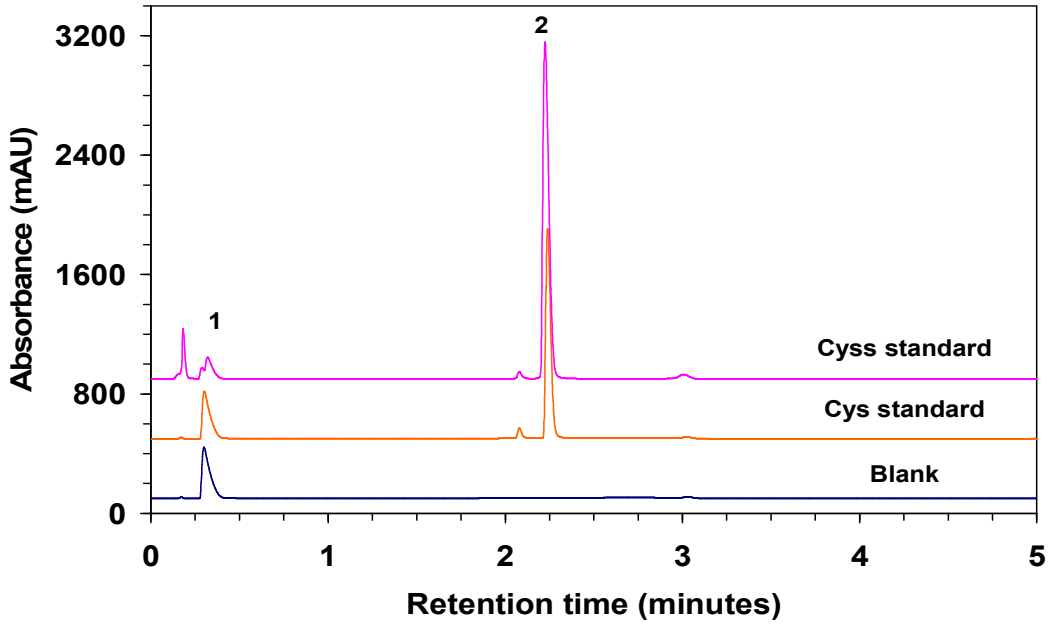

Figure 5.8: HPLC chromatograms of Cys and Cyss standards overlaid with a blank. Column: 50 mm × 2 mm Phenomenex Onyx C_{18} monolith. Mobile phase A: 10 mmol.L^{-1} ammonium acetate buffer pH 5. Mobile phase B: ACN. Gradient program: 0-1 minutes (2 % B), 1.1-5 minutes (10 % B), 5.1-7 minutes (2 % B) delivered at 1.5 mL.min^{-1}. Injection volume: 100 µL. Column temperature: 25 ^{o}C. Detection at 355 nm. Peaks: (**1**) excess CMQT, (**2**) CMQT-Cys.

5.3.3. The effect of sample matrices

When the isocratic method was developed and applied to the real samples, it was expected to get only one peak for CMQT-Cys due to the selectivity of the reagent towards thiol-containing compounds as Cyss is the only thiol-containing compound in the samples. However, as it can be seen in Figure

5.7, unexpected peaks appeared after derivatising the sample with CMQT. Unsuccessful attempts were made in order to clean up the samples such as passing the samples through solid phase extraction cartridge before and after derivatisation with no success. These extra peaks did not occur when underivatised samples were injected.

For the purpose of investigating the origin of interfering sample matrix peaks, the separation was further developed to the gradient method. The chromatograms shown in Figure 5.9 were obtained for a CD media sample which was also spiked with different Cys concentrations. The sample was derivatised using the purified reagent. The gradient was complete, with all peaks eluted in less than 7 minutes, with the target CMQT-Cys peak now very well resolved from all other peaks. However, as shown in Figure 5.9, although recrystallisation yielded a cleaner mass spectrum and ^{1}H NMR spectrum (Appendix I), many extra such peaks still appeared in sample chromatograms, clearly suggesting the peaks observed are indeed CMQT derivatives of unknown sample components.

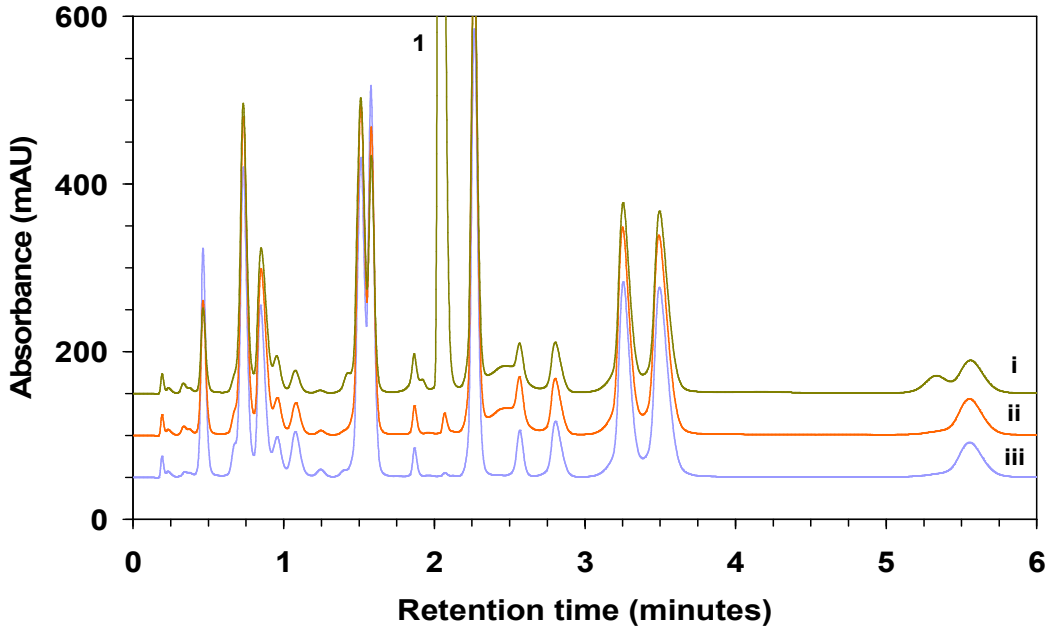

Figure 5.9: HPLC chromatograms showing (**i**) a CD media sample derivatised with recrystallised CMQT reagent and then spiked with (**ii**) 6 and (**iii**) 125 µmol.L^{-1} Cys standard. Chromatographic conditions are as described in Figure 5.8. Peaks: (**1**) CMQT-Cys.

In addition, a number of sample preparation parameters were varied to investigate their effect upon the resultant chromatograms and overall method ruggedness. Firstly, the effect of sample dilution upon quantitation was investigated. A CD media sample spiked with Cys was serially diluted up to a 1/100 dilution factor prior to derivatisation. As expected, the CMQT-Cys peak area decreased linearly as the dilution factor increased (R^2 = 0.998). However, this was not the case for many of the unknown sample component peaks, which showed decreases but unlike CMQT-Cys, such decreases were not linear. For example the peak at ~1.6 minutes in Figure 5.10 decreased in area by a factor of only 1.3 after a ten-fold dilution of the sample. Figure 5.10 shows how the peak area for CMQT-Cys is linearly proportional to sample dilution.

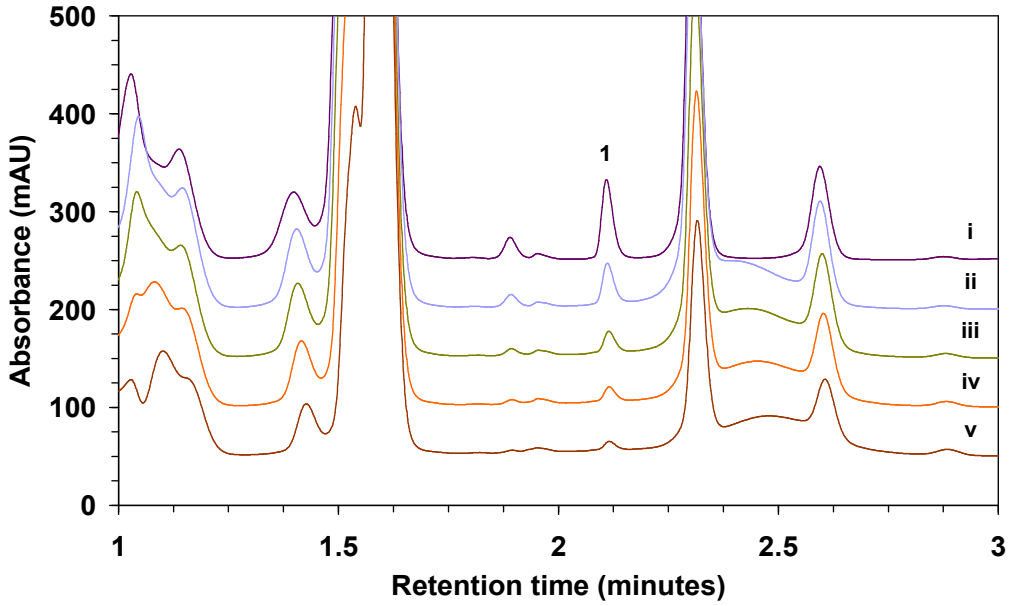

Figure 5.10: HPLC chromatograms showing the effect of sample dilution prior to derivatisation. The sample was diluted by a factor of (**i**) 0, (**ii**) 2, (**iii**) 4, (**iv**) 6 and (**v**) 10. Chromatographic conditions are as described in Figure 5.8. Peaks (**1**): CMQT-cysteine.

Moreover, increasing the amount of CMQT used during the derivatisation step also yielded unexpected results. As shown in Figure 5.11, the peak area for Cys remained constant as the CMQT volume increased,

reflecting the fixed amount of Cys present in the sample. This demonstrated the reaction of Cys with CMQT to be quantitative, despite clear competition with other sample components. Over a factor of ten increase in CMQT concentration, the CMQT-Cys peak varied in peak area by less than 5 %, and such variation was not proportional to CMQT concentration. However, the extra sample peaks continued to increase in area as CMQT volume increased. This indicates such components firstly form less stable derivatives than Cys, and secondly that under the initial conditions used the reaction of these components with CMQT was not quantitative. For example, peaks at ~1.5 and ~2.3 minutes both increased by over 400 % as CMQT concentration was increased by a factor of 10.

As CD media samples were provided from industry in an acidic medium, aliquots were first neutralised and then buffered at a selected pH prior to derivatisation. Based upon the work of Bald and Glowacki [15], this pH was initially selected as pH 7.6. Changing the pH at which sample derivatisation was carried out also had a significant effect upon sample matrix peaks, whilst the target CMQT-Cys peak remained constant. Figure 5.12 illustrates that a decrease in derivatisation pH from 7.6 to 6.0 led to a significant decrease in the peak area of these peaks. For example, there was a 27-fold decrease in peak area for the peak doublet at ~1.5 minutes, with other peaks decreasing by similar amounts, even when the pH was decreased by a mere 1.6 pH units. Thus the extreme sensitivity of unknown sample peaks to small changes in pH allowed for their selective reduction while CMQT-Cys sensitivity was only slightly affected (~6 % peak area variation over pH range studied). Outside the pH range studied, there was a more pronounced decrease in sensitivity. For example, the CMQT-Cys peak area decreased sharply by 34 % between pH 6.0 and pH 5.8. Therefore, all subsequent determinations of Cys/Cyss in the samples were carried out at pH 6.2.

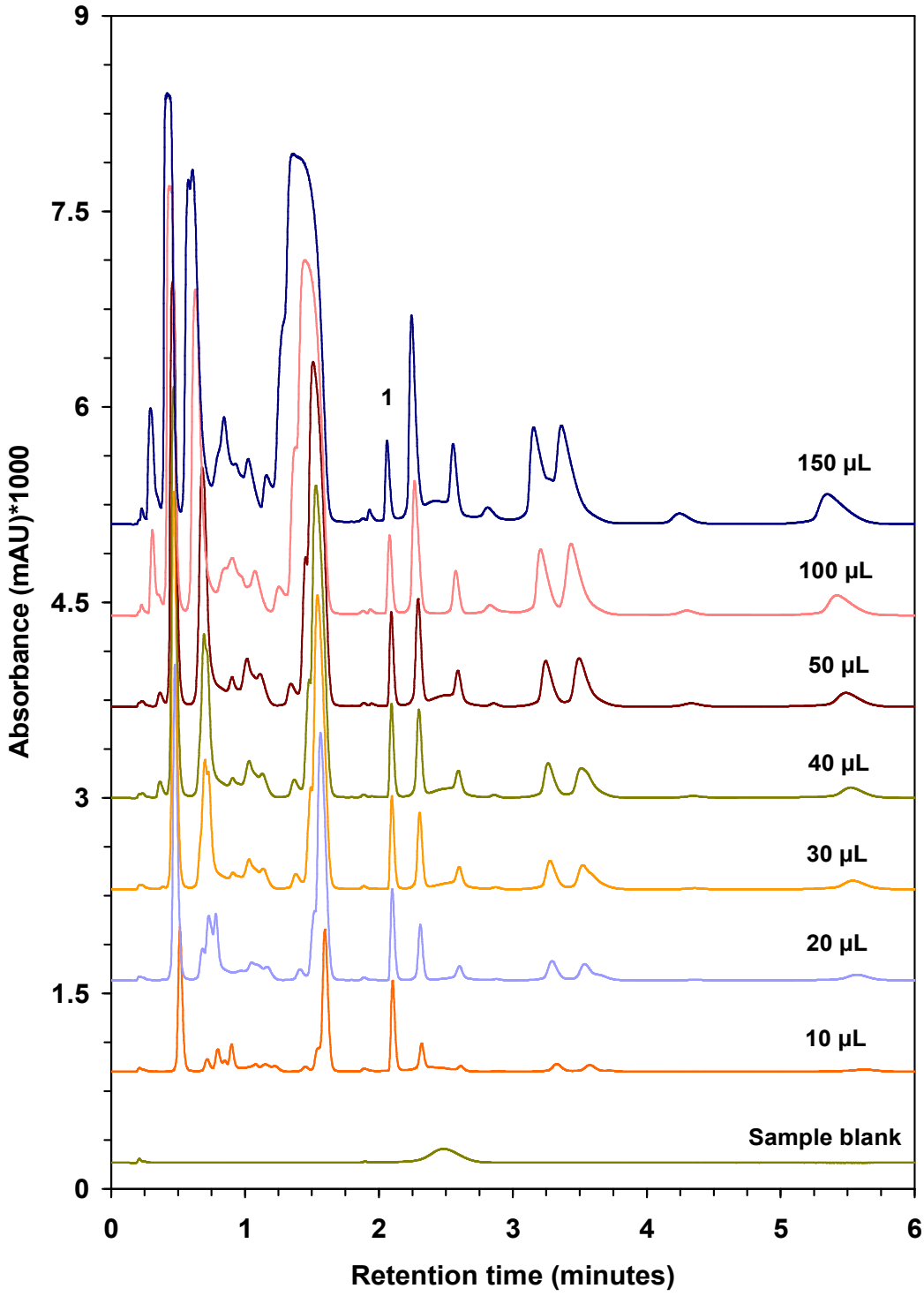

Figure 5.11: Selected HPLC chromatograms showing the effect upon extra peaks of increasing the amount of CMQT used for derivatisation. A Cys-spiked sample was derivatised as described in the Experimental section. Chromatographic conditions are as described in Figure 5.8. Peaks (**1**): CMQT-Cys.

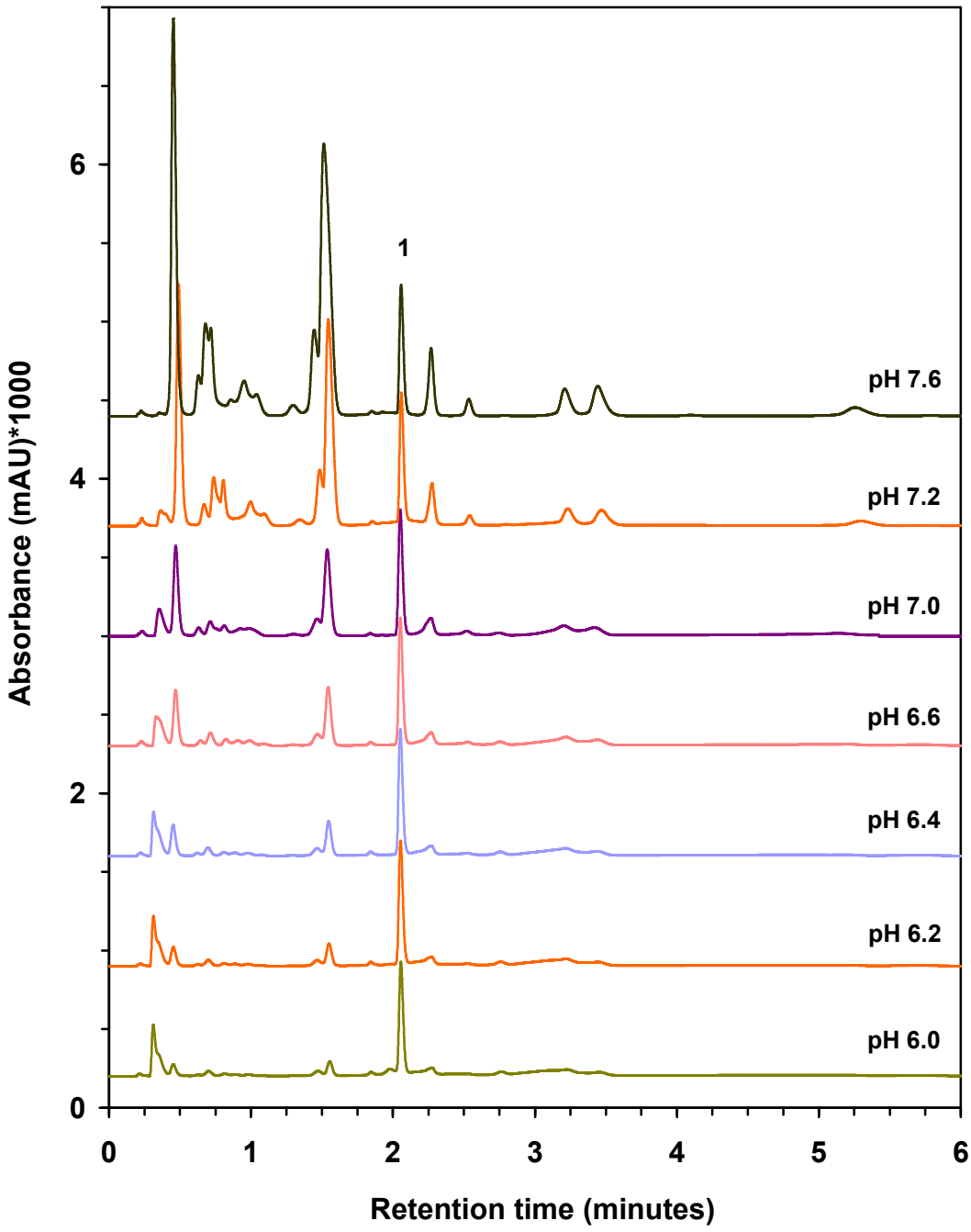

Figure 5.12: Selected HPLC chromatograms showing the effect upon extra peaks of derivatisation at different pH values. Chromatographic conditions are as described in Figure 5.8. Peaks (**1**): CMQT-Cys.

5.3.4. Effect of Cu(II) on Cys determination

Presence of trace metals in the samples, such as Cu(II), may affect the determination of Cys as they have a high affinity for thiol groups [26] and thus prevent the reaction between the thiol group and the derivatisation reagent. Therefore, to investigate the effect of the presence of Cu(II) traces on the determination of Cys, 50 µL of Cu(II) solution within the concentration range 0 - 30 ppm was added to 150 µL of Cys standard (0.5 mmol.L^{-1}) in a 2 mL polypropylene plastic sample tube. The reaction was left for 5 minutes at room temperature. Then 150 µL of that was derivatised as described in the Experimental section. Figure 5.13 indicates the effect of Cu(II) concentration on the formation which shows that increasing the Cu(II) concentration leads to decrease the CMQT-Cys derivative. On the other hand, this effect was completely prevented by the presence of EDTA as it forms a complex with Cu(II). Figure 5.14 shows a separation of derivatised cysteine standard in the presence of Cu(II) only and in the presence of both Cu(II) and EDTA overlaid with derivatised cysteine standard.

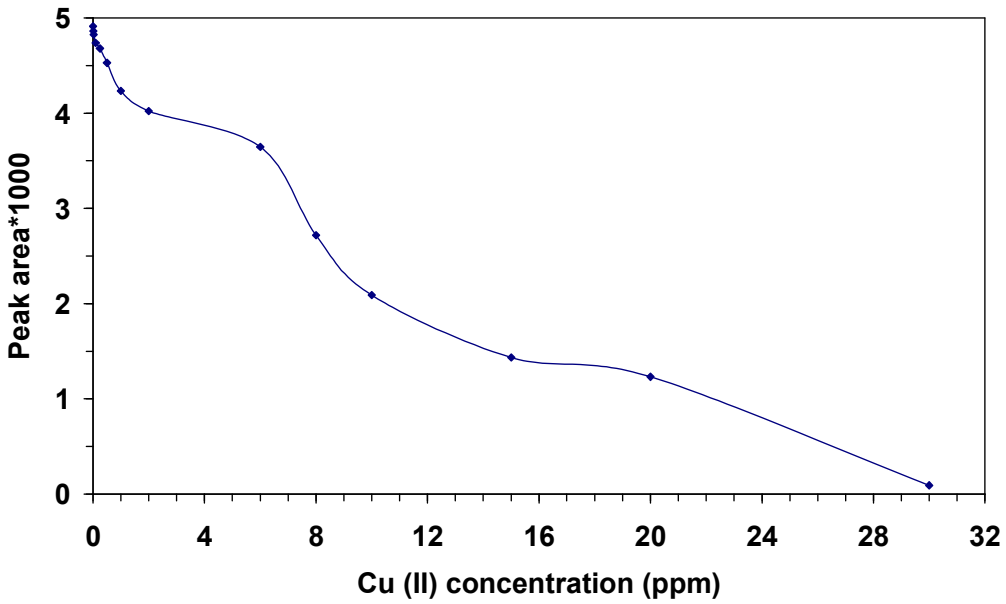

Figure 5.13: A study shows the effect of increasing Cu (II) concentration upon the reaction between CMQT and Cys standard. Derivatisation reaction was carried out as described in the Experimental section.

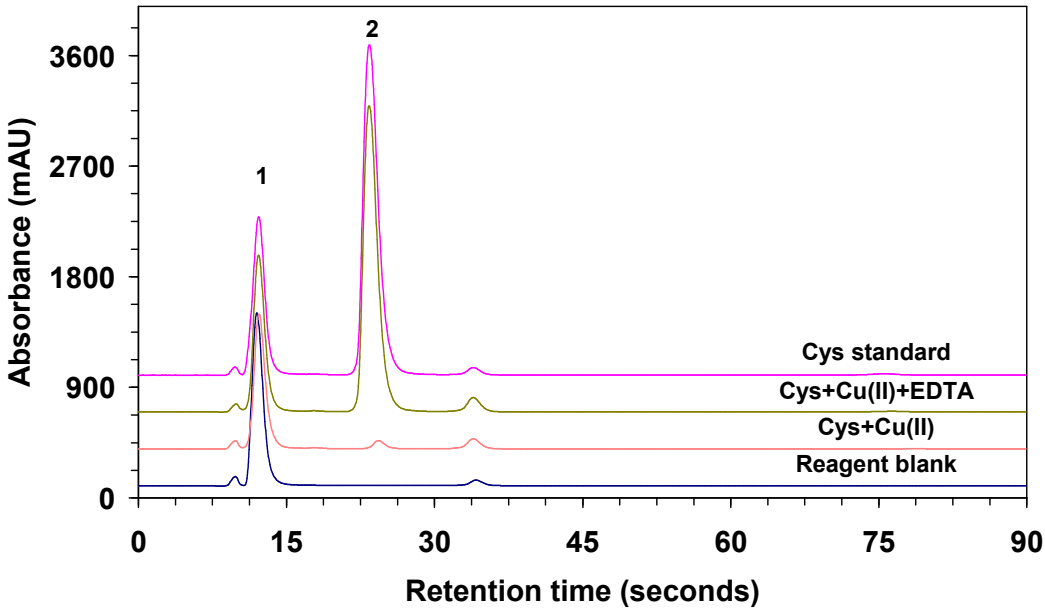

Figure 5.14: HPLC chromatograms showing the effect of Cu(II) on Cys determination in the presence and absence of EDTA. Chromatographic conditions are as described in Figure 5.8. Peaks: (**1**) excess CMQT, (**2**) CMQT-Cys.

5.3.5. Method validation

5.3.5.1. Method selectivity

In order to evaluate the selectivity of the reagent towards thiol-containing compounds, the following amino acid standards were prepared and subjected to the full derivatisation process as described in the Experimental section: 0.1 mmol.L^{-1} L-phenylalanine, L-leucine, D-threonine, L-proline, L-arginine, L-tyrosine, D-methionine, L-histidine, L-methionine, L-aspartic acid, L-isoleucine, L-valine, L-serine, trans-4-hydroxy-l-proline, L-lysine, L-threonine, L-alanine, L-glutamine, L-glutamic acid, L-asparagine, L-tryptophan, D-tryptophan and D-valine. The above listed amino acids were also injected in the column without derivatisation. As a result, all the tested amino acids gave no detectable peaks which confirm the selectivity of the reagent for Cys over other amino acids.

5.3.5.2. Linearity

Linear curves for Cys and Cyss were obtained based on duplicate injection of Cys- and Cyss-CMQT derivatives across the range 0.25-500 μmol.L^{-1} for Cys (n = 9) and 0.25-250 μmol.L^{-1} for Cyss (n = 8). The method was linear over at least three orders of magnitude with correlation coefficients of > R^2 = 0.999 obtained for both analytes. At concentrations greater than 500 μmol.L^{-1} for Cys the standard curve deviated significantly from linearity. Although the initial intention was to begin the Cys linearity at the Cys LOQ (360 nmol.L^{-1}), nevertheless it was found that linearity was maintained at a lower limit of 0.25 μmol.L^{-1}. No investigation was made into whether linearity was conserved below this range.

5.3.5.3. Precision

Precision of the method was studied for the reduction/derivatisation step and for the chromatographic instrument. The repeatability of the reduction/derivatisation step was studied by subjecting six different solutions of Cys and six different solutions of Cyss to reduction/derivatisation processes and the resultants were injected in the HPLC. The precision of the instrument was evaluated by injecting a CMQT-Cys derivative solution in the HPLC system six times and the % RSD was calculated for both peak areas and retention times and the results are listed in Table 5.2. From the results obtained, it can be confirmed that the method was highly reproducible.

5.3.5.4. Sensitivity

Under the optimised conditions, the sensitivity was determined by preparing a series of Cys standard solutions. The LOD of the assay was based on a signal-to-noise ratio of 3 and found to be 36 nmol.L^{-1} (Table 5.2).

5.3.5.5. Recovery studies

The recovery was studied by spiking real samples with three different known concentrations of Cys standard. The spiked samples were derivatised with CMQT as described in the Experimental section. The recovery values were 103, 88 and 97 % for the samples spiked with 5, 10 and 50 $\mu mol.L^{-1}$ of Cys standard respectively.

Table 5.2
Method validation data

	Cys
Area precision % RSD (*n* = 6)	1.1 %
RT precision % RSD (*n* = 6)	0.1 %
Derivatisation precision for Cys % RSD (*n* = 6)	0.55 %
Reduction/derivatisation precision for Cyss % RSD (*n* = 6)	0.51 %
LOD	36 $nmol.L^{-1}$
Cys Linear range ($\mu mol.L^{-1}$), linearity	0.25-500, $R^2 > 0.999$
Cyss Linear range ($\mu mol.L^{-1}$), linearity	0.25-250, $R^2 > 0.999$
Average of Cys recovery from real samples	96 %

5.3.6. Quantitative determination of Cys/Cyss in chemically defined media

Under the optimised sample preparation protocol, the method was applied to the analysis of 31 CD media samples sourced from biopharmaceutical industry. Figures 5.15 and 5.16 show the HPLC chromatograms obtained from the analysis of these samples. Cys/Cyss were found in all samples tested and their presence was verified by a comparison with standard chromatograms. Cys/Cyss presented in the samples were quantified against linear curves of Cys/Cyss standards and the results obtained are listed in Table 5.3. The average amount of Cys found in the samples was 1.7 $\mu g.mL^{-1}$ (S.D. = 0.16 $\mu g.mL^{-1}$) and ranged between 1.6 and 2.3 $\mu g.mL^{-1}$, whereas the average of Cyss was 1196.5 $\mu g.mL^{-1}$ (S.D. = 80.5 $\mu g.mL^{-1}$) and ranged from 1060 and 1347 $\mu g.mL^{-1}$. Moreover, the % RSD values of Cys and Cyss in

the samples were 9.4 % and 6.7 %, respectively, which shows low lot-to-lot variation. Interestingly, Cys was found in all samples tested although initial advice received from the suppliers of the samples was that of the redox pair, only Cyss was expected to be present based on the formulation recipe for the CD media. Clearly the samples had been inadvertently subjected to unwanted redox activity and this method thus has potential as a stability indicating assay within the biopharmaceutical industry. The thiol redox status is defined in this work as the ratio of the reduced form (Cys) to the oxidised form (Cyss) and can be used as an important quality indicator for these raw materials used in biofermentation processes. Table 5.3 details the Cys/Cyss ratio as well as the percentage of total thiols present as Cys. To our knowledge this work represents the first time that Cys/Cyss analysis has been performed in CD media samples and so no alternative method was suitable for the purposes of cross-validation.

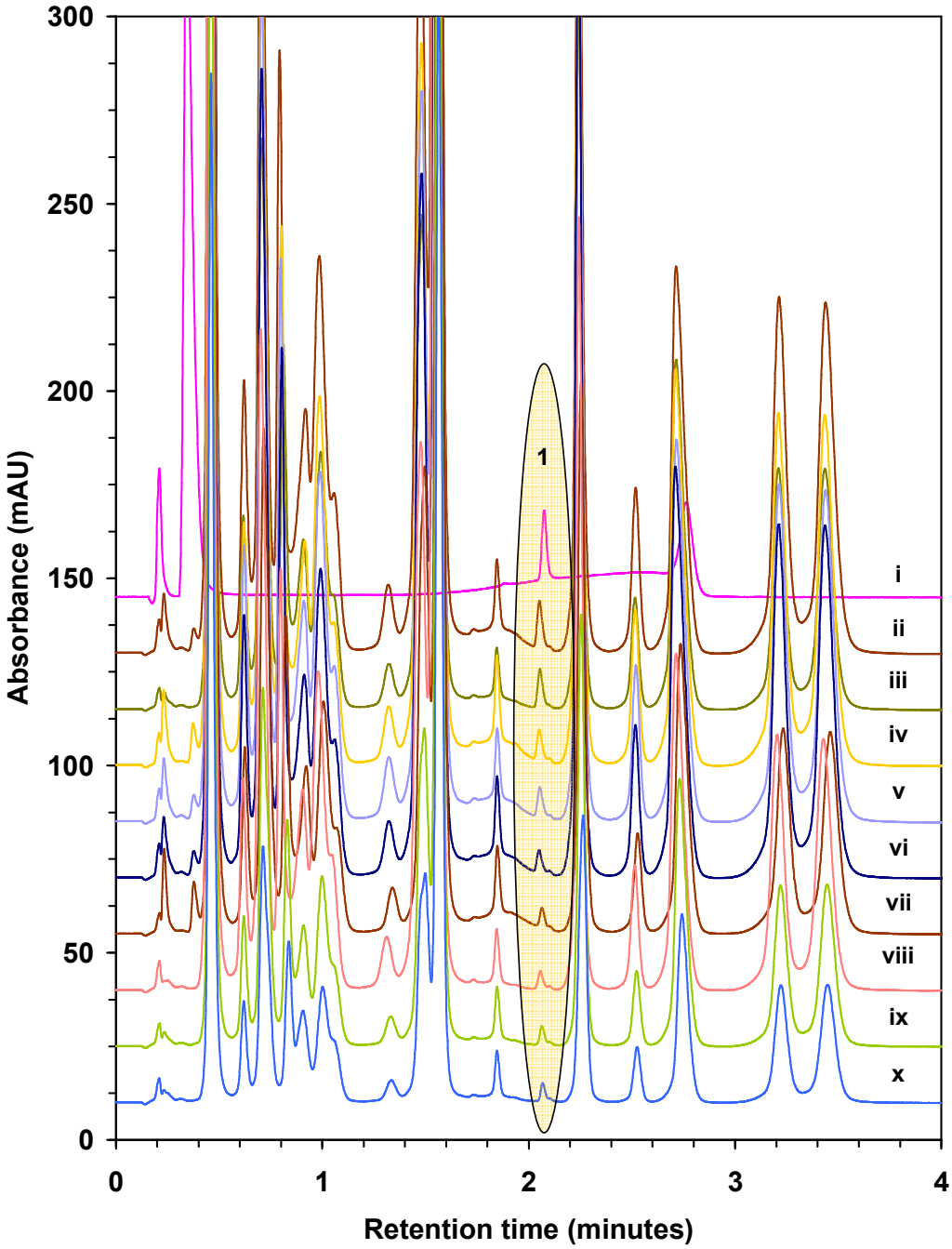

Figure 5.15: Determination of Cys in selected CD media samples. Chromatograms (**ii**-**x**) are selected samples overlaid with (**i**) a Cys standard. Chromatographic conditions are as described in Figure 5.8. Peaks: (**1**) CMQT-Cys.

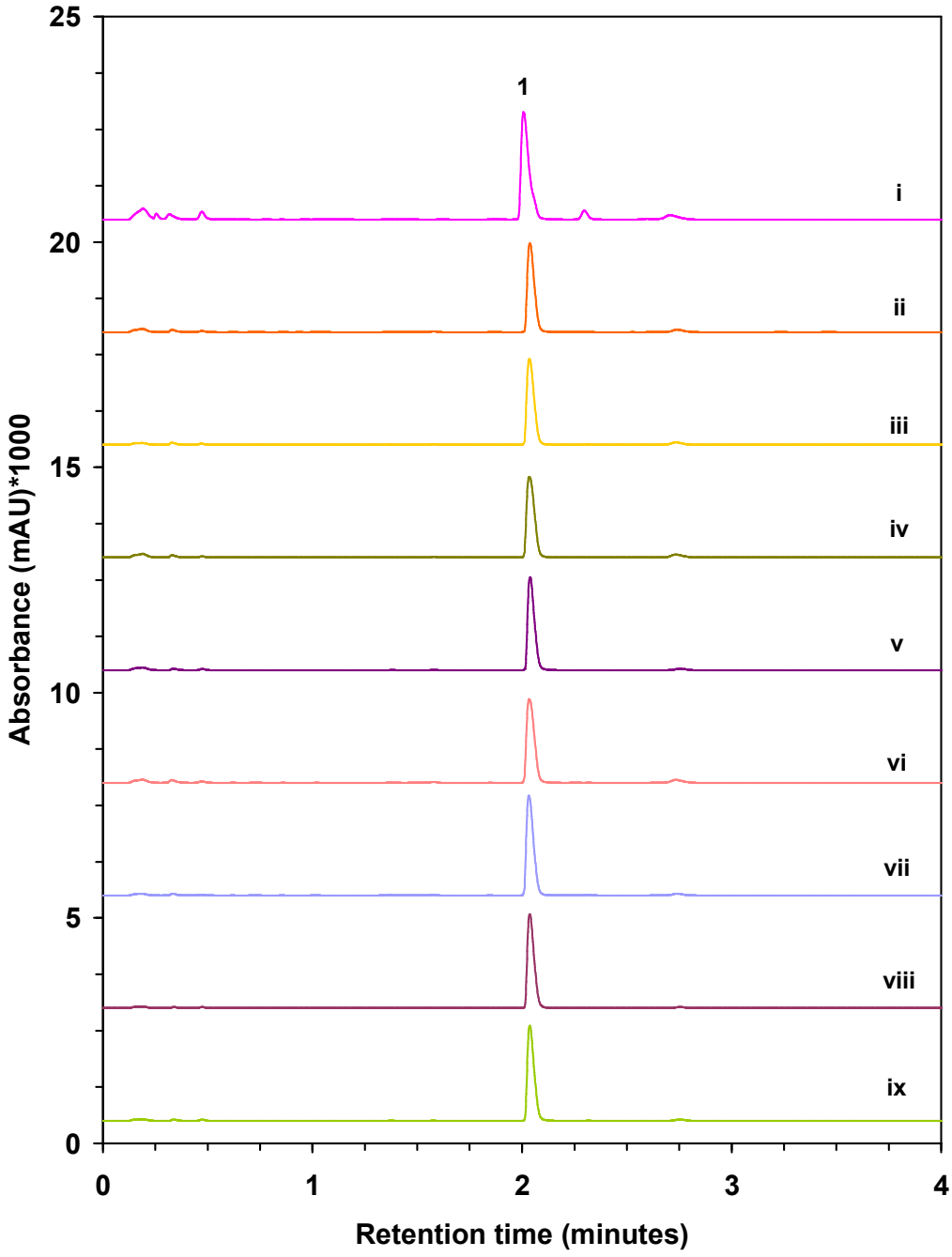

Figure 5.16: Determination of Cyss in selected CD media samples. Chromatograms (**ii**-**ix**) are selected samples overlaid with (**i**) a Cyss standard. Chromatographic conditions are as described in Figure 5.8. Peaks: (**1**) CMQT-Cys.

Table 5.3
Quantitative data of Cys/Cyss in the CD media samples. Date of analysis: 10/07/2009.

Sample	Sample ID	Cys ($\mu g.mL^{-1}$)	Cyss ($\mu g.mL^{-1}$)	% Cys	Cys/Cyss ratio
Sample 1	ITP-2007-000066	1.7	1165.4	0.15	0.0015
Sample 2	ITP-2006-000637	1.6	1179.7	0.14	0.0014
Sample 3	ITP-2006-000062	1.6	1183.9	0.14	0.0014
Sample 4	ITP-2007-000007	1.8	1139.3	0.16	0.0016
Sample 5	ITP-2006-000102	1.7	1341.5	0.13	0.0014
Sample 6	ITP-2007-000054	1.6	1164.1	0.14	0.0014
Sample 7	ITP-2006-000532	1.6	1167.9	0.14	0.0014
Sample 8	ITP-2006-000595	1.6	1168.4	0.14	0.0015
Sample 9	ITP-2007-000089	1.6	1346.5	0.12	0.0014
Sample 10	ITP-2006-000591	1.8	1170.2	0.15	0.0014
Sample 11	ITP-2007-000081	1.7	1147.2	0.14	0.0017
Sample 12	ITP-2006-000538	1.6	1154.2	0.14	0.0017
Sample 13	ITP-2007-000019	2.0	1173.2	0.17	0.002
Sample 14	ITP-2006-000534	2.0	1157.6	0.17	0.0015
Sample 15	ITP-2006-000408	1.8	1322.4	0.14	0.0015
Sample 16	ITP-2006-000599	2.3	1147.8	0.20	0.0015
Sample 17	ITP-2006-000106	1.6	1060.4	0.15	0.0014
Sample 18	ITP-2006-000611	1.6	1066.9	0.15	0.0015
Sample 19	ITP-2006-000603	1.9	1212.9	0.15	0.0015
Sample 20	ITP-2007-000085	1.6	1147.6	0.14	0.0013
Sample 21	ITP-2007-000023	1.6	1317.1	0.12	0.0015
Sample 22	ITP-2007-000084	1.6	1336.5	0.12	0.0014
Sample 23	ITP-2007-000063	1.8	1197.2	0.15	0.0015
Sample 24	ITP-2007-000032	1.8	1175.6	0.15	0.0018
Sample 25	ITP-2006-000607	1.6	1171.2	0.13	0.0013
Sample 26	ITP-2007-000057	1.7	1142.5	0.15	0.0012
Sample 27	ITP-2007-000027	1.6	1179.0	0.14	0.0014
Sample 28	ITP-2006-000098	1.7	1340.9	0.12	0.0012
Sample 29	ITP-2007-000015	1.6	1320.9	0.12	0.0012
Sample 30	ITP-2006-000068	1.6	1130.3	0.15	0.0012
Sample 31	ITP-2007-000002	2.1	1161.9	0.181	0.0012
S.D. (% RSD)		**0.16 (9.4 %)**	**80.5 (6.7 %)**	---	---

5.3.7. LC-ESI-MS qualitative sample analysis

For the confirmation of the presence of Cys/Cyss, the samples were analysed by LC-ESI-MS using the optimised conditions described in the Experimental section. This is the first use of ESI-MS detection with this specific derivatisation chemistry. Under the LC conditions used, the CMQT-Cys peak eluted at 9.5 minutes, as verified by comparison with a standard. Figures 5.17 and 5.18 show representative extracted ion chromatograms (EICs) of a derivatised Cys standard and a derivatised CD media sample before and after reduction. The product ion spectra of the CMQT-Cys derivative shows a fragment ion at *m/z* 185.4, which corresponds to $[M-C_2O_2NH_7]^+$, therefore this fragment ion was used to confirm the presence of the CMQT-Cys derivative. The LC-ESI-MS chromatograms confirm that the method is indeed specific to Cys and Cyss in the complex media samples. In addition, the sample was spiked with Cys standard and the results are shown in Figure 5.19.

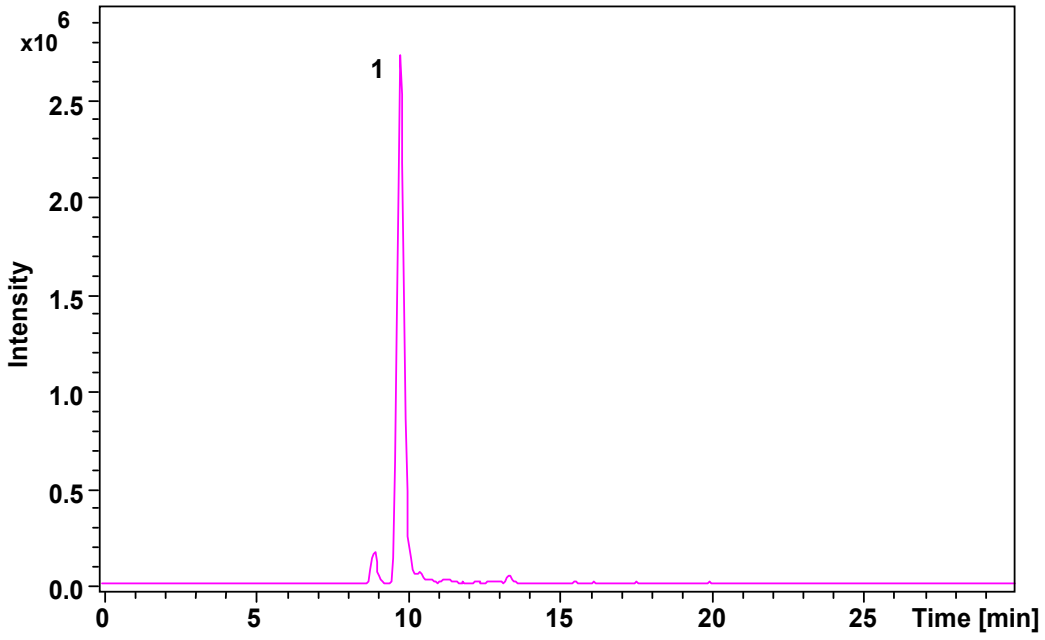

Figure 5.17: Extracted ion chromatogram (EIC) of derivatised Cys standard. Peak eluted at 9.5 minutes with *m/z* 185.4 corresponds to CMQT-Cys derivative. Chromatographic conditions as in Figure 5.8 with flow rate reduced to 0.3 $mL.min^{-1}$.

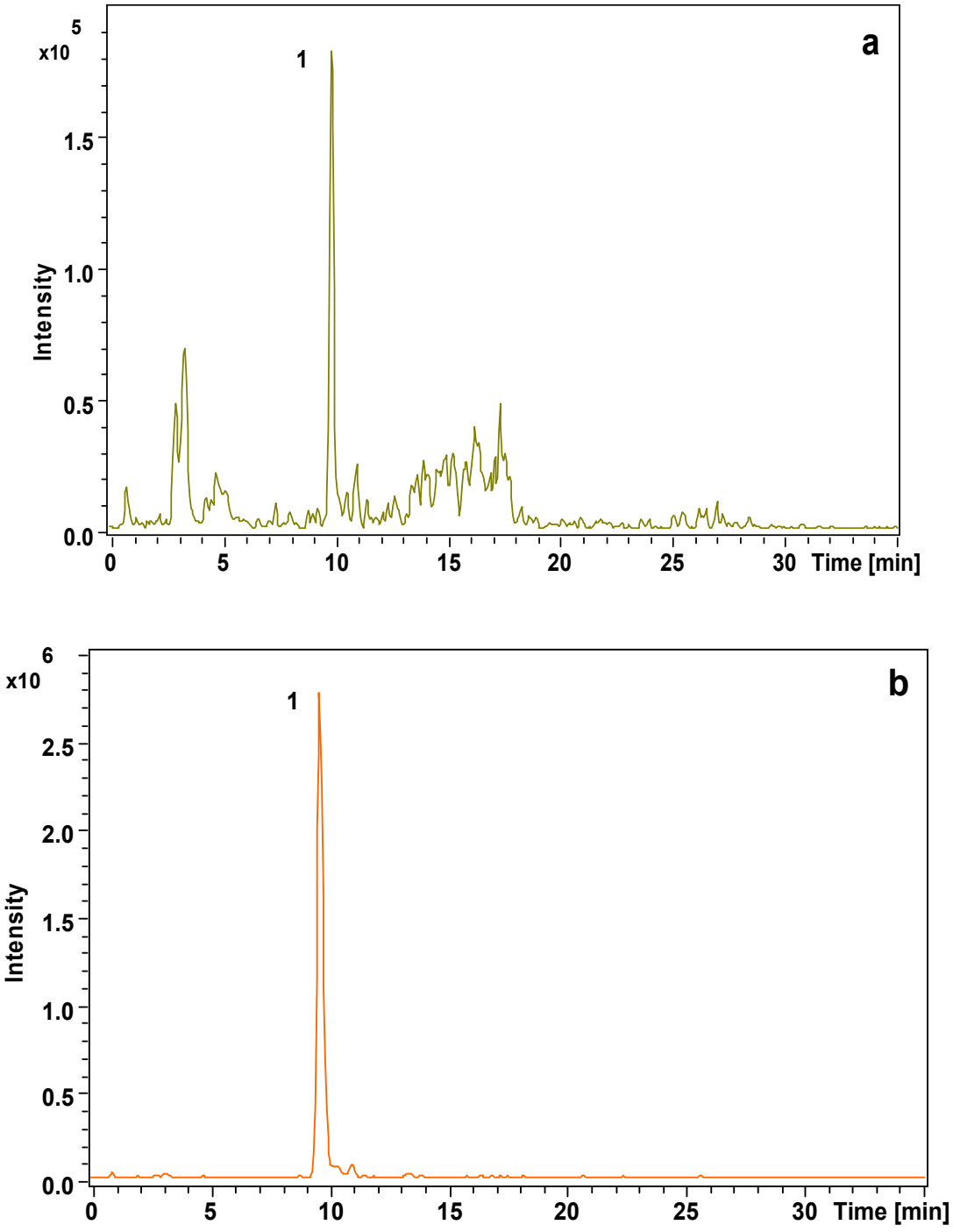

Figure 5.18: Extracted ion chromatograms (EICs) of (**a**) CD media sample and (**b**) reduced CD media sample. Peaks eluted at 9.5 minutes with *m/z* 185.4 correspond to CMQT-Cys derivative. Chromatographic conditions as in Figure 5.8 with flow rate reduced to 0.3 mL.min^{-1}.

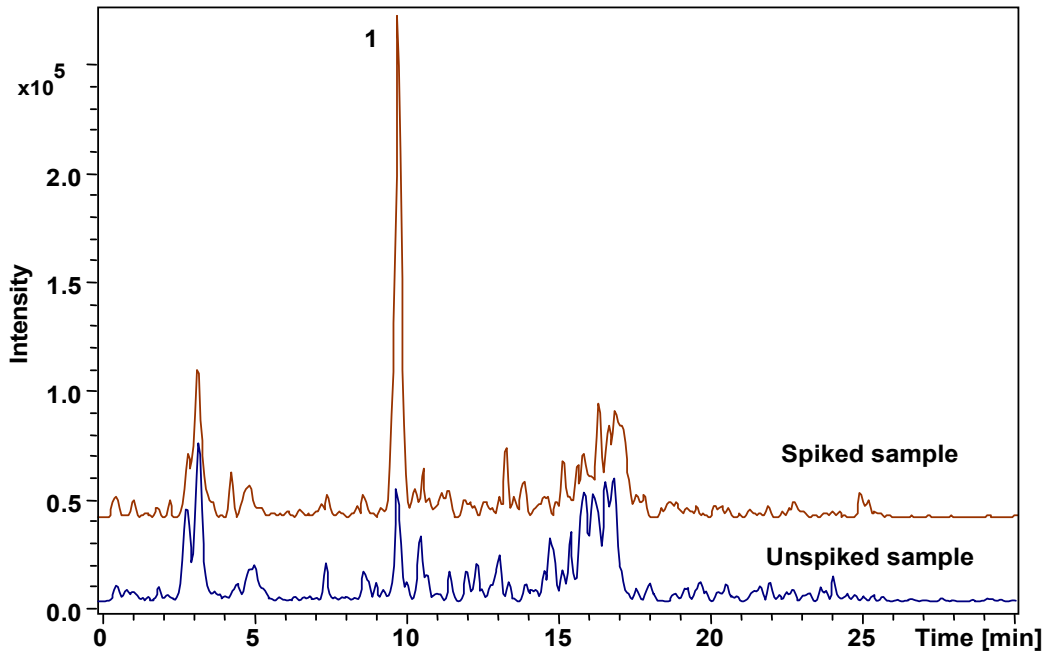

Figure 5.19: Extracted ion chromatograms (EICs) of a CD media sample (unspiked and spiked with Cys standard). Peaks eluted at 9.5 minutes with *m/z* 185.4 correspond to CMQT-Cys derivative. Chromatographic conditions as in Figure 5.8 with flow rate reduced to 0.3 mL.min^{-1}.

5.4. Conclusions

Two pre-column derivatisation methods for determination of Cys and Cyss by monolithic reversed-phase LC and LC-ESIMS were developed. Samples were divided into two aliquots and analysed for Cys first, followed by the determination of Cyss after its reduction to Cys using tris(2-carboxyethyl)phosphine (TCEP). The reagent used (CMQT) is thiol selective and the detection wavelength negated any possible interference from other potential interfering sample components such as monosaccharides or other amino acids. The method performance data reveal that the methods are linear, sensitive and precise. The developed methods are useful for routine analysis for large numbers of CD media samples due to their reduced sample handling steps, quantitative nature, ruggedness and non-harsh conditions.

5.5. References

[1] E. A. McGaw, K. W. Phinney, M. S. Lowenthal, J. Chromatogr. A, 2010, **1217**, 5822 - 5831.

[2] S.W. Myung, M. Kim, H.K. Min, F.A. Yoo, K.R. Kim, *J. Chromatogr. B,* 1999, **727**, 1 - 8.

[3] A.R. Ivanov, I.V. Nazimov, L.A. Baratova, *J. Chromatogr. A*, 2000, **895**, 167 - 171.

[4] S.H. Kang, J.W. Kim, D.S. Chung, J. Pharm. Biomed. Anal. 1997, **15**, 1435 - 1441.

[5] P. Kubalczyk, E. Bald, *Electrophoresis,* 2009, **30**, 2280 - 2283.

[6] N. Ercal, K. Le, P, Treeratphan, R. Matthews, *Biomed. Chromatogr.* 1996, **10**, 15 - 18.

[7] Y. Rao, B. Xiang, E. Bramanti, A. D'Ulivo, Z. Mester, *J. Agric. Food Chem.* 2010, **58**, 1462 - 1468.

[8] J. M. Johnson, F. H. Strobel, M. Reed, J. Pohl, D. P. Jones, *Clin. Chim. Acta* 2008, **396**, 43-48.

[9] X. Guan, B. Hoffman, C. Dwivedi, D. P. Matthees, *J. Pharm. Biomed. Anal.* 2003, **31**, 251 - 261.

[10] J. H. Suh, R. Kim, B. Yavuz, D. Lee, A. Lal, B. N. Ames, M. K. Shigenaga, *J. Chromatogr. B,* 2009, **877**, 3418 - 3427.

[11] E. Bald, G. Chwatko, R. Glowacki, K. Kusmierek, *J. Chromatogr. A,* 2004, **1032**, 109 - 115.

[12] K. Kusmierek, R. Glowacki, E. Bald, *Anal. Bioanal. Chem.* 2006, **385**, 855 - 860.

[13] K. Kusmierek, E. Bald, *Chromatographia*, 2008, **67**, 23 - 29.

[14] Y. Wang, X. Kang, W. Ge, X. Sun, J. Peng, *Chromatographia* 2007, **65**, 527 - 532.

[15] E. Bald, R. Glowacki, *J. Liq. Chromatogr. Rel. Technol.* 2001, **24**, 1323-1339.

[16] R. Glowacki, E. Bald, *J. Liq. Chromatogr. Rel. Technol.* 2009, **32**, 2530 - 2544.

[17] R. Glowacki, E. Bald, *J. Chromatogr. B,* 2009, **877**, 3400 - 3404.

[18] K. Kuśmierek, G. Chwatko, E. Bald, *Chromatographia*, 2008, **68**, S91 - S95.

[19] K. Kuśmierek, E. Bald, *Food Chem.* 2008, **106**, 340 - 344.

[20] K. Kuśmierek, E. Bald, *Biomed. Chromatogr.* 2009, **23**, 770 - 775.

[21] E. Bald, R. Glowackia, J. Drzewoski, *J. Chromatogr. A,* 2001, **913**, 319 - 329.

[22] G. Chwatko, E. Bald, *Talanta*, 2000, **52**, 509 - 515.

[23] A. Pastore, R. Massoud, C. Motti, A. Lo Russo, G. Fucci, C. Cortese, G. Federici, *Clin. Chem.* 1998, 44, 825 - 832.

[24] A.R. Ivanov, I.V. Nazimov, L. Baratova, *J. Chromatogr. A,* 2000, **895**, 157 - 166.

[25] A.R. Ivanov, I.V. Nazimov, L. Baratova, A.P. Lobazov, G.B. Popovich, *J. Chromatogr. A,* 2001, 913, 315 - 318.

[26] D. Tang, L.S. Wen, P.H. Santschi, *Anal. Chim. Acta* 2000, **408**, 299 - 307.

[27] Y. V. Tcherkas, A. D. Denisenko, *J. Chromatogr. A,* 2001, **913**, 309 - 313.

[28] L. Pripis-Nicolau, G. de Revel, S. Marchand, A. A. Beloqui, A. Bertrand, *J. Sci. Food Agric.* 2001, **81**, 731 - 738.

[29] L. Campanella, G. Crescentini, P. Avino, *J. Chromatogr. A,* 1999, **833**, 137 - 154.

[30] K. Kuśmierek, G. Chwatko, R. Glowacki, P. Kubalczyk, E. Bald, *J. Chromatogr. B,* 2011, **879**, 1290 - 1307.

[31] K. Kuśmierek, G. Chwatko, R. Glowacki, P. Kubalczyk, E. Bald, *J. Chromatogr. B,* 2009, **877**, 3300 - 3308.

[32] E. Bald, E. Kaniowska, G. Chwatko, R. Glowacki, *Talanta*, 2000, **50**, 1233 - 1243.

[33] E. Kaniowska, G. Chwatko, R. Glowacki, P. Kubalczyk, E. Bald, *J. Chromatogr. A,* 1998, **798**, 27 - 35.

[34] J. Krijt, M. Vackova, V. Kozich, *Clin. Chem.* 2001, 47, 1821 - 1828.

[35] W. Chen, Y. Zhao, T. Seefeldt, X. Guan, *J. Pharm. Biomed. Anal.* 2008, **48**, 1375 - 1380.

[36] S. Pelletier, C. A. Lucy, *Analyst*, 2004, **129**, 710- 713.

[37] I. J. Kim, S. J. Park, H. J. Kim, *J. Chromatogr. A,* 2000, **877**, 217 - 223.

[38] R. Sack, A. Willi, P. E. Hunziker, *J. Liq. Chromatogr. Rel. Technol.* 2000, **23**, 2947 - 2962.

[39] J. C. Han, G. Y. Han, *Anal. Biochem.* 1994, **220**, 5 - 10.

[40] E. B. Getz, M. Xiao, T. Chakrabarty, R. Cooke, P. R. Selvin, *Anal. Biochem.* 1999, **273**, 73 - 80.

Chapter 6

Lectin-modified gold nano-particles immobilised on a monolithic pipette-tip for selective enrichment of glycoproteins

6.1. Introduction

In general, SPE is a simple effective and most versatile technique. It is applied to the selective capture and preconcentration of the target analyte and/or the removal of potentially interfering components from the sample matrix [1-4]. Micro-scale SPE devices consist of a selective adsorbant material encased within a housing, such as a column, capillary, the channels of a micro-fluidic device, or in commercial pipette-tips when working with small volumes. The advantages of SPE in pipette-tip format include ease of use, small sample and solvent volumes, as well as the possibility to process many samples simultaneously, using either multi-channel hand-held pipettes or robotic liquid handling systems [5-7].

Packed SPE in micro-pipette tips have been applied for the enrichment, purification, desalting and fractionation of different biological samples using either home-made or commercially available tips [8-14]. For example, Kussmann *et al.* used a home-made tip that was prepared by filling a bottom-end squeezed GelLoader tip (Eppendorf, Hamburg, Germany) with a suspension of Poros materials (PerSeptive Biosystems, Framingham, MA, USA) to form a purification column [10]. However, there are some difficulties and drawbacks associated with the preparation of these kinds of tips [8, 15-17], most notably the requirement for inclusion of retaining frits. As an alternative, many packed sorption material related drawbacks can be overcome through the use of monolithic sorption beds.

Great attention has been paid recently to the monolithic sorption beds due to the various features they possess [18, 19], as discussed in Chapter 1. Silica monoliths are manufactured by sol-gel technology with phase separation and have been used for '*in-tip*' SPE previously [16, 20-23]. For example, Miyazaki *et al.* prepared a monolithic silica bed fixed in a 200 µL pipette-tip in which the silica surface was modified with a C_{18} phase or coated with a titania phase and applied to the selective extraction, concentration, desalting and purification of phosphorylated peptides [16].

Organic polymer monoliths are produced by the one-step polymerisation of a mixture consisting of organic monomers, cross-linkers, porogenic solvents and initiators. The mixture is typically sonicated, purged under nitrogen, filled into the tip itself and in most cases polymerised using UV irradiation. Monolithic materials have shown excellent utility as support for affinity chromatography of bimolecules. Different bioligands have been immobilised on monolithic surface such as Protein A for biospecific separation of immunoglobulins [24], mannan for separation of mannose-binding proteins [25], concanavalin A (Con A) and wheat germ agglutinin (WGA) for isolation and preconcentration of glycoconjugates [26], carbohydrate for affinity of lectins [27] and trypsin immobilised a monolithic pipette-tip for rapid proteins digestion [28]. Several studies have described the preparation and application of polymer monoliths in such tips in the analysis of the biological samples [15, 29-34]. For example, Rainer and co-workers fabricated a divinylbenzene-based extraction tip for selective enrichment of phosphorylated peptides and successfully applied this to the study of *in vitro* phosphorylation [29].

Despite of all the advantages of monoliths, the low surface area of the polymer materials, relative to silica monoliths, somewhat restricts the applicability of these materials. However, the surface of the polymer monolith can be modified with nano-particles to increase the surface area simultaneous with the introduction of new chemistry to the surface for specific applications. This modification could be utilised in two different strategies: either embedding nano-particles within the polymerisation mixture during the fabrication of the monolith in one step [15, 29, 34-36] or immobilising the nano-particles on the surface of the pre-formed monolith [37-39]. Following the first strategy, Hsu *et al.* [15], for example, encapsulated C_{18} and IMAC beads into a methacrylate monolith formed within the confines of a pipette-tip, either for desalting of protein solutions (using the C_{18} monolith) or enrichment of phosphopeptides (using the IMAC bead monolith). Building upon this work, Hsieh *et al.* [34] and Rainer *et al.*

[29] formed a polymer monolith within a pipette-tip which incorporated titanium dioxide nano-particles for the selective enrichment of phosphopeptides. However, this strategy is inherently flawed since rather than all nano-particles being presented at the monolith surface, the majority of nano-particles will either be located deep within the bulk polymer or will be only partially exposed at the polymer surface, leading to limitations on binding capacity. Therefore, a preferred strategy for the preparation of nano-structured monoliths is the coating of an activated monolith surface with selected nano-particles resulting in higher surface coverage. Recently, Connolly *et al.* produced a high-density Au-immobilised monolith in which the AuNPs were immobilised on the surface of the preformed monolith utilising azlactone chemistry surface modification [40]. Moreover, Xu *et al.* prepared a GMA-*co*-EDMA monolithic capillary column which was aminated prior to the *in-situ* generation of citrate-stabilised gold nano-particles for the selective capturing of cysteine-containing peptides [41]. This work was quickly followed by Cao *et al.* [42] who used the same gold modified monolith as an “exchangable” surface, which could be readily functionalised with either reversed-phase or ion-exchange functionalities for the separation of selected peptides and proteins.

In this Chapter, the significant enhancement of the surface area of a polymer monolithic phase fabricated in a pipette-tip was achieved by immobilising AuNPs on the surface of the monolith. Then, a selective lectin was immobilised upon the attached AuNPs via a cross-linker for lectin-affinity extraction of target glycoproteins from samples of varying complexity.

6.2. Experimental

6.2.1. Reagents and materials

BP (99 %), 2,2-dimethoxy-2-phenylacetophenone (DPA, 99 %), EDMA (98 %), lauryl methacrylate (LMA, 96 %), 1-decanol (99 %), ethylenediamine

(SigmaUltra), gold(III) chloride trihydrate ($HAuCl_4.3H_2O$, ≥ 99.9 % trace metals basis), 3,3′-dithiodipropionic acid di(N-hydroxysuccinimide ester) (DTSP), transferrin (human, 98 %), ribonuclease B (≥ 80 %), insulin (bovine pancreas), insulin chain B (oxidised from bovine pancreas), enolase (*S. cerevisiae*), thyroglobulin from porcine thyroid gland, carbonic anhydrase (bovine), cytochrome c (equine), manganese (II) chloride tetrahydrate (≥ 99 %), calcium chloride hexahydrate (98 %), D-(+)-galactose (Gal), 1,4-butanediol, 1-propanol, Trizma hydrochloride (≥ 99.0 %), sodium citrate, 4-(2-hydroxyethyl)piperazine-1-ethanesulfonic acid (HEPES, ≥ 99.0 %), DMSO and trifluoroacetic acid (TFA, 99 %) were all purchased from Sigma-Aldrich (Dublin, Ireland). Trizma base (≥ 99.0 %), sodium chloride (NaCl, ≥ 99.5 %) and bovine serum albumin were from Fluka (Buchs, Switzerland). 4,4-Dimethyl-2-vinyl-2-oxazolin-5-one (Vinyl azlactone, 95 % GC) was purchased from TCI Europe (Zwijndrecht, Belgium). Unconjugated *Erythrina cristagalli* lectin (ECL) was provided by Vector Laboratories (Peterborough, UK). *Clostridium perfringens* neuraminidase and *Flavobacterium meningosepticum* PNGase F were purchased from New England BioLabs (Hitchin, UK). The 20-µL polypropylene (PP) tips used for *in-situ* fabrication of the monolith were from Brand (Wertheim, Germany). MeOH, EtOH, acetone and ACN were of HPLC grade and purchased from Fisher Scientific (Dublin, Ireland). All chemicals were used as received and without any further purification. Teflon-coated fused silica capillary (100 µm i.d.) was supplied by Composite Metal Services (Shipley, England).

6.2.2. Instrumentation

Photo-polymerisation and photo-grafting were carried out using a Spectrolinker XL-1000 UV Crosslinker at 254 nm (Spectronics Corp., Westbury, NY, USA). The balance used was a Sartorius Extend (Sartorius, Goettingen, Germany). The sonication bath used was from Branson Ultrasonics Corporation (Danbury, CT, USA). A KD Scientific syringe pump

(KDS-100-CE, KD Scientific Inc, Holliston, MA, USA) was used for all washing and functionalisation of monoliths within pipette-tips, as well as for the trap/release of protein mixtures. SEM was performed on a 1 mm long cross-section of the unmodified monolith using a Hitachi S-3400N instrument (Hitachi, Maidenhead, UK), after sputtering the sample with gold using a SputterCoater S150B (BOC Edwards, Sussex, UK). To visualise the coverage of AuNPs on cross-sections of gold-modified monoliths previously removed from their housings (as described later) and mounted on carbon grids, a Hitachi S-5500 field emission SEM (Hitachi, Maidenhead, UK) was used.

Chromatography was performed using a Dionex Ultimate 3000 capillary LC system (Dionex, Sunnyvale, USA) at a flow rate of 2 $\mu L.min^{-1}$. The injection volume was 1 µL, with detection by UV at 214 nm using a 3 nL flow-cell. Mobile phase A was 0.1 % TFA in water and mobile phase B was 0.1 % TFA in 90 % ACN. For the separation of ribonuclease B and desialylated transferrin a 10 minute gradient of 5 % B to 100 % B was applied at 25 ^{o}C. All other separations involved a 9 minute gradient (5 % B to 100 % B) at 40 ^{o}C. The monolithic column used was prepared by filling a 100 µm x 15 cm vinylised [43] fused silica capillary with a deoxygenated mixture of 24 wt % LMA, 16 wt % EDMA, 14.5 wt % 1,4 butandiol, 45.5 wt % propanol and 1 wt % DPA (w.r.t monomers), followed by irradiation with 2 $J.cm^{-2}$ UV energy at 254 nm. The resulting monolith was washed with MeOH for 2 hours at the flow rate of 2 $\mu L.min^{-1}$ to remove the porogen and unreacted monomers.

6.2.3. Fabrication of a monolith in a pipette-tip

6.2.3.1. Modification of the polypropylene tip inner-wall

Prior to *in-situ* fabrication of the monolith, the inner-wall of the polypropylene tip was modified with grafted chains of EDMA. Firstly, the tip was washed with 10 µL EtOH (10 times) and 10 µL acetone (10 times) and

dried using nitrogen to remove any impurities on the surface of the polypropylene. A solution of BP in MeOH (5 %) was prepared and deoxygenated with nitrogen for 10 minutes. Then the tip was filled with 10 µL of BP and placed in a capped 5-mL polypropylene UV transparent sample tube irradiated with 1 $J.cm^{-2}$ UV energy at 254 nm, followed by a thorough MeOH rinse. The tip was then filled with deoxygenated 15 % EDMA in MeOH and irradiated using the same conditions. Finally, the tip was washed thoroughly with MeOH and dried with nitrogen before use.

6.2.3.2. In-situ fabrication of the polymer monolith within the modified pipette-tip housing

A polymerisation mixture consisting of EDMA (40 wt %), 1-decanol (60 wt %) and DPA (1 wt %, w.r.t monomer) was prepared, sonicated for 30 minutes and deoxygenated with a nitrogen flow for 10 minutes. In order to ensure a constant and repeatable bed volume for each monolith, a 2-mm o.d. guide ring of polypropylene was slipped over the outside of the modified tip, which was subsequently filled by capillary action until the meniscus reached the bottom of the guide ring as shown in Figure 6.1. The filled tip was placed upright in a coned centrifuge tube (polypropylene) and irradiated with 3 $J.cm^{-2}$ UV energy at 254 nm. The resulting monolith was washed thoroughly with MeOH at flow rate of 100 $\mu L.h^{-1}$ to remove the porogen and any unreacted monomers.

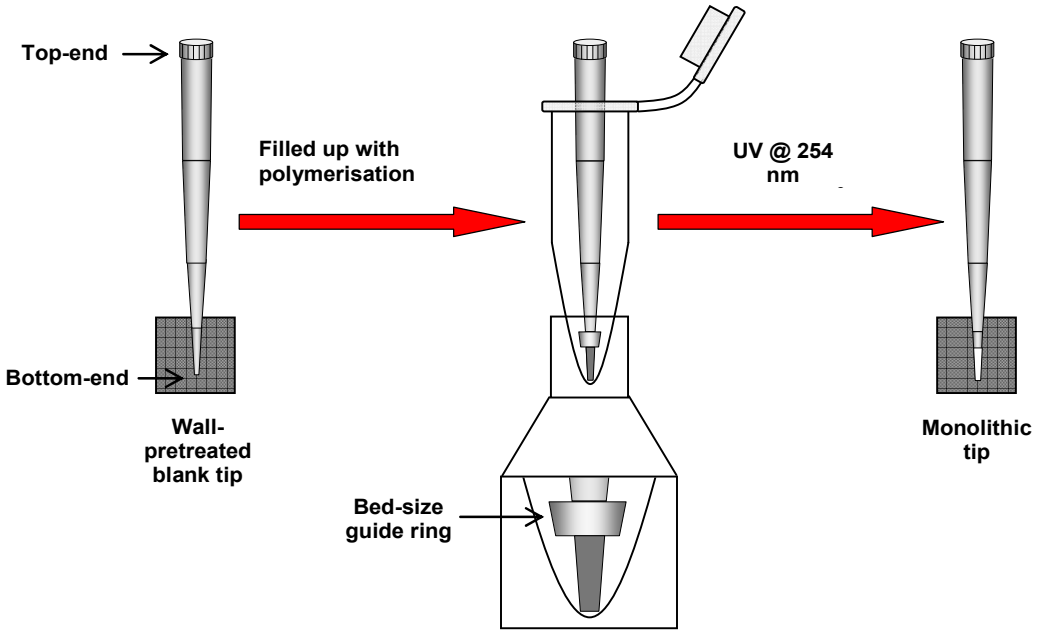

Figure 6.1: Schematic description of the monolithic tip preparation.

In some instances, an attempt was made to prepare a main channel through the centre of the monolith to facilitate lower operating backpressures. This was achieved by inserting a section of either 150 µm o.d. or 360 µm o.d. fused silica capillary down the bore of the monomer-filled tip prior to polymerisation followed by the removal of this template afterwards as described by Hsu *et al.* [15].

6.2.4. Modification of the preformed monolithic surface with gold nano-particles (AuNPs)

6.2.4.1. Preparation of citrate-stabilised AuNPs

AuNPs (20 nm) were prepared using the citrate reduction method as described by Frens [44]. All glassware was acid-washed with 1 mol.L^{-1} HNO_3 prior to use followed by copious rinsing with deionised water. Gold chloride (50 mL, 5 mmol.L^{-1}) was added to a stirred 425 mL volume of boiling deionised water. While the solution was boiling, 25 mL of 30 mmol.L^{-1} sodium citrate was rapidly added during vigourous stirring. After the

evolution of a deep red wine colour, (< 3 minutes), boiling and stirring were continued for 5 minutes, followed by stirring for an additional 30 minutes at room temperature. Finally upon cooling, the solution was made up to 500 mL with water and stored at 4 ^{o}C until use.

6.2.4.2. Immobilisation of AuNPs on the monolithic surface

Attachment of AuNPs to the monolith surface first involved the amination of the monolith surface as described by Connolly *et al*. [40]. The monolith was first conditioned with 50 µL MeOH followed by flushing the monolith with a deoxygenated solution of 5 % BP in MeOH for 30 minutes. The monolith was then irradiated with 3 J.cm^{-2} UV energy at 254 nm followed by washing with MeOH for 30 minutes. The monolith was then flushed with a deoxygenated solution of 15 % vinyl azlactone in MeOH for 30 minutes and subjected to the same irradiation cycle. After a preliminary wash with MeOH, the monolith was washed with H_2O for 30 minutes prior to flushing with 1 mol.L^{-1} ethylenediamine for a nominal time of 4 hours. The monolith was again washed with water (until monolith rinsings were pH neutral) to remove free ethylenediamine. Finally, the aminated monolith was flushed with AuNPs (approx. 2 mL). Immobilisation of AuNPs was considered to be complete after the entire monolith bed had turned a deep red colour. The Au-modified monolith was washed with 1 mL water to remove unbound AuNPs. The axial homogeneity of AuNPs coverage along the monolith bed was readily evaluated using an optical microscope. The density of coverage of AuNPs on the monolith was examined using FE-SEM.

6.2.5. Functionalisation of Au-modified monolith with ECL for affinity extraction of glycoproteins

The Au-modified monolith prepared above was conditioned with 50 µL of DMSO and then flushed with 25 mmol.L^{-1} coupling agent, DTSP in DMSO for 4 hours. The monolith was then washed with DMSO for 30 minutes to remove any unreacted DTSP, followed by deionised water for 30 minutes.

Subsequently, the monolith was conditioned for 30 minutes with 10 mmol.L^{-1} HEPES buffer pH 8.2 containing 1 mmol.L^{-1} Ca^{2+} and 1 mmol.L^{-1} Mn^{2+}, followed by flushing a 1 mg.mL^{-1} solution of ECL prepared in the same buffer for 4 hours at room temperature. Finally, in order to block any unreacted succinimidyl groups, the resulting ECL-Au-modified monolith was flushed with a primary amine (1 mol.L^{-1} Tris buffer pH 7.4) followed by a 100 µL deionised water wash. When not in use, the ECL-Au-modified monolith was kept immersed in 10 mmol.L^{-1} Tris buffer pH 7.4 containing 150 mmol.L^{-1} NaCl, 1 mmol.L^{-1} Ca^{2+} and 1 mmol.L^{-1} Mn^{2+} at 4 ^{o}C. For the sake of clarity, this monolith shall be referred to hereafter as **Monolith A**.

In order to investigate the effect of immobilising AuNPs on the monolith surface, a comparison monolith (**Monolith B**) was also prepared which did not incorporate immobilised AuNPs. Instead, the monolith was grafted with vinyl azlactone as described, and then ECL was immobilised onto the resulting pendant azlactone moieties using the same immobilisation buffer, followed by blocking with 1 mol.L^{-1} Tris buffer.

6.2.6. Non-specific binding studies

In order to investigate the origin of unwanted non-specific interactions between test proteins and the Au-modified substrate, a further four monoliths were prepared (referred to as “blank” monoliths in that they did not include immobilised ECL). **Blank Monolith 1** did not include immobilised AuNPs, but was grafted with polymer chains of vinyl azlactone and blocked with 1 mol.L^{-1} Tris buffer. **Blank Monolith 2** was modified with AuNPs which were not blocked with 1 mol.L^{-1} Tris buffer. **Blank Monolith 3** was modified with AuNPs which were subsequently blocked with 1 mol.L^{-1} Tris buffer. **Blank Monolith 4** was modified with AuNPs, functionalised with DTSP and the resulting succinimidyl groups blocked with 1 mol.L^{-1} Tris buffer. Figure 6.2 illustrates a schematic diagram of the different monoliths prepared and Table 6.1 summarises them.

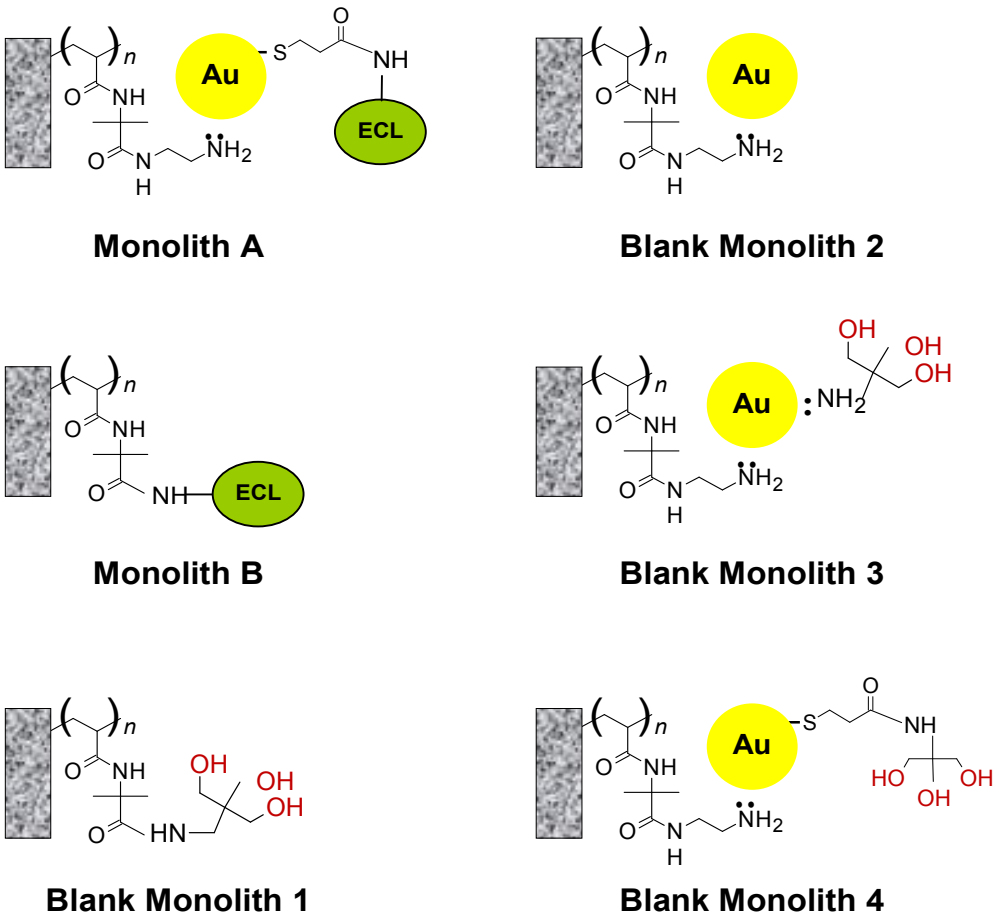

Figure 6.2: Schematic diagram of all affinity monoliths and blank monoliths prepared in this study.

Table 6.1
Summary of different monoliths prepared throughout this study

Monolith	Surface chemistry	Expected protein retention
Monolith A	ECL immobilised on AuNPs	Galactosylated proteins
Monolith B	ECL immobilised on azlactone moieties (no AuNPs)	Galactosylated proteins
Blank monolith 1	Azlactone blocked with Tris buffer	None
Blank monolith 2	Bare AuNPs	Amines and thiols
Blank monolith 3	AuNPs blocked with Tris buffer	None
Blank monolith 4	AuNPs functionalised with DTSP and then blocked with Tris buffer	None

6.2.7. Desialylation of transferrin and thyroglobulin

Desialylated transferrin and thyroglobulin was prepared by treating each with *Clostridium perfringens* neuraminidase and following supplier instructions. Briefly, 100 µg of the protein was prepared in 50 mmol.L^{-1} sodium citrate, pH 6.0, mixed with 50 U neuraminidase and left to react at 37 ^{o}C for overnight.

6.2.8. Deglycosylation of transferrin

Transferrin was deglycosylated using *Flavobacterium meningosepticum* PNGase F, following supplier instructions. Briefly, 100 µg of the protein was prepared in 50 mmol.L^{-1} sodium phosphate, pH 7.5, mixed with 500 U PNGase F and left to react at 37 ^{o}C for overnight.

6.2.9. Bind and elute studies

A number of selected proteins were used to study the binding affinity of all fabricated monoliths and also to evaluate the blocking strategies used to eliminate non-specific interactions (i.e. binding which was not due to sugar-lectin interactions). All lectin affinity monoliths and blank monoliths were tested using the syringe pump at a flow rate of 50 µL.$hour^{-1}$. The monolith was first conditioned with 20 µL of loading buffer (10 mmol.L^{-1} Tris, pH 7.4, containing 150 mmol.L^{-1} NaCl, 1 mmol.L^{-1} Ca^{2+} and 1 mmol.L^{-1} Mn^{2+}). A test mix of selected proteins (total volume: 20 µL) was prepared in loading buffer and loaded from the top-end, pumped through the monolith and collected in a clean 1.5 mL centrifuge tube, followed by a 20 µL buffer wash which was collected in the same tube and combined with the extracted mixture. Preliminary binding studies and all evaluations of “blank monoliths” (**Blank Monoliths 1** to **4**) involved the use of a simple mixture of two glycoproteins: desialylated transferrin and ribonuclease B (20 µg.mL^{-1} each) and denoted as **Standard A.** Further more rigourous testing of the affinity monoliths involved the use of a more complex protein mixture containing up to nine

proteins as described later and denoted as **Standard B.** Finally, an *Escherichia coli* (*E. coli*) cell lysate spiked with transferrin was also used to test the affinity monolith. In all cases, to elute any retained glycoprotein, 40 µL of 0.8 mol.L^{-1} galactose prepared in buffer solution was flushed through the monolith and collected for analysis by nano-LC. All affinity monoliths prepared in this study could be re-used numerous times after a rinse with loading buffer.

6.3. Results and discussion

The fabrication of porous polymer monoliths within pipette-tips has been reported before [15, 29-34], however in the work described herein, it is reported for the first time the *in-situ* covalent attachment of AuNPs to the polypropylene-encased monolith, resulting in two distinct benefits. Firstly, the surface area can be significantly increased, resulting in increased loading capacity when a selected lectin is immobilised onto the gold surface. Secondly, the use of a gold surface and a commercially available bi-functional linker (DTSP) means that the extraction device is readily suited for the immobilisation of any bio-recognition molecule via the reaction between pendant succinimidyl groups and native lysine residues (ranging from Protein A for trapping immunoglobulins, to enzymes such as trypsin or PNGase for off-line enzymatic digestion). In this study however, a galactose-selective lectin (ECL, Figure 6.3) was elected to be immobilised on the gold surface as a simple test-case, in order to examine the trap-and-release of various selected glycoproteins with terminal beta-galactose. Terminal beta-galactose is of concern in biopharmaceuticals since proteins with these structures get cleared from the bloodstream by the liver [45]. ECL is a well-characterised commercially available lectin [46]. The performance of the resulting ECL affinity monolith was also compared directly with that of an ECL affinity monolith which did not incorporate AuNPs, but rather where the lectin was instead immobilised directly onto the lower surface area

monolithic substrate itself via grafted chains of amine-reactive poly(vinyl azlactone).

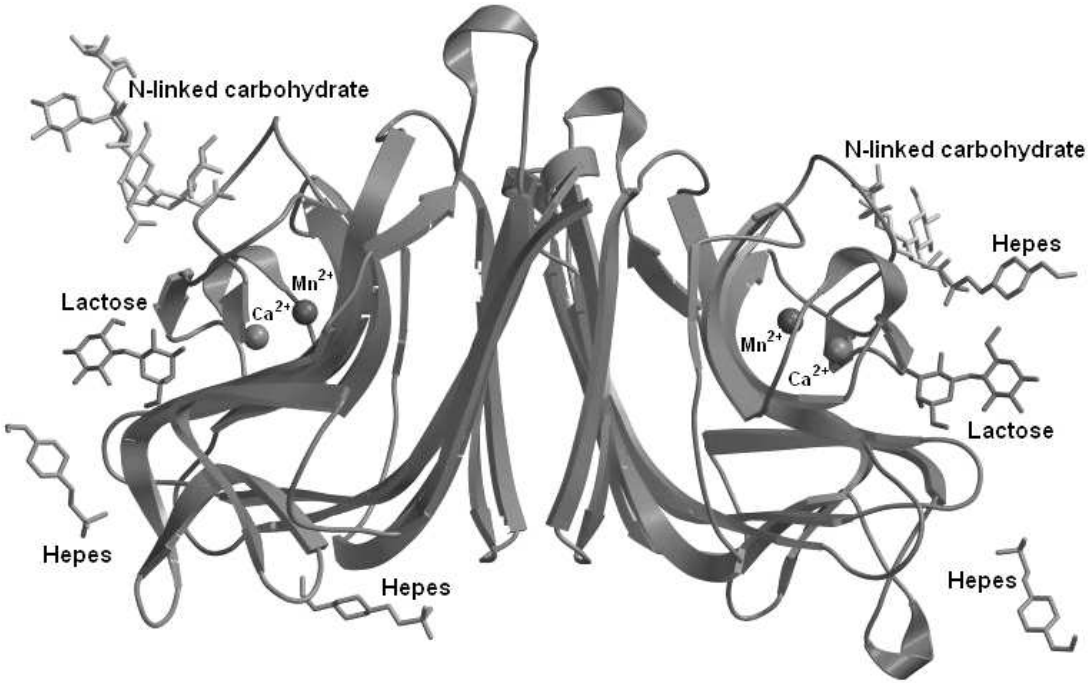

Figure 6.3: The structure of ECL dimer. The N-linked carbohydrate, lactose bound at the combining site and HEPES molecules are shown. The manganese and calcium ions bound in the vicinity of the combined site are shown as small spheres [47].

6.3.1. Fabrication of porous polymer monoliths within pipette-tips

In the study described here, an EDMA monolith was *in-situ* fabricated within the confines of a commercial 20 µL plastic pipette-tip. Pipette-tips used in this study were manufactured from polypropylene as polypropylene is resistant to all solvents employed in this study and was found to be appropriate for all UV-initiated photo-grafting and polymerisation events. In addition, polypropylene is highly suited as a substrate for the photo-grafting of selected monomers as it contains easily abstractable hydrogens (photo-grafting is mediated by BP and proceeds due to hydrogen abstraction from the surface of the substrate [48-50]). Therefore, as illustrated in Figure 6.4,

the surface chemistry of the tip inner-wall was modified by grafting EDMA chains for subsequent attachment to the monolith.

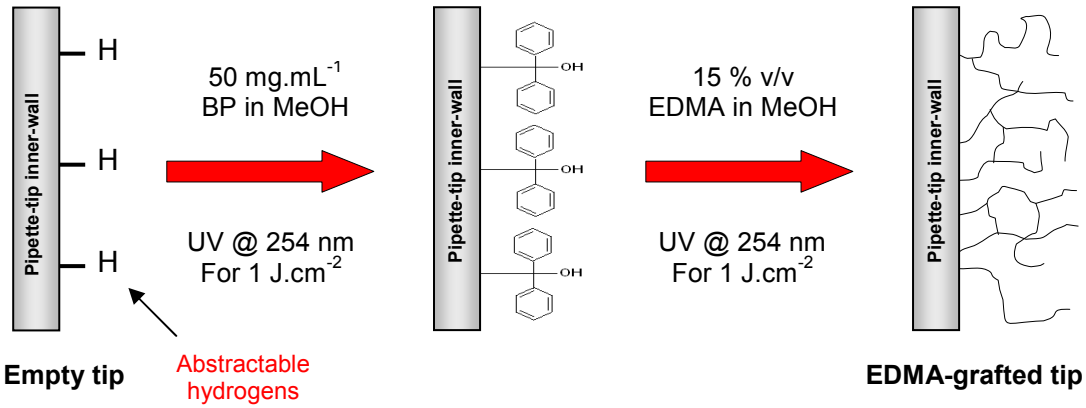

Figure 6.4: Schematic diagram of pipette-tip inner-wall modification.

The inner-wall surface of the tip was modified to ensure covalent attachment between the EDMA monolith and the tip. This monolith/wall attachment is significant (i) to increase the rigidity of the monolithic bed to withstand high backpressures and thus prevent the bed from slipping out of the tip either during the tip fabrication and surface modification (i.e. grafting, Au-immobilisation and ECL-modification) or during the sample analysis as some of the tips are not tapered enough at the bottom-end to hold the monolithic bed, and (ii) to prevent unwanted voids between the wall and the monolithic bed that occur due to the shrinkage of the monolith during the polymerisation, which could has an impact on the recovery and thus the sample to pass through the monolithic bed. In addition, there is no need for supporting frits when the monolithic bed is bonded to the wall.

The monolith/wall attachment evaluation was carried out by flowing a stream of nitrogen from the bottom-end of the tip. The monolithic bed was easily detached from the unmodified pipette-tip whereas the resistance of the monolith prepared in the modified tip was significantly higher which

indicates the strong covalent attachment between the inner-wall of the tip and the monolithic bed. As a result of this attachment, the tip could be operated at high flow rates. Figure 6.5 shows SEM images of an EDMA monolith fabricated in a pipette-tip, with and without wall modification. As it can be seen, the monolith fabricated in a wall-modified tip was covalently attached to the tip inner-wall (Figure 6.5(**i**-**iv**)), whereas the monolith fabrication in the unmodified tip resulted in a void between the monolith and the tip inner-wall (Figure 6.5(**v**) and (**vi**)).

Unlike capillary fused silica or microfluidic channels, the *in-situ* fabrication of the monolith in a pipette-tip is technically challenging. For example, because the tips are not sealable, polymerisation can not be carried out thermally (i.e. in a water bath). Moreover, some of the porogens can not be used due to the volatility issues. Another issue is how to control the bed size for a reproducible preparation of the monolithic tips. Unsuccessful attempts were made to adjust the monolith bed size utilising a photomask as illustrated in Figure 6.6(**i**) because some of the monolith was partially polymerised underneath the mask which was over the requested bed size. Also, other studies have reported the placement of guide ring inside the tip for this purpose [15]. However, this strategy was avoided due to the possible generation of a void volume between the top of the monolith bed and the ring.

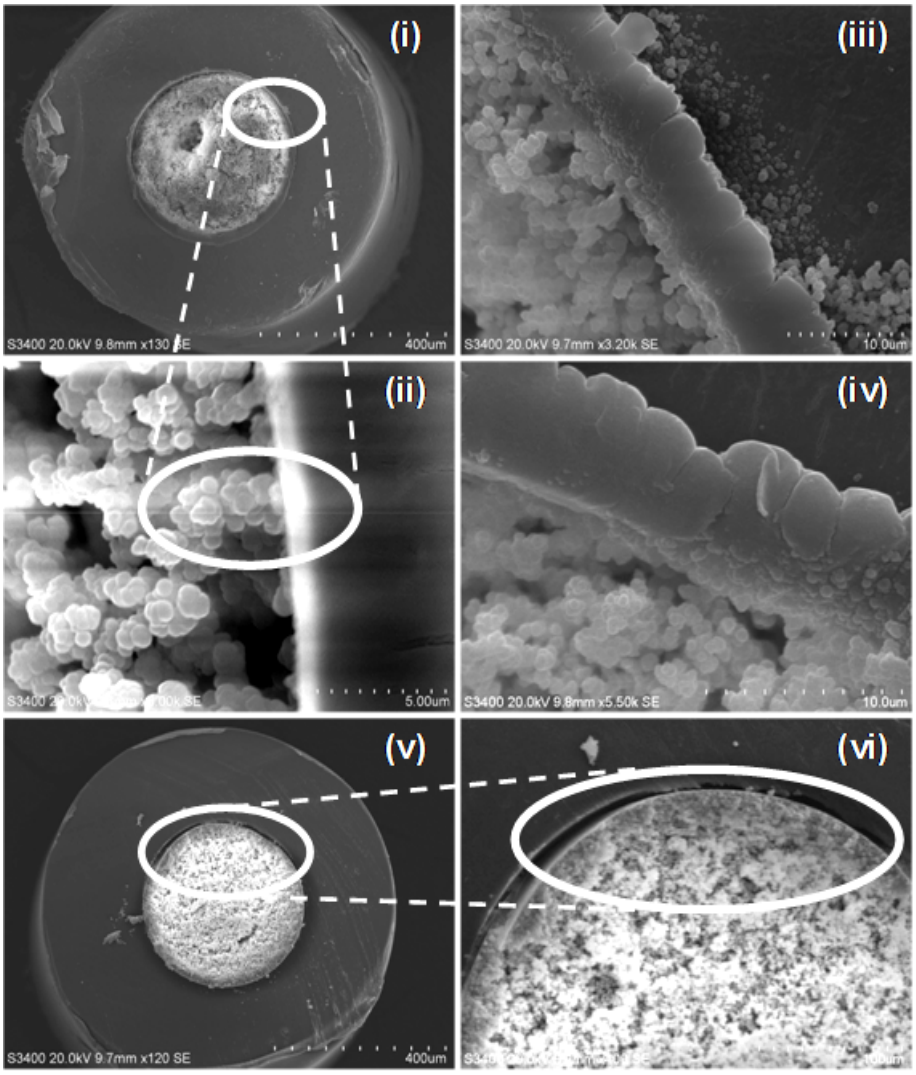

Figure 6.5: Scanning electron microscopy images of a porous polymer monolith formed within a polypropylene pipette-tip, which was modified by photo-grafting (**i**-**iv**) and unmodified (**v**, **vi**) prior to monolith polymerisation.

Therefore, the monolithic bed size was adjusted during the fabrication using a 2-mm guide ring as described in the Experimental section. The guide ring was placed outside the tip and removed when the polymerisation was completed (Figure 6.6(**ii**-**iii**)). The monolith bed length was measured under an optical microscope using a vernier caliper and a % RSD of 8 % was achieved for 11 separately prepared monoliths. In addition, different bed size could be prepared by changing the ring size, as illustrated in Figure 6.6(**iv**).

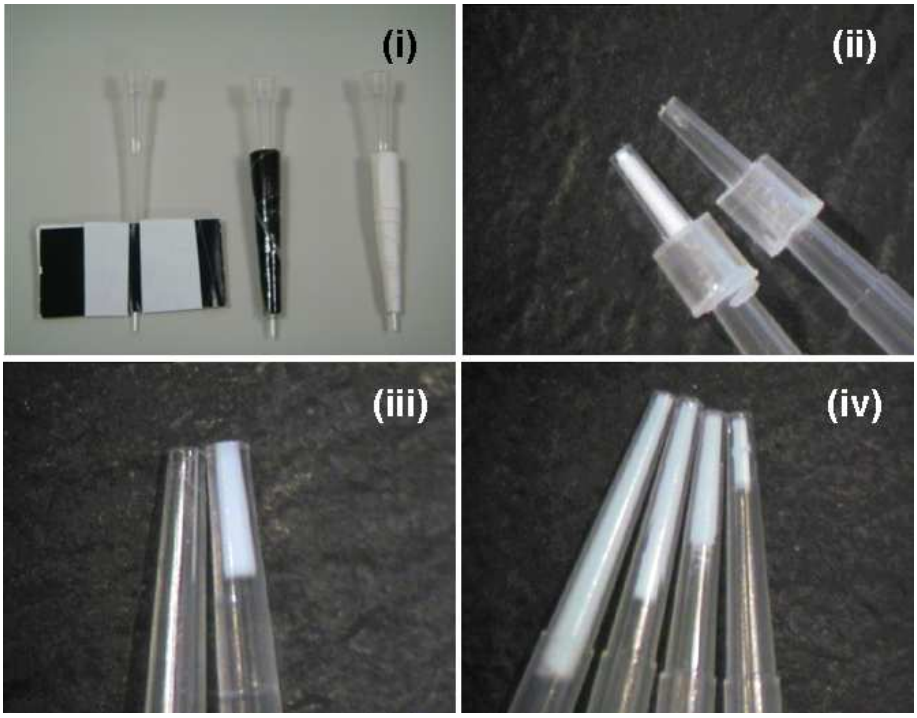

Figure 6.6: Images of a monolith bed size adjustment using a photomask (**i**) and a guide ring (**ii**-**iii**). (**iv**) preparation of different bed size.

To facilitate aspirating and expelling the sample during analysis and to reduce operating backpressures and thus facilitate the use of laboratory auto-pipettes, previous studies have suggested creating a main flow-through channel through the monolithic bed [15, 34]. However, two issues occurred during the fabrication and modification process of the monolithic tip when the channel was created. Firstly, the channel was close to the tip wall and it was difficult to have it right in the centre of the monolithic bed. This could negatively affect the trap-elution of the sample analytes due to uneven fluid flow through the monolithic bed (Figure 6.7(**ii**)). Secondly, which was more significant in this study, the subsequent immobilisation of AuNPs on monoliths incorporating a main channel did not occur evenly throughout the entire monolith. Rather, the coverage of AuNPs was centred around the bore of the main channel such that the radial homogeneity of immobilised AuNPs was poor (Figure 6.7(**iii**-**iv**)). This is because the fluid followed the path of

least resistance through the channel rather than flowing through the pores of the monolith. Thus, the preparation of the monolithic bed without the main flow-through channel was unavoidable even though it lead to high backpressures during operation, which prohibited the use of hand-held auto-pipettes for sample loading and rinsing and obliged the use of a syringe pump.

Unsuccessful attempts were made to reduce the backpressure by varying the monomer concentration between 20 % and 40 % prior to polymerisation, but all monoliths with < 40 % EDMA had very poor mechanical rigidity. However the main focus of our efforts in this work was to demonstrate the use of Au-modified monoliths in pipette-tips for affinity applications and thus the means by which the monolith was flushed (i.e. via syringe pump or auto-pipette) was considered incidental at this stage of the project.

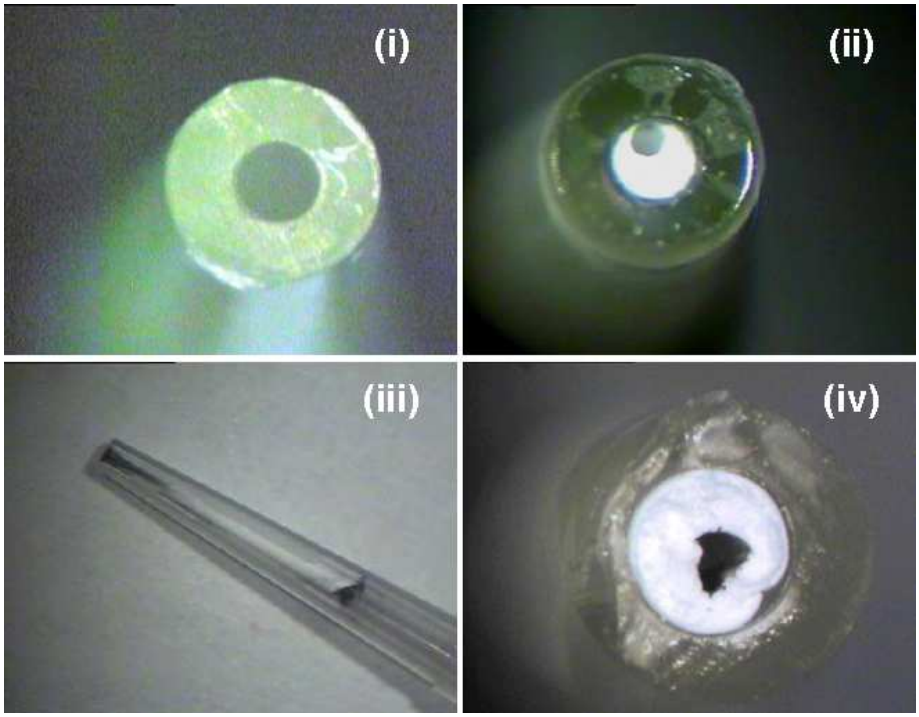

Figure 6.7: Optical microscope images of (**i**) empty pipette-tip, (**ii**) bottom-end of monolithic tips with a 150 µm o.d. flow-through channel, and (**iii**-**iv**) monolithic tips with flow-through channel after AuNPs immobilisation.

6.3.2. Modification of the monolith surface with AuNPs

The focus of this Chapter was to increase the capacity of the monolithic extraction device by increasing the number of extraction active sites (ECL in this case). The surface of the preformed monolith was modified utilising photografting since it is one of the techniques used to modify the chemistry of the surface of synthetic polymers [51] and it does not require re-optimisation of the polymerisation conditions for each new monolith (as discussed in Chapter 1) [52].

Therefore, the surface area of the monolithic substrate, which had a high surface density of primary amine groups, was increased by immobilising 20 nm citrate-stabilised AuNPs. The immobilisation of AuNPs onto the polymer monolith with a high density of coverage was achieved using a protocol originally described by Connolly *et al*. [40] with minor modifications. Figure 6.8 illustrates the scheme of the monolith surface modification with AuNPs. The immobilisation procedure was divided into two main steps: amination of the monolith surface by flushing the vinyl azlactone photo-grafted polymer monolith with ethylenediamine and then the resulting aminated monolith was flushed with the 20 nm citrate-stabilised AuNPs subsequently.

One particular matter of concern was the possibility that the UV radiation (during grafting of azlactone) might not penetrate through the entire bulk of the monolith (due to the screening effect of UV absorbing monomers, solvents and the monolith itself) leading to an unwanted radial gradient of graft density. Rohr *et al*. have previously demonstrated that homogeneous grafting can be achieved through a 200 µm thick layer of monomer and also investigated the effect of rotating the substrate during grafting events [50]. In their study, they used electron probe microscopy to evaluate the homogeneity of graft density (for sulphonated polymer grafts) [53].

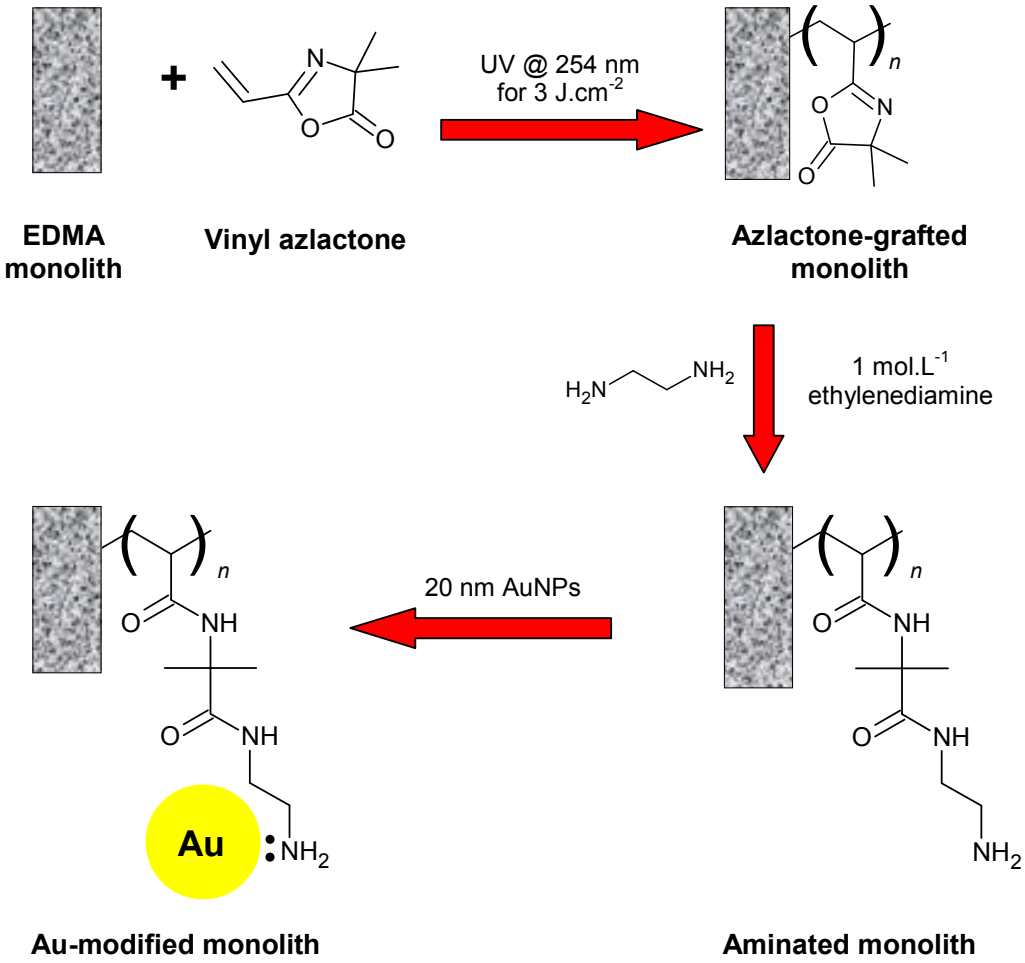

Figure 6.8: Reaction scheme showing the surface modification of the pre-formed monolith with AuNPs.

However, in the work described here, FE-SEM was used to image the high coverage of the monolith surface with the AuNPs, which was indicative of graft homogeneity since each nano-particle was strongly attached by multi-point interactions to the grafted surface, via primary amine lone-pair electrons [40-42]. Figures 6.9 and 6.10 show images of an Au-modified monolith which have been taken under optical microscope and FE-SEM, respectively. As it can be seen in Figure 6.9, the monolith colour turned from white to dark red indicating the complete radial and axial coverage with AuNPs. The images (**i-iii**) in Figure 6.10 were taken using the FE-SEM for a

piece of monolith that was prepared in a pipette-tip that had not been treated. These images illustrate the excellent coverage of AuNPs represented by the white dots. This high surface coverage of AuNPs clearly confirmed the achieved significant increase in surface area even though it was not specifically measured here due to the very small bed volume (which prevents the use of Brunauer-Emmett-Teller (BET) surface area analysis to accurately quantitate the surface area increase).

The image (**i**) in Figure 6.10 shows that the edge of the monolith close to the wall of the tip had rather a sparse coverage of AuNPs. It is believed that the poor coverage in this very narrow zone (representing about 3.5 % of the entire 400 µm monolith radius) was due to poor convective fluid flow at the extremities of the monolith compared with flow through the remaining monolith bulk. In relation to the work of Rohr *et al*. [50, 53] regarding the radial homogeneity of grafting, for the work presented here, no gradient of grafting density was observed, either axially or radially even though the monolith here was of considerably larger dimensions.

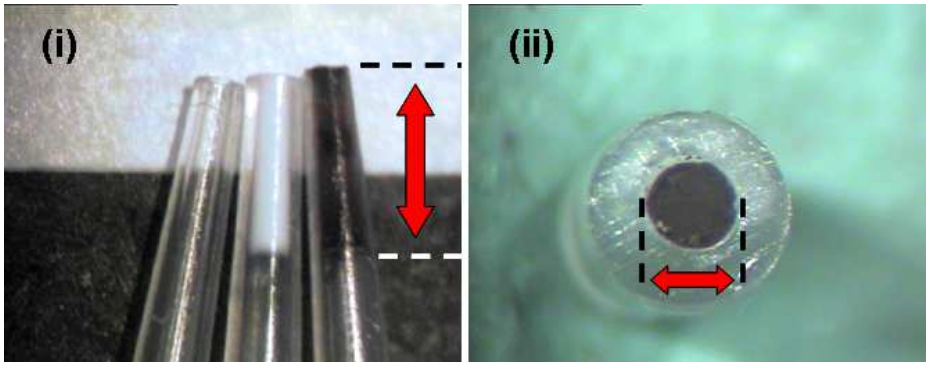

Figure 6.9: Optical microscope images showing the monolithic tips before and after coverage with AuNPs.

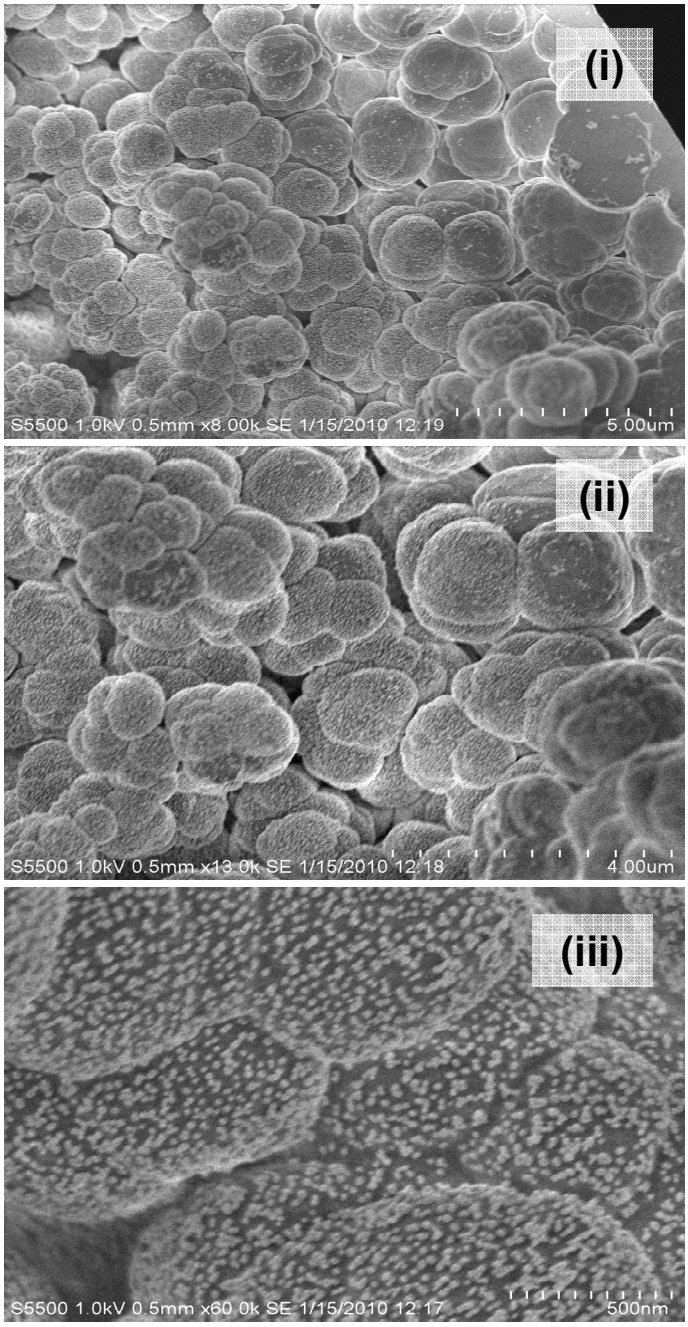

Figure 6.10: Field emission scanning electron microscopy images showing dense coverage of AuNPs. (**i**) 8,000X magnification, (**ii**) 13,000X magnification and (**iii**) 60,000X magnification. The white dots on the globule surfaces represent the immobilised AuNPs.

6.3.3. Modification of the Au-modified monolith with ECL

For the preparation of a lectin-affinity extraction phase, ECL was chosen due to its commercial availability as well as that its bind/release mechanism is well known [46]. Therefore, the Au-immobilised monolith was subsequently modified with ECL for the preparation of the lectin-affinity extraction monolith for selective enrichment of galactosylated proteins.

The immobilisation of ECL on the Au surface can be carried out utilising different strategies. The easiest and quickest method would be to flush the Au-modified monolith with a solution of ECL as suggested by Storri *et al*. [54], such that the lectin is physically adsorbed on the bare gold surface. However, this interaction is known to be weak and the adsorbed lectin could be easily detached from the Au surface during the subsequent use of the extraction device [54].

An alternative method that resulted in a strong covalent attachment between the ECL and the Au surface involved the use of a bi-functional linker, DTSP, as described by Katz [55] and illustrated in Figure 6.11. The Au surface modification was carried out utilising a two-step strategy in which the Au-modified monolith was first flushed with DTSP to form self-assembled monolayers (SAM) of N-succinimidyl-3-thiopropionate (NSTP) [55-57], via strong gold-sulphur bonds. Since disulphides are known to interact with gold surfaces via dissociative chemisorption, thus NSTP monolayers are formed from the dissociation of the DTSP disulfide bond on the gold surface [58]. NSTP has an exposed active NHS group that is reactive towards primary amines. Covalent immobilisation of ECL was achieved by flushing a solution of ECL as a second step and the attachment took place by the nucleophilic attack of the lysine primary amine group of the ECL [56]. The final step was to block any possible remaining active NHS groups or bare gold by flushing the ECL-Au-modified monolith with amine-containing buffer. This blocking is crucial to eliminate non-specific binding of sample components to the SAM or the bare gold surface as illustrated in Figure 6.12.

The Au surface could also be modified with ECL in a faster way utilising a one-step immobilisation strategy in which ECL is mixed with the bi-functional linker first and then the resultant solution is flushed through the Au-modified monolith. However, the two-step immobilisation strategy was preferred to the one-step because unspecific adsorption of the ECL on the Au surface was prevented by the pre-formed NSTP SAM [57].

The immobilisation buffer was selected to have a pH of 8.2, which was close to the optimum pH for lectin/glycan binding as dictated by the vendor. The buffer also incorporated 1 mmol.L^{-1} of Ca^{2+} and 1 mmol.L^{-1} of Mn^{2+}, which are known to play a role in maintaining the spatial arrangement of the carbohydrate binding site residues [59]. By maintaining optimum buffer conditions for ECL during immobilisation and subsequent testing of the affinity monoliths, the risk of deactivation of ECL was minimised.

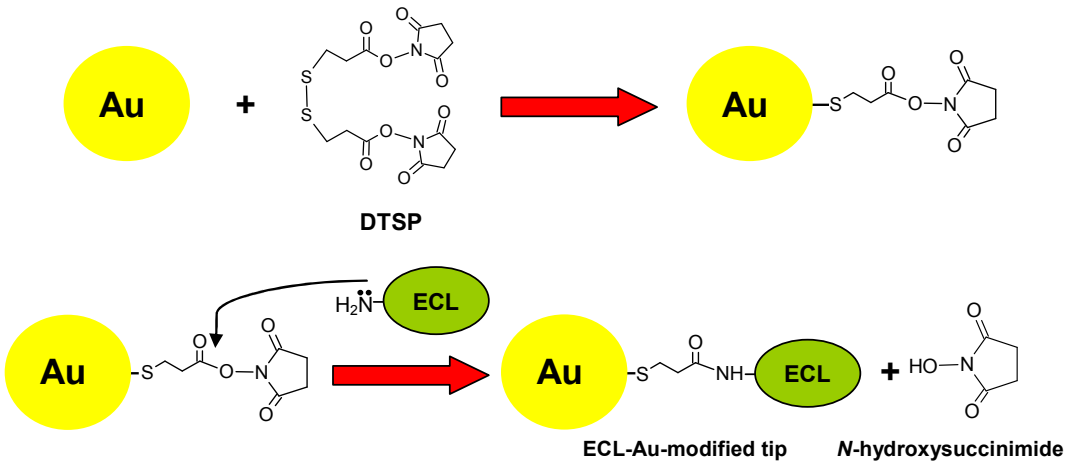

Figure 6.11: Reaction scheme showing the adsorption of NSTP via the dissociation of the DTSP disulphide bond, followed by the subsequent immobilisation of ECL.

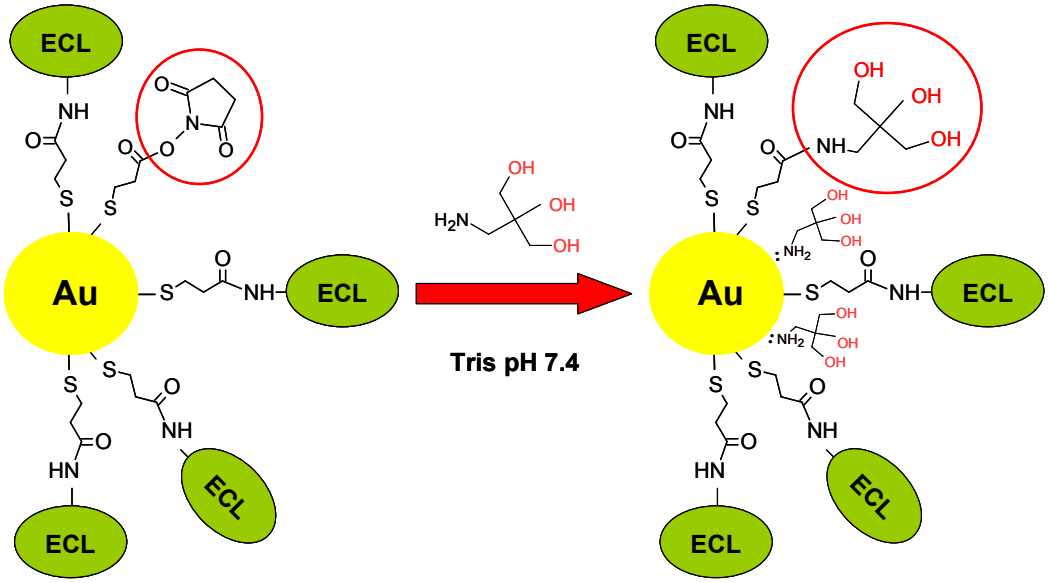

Figure 6.12: Reaction scheme showing the blocking of remaining unreacted NHS groups and bare gold sites with Tris buffer.

6.3.4. Trap-elute studies of a simple standard mixture of glycoproteins

ECL is known to be selective towards glycoproteins with terminal galactose residues. Therefore, a simple mixture (**Standard A**) consisting of two test glycoproteins were chosen both for selectivity studies and evaluation of non-specific protein binding. The mixture consisted of ribonuclease B as the negative control since it contains high mannose glycan structures [60], and thus this glycoprotein is not expected to be retained by the ECL affinity monolith. Transferrin was selected as the positive control protein since the glycan of transferrin is terminated by neuraminic acid residues, [61] which were removed by neuraminidase to expose galactose residues and thus maximise the transferrin extraction. To validate the extraction efficiency and selectivity of the extraction monoliths, all samples treated with the extraction monoliths were injected in a capillary HPLC and separated on a reversed-phase monolithic column as described in the Experimental section.

6.3.4.1. Investigation of non-specific interactions

In order to insure that the retention of the galactosylated proteins was due to sugar-lectin interactions which prove the specificity of ECL and to investigate non-specific binding, several monolithic tips containing no immobilised ECL were used as blank comparisons. The unwanted non-specific binding of proteins could occur, either due to hydrophobic interactions with the polymer monolith, gold-sulphur/gold-amine interactions with the immobilised AuNPs, or via the covalent attachment between the proteins and the exposed unreacted succinimidyl groups. Therefore, four blank monoliths were prepared as described in Section 6.2.6 and illustrated in Figure 6.2 and summarised in Table 6.1. The test mixture, **Standard A**, was used for the evaluation purposes. Note: different batch of **Standard A** was used for each of the following experiments. Figure 6.13(**a**) shows chromatograms obtained for **Standard A** before and after flushing through **Blank Monolith 1** in which the hydrophobicity of the EDMA base monolith was modified by photografting azlactone moieties, followed by blocking with Tris buffer. This modification increased the hydrophilicity of the monolith surface, which then minimised any unwanted hydrophobic interactions, as evidenced by the complete lack of retention of either test protein on the monolith surface after **Standard A** passage.

Conversely, as it can be seen in Figure 6.13(**b**), both test proteins (both glycosylated) were retained on **Blank Monolith 2** which incorporated bare unfunctionalised AuNPs, presumably due to adsorption of protein on the gold surface as described by Storri *et al*. [54].

The % relative areas of the two test proteins before and after treatment with the **Blank Monolith 1** are listed in Table 6.2.

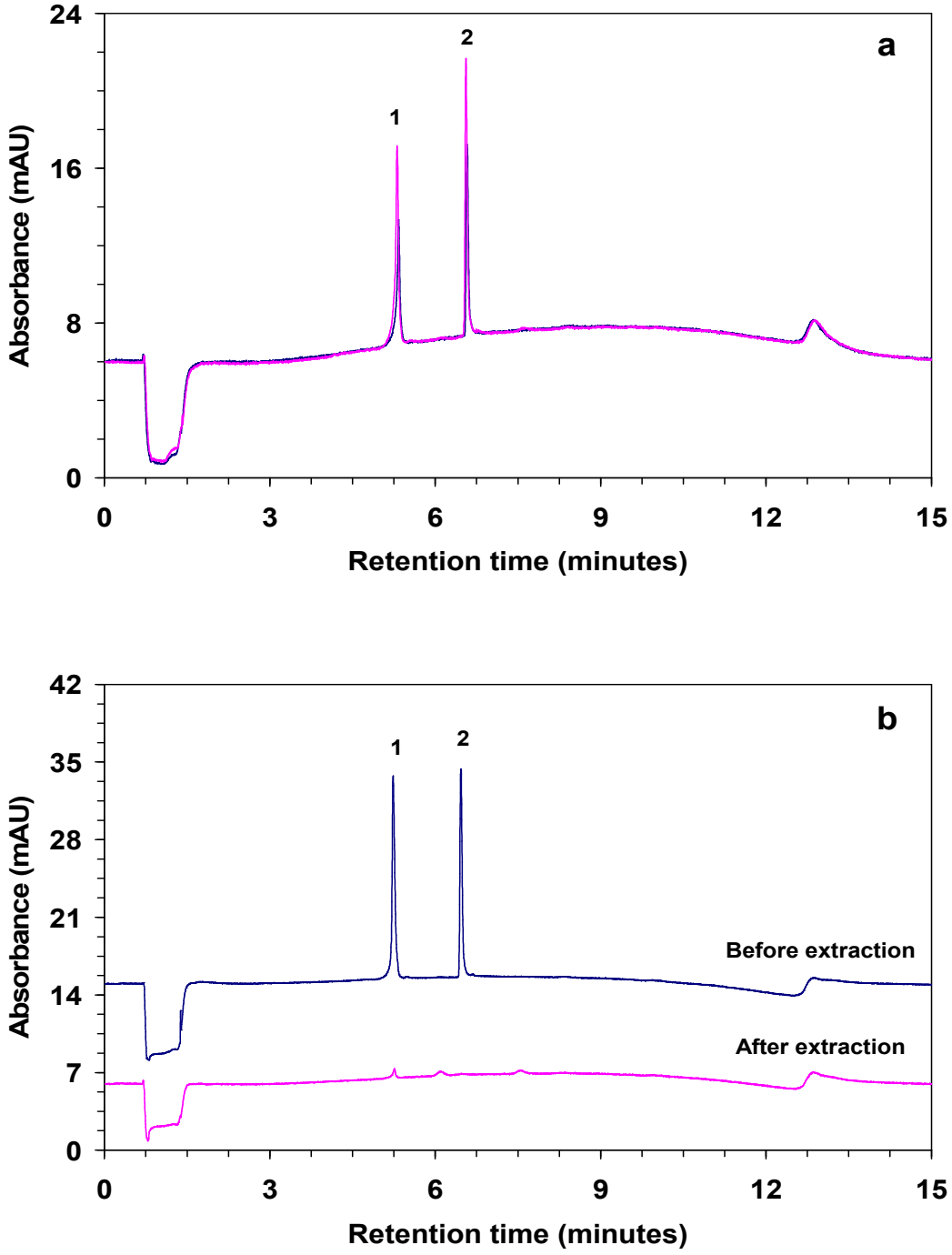

Figure 6.13: HPLC chromatograms of **Standard A** before (blue) and after (pink) passage through: (**a**): **Blank Monolith 1** showing the elimination of non-specific protein adsorption and (**b**): **Blank Monolith 2** showing adsorption of the two-test proteins on the bare AuNPs. Chromatographic conditions: Column: 100 µm x 15 cm LMA-*co*-EDMA monolith, Gradient: 10 minute gradient from 5 % B to 100 % B at 2 µL.min^{-1}, Column temperature: 25 ^{o}C, Injection volume: 1 µL, Detection: UV at 214 nm. Peaks: (**1**) ribonuclease B, (**2**) desialylated transferrin.

Table 6.2
Peak areas of the two-test proteins and the deglycosylated transferrin before and after treatment with the different monoliths.

Monolithic tip	Test-protein	% Peak area*	
		Before extraction	After extraction
Blank Monolith 1	Ribonuclease B	48.4 %	52.0 %
	Desialylated transferrin	51.6 %	48.0 %
Blank Monolith 3	Ribonuclease B	60.9 %	62.6 %
	Desialylated transferrin	39.1 %	37.4 %
Blank Monolith 4	Ribonuclease B	37.1 %	39.1 %
	Desialylated transferrin	62.9 %	60.9 %
Monolith A	Deglycosylated transferrin	1.085**	1.086**

*Relative peak area expressed as a percentage.
**Actual peak areas rather than percentage.

However, no detectable retention of either test protein was observed when the bare AuNPs were blocked with Tris to produce **Blank Monolith 3** (Figure 6.14) as well as when AuNPs were functionalised with DTSP and then blocked with Tris (**Blank Monolith 4**) as indicated in Figure 6.15. This is suggesting that Tris, as a small hydrophilic amine, was well suited to providing efficient blocking of unreacted succinimidyl groups. The % relative areas of the two test proteins before and after treatment with the **Blank Monolith 3** and **Blank Monolith 4** are listed in Table 6.2.

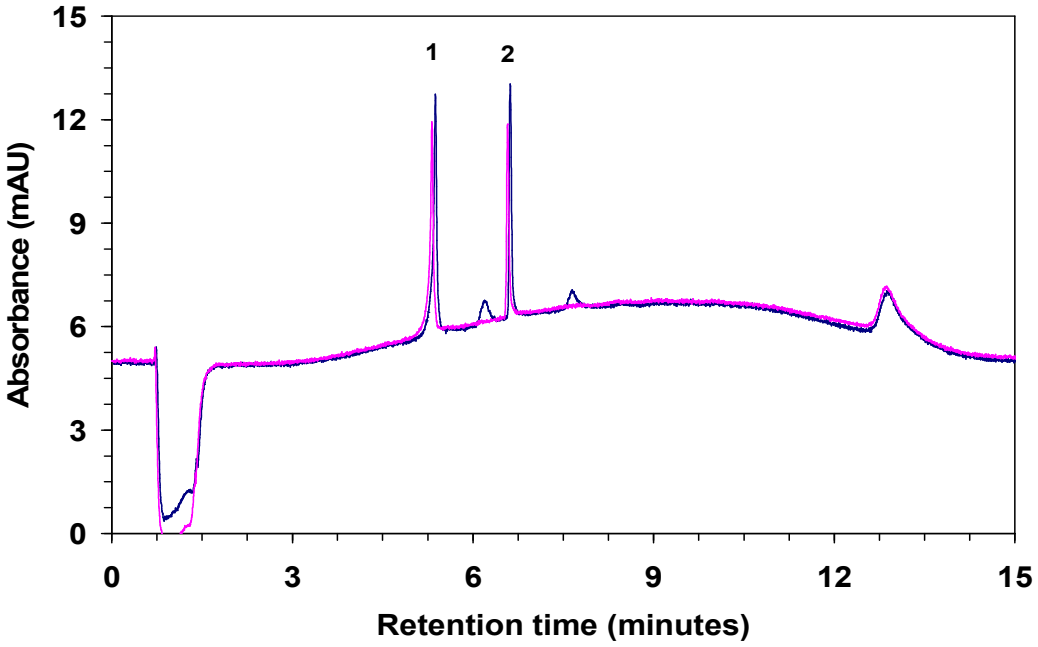

Figure 6.14: HPLC chromatograms of **Standard A** before (blue) and after (pink) passage through **Blank Monolith 3** showing the effect of blocking the bare AuNPs with Tris buffer. Chromatographic conditions are as in Figure 6.13. Peaks: (**1**) ribonuclease B, (**2**) desialylated transferrin.

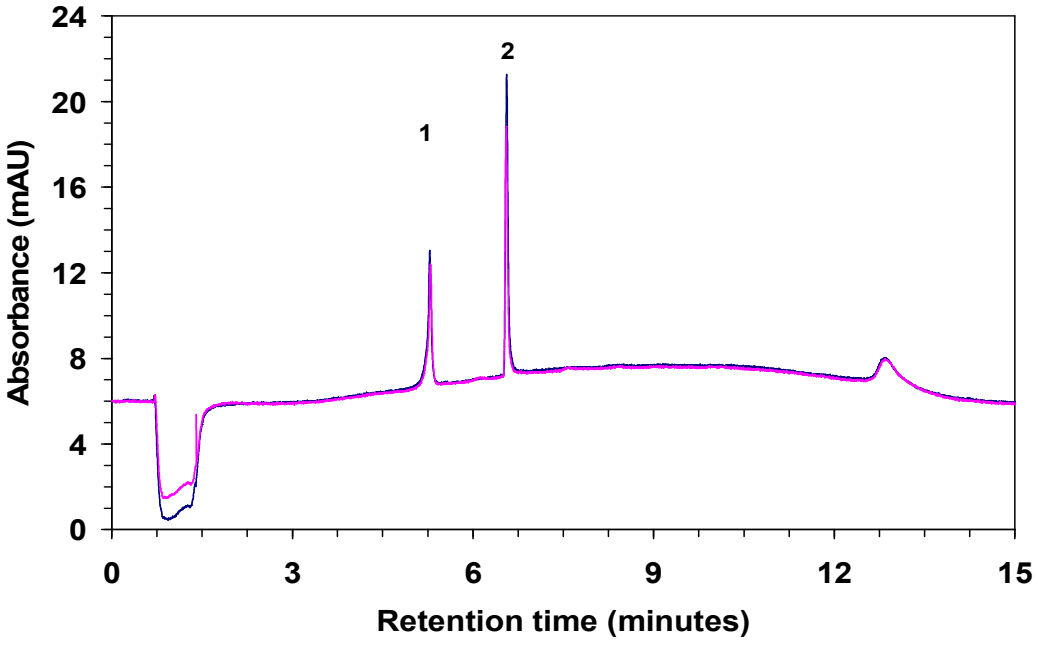

Figure 6.15: HPLC chromatograms of **Standard A** before (blue) and after (pink) passage through **Blank Monolith 4** showing the effect of blocking the DTSP-functionalised AuNPs with Tris buffer. Chromatographic conditions are as in Figure 6.13. Peaks: (**1**) ribonuclease B, (**2**) desialylated transferrin.

In addition, Figure 6.16 shows that no retention was observed when a deglycosylated transferrin was passed through **Monolith A** as it did not contain galactose residues indicating the specificity of **Monolith A** towards galactosylated proteins. The peak area of the deglycosylated transferrin before and after treatment with **Monolith A** is listed in Table 6.2. As a consequence of all of the results obtained above, the retention of the galactosylated transferrin was due to the specific sugar-lectin interactions and all other possible interactions were eliminated.

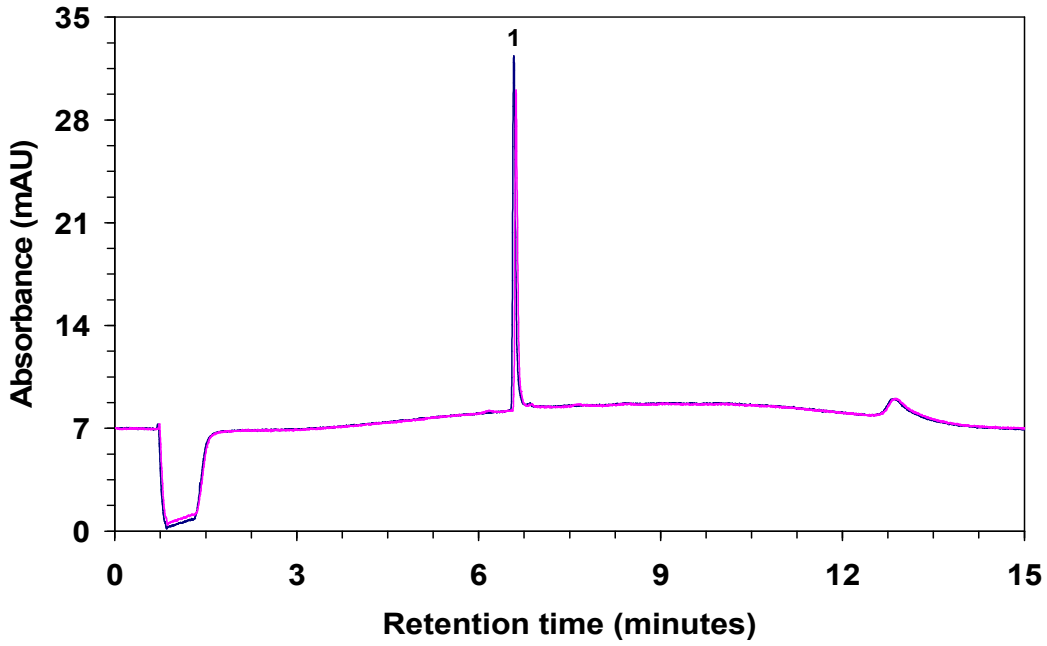

Figure 6.16: HPLC chromatograms of deglycosylated transferrin before (blue) and after (pink) passage through **Monolith A** showing its specificity towards galactosylated proteins. Chromatographic conditions are as in Figure 6.13. Peaks: (**1**) deglycosylated transferrin.

6.3.4.2. Investigation of affinity extraction of ECL-functionalised monoliths

Due to the specificity of ECL towards galactose residues, the extraction efficiency of the ECL-functionalised monoliths (**Monolith A** and **Monolith B**) was evaluated by examining its ability in extracting desialylated transferrin (e.g. a protein terminated with galactose residues). The evaluation of the monoliths involved loading 20 µL of **Standard A** from the top-end of the affinity monoliths followed by a buffer rinse as described in Section 6.2.9. All fractions and combined monolith rinsings were collected and subjected to capillary LC analysis to determine if selective binding had occurred.

The aim of immobilising AuNPs on the monolithic surface was to increase the area of that surface and therefore increase the extraction capacity of the affinity monolithic tip by increasing the available lectin immobilised on the gold surface (**Monolith A**). Therefore, for comparative purposes, **Monolith B** was prepared in which the ECL was immobilised on a monolith containing no AuNPs (ECL covalently attached via amine-reactive azlactone polymer grafts) as illustrated in Figure 6.17.

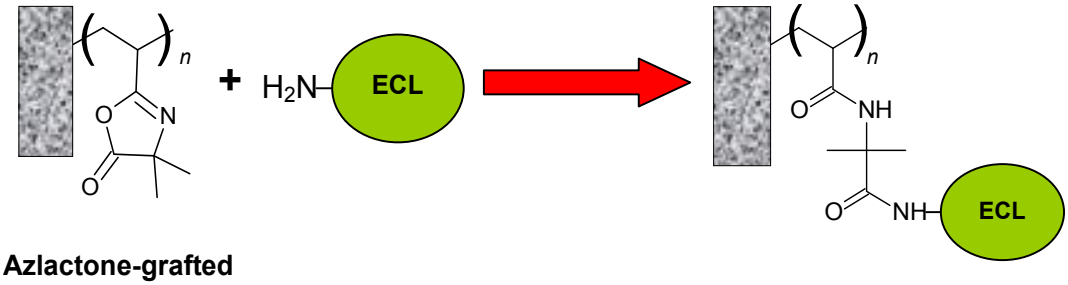

Figure 6.17: Reaction scheme showing the immobilisation of ECL on the surface of the pre-formed monolith for the preparation of **Monolith B**.

As mentioned above, 20 µL of **Standard A** was passed through both affinity monoliths and the chromatograms obtained are in Figure 6.18. As it can be seen, in both affinity monoliths, ribonuclease B was not retained as

expected whereas desialylated transferrin was retained by both **Monolith A** and **Monolith B**. This is clearly indicative of the selective retention of desialylated transferrin over ribonuclease B due to galactose-lectin interactions. Moreover, using relative peak areas in standard Chromatogram (**i**) as a reference, ~ 95 % more desialylated transferrin was retained on **Monolith A** relative to **Monolith B**, clearly showing the advantage of Au-modified monoliths as substrates which lead to much more immobilised ECL lectin for affinity extraction. The relative peak area of desialylated transferrin before extraction was 1.6 and decreased to 1.28 after treatment with **Monolith B**, whereas the treatment with **Monolith A** lead to a decrease to 0.55. The loading capacity is estimated to be 138 ng/monolith. A subsequent monolith rinse of **Monolith A** with 40 µL of 0.8 mol.L^{-1} galactose in loading buffer revealed that the bound desialylated transferrin could be readily recovered, appearing as a single peak in Chromatogram (**iv**).

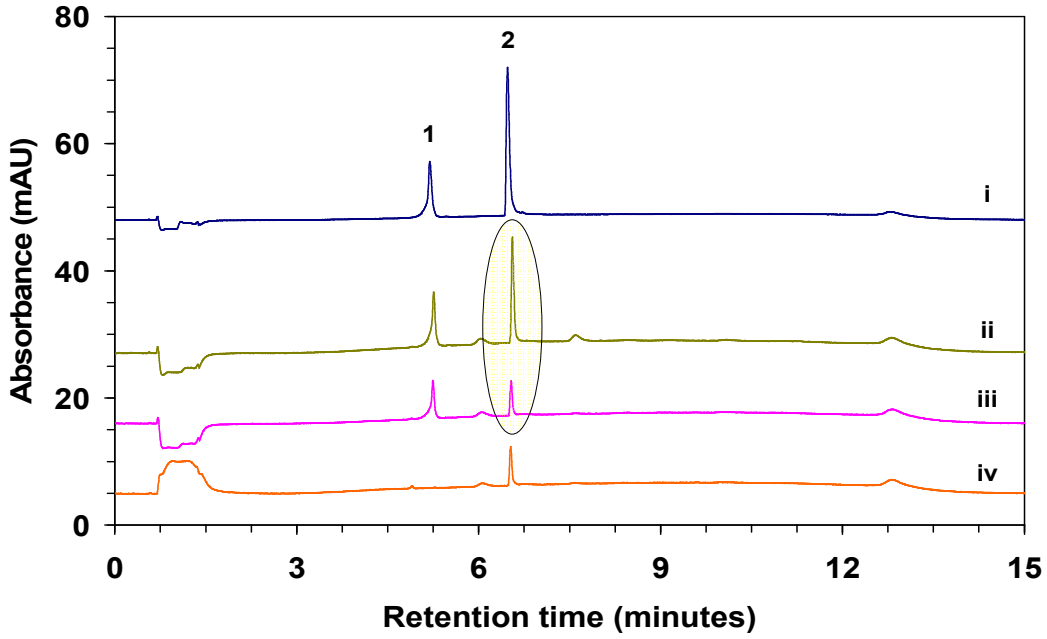

Figure 6.18: HPLC chromatograms of (**i**) untreated **Standard A**, (**ii**) **Standard A** after passage through **Monolith B**, (**iii**) **Standard A** after passage through **Monolith A**, (**iv**) release of bound transferrin from **Monolith A** with a galactose rinse. Chromatographic conditions are as described in Figure 6.13. Peaks: (**1**) ribonuclease B, 2- desialylated transferrin.

6.3.5. Application of affinity monoliths to complex protein mixtures

The extraction efficiency of **Monolith A** was further evaluated by applying the affinity monolith to extract two galactosylated proteins from a complex mixture of proteins. The complex mixture (**Standard B1**) consisting of nine selected proteins in which six of them are non-glycosylated proteins (insulin chain B, insulin, cytrochrome C, BAS, enolase and carbonic anhydrase) as well as glycoproteins which had either terminal mannose (ribonuclease B), or terminal galactose (desialylated transferrin and desialylated thyroglobulin). In order to mimic a real sample, the non-glycosylated proteins were specifically selected to span a wide range of molecular masses from insulin chain B (3.5 kDa) to enolase (82 kDa to 100 kDa, depending on the isoform).

For the evaluation purposes, a chromatographic method was developed for the separation of the nine proteins. The effect of the column temperature on the separation was investigated on the range between 25 ^{o}C and 75 ^{o}C at 5 ^{o}C intervals and the results are shown in Figure 6.19. As it can be seen, there was no significant influence on the retention times across this range as the retention time of the last eluted peak was decreased by only 0.4 minutes when the column temperature increased from 25 ^{o}C to 75 ^{o}C. However, the remarkable effect was upon selectivity, particularly for three adjacent peak pairs. Resolution between Peak 2 and 3 increased from 0.9 at 25 ^{o}C to 2.5 at 75 ^{o}C, resolution of Peak 3 and 4 decreased from 3.6 at 25 ^{o}C to 1.2 at 75 ^{o}C and resolution of Peak 7 and 8 decreased from 2.0 at 25 ^{o}C to complete co-elution at 75 ^{o}C. As a compromise, a column temperature of 40 ^{o}C was selected which resulted in resolution between Peaks 2/3, 3/4 and 7/8 of 1.4, 2.5 and 1.7 respectively. The optimised gradient conditions resulted in a peak capacity of 102 which was calculated based on the following equation [62].

$$Pc = 1 + \left(\frac{t_g}{w} \right) \qquad \text{(Eq. 6.1)}$$

where t_g is the gradient time and w is the average peak width measured 13.4% above the baseline. The concentration of enolase and desialylated thyroglobulin in **Standard B1** was higher than the others due to the lower absorbance at 214 nm.

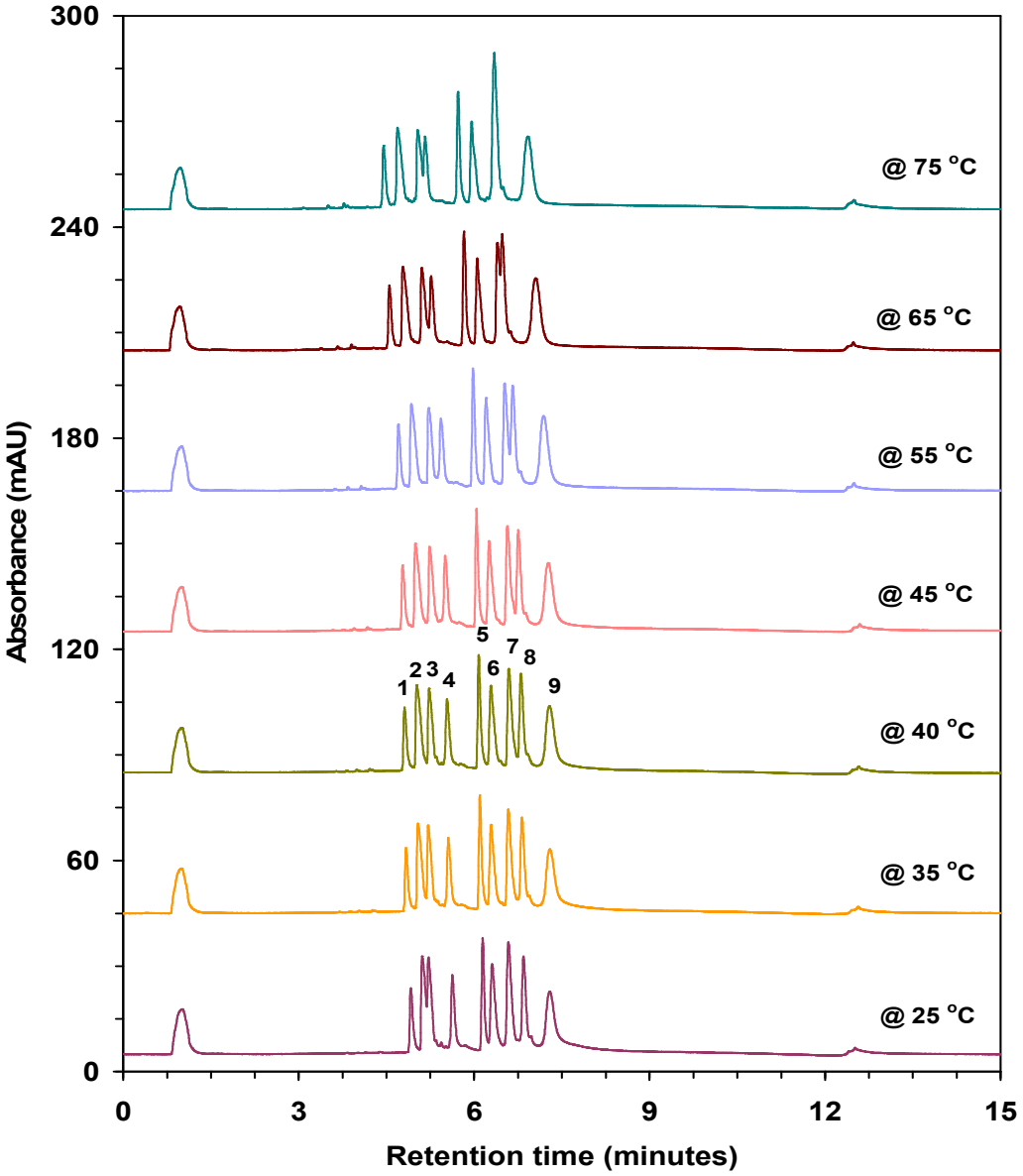

Figure 6.19: Selected HPLC chromatograms showing the effect of column temperature on the separation of **Standard B1** proteins. Chromatographic conditions are as described in Figure 6.13 except: Gradient: 9 minute gradient from 5 % B to 100 % B. Peaks: (**1**) 20 µg.mL^{-1} ribonuclease B, (**2**) 20 µg.mL^{-1} insulin chain B, (**3**) 20 µg.mL^{-1} insulin, (**4**) 20 µg.mL^{-1} cytrochrome C, (**5**) 25 µg.mL^{-1} desialylated transferrin, (**6**) 25 µg.mL^{-1} BSA, (**7**) 20 µg.mL^{-1} carbonic anhydrase, (**8**) 40 µg.mL^{-1} enolase, (**9**) 80 µg.mL^{-1} desialylated thyroglobulin.

Figure 6.20 shows chromatograms of **Standard B1** before and after its passage through **Monolith A**. The results show that all of the non-glycosylated proteins (Peaks 2-4 and 6-8) were unretained as well as Peak 1 (ribonuclease B) since this glycoprotein has high mannose glycans. On the other hand, significant retention (i.e. significant decrease in their peak areas) was observed for both desialylated transferrin and desialylated thyroglobulin (Peaks 5 and 9) and subsequently recovered with a galactose wash step. The lack of interfering peaks in the galactose wash is indicative of the specificity of binding. Interestingly, the affinity monolith was demonstrated to simultaneously extract both transferrin and thyroglobulin even in the presence of other proteins and glycoproteins. This was despite the considerable difference in size of both target glycoproteins (80 kDa and 670 kDa, respectively) and also the difference in glycan structure and coverage. Specifically, thyroglobulin has 25-30 N-linked glycans having both high-mannose- and complex structures, some of which are teminated in galactose [63]. Other complex glycans on thyroglobulin are terminated in sialic acid and so treatment with neuraminidase revealed underlying galactose residues in order to maximise the ECL binding of the protein. Conversely, transferrin contains only 2 N-linked glycans, both of which have the same complex-type structure [61].

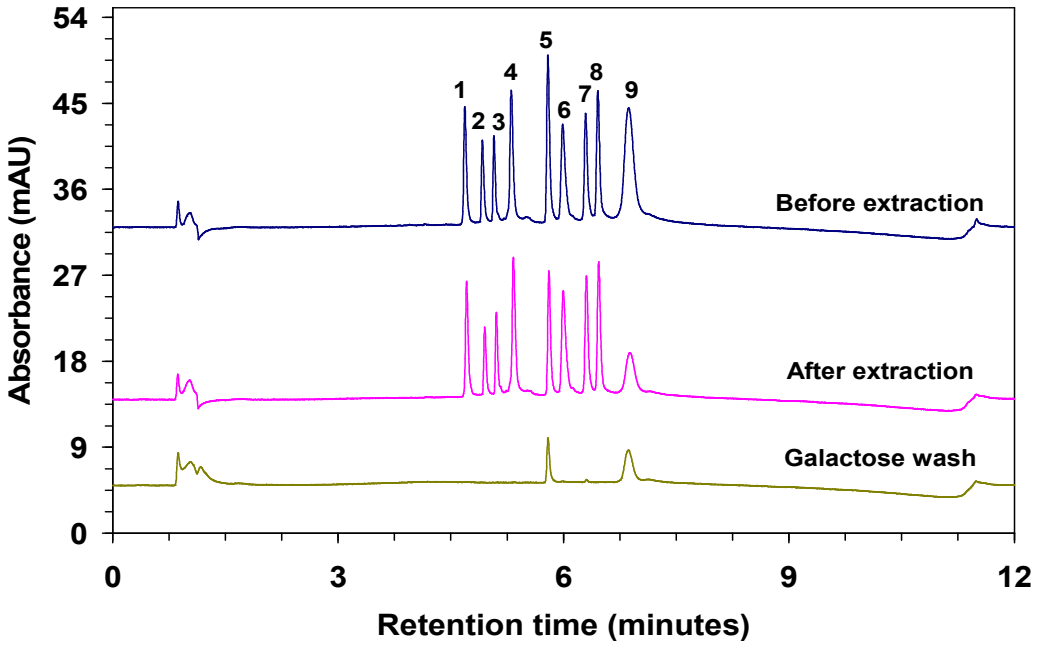

Figure 6.20: HPLC chromatograms of **Standard B1** before and after extraction with **Monolith A8**. Chromatographic conditions and peak assignment are as described in Figure 6.19.

In a further effort to verify that transferrin had indeed been retained due to sugar-lectin interactions, rather than non-specific protein-protein interactions, two further complex mixtures (**Standard B2** and **B3**) were prepared. Both mixtures do not contain galactosylated proteins; therefore no retention was expected from any of the proteins presented in these two mixtures. **Standard B2** consists of the six non-glycosylated proteins (insulin chain B, insulin, cytrochrome C, BSA, enolase and carbonic anhydrase) in addition to ribonuclease B (terminated with mannose) and asialotransferrin (terminated with sialic acid). The proteins presented in **Standard B3** are the same as **Standard B2** except that it does not contain asialotransferrin. The two mixtures were treated with **Monolith A** and the results obtained are in Figure 6.21. As expected, the retention of the target proteins was due to the sugar-lectin interaction.

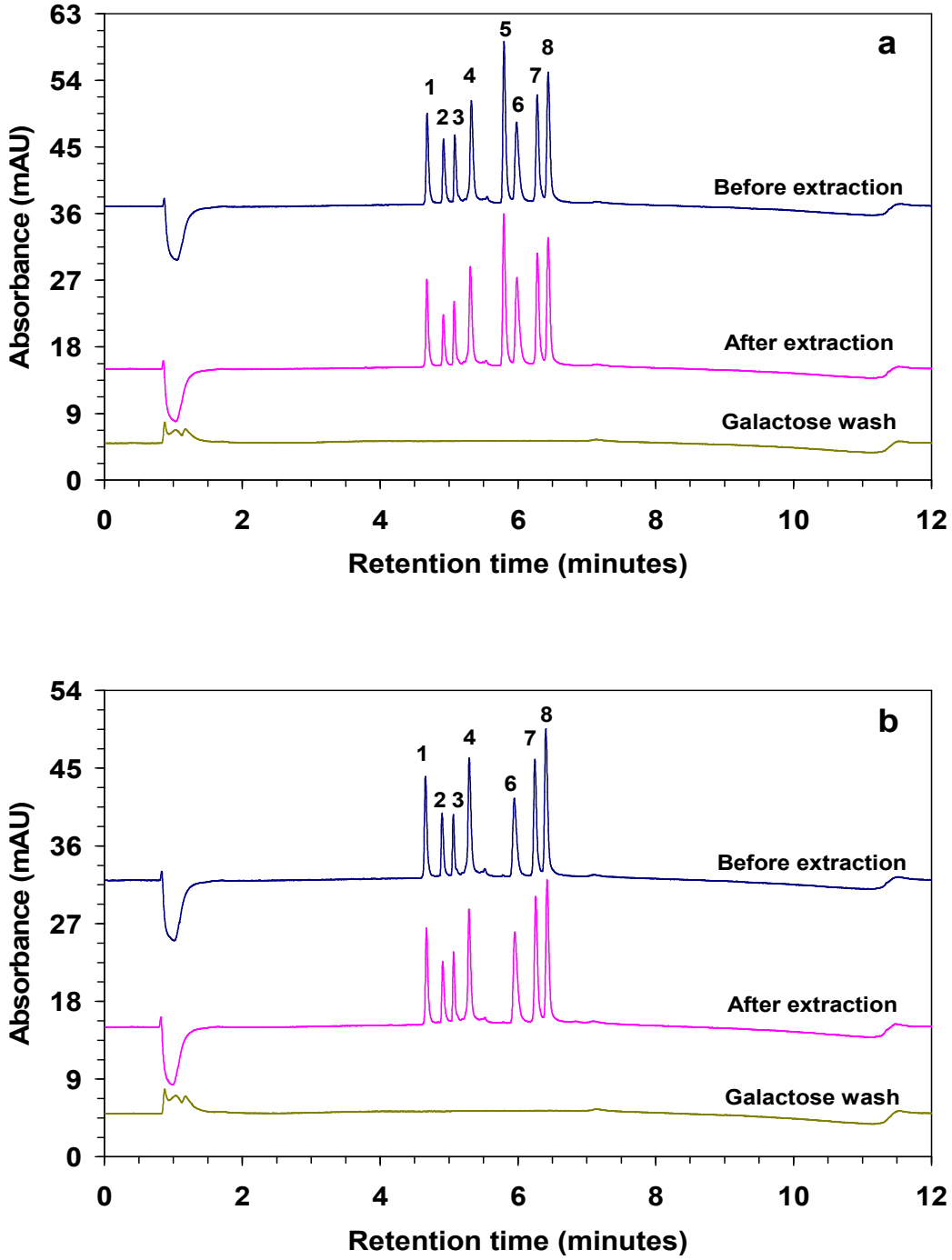

Figure 6.21: HPLC chromatograms of: (a) **Standard B2** and (b) **Standard B3** before and after extraction with **Monolith A8**. Chromatographic conditions and peak assignment are as described in Figure 6.19.

6.3.6. Evaluation of transferrin extraction repeatability on **Monolith A**

The % of desialylated transferrin extracted during the loading step was calculated using relative peak areas with ribonuclease B as an internal standard. Three repeat extraction cycles were performed on a **Monolith A** (regenerated each time with a galactose rinse). The average % extraction for desialylated transferrin for a single selected affinity monolith (*n* = 3) was 31 % which suggests that either (a): the affinity monolith was overloaded at the employed sample concentration (20 $\mu g.mL^{-1}$; equivalent to 400 ng of protein loaded per 20 µL aliquot of test mix) or (b): the loading flow-rate and thus contact time was not optimum. The % RSD for the three repeat extractions using the stated loading conditions on a single extraction monolith was 4.3 %, indicating that the affinity monolith could be reused for repeat extractions.

Although a rigourous study of the stability of prepared affinity monoliths was not conducted, it was observed that affinity monoliths could retain their extraction capabilities after numerous consecutive periods of storage at 4 ^{o}C and re-use at room temperature. For example, immediately after preparation, a particular monolith was stored for 12 hours at 4 ^{o}C, used for one extraction cycle (bind/elute), stored for a further 5 days at 4 ^{o}C, re-used for 6 consecutive extraction cycles, stored for 36 hours at 4 ^{o}C and finally used for three extraction cycles. In all cases, the extraction device was able to retain galactosylated proteins. More detailed stability testing should be the subject of future studies. However, the extraction performance dropped off significantly after prolonged storage (> 1 month). For example, the peak areas of the ribonuclease (i.e. non-galactosylated protein) B before and after extraction were 0.54 and 0.53, respectively. Also, the peak area of the desialylated transferrin (i.e. galactosylated protein) before and after extraction were 0.84 and 0.83, respectively.

6.3.7. Repeatability of nano-agglomerated affinity monolith fabrication procedures

During the course of this work, a total of eight nano-agglomerated affinity monoliths were prepared (denoted **A1** to **A8**) and their extraction performance was evaluated as described. For six of the eight monoliths, (Figure 6.22) the average extraction of transferrin (from 20 µL of **Standard A**) was again 31 %, with a % RSD between monoliths of 14.0 %. This level of agreement between separate affinity monoliths is acceptable considering that each individual monolith was subject to no less than 11 discrete steps during fabrication (2 steps for polypropylene wall modification, 2 steps for monolith polymerisation (critical for control of base-monolith surface area and bed volume), 4 steps for nano-agglomeration with gold and 3 steps for protein immobilisation/blocking procedures). Two of the eight affinity monoliths (**A7** and **A8**) displayed disproportionately high % extraction of desialylated transferrin (72 % and 65 %) relative to the other six monoliths. The most likely reason for higher extraction of transferrin is (a): an erroneously higher surface area for the base monolith due to the human error involved in preparing the monomer mixture or (b): a larger bed volume due to inaccurate filling of the tip with monomer mixture.

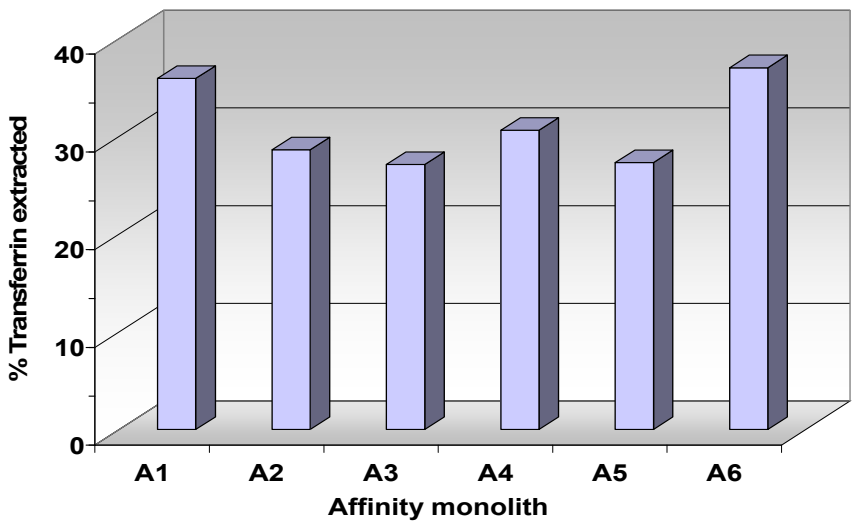

Figure 6.22: Repeatability of extraction of desialylated transferrin from **Standard A** on multiple nano-agglomerated affinity monoliths.

6.3.8. Extraction of glycoprotein from spiked real samples: *E. coli*

Finally, the extraction performance of the affinity monolith tip (**Monolith A**) was examined with real sample matrices similar to those typical of a biofermentation process reaction. An *E. coli* cell lysate sourced from a KRX strain (filtered and passed through a 10 kDa ultrafiltration unit) was spiked with 20 $\mu g.mL^{-1}$ desialylated transferrin. The cell lysate was from *E. coli*, which is a prokaryotic organism and so does not have the type of glycosylation system that produces the complex glycoproteins that ECL interacts with. Thus, 20 µL of the spiked sample was passed through the monolith and the results before and after are shown in Figure 6.23. The peak of the desialylated transferrin decreased significantly as a result of extraction despite the presence of unknown matrix protein. Indeed the peak profile of the *E. coli* proteins was unchanged before and after extraction, as expected, which indicates that unwanted non-specific protein binding or protein-protein interactions were largely eliminated. In addition, the retained transferrin was recovered from the extraction phase with an extraction recovery of about 83

% and there was a marked absence of interfering proteins in this galactose elution step.

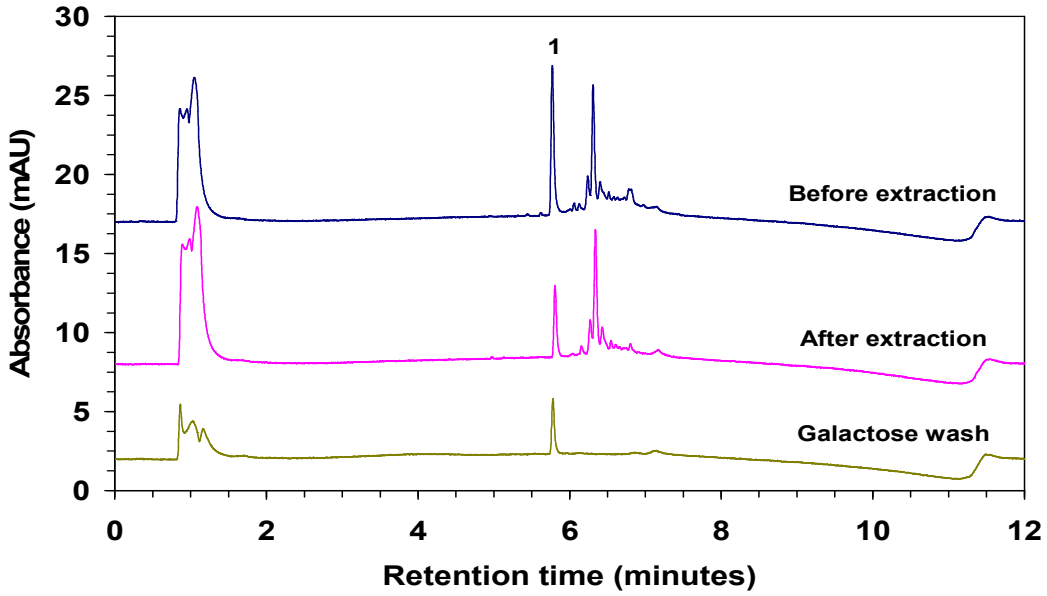

Figure 6.23: HPLC chromatograms of spiked *E. coli* cell lysate before and after passage through **Monolith A**. Chromatographic conditions are as described in Figure 6.20. Peaks: (**1**) desialylated transferrin.

6.4. Conclusions

A novel affinity monolithic extraction phase has been described which incorporates covalently attached AuNPs, providing a significant increase in surface area. By using the well studied bifunctional coupling agent DTSP, a selected lectin was successfully immobilised on the gold surface, while retaining its activity. The obvious advantage of this new Au-modified substrate is that using DTSP chemistry, any bio-recognition molecule (lectins, enzymes, Protein A etc) can be immobilised depending upon the required application while taking full advantage of the excellent mass-tranfer characteristics afforded by the underlying porous polymer monolith. Although a comprehensive quantitative assessment of extraction and recovery was not performed, nevertheless enhanced capacity and excellent phase selectivity was clear.

6.5. References

[1] M. Gilar, E. S. Bouvier, B. J. Compton, *J. Chromatogr. A* 2001, **909**, 111 - 135.

[2] D. Martinez, M. J. Cugat, F. Borrull, M. Calull, *J. Chromatogr. A* 2000, **902**, 65 - 89.

[3] G. L. Duan, L. X. Zheng, J. Chen, W. B. Cheng, D. Li, *Biomed. Chromatogr.* 2002, **16**, 282 - 286.

[4] J. L. Luque-Garcia, T. A. Neubert, *J. Chromatogr. A* 2007, **1153**, 259 - 276.

[5] L. Xu, Z. G. Shi, Y. Q. Feng, *Anal. Bioanal. Chem.* 2011, **399**, 3345 - 3357.

[6] T. Kumazawa, C. Hasegawa, X. P. Lee, K. Sato, *Forensic Toxicol.*, 2010, **28**, 61 - 68.

[7] Z. Altun, C. Skoglund, M. Abdel-Rehim, *J. Chromatogr. A* 2010, **1217**, 2581 - 2588.

[8] D. Moravcová, V. Kahle, H. Řehulková, J. Chmelík, P. Řehulka, *J. Chromatogr. A* 2009, **1216**, 3629 - 3636.

[9] J. Jiang, C. A. Lucy, *Talanta* 2007, **72**, 113 - 118.

[10] M. Kussmann, E. Nordho, H. Rahbek-Nielsen, S. Haebel, M. Rossel-Larsen, L. Jakobsen, J. Gobom, E. Mirgorodskaya, A. Kroll-Kristensen, L. Palmp, P. Roepstor, *J. Mass Spectrom.* 1997, **32**, 593 - 601.

[11] Y. Ishihama, J. Rappsilber, M. Mann, *J. Proteome Res.* 2006, **5**, 988 - 994.

[12] J. Šalplachta, P. Řehulka, J. Chmelík, *J. Mass Spectrom.* 2004, **39**, 1395 - 1401.

[13] T. Keough, M. P. Lacey, R. S. Youngquist, *Rapid Commun. Mass Spectrom.* 2002, **16**, 1003 - 1015.

[14] M. Palmblad, J. S. Vogel, *J. Chromatogr. B* 2005, **814**, 309 - 313.

[15] J. L. Hsu, M. K. Chou, S. S. Liang. S. Y. Huang, C. J. Wu, F. K. Shi, S. H. Chen, *Electrophoresis* 2004, **25**, 3840 - 3847.

[16] S. Miyazaki, K. Morisato, N. Ishizuka, H. Minakuchi, Y. Shintani, M. Furuno, K. Nakanishi, *J. Chromatogr. A* 2004, **1043**, 19–25.

[17] Z. Altun, L. Blomberg, M. Abdel-Rehim, *J. Liq. Chromatogr. Rel. Technol.* 2006, **29**, 1477 - 1489.

[18] E. F. Hilder, F. Svec, J. M. J. Frèchet, *J. Chromatogr. A* 2004, **1044**, 3 - 22.

[19] D.S. Peterson, T. Rohr, F. Svec, J. M. J. Frèchet, *Anal. Chem.* 2002, **74**, 4081 - 4088.

[20] T. Kumazawa, C. Hasegawa, X. P. Lee, A. Marumo, N. Shimmen, A. Ishii, H. Seno, K. Sato, *Talanta* 2006, **70**, 474 - 478.

[21] C. Hasegawa, T. Kumazawa, X. P. Lee, M. Fujishiro, A. Kuriki, A. Marumo, H. Seno, K. Sato, *Rapid Commun. Mass Spectrom.* 2006, **20**, 537 - 543.

[22] T. Kumazawa, C. Hasegawa, X. P. Lee, K. Hara, H. Seno, O. Suzuki, K. Sato, *J. Pharm. Biomed. Anal.* 2007, **44**, 602 - 607.

[23] C. Hasegawa, T. Kumazawa, X. P. Lee, A. Marumo, N. Shinmen, H. Seno, K. Sato, *Anal. Bioanal. Chem.* 2007, **389**, 563 - 570.

[24] L. Berruex, R. Freitag, T. Tennikova, *J. Pharm. Biomed. Anal.* 2000, **24**, 95 - 104.

[25] M. Bedair, Z. El Rassi, *J. Chromatogr. A* 2004, **1044**, 177 - 186.

[26] M. Bedair, Z. El Rassi, *J. Chromatogr. A* 2005, **1079**, 236 - 245.

[27] K. K. R. Tetala, B. Chen1, G. M. Visser, T. A. van Beek, *J. Sep. Sci.* 2007, **30**, 2828 - 2835.

[28] S. Ota, S. Miyazaki, H. Matsuoka, K. Morisato, Y. Shintani, K. Nakanishi, *J. Biochem. Biophys. Methods* 2007, **70**, 57 - 62.

[29] M. Rainer, H. Sonderegger, R. Bakry, C. W. Huck, S. Morandell, L. A. Huber, D. T. Gjerde, G. K. Bonn, *Proteomics* 2008, **8**, 4593 - 4602.

[30] M. Abdel-Rehim, C. Persson, Z. Altun, L. Blomberg, *J. Chromatog. A* 2008, **1196–1197**, 23 - 27.

[31] S. S. Liang, S. H. Chen, *J. Chromatogr. A* 2009, **1216**, 2282 - 2287.

[32] Z. Altun, A. Hjelmström, M. Abdel-Rehim, L. G. Blomberg, *J. Sep. Sci.* 2007, **30**, 1964 - 1972.

[33] Z. Altun, A. Hjelmström, L. G. Blomberg, M. Abdel-Rehim, *J. Liq. Chromatogr. Rel. Technol.* 2008, **31**, 743 - 751.

[34] H. C. Hsieh, C. Sheu, F. K. Shi, D. T. Li, *J. Chromatogr. A* 2007, **1165**, 128 - 135.

[35] J. Thabano, M. Breadmore, J. Hutchinson, C. Johns, P. R. Haddad, *J. Chromatogr. A* 2009, **1216**, 4933 - 4940.

[36] J. Krenkova, N. A. Lacher, F. Svec, *Anal. Chem.* 2010, **82**, 8335 - 8341.

[37] E. F. Hilder, F. Svec, J. M. J. Frèchet, *J. Chromatogr. A* 2004, **1053**, 101 - 106.

[38] J. P. Hutchinson, P. Zakaria, A. R. Bowie, M. Macka,N. Avdolovic, P. R. Haddad, *Anal. Chem.* 2005, **77**, 407 - 416.

[39] Comparison of ion-chromatography and portable capillary electrophoresisfor identification of improvised inorganic explosives used in terrorist attacks: P. Haddad, G. Dicinoski, E. Hilder, R. Guijt, J. Hutchinson, C. Johns, E. Tyrrell, Euroanalysis 2009, Innsbruck, Austria.

[40] D. Connolly, B. Twamley, B. Paull, *Chem. Commun.* 2010, **46**, 2109 - 2111.

[41] Y. Xu, Q. Cao, F. Svec, J. M. J. Frèchet, *Anal. Chem.* 2010, **82**, 3352 - 3358.

[42] Q. Cao, Y. Xu, F. Liu, F. Svec, J. M. J. Frèchet, *Anal. Chem.* 2010, **82**, 7416 - 7421.

[43] D. Connolly, V. O'Shea, P. Clark, B. O'Connor, B. Paull, *J. Sep. Sci.* 2007, **30**, 3060 - 3068.

[44] G. Frens, *Nature* 1973, **241**, 20 - 22.

[45] A. Varki, R. D. Cummings, J. D. Esko, H. H. Freeze, P. Stanley, C. R. Bertozzi, G. W. Hart, M. E. Etzler, *Essentials of Glycobiology*, 2nd edn, Cold Spring Harbor Laboratory Press, NY, USA, 2009.

[46] A. M. Wu, J. H. Wu, M. S. Tsai, Z. Yang, N. Sharon, A. Herp, *Glycoconj. J.* 2007, **24**, 591 - 604.

[47] K. Turton, R. Natesh, N. Thiyagarajan, J. A. Chaddock, K. R. Acharya, *Glycobiology* 2004, **14**, 923 - 929.

[48] T. B. Stachowiak, T. Rohr, E. F. Hilder, D. S. Peterson, M. Yi, F. Svec, J. M. J. Fréchet, *Electrophoresis* 2003, **24**, 3689 - 3693.

[49] B. Rånby, W. T. Yang, O. Tretinnikov, *Nucl. Instrum. Methods Phys. Res. Sect. B* 1999, **151**, 301 - 305.

[50] T. Rohr, D. F. Ogeltree, F. Svec, J. M. J. Fréchet, *Adv. Funct. Mat.* 2003, **13**, 264 - 270.

[51] Y.Uyama, K. Kato, Y. Ikada, *Adv. Polym. Sci.* 1998, **137**, 1 - 39.

[52] F. Svec, *J. Chromatogr. A* 2010, **1217**, 902 - 924.

[53] T. Rohr, E. F. Hilder, J. J. Donovan, F. Svec, J. M. J. Fréchet, *Macromolecules* 2003, **36**, 1677 - 1684.

[54] S. Storri, T. Santoni, M. Minunni, M. Mascini, *Biosens. Bioelectron.* 1998, **13**, 347 - 357.

[55] E. Y. Katz, *J. Electroanal. Chem.* 1990, **291**, 257 - 260.

[56] M. Darder, K. Takada, F. Pariente, E. Lorenzo, H. D. Abruña, *Anal. Chem.* 1999, **71**, 5530 - 5537.

[57] J. C. Feldner, M. Ostrop, O. Friedrichs, S. Sohn, D. Lipinsky, U. Gunst, H. F. Arlinghaus, *Appl. Surf. Sci.* 2003, **203**-**204**, 722 - 725.

[58] L. H. Dubois, R. G. Nuzzo, *Annu. Rev. Phys. Chem.* 1992, **43**, 437 - 463.

[59] K. Turton, R. Natesh, N. Thiyagarajan, J. A. Chaddock, K. R. Acharya, *Glycobiology* 2004, **14**, 923 - 929.

[60] R. A. Dwek, *Chem. Rev.*, 1996, **96**, 683–720.

[61] T. Iskratsch, A. Braun, K. Paschinger, I. B.H. Wilson, *Anal. Biochem.* 2009, **386**, 133 - 146.

[62] J. W. Dolan, L. R. Snyder, M. Djordjevic, D. W. Hill, T. J. Waeghe, *J. Chromatogr. A* 1999, **857**, 1 - 20.

[63] J. Charlwood, H. Birrell, A. Organ, P. Camilleri, *Rapid Commun. Mass Spectrom.* 1999, **13**, 716 - 723.

Chapter 7

Final conclusions

The effectiveness of biotherapeutic drugs for the treatment of different diseases, e.g. cancer, diabetes, etc., has accelerated their development and manufacturing. The production processes of such drugs are strictly regulated to ensure the consistency of the processes and to produce high quality drugs. Therefore, the aim of this project was to develop rapid and efficient chromatographic methods for the analysis of real samples sourced from the biopharma industry and to evaluate lot-to-lot variability. The samples included complex and CD cell culture media, raw materials (i.e. yeastolate) and in-process samples. The samples were complex and comprised a variety of components. The challenge was to develop methods for the determination of the target analytes with minimal interference from sample matrices.

The results in Chapter 3 showed the development of a relatively rapid and efficient RPLC-FLD based method for the qualitative and semi-quantitative determination of up to ten common monosaccharides. The method involved a sample pretreatment step using a C_{18} SPE cartridge to trap hydrophobic peptides and vitamins, with recovery of all test monosaccharides exceeding 90 %. The selectivity of the method was also achieved by the pre-column derivatisation of monosaccharides with anthranilic acid. The derivatives were efficiently separated on a C_{18} particle-based column packed with sub-2 µm particles. The method used considerably less mobile phase while running at lower flow rates. Standard analytical performance criteria were used for evaluation purposes, with the method found to exhibit LOD's as low as 10 fmol, and be linear and precise (% RSD < 2.2 % (n = 7). The method was applied to the analysis of different lots of complex biopharmaceutical production samples, including yeastolate powders, cell culture media and in-process fermentation broth samples in order to estimate lot-to-lot variability.

The second developed method, as described in Chapter 4, showed the successful application of a rapid, sensitive and specific RRLC-UV-Vis assay for the quantitative determination of total free sialic acid in the same

sample matrices analysed in Chapter 3. The method also involved a sample pretreatment step utilising a C_{18} SPE cartridge. It also involved a pre-column derivatisation step employing thiobarbituric acid as pre-column tagging agent followed the oxidation of sialic acid with periodic acid. However, the derivatives here were separated on a short C_{18} monolithic column in less than 90 seconds. The separation was carried out at high flow rates showing the advantage of using such columns. The method was linear over a wide range (0.25 - 25 $\mu mol.L^{-1}$), reproducible (average % RSD = 1.2 (*n* = 6) and sensitive (LOD = 842 fmol based upon a 100 µL injection volume).

Monolithic columns were also effectively used for the development of a rapid and sensitive method for the quantitative determination of the Cys and Cyss ratio in CD media feedstock as presented in Chapter 5. Cys was pre-derivatised with purified CMQT and separated from other derivatisation products on a narrow-bore C_{18} monolithic column and monitored with UVD at 355 nm and MS. The derivatisation reagent (CMQT) is thiol selective and the detection wavelength negated any possible interference from other potential interfering sample components such as monosaccharides or other amino acids. The treatment of the samples consisted of dividing them into two aliquots, the first aliquot was analysed for Cys and the second aliquot is analysed for Cyss after its quantitative reduction to cysteine using TCEP. The method performance data revealed that the method w linear, sensitive and precise. Samples (*n* = 31) of an industry-supplied CD media feedstock were analysed, finding Cys ranging from 1.56 to 2.26 $\mu g.mL^{-1}$ (S.D. 0.2 $\mu g.mL^{-1}$) and Cyss from 1062.02 to 1348.13 $\mu g.mL^{-1}$ (S.D. 80.5 $\mu g.mL^{-1}$). The developed methods are useful for routine analysis for large numbers of samples due to their minimal sample handling steps, quantitative nature and fast analysis.

The final section of this project, which is presented in Chapter 6, demonstrated a novel affinity monolithic extraction phase for selective enrichment of galactosylated proteins. The inner-wall of pipette-the tip was pretreated by grafting methacrylate anchor sites to ensure a subsequent

attachment between the tip and the extraction phase (i.e. EDMA porous polymer monolith), which was then photopolymerised *in-situ* within the confines of 20 µL polypropylene pipette-tips. Then the surface of the monolith was significantly enhanced by immobilising AuNPs. AuNPs were immobilised onto the monolith after surface amination (via an azlactone grafting step) and coverage was verified using FE-SEM. The obvious advantage of this new Au-modified substrate is that any bio-recognition molecule (lectins, enzymes, Protein A etc) can be immobilised by using the bifunctional coupling agent DTSP. However, ECL was selected in this study since it is commercially available and its bind/elute mechanism is well known [1]. Therefore, the immobilised AuNPs were functionalised with ECL. The ECL-modified tip was successfully applied for the enrichment of galactosylated protein (desialylated transferrin) versus a non-galactosylated protein (Ribonuclease B) due to the specificity of ECL. Reversed-phase capillary HPLC was used to validate the efficiency and selectivity of the developed extraction device which resulted in an increase in extraction recovery of ~95 % due to the AuNPs enhanced surface area. Further specificity of the ECL-modified tip was demonstrated with a complex mixture of non-glycosylated and glycosylated proteins with differing terminal sugar structures. Although the affinity monolith was not applied to industry-supplied complex samples, it was applied to a galactosylated protein spiked *E. coli* cell lysate to successfully demonstrate matrix tolerance.

The primary focus in the work presented in Chapter 6 was a qualitative assessment of the selectivity of the affinity monolith for galactosylated glycoproteins (e.g. transferrin) over non-glycosylated glycoproteins (e.g. ribonuclease B) rather than a comprehensive quantitative assessment of extraction/recovery. The preliminary results obtained were extremely promising in terms of the development of a novel AuNP-modified monolithic substrate for affinity applications. The enhanced capacity and excellent phase selectivity of the affinity monolith were clear. Future work

shall involve a more detailed examination of extraction/recovery, loading flow-rates and stability testing of the affinity monolith tip.

7.1. References

[1] A. M. Wu, J. H. Wu, M. S. Tsai, Z. Yang, N. Sharon, A. Herp, *Glycoconj. J.* 2007, **24**, 591 - 604.

Appendix I: Recrystallisation of CMQT

Experimental

Instrumentation

^{1}H NMR spectra of CMQT before and after recrystallisation were collected with a Bruker Avance 400 UltraShield spectrometer (Fällanden, Switzerland). Accumulation parameters are listed in Table I.1. The chemical shifts were referenced with respect to deuterium oxide (D_2O), used as internal reference.

Table I.1
Experimental acquisition conditions for ^{1}H NMR spectroscopy

State	Frequency (MHz)	Recycle delay time (µs)	Pulse duration (s)	Spectral width (ppm)	Scans
Liquid	400	60	3.95	20.68	16

Recrystallisation of CMQT

1.3 g of CMQT produced in Section 5.2.4 was dissolved in 3 mL ACN and placed in a 25-mL beaker, which was in turn placed within a larger beaker containing 25 mL diethyl ether. The system was made airtight and left overnight. The resulting crystals in the inner beaker (formed due to solvent exchange) were isolated and dried by vacuum filtration for 60 minutes. The recrystallisation yield was calculated as 93.9 %.

Results and discussion

Recrystallisation of the prepared CMQT reagent was carried out in order to minimise unknown reagent components that were observed when the CMQT was injected in the HPLC which possibly lead to increase chromatogram complexity.

Choosing the proper solvent for recrystallisation is the most critical point. Unsuccessful attempts have been made to use single-solvent or hot-filtration recrystallisation due to either the solubility of CMQT at room temperature in the more polar solvents or due to insolubility of CMQT in the less or non polar solvents. The only two solvents that CMQT was insoluble in at room temperature and soluble at boiling point were ethanol and 1-propanol. Figure I.1 shows chromatograms of CMQT-Cys using CMQT recrystallised in three different solvents; diethyl ether, ethanol and 1-propanol. As it can be seen, CMQT was successfully recrystallised from ACN:diethyl ether. Purified CMQT crystals were verified using HPLC (Figure I.2), mass spectrometry (Figure I.3) and ^{1}H NMR (Figure I.4).

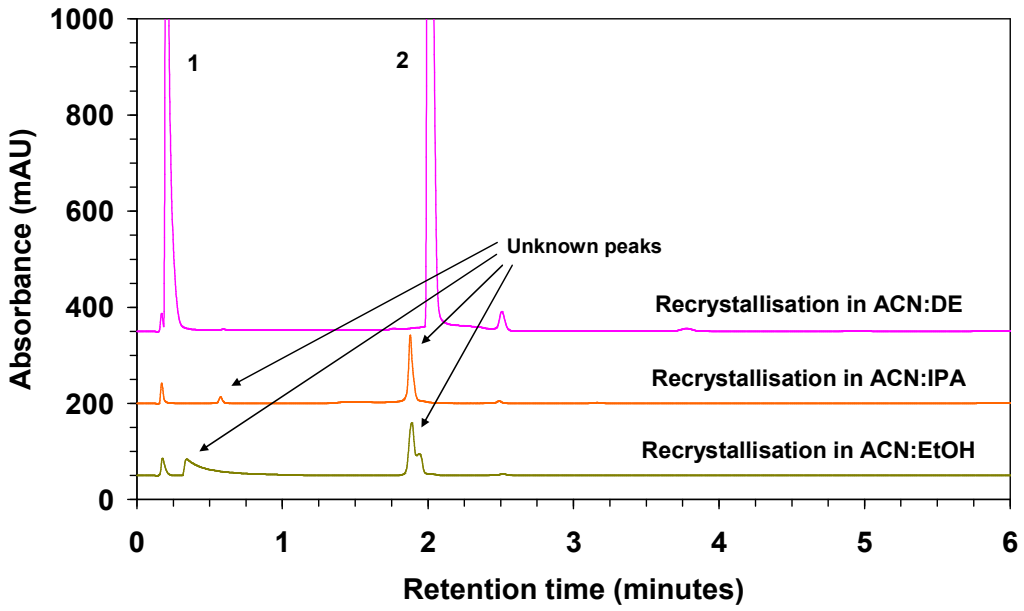

Figure I.1: HPLC chromatograms showing Cys standard drivatised with CMQT that was recrystallised in different solvents. Chromatographic conditions are as described in Figure 5.8. Peaks: (**1**) excess CMQT, (**2**) CMQT-Cys.

Figure I.2 shows HPLC chromatograms of Cys standard derivatised with CMQT before and after recrystallisation in diethyl ether. The chromatograms were obtained using a gradient method. As it can be seen, the recrystallisation of CMQT lead to disappearance of the extra peaks eluted after the excess CMQT reagent peak.

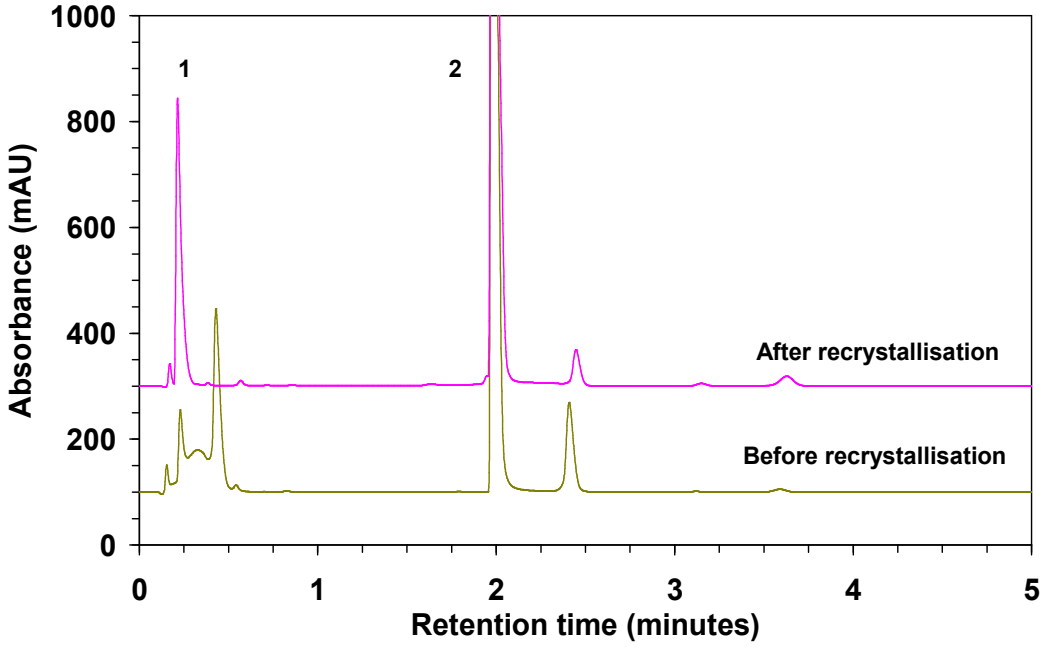

Figure I.2: HPLC chromatograms showing the CMQT-Cys standard before and after recrystallisation of CMQT. Chromatographic conditions are as described in Figure 5.8. Peaks: (**1**) excess CMQT, (**2**) CMQT-Cys.

CMQT purification was also confirmed using MS. Figure I.3 shows the mass spectra of CMQT before and after recrystallisation. The spectra was obtained from direct infusing of a solution of CMQT (1 $\mu g.L^{-1}$) prepared in H_2O/MeOH (80:20). Apart from CMQT signal at *m/z* of 178, which remained relatively constant, other signals at *m/z* 174, 159 and 131 were present. The intensities of these signals were decreased by over 96 % after recrystallisation. A characteristic mass spectral isotope pattern was produced by CMQT corresponding to the chlorine natural isotopic abundance. The molecular ion of CMQT at *m/z* 178 shows a +2 amu peak

with about 30 % intensity, which corresponds to the ^{37}Cl isotope contribution as illustrated in Figure I.3. (It should be noted that this characteristic pattern is not produced by the CMQT-Cys derivative since the chlorine atom is replaced by the thiol.)

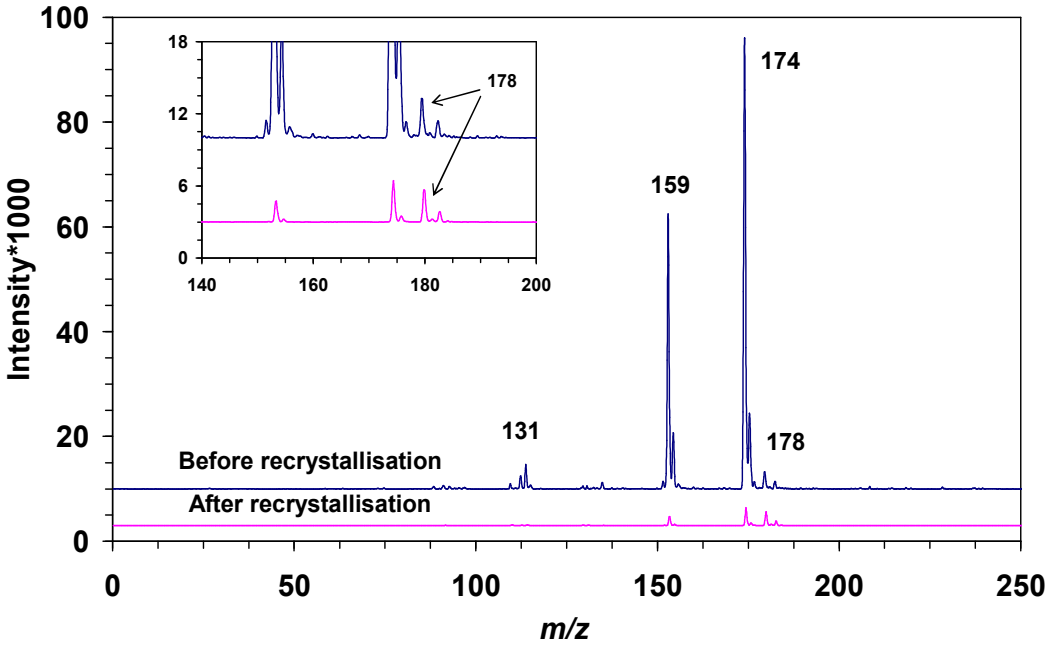

Figure I.3: Mass spectra of CMQT (1 µg.L^{-1}) before and after recrystallisation.

To identify the origin of these peaks, CMQT was further analysed using ^{1}H NMR. Figure I.4 shows the ^{1}H NMR spectra of CMQT before and after recrystallisation. Both spectra exhibit 6 different NMR signals located at 7.9, 8.03, 8.15, 8.17, 8.3 and 8.9 ppm. Apart from signals located at 7.9 and 8.15, which are triplet signals, all other signals are doublet. This demonstrates that CMQT structure consisted of four different protons having one single neighbouring proton, and two different protons having two neighbouring protons. Moreover, the triplet signal observed around 8.15 ppm is composed of a superposition of two triplet signals translating the presence of two different protons of similar electronical environment. According to these observations, the ^{1}H NMR spectra show the presence of seven

different protons within the structure of CMQT. This is in a perfect agreement with the theoretical expectation as CMQT is consisting of nine protons in which three of them (within the methyl group, $-CH_3$) have an identical electronical environment and thus appearing with the same NMR signal (Figure I.4(**a**)). Assignments of the different chemical shifts are summarised in Table I.2.

Table I.2
Assignment of ^1H NMR signals obtained from CMQT

Attribution	Chemical shift (ppm)
H_6	7.9
H_7	8.03
$H_{4,5}$	8.15
H_3	8.17
H_2	8.3
H_1	8.9

Even if both spectra (before and after recrystallisation) show the same number of signals at closely related chemical shifts, it is important to highlight the slight shift toward the lower chemical shifts of CMQT characterised before recrystallisation, as indicated by the dash-lines in Figure I.4(**a**). This shift could be caused by the presence of strong nucleophilic groups such as oxygenated or fluorinated groups, which could be present in the reagent before purification.

In addition, Figure I.4(**b**) shows the disappearance of several signals in the 3 - 4.5 ppm region, where methoxy- protons (CH_3-O) linked to either aliphatic or aromatic groups usually appear. Thus, it is very likely that unpurified CMQT contains methoxy groups covalently linked to the aromatic skeleton in place of the chloride group. Furthermore the presence of a peak at *m/z* 174 in the mass spectrum of the material before recrystallisation suggests the presence of a methoxy group on the aromatic skeleton rather than the intended chloride atom.

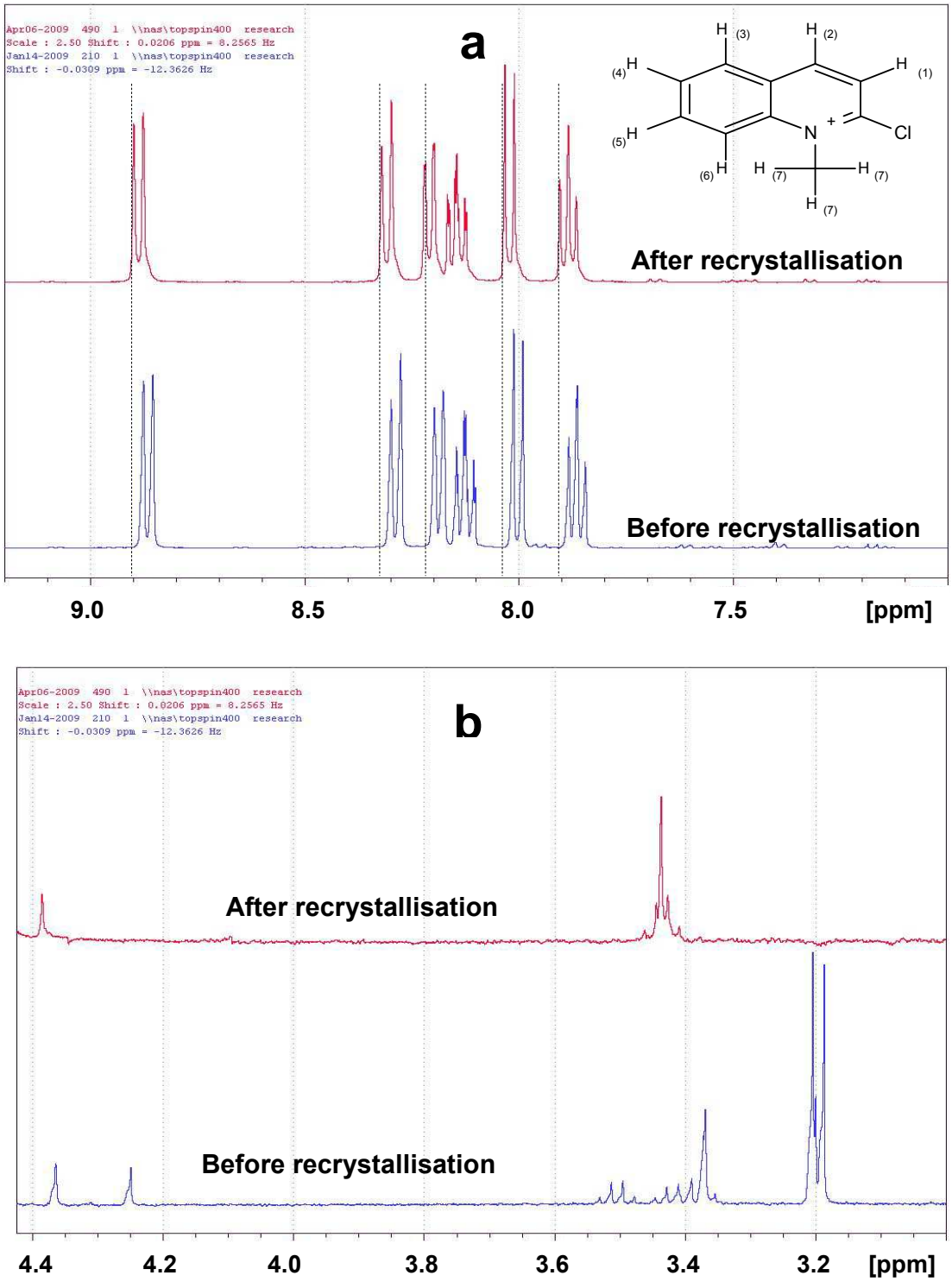

Figure I.4(a and b): ^{1}H NMR spectra of CMQT (20 mg/1 mL D_2O) before and after recrystallisation